

AWARD NUMBER: **W81XWH-15-1-0489**

TITLE: **Role of C/EBP Delta in IR-Induced Sepsis**

PRINCIPAL INVESTIGATOR: **SNEHALATA A PAWAR**

CONTRACTING ORGANIZATION: **UNIVERSITY OF ARKANSAS FOR MEDICAL SCIENCES
Little Rock, AR 72205**

REPORT DATE: **Nov 2019**

TYPE OF REPORT: **Final Report**

PREPARED FOR: **U.S. Army Medical Research and Materiel Command
Fort Detrick, Maryland 21702-5012**

DISTRIBUTION STATEMENT: **Approved for Public Release;
Distribution Unlimited**

The views, opinions and/or findings contained in this report are those of the author(s) and should not be construed as an official Department of the Army position, policy or decision unless so designated by other documentation.

| REPORT DOCUMENTATION PAGE | | | Form Approved OMB No. 0704-0188 | | |
|--|--------------|--------------------------------|--|---|---|
| Public reporting burden for this collection of information is estimated to average 1 hour per response, including the time for reviewing instructions, searching existing data sources, gathering and maintaining the data needed, and completing and reviewing this collection of information. Send comments regarding this burden estimate or any other aspect of this collection of information, including suggestions for reducing this burden to Department of Defense, Washington Headquarters Services, Directorate for Information Operations and Reports (0704-0188), 1215 Jefferson Davis Highway, Suite 1204, Arlington, VA 22202-4302. Respondents should be aware that notwithstanding any other provision of law, no person shall be subject to any penalty for failing to comply with a collection of information if it does not display a currently valid OMB control number. PLEASE DO NOT RETURN YOUR FORM TO THE ABOVE ADDRESS. | | | | | |
| 1. REPORT DATE Nov 2019 | | 2. REPORT TYPE FINAL REPORT | | 3. DATES COVERED 09/01/2015 - 08/31/2019 | |
| 4. TITLE AND SUBTITLE ROLE OF C/EBP DELTA IN IR-INDUCED SEPSIS | | | 5a. CONTRACT NUMBER | | |
| | | | 5b. GRANT NUMBER W81XWH-15-1-0489 | | |
| | | | 5c. PROGRAM ELEMENT NUMBER | | |
| 6. AUTHOR(S) SNEHALATA A PAWAR E-Mail: SAPawar@uams.edu | | | 5d. PROJECT NUMBER | | |
| | | | 5e. TASK NUMBER | | |
| | | | 5f. WORK UNIT NUMBER | | |
| 7. PERFORMING ORGANIZATION NAME(S) AND ADDRESS(ES) University of Arkansas for Medical Sciences, Little Rock, Arkansas-72205 | | | 8. PERFORMING ORGANIZATION REPORT | | |
| 9. SPONSORING / MONITORING AGENCY NAME(S) AND ADDRESS(ES) U.S. Army Medical Research and Materiel Command Fort Detrick, Maryland 21702-5012 | | | 10. SPONSOR/MONITOR'S ACRONYM(S) | | |
| | | | 11. SPONSOR/MONITOR'S REPORT NUMBER(S) | | |
| 12. DISTRIBUTION / AVAILABILITY STATEMENT Approved for Public Release; Distribution Unlimited | | | | | |
| 13. SUPPLEMENTARY NOTES | | | | | |
| 14. ABSTRACT It is known that exposure to ionizing radiation (IR) induces a plethora of responses in the cells to counteract oxidative stress, DNA damage response and inflammation by inducing the expression of inflammatory and anti-inflammatory cytokines. We have previously shown that <i>Cebpd</i> -knockout (KO) mice are highly sensitive to IR and the underlying cause of lethality is due to injury to the intestine and bone marrow. In this study, we investigated whether impaired inflammation signaling and oxidative/nitrosative stress promoted radiation-induced intestinal injury and sepsis-associated lethality of <i>Cebpd</i> ^{-/-} mice after exposure to total body irradiation. We showed that <i>Cebpd</i> -KO mice display increased expression of the pro-inflammatory cytokines such as <i>Il-6</i> , <i>Tnf-α</i> in the intestine tissues as well as in the plasma and increased expression of chemokines such as <i>Mcp-1</i> , <i>Cxcl1</i> and <i>Mif-1a</i> . <i>Cebpd</i> -KO mice showed increased expression of Claudin-2, a protein associated with <i>in vivo</i> intestinal barrier disruption, which correlated with an increase in increased plasma levels of lipopolysaccharide-binding protein, <i>in vivo</i> intestinal permeability and bacterial translocation. We also uncovered that the IR-induced upregulation of TLR4 signaling in <i>Cebpd</i> -KO mice is due to upregulation of TRAF6 (a positive regulator) and decrease in expression of TOLLIP (a negative regulator). We also found that <i>Cebpd</i> is essential for gamma tocotrienol-mediated protection against radiation-induced intestinal and bone marrow injury. Lastly, our results reveal that <i>Cebpd</i> -deficiency does not perturb the response of KO macrophages to promote increased intestinal injury in response to TBI exposure. Lastly, we also found that treatment with TLR4 inhibitor-C34 immediately post-irradiation showed a significant protection of intestinal crypts at day 3.5 post-10 Gy, however the effect on overall survival remains unexplored. Given that TLR4 does play an important role in intestinal homeostasis as well as in hematopoietic system, the time and dosing regimen will play a critical role. In this regards, the pharmacokinetics and pharmacodynamics of the TLR4 inhibitor C34 will need to be determined. | | | | | |
| 15. SUBJECT TERMS <i>C/EBPδ</i> , <i>Cebpd</i> , ionizing radiation, sepsis, inflammation, oxidative stress, intestinal injury, hematopoietic injury, macrophages, bone marrow-derived macrophages, toll-like receptor, tight junction proteins, total body irradiation | | | | | |
| 16. SECURITY CLASSIFICATION OF: | | | 17. LIMITATION OF ABSTRACT | 18. NUMBER OF PAGES | 19a. NAME OF RESPONSIBLE PERSON |
| a. REPORT | b. ABSTRACT | c. THIS PAGE | | | USAMRMC |
| Unclassified | Unclassified | Unclassified | Unclassified | 168 | 19b. TELEPHONE NUMBER (include area code) |

TABLE OF CONTENTS

| # | Description | Page numbers |
|---|---|--------------|
| 1 | Introduction..... | 1 |
| 2 | Keywords..... | 1 |
| 3 | Accomplishments..... | 1-32 |
| 4 | Impact..... | 32 |
| 5 | Changes/Problems..... | 32-33 |
| 6 | Products..... | 33-39 |
| 7 | Participants & Other Participating Organizations..... | 40-42 |
| 8 | Special Reporting Requirements..... | 41-42 |
| 9 | Appendices..... | 42-168 |

1. INTRODUCTION:

Sepsis is characterized by increased myelosuppression, disruption of intestinal barrier and bacterial translocation and an exaggerated inflammatory response. Current evidence indicates that dysregulation of the host inflammatory response to the infectious agent is central to the mortality of patients with sepsis. Although regulated inflammation is important to control bacterial infection, an excessive systemic inflammatory response can lead to shock and early mortality. Factors related to the infectious agent that trigger the immune/inflammatory responses are amplified by molecules of the host origin including cytokines, chemokines, lipid mediators, and reactive oxygen species. These inflammatory mediators influence the recruitment and activation of leukocytes affecting pathogen clearance at a potential cost of promoting tissue damage. There have been no studies investigating the role of C/EBP δ in the inflammation and toll-like receptor (TLR) responses in the context of radiation-injury and sepsis.

Our recently published studies on *Cebpd*-deficient mice revealed thrombocytopenia, neutropenia, myelosuppression and loss of intestinal crypts as the underlying cause of TBI-induced lethality. Further our preliminary results show that radiation-induced increased expression of pro-inflammatory cytokines and TLRs in the intestines of *Cebpd*-KO mice. All these results point to a role for IR-mediated sepsis-induced lethality in *Cebpd*-KO mice. Because gut-associated sepsis is the major cause of lethality after exposure to TBI, we hypothesize that the inflammatory responses mediated via TLR4 are regulated by C/EBP δ and may play an important role in post-radiation survival. We will test this hypothesis as follows- In **Aim1**: we will determine whether IR-induced intestinal injury in *Cebpd*-KO mice is due to increased TLR4-mediated inflammatory response and in **Aim2**, we will determine whether *Cebpd*-KO mice show perturbed macrophage response post-IR.

Protection of first responders who are deployed in a radiation exposure field for rescue or military operations is an urgent need. There is a greater need for understanding the mechanisms of radiation-induced sepsis and the underlying lethality especially due to the increasing global threat of nuclear terrorism and or due to accidental radiation exposure to populations, due to nuclear accidents such as the recent Fukushima incident. This proposal addresses a **novel function of C/EBP δ** in the context of **radiation-induced sepsis** at a cellular and mechanistic level and may lead to new avenues for therapeutic intervention. Successful completion of the proposed studies will establish an important function for C/EBP δ in IR-induced sepsis and in macrophage function.

The **long term goal** will be to determine if activation of the C/EBP δ -specific pathways can protect cells from IR injury and sepsis. After specific targets of C/EBP δ are determined that are transcriptionally or post-translationally regulated after IR exposure, our next step will be to investigate possible pharmacologic interventions to manipulate C/EBP δ function to protect from IR-induced sepsis and promote recovery of the GI and hematopoietic systems.

2. **KEYWORDS:** C/EBP δ , *Cebpd*, ionizing radiation, sepsis, inflammation, oxidative stress, intestinal injury, hematopoietic injury, macrophages, bone marrow-derived macrophages, toll-like receptor, tight junction proteins, total body irradiation

3. ACCOMPLISHMENTS:

a. What were the major goals of the project?

Major Goals of the Project as approved in the SOW:

Specific Aim1: Determine whether IR-induced intestinal injury in *Cebpd*-KO mice is due to increased TLR4-mediated inflammatory response.

*Aim 1.1. Determine whether expression of pro-inflammatory cytokines and TLR genes is upregulated in *Cebpd*-KO mice but not WT mice after exposure to TBI.*

(4-12 mths)- Completion-100%

Milestones: (1) Demonstrate increased expression of pro-inflammatory cytokines, chemokines and TLR genes in intestines of *Cebpd*-KO mice using q-PCR and ELISA; (2) Identify differentially regulated cytokine

/chemokine/TLR targets of C/EBP δ that are induced by radiation (3) Present findings at a National meeting and publish results.

Aim 1.2 a. Determine whether IR-induced increased intestinal permeability in the *Cebpd*-KO mice. (6-9 mths) Completion-100%

Milestone: Demonstrate that *Cebpd*-KO mice show increased intestinal permeability after IR exposure compared to WT mice using an *in vivo* assay.

Aim 1.2 b. Determine the expression of tight junction proteins in WT and KO mice before and after irradiation.

(9-12mths) Completion-100%

Milestone: Demonstrate downregulation of tight junction proteins in intestines tissues of KO mice compared to that of WT mice after IR exposure.

Aim 1.2 c Determine whether lack of *Cebpd* increased bacterial translocation post-TBI.

(12-18mths) Completion-100%

Milestone: (1) Demonstrate evidence of translocation of bacteria to distant sites such as liver indicative of sepsis-like conditions in *Cebpd*-KO mice; (2) Present results at a National meeting and publish results obtained in 1.2 a, b, c.

Aim 1.3 a. Determine the effect of TLR inhibitor in alleviating the TLR4-mediated inflammation and intestinal injury.(15-21 mths) Completion -100%

Milestone: These studies will identify a role for TLR4 in aggravating IR-induced loss of intestinal crypts and lethality to TBI in *Cebpd*-KO mice.

Aim 1.3 b. Determine the role of gamma-tocotrienol (GT3) in alleviating the TLR4-mediated inflammation and intestinal injury. (18-24mths) Completion-100%

Milestone: These studies will identify a role for inflammatory response-mediated upregulation of ROS in promoting intestinal injury and IR-induced lethality which is rescued by GT3 treatment in *Cebpd*-KO mice. Publish results obtained from 1.3 a, b.

Specific Aim 2: Determine whether *Cebpd*-KO mice show perturbed macrophage response post-IR.

Aim 2.1 Determine effects of TBI on immune cells in WT and KO mice.

(24-30mths) Completion -100%

Milestone: Demonstrate using immunohistochemistry that there is increased recruitment of the inflammatory cells in response to IR in intestines of KO mice compared to that of respective WT counterparts.

Aim 2.1 b. Determine whether *Cebpd*-deficient macrophages show increased pro-inflammatory cytokines and oxidative stress post-irradiation. (27-33 mths) Completion -100%

Milestone: (1) Optimize protocols to isolate and characterize peritoneal and intestinal macrophages by flow cytometry. (2) We will demonstrate that *Cebpd*-KO macrophages are impaired in their inflammatory responses and are polarized to a M2 phenotype which promotes the increased intestinal injury.

Aim 2.1 c. Determine whether transplantation of *Cebpd*-KO macrophages enhance post-TBI intestinal injury in a macrophage-depletion mouse model. (30-36mths) Completion -100%

Milestone: (1) These studies will confirm that the altered/impaired functions of *Cebpd*-KO macrophages promote TBI-induced lethality and promote increased intestinal injury. (2) Present results at a National meeting and publish results.

b. What was accomplished under these goals?

Major Accomplishments

The major accomplishments under the goals for objectives of Aims 1 and 2 were achieved successfully and are listed below.

1) For this reporting period between September 1, 2015-Aug 31, 2018, our studies in Aim 1 confirmed that IR-induced inflammatory responses and TLR4 signaling in the intestines of *Cebpd*-KO mice led to the increased intestinal injury as indicated by increase in *in vivo* intestinal permeability, alterations in tight junction proteins, and showed elevated levels of oxidative and nitrosative stress. These findings were recently accepted in Scientific Reports (1).

We also reported that the antioxidant gamma-tocotrienol (GT3) imparts protection against radiation-induced hematopoietic as well as intestinal injury in a *Cebpd*-dependent manner and independent of G-CSF (2). Further our unpublished results show that the IR-induced upregulation of inflammatory cytokines and chemokines as well as nitrosative stress is due to upregulation of TLR4 signaling in the intestines of irradiated *Cebpd*-KO mice.

We found that the upregulation of TLR4 signaling in intestines of KO mice occurs due to decreased expression of the negative regulator -TOLLIP and upregulation of the positive regulator -TRAF6. Lastly we showed that using a TLR4 inhibitor, the increased intestinal injury by radiation can be alleviated by suppressing the IR-induced inflammatory as well as nitrosative stress in KO mice. Interestingly, we were able to also see significant protection of intestinal crypts in *Cebpd*-WT mice. Thus our results uncover a novel role for TLR4 inhibitors as potential agents to protect from radiation-induced intestinal injury. These results are currently in preparation to be submitted as a manuscript for publication.

2) In contrast the results from Aim 2, show that *Cebpd*-KO macrophages may not play a pertinent role in promoting increased intestinal injury in response to ionizing radiation exposure.

The details of the key findings from Aims 1 & 2 are as described below:

Specific Aim1: Determine whether IR-induced intestinal injury in *Cebpd*-KO mice is due to increased TLR4-mediated inflammatory response.

Aim 1.1. Determine whether expression of pro-inflammatory cytokines and TLR genes is upregulated in *Cebpd*-KO mice but not WT mice after exposure to TBI.

Methodology: Mice were exposed to isoflurane and blood was collected by orbital puncture, followed by harvesting intestine tissues from *Cebpd*-WT and KO mice (n=4-10/timepoint/genotype) at various timepoints (0h,1h,4h, 24h, 3.5d, 7d and 12d) after exposure to TBI (8.5 Gy). The gene expression for some pro-inflammatory cytokines, toll-like receptor genes and anti-inflammatory markers at early timepoints (0-24h) were measured by quantitative real-time PCR and normalized to *Gapdh* as an endogenous reference. The data are presented as fold change normalized to unirradiated *Cebpd*-WT group. Plasma samples were collected from the blood by centrifugation at 2000 rpm for 10mins and the supernatants were stored at -80°C. The plasma levels of cytokines and chemokines were measured by multiplex ELISA assays by Quansys Biosciences.

Results: 1) We confirmed that the *Cebpd*-KO mice expressed elevated mRNA levels of pro-inflammatory cytokines such as *Il-6*, *Tnf- α* and chemokines such as *Mcp-1*, *Cxcl1* and *Mif-1 α* (**Fig. 1**). 2) We further validated the gene expression data on the pro-inflammatory cytokine and chemokine expression by ELISA in systemic circulation by analyzing the plasma levels (**Fig. 2**). These findings correlated with the increased expression of mRNA levels of pro-inflammatory cytokines and chemokines in the intestine tissues of *Cebpd*-KO mice post-irradiation as described in **Fig. 1**.

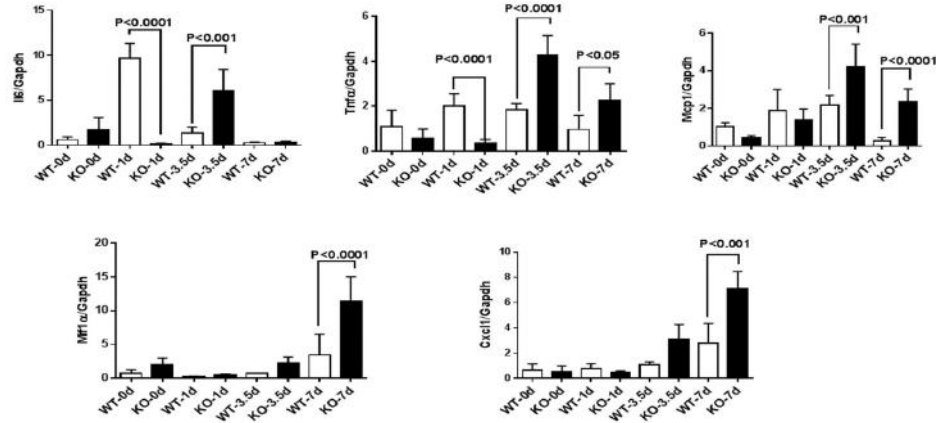


Fig. 1. *Cebpd*-deficient mice display increased pro-inflammatory cytokines and chemokine expression in intestine tissues after exposure to IR. WT and KO animals were sacrificed at days 0, 1, 3.5 and 7 post-TBI exposure of 8.5 Gy. The mRNA expression of (A) (Il-6, (B) Tnf- α , (C) Mcp-1, (D) Mif-1 α , (E) Cxcl1 were analyzed. The data are presented as average+ S.E.M. of n=4-10 mice /genotype/treatment group.

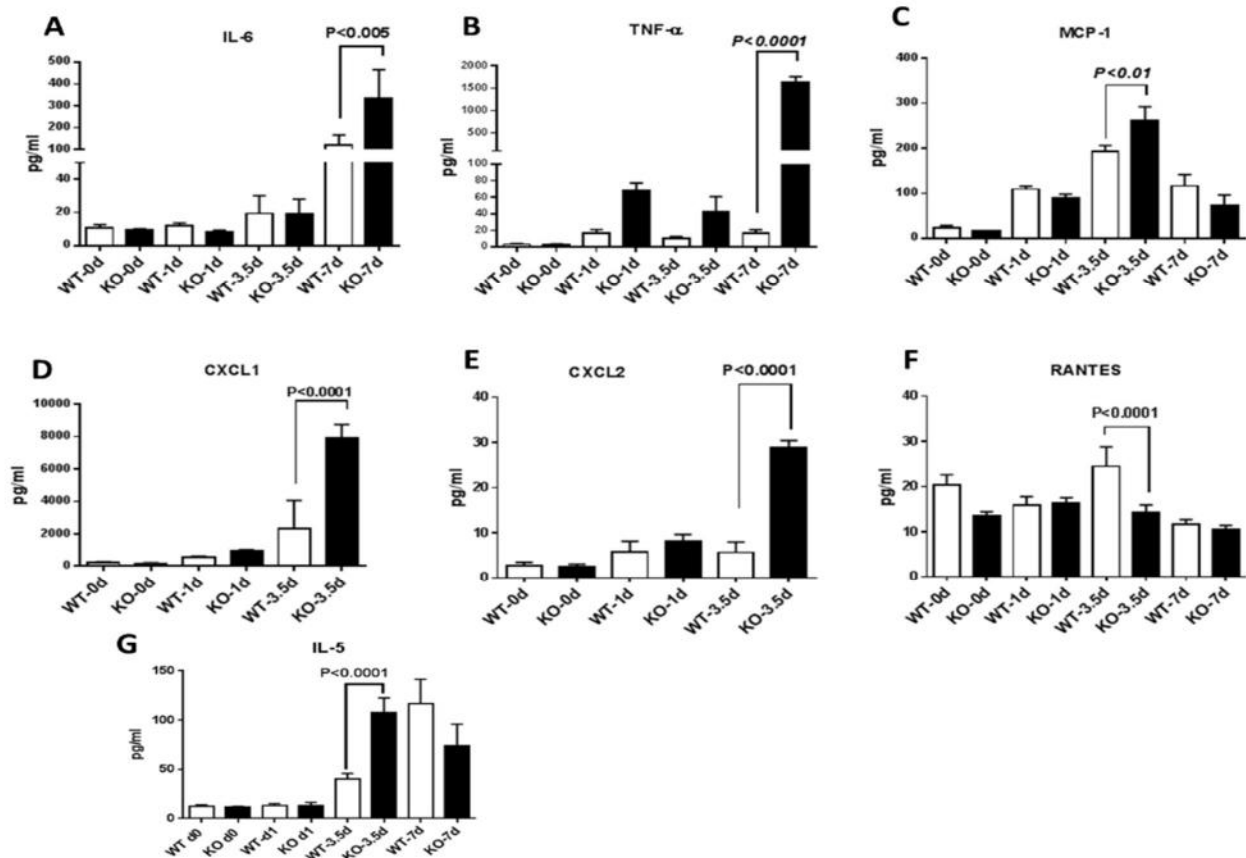


Fig. 2. *Cebpd*-deficient mice showed an increase in expression of pro-inflammatory cytokines and chemokines in the plasma after exposure to IR. *Cebpd*-WT and *Cebpd*-KO animals were sacrificed at 0, 1, 3.5 and 7 days post TBI dose of 8.5 Gy. Plasma levels of cytokines were measured in the plasma samples of *Cebpd*-KO and WT mice at various timepoints post-irradiation using either Single-plex or multiplex assay. The data represent the average+ S.E.M. of n=8-9 mice per genotype per timepoint.

3) Irradiated *Cebpd*-KO mice showed elevated expression of toll-like receptor 2 (*Tlr2*) and toll-like receptor 4 (*Tlr4*) genes, while the expression of *Tollip* expression was not significantly different at various timepoints post-irradiation between *Cebpd*-WT and KO mice.

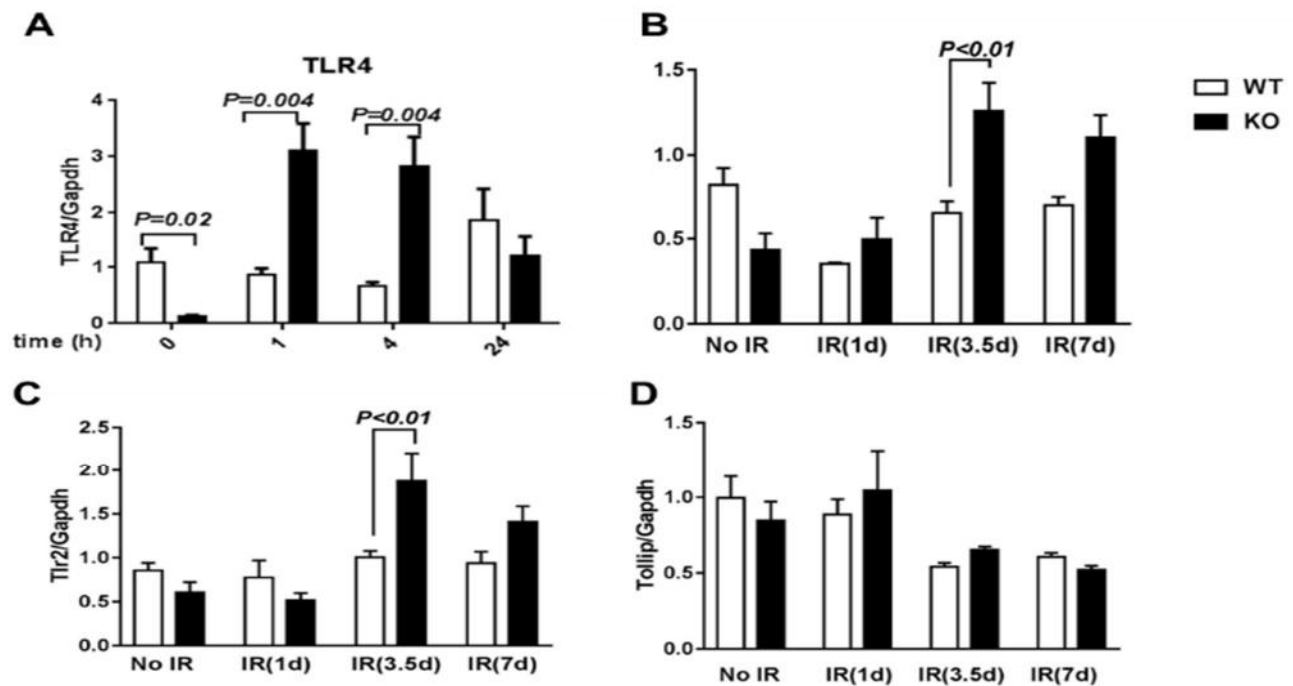


Fig. 3. *Cebpd*-deficient mice display elevated expression of *Tlr2* and *Tlr4* at early as well as later timepoints post-TBI exposure to 8.5 Gy. WT and KO animals were sacrificed at days 0, 1, 3.5 and 7 post-TBI exposure of 8.5 Gy. The mRNA expression of (A and B) *Tlr4*, (C) *Tlr2* and (D) *Tollip* were analyzed. The data are presented as average+ S.E.M. of n=4-10 mice /genotype/treatment group.

4) In order to determine the source of the pro-inflammatory cytokines, we examined the recruitment of neutrophils to the intestine at various timepoints post-irradiation using antibody specific to the neutrophil-specific marker myeloperoxidase (MPO). We also examined the mRNA expression of the macrophage-specific gene *Trem-2*, a gene which has been positively correlated with sepsis. We examined *Trem-2* expression in unirradiated and irradiated *Cebpd*-WT and KO mice.

Methodology: *Cebpd*-KO and WT mice (n=8-9) were exposed to 8.5 Gy and intestine tissues were harvested at various timepoints such as 0, day1, day 3.5 and day7 post-TBI. We examined the neutrophil infiltration in the irradiated intestine tissues of *Cebpd*-KO and WT by antibody specific to myeloperoxidase which is primarily expressed by neutrophils. The data presented here is the average of MPO positive cells enumerated from 10 fields observed under 20x magnification for each mouse per timepoint + standard error mean (SEM).

Results: *Cebpd*-KO mice showed a slight increase at day 1 and day 3.5 post-IR, but decline in neutrophils by day 7 post-irradiation, whereas WT mice showed significant down regulation by day 3.5 post-irradiation and slight recovery to baseline by day 7 post-irradiation. Interestingly, the macrophage-specific gene *Trem2* was significantly elevated in the intestine tissues at days 3.5 and 7 post-irradiation.

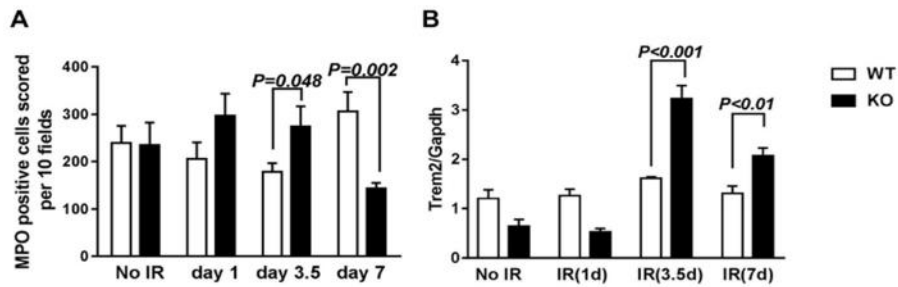


Fig. 4. *Cebpd*-deficient mice display (A) a rapid increase in the recruitment of neutrophils in the intestine at early timepoints and sharp decline at day 7 post-irradiation, (B) while the macrophage-specific gene *Trem-2* is elevated by day 3.5 and 7 post-TBI exposure to 8.5 Gy. The data are presented as an average + SEM, n=8-9 mice/genotype/timepoint.

5) Examined for markers of nitrosative and oxidative stress in intestine tissue at various timepoints post-irradiation.

Methodology: *Cebpd*-KO and WT mice (n=8-9) were exposed to 8.5 Gy and intestine tissues were harvested at various timepoints such as 0, day1, day 3.5 and day7 post-TBI. The intestine tissues were harvested from *Cebpd*-WT and KO mice and GSH, GSSG, GSNO and 3-nitrotyrosine levels were measured by HPLC-EC and normalized to protein content measured by Bradford assay.

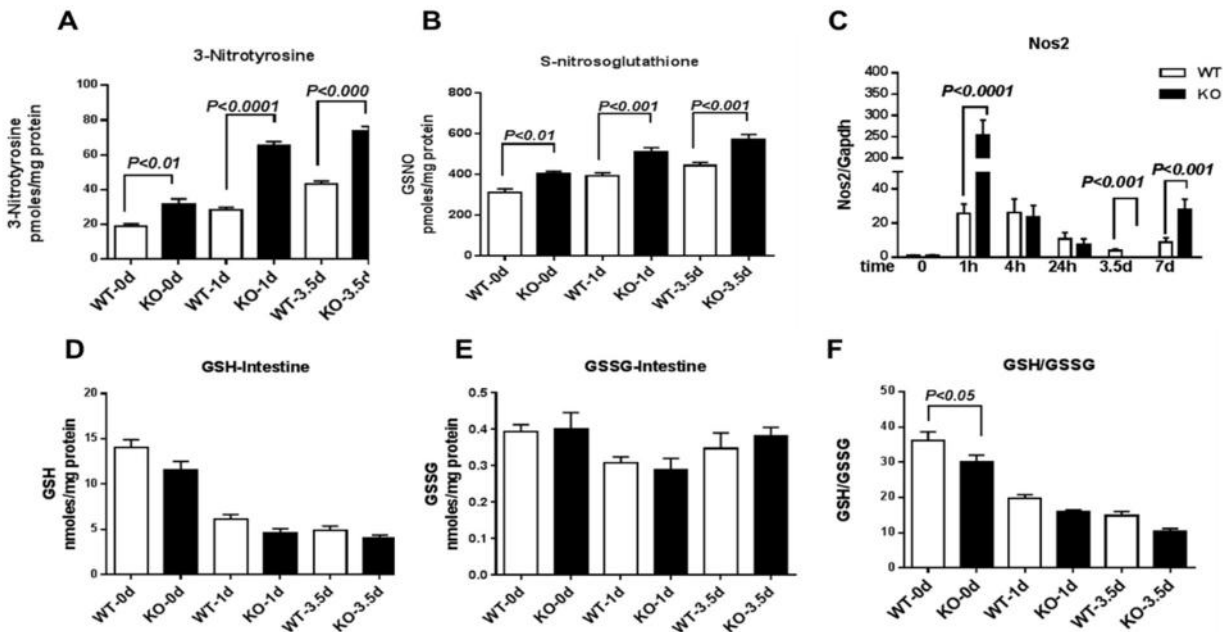


Fig. 5. *Cebpd*-deficient mice show basal oxidative and nitrosative stress, which is further exacerbated by exposure to TBI. *Cebpd*-KO and WT mice were sacrificed at days 0, 1, 3.5 and 7 post 8.5 Gy TBI. The intestinal tissue was analyzed for (A) 3-nitrotyrosine; (B) S-nitrosoglutathione; (C) Nos2 mRNA levels; (D) GSH, (E) GSSG; (F) GSH/GSSG using HPLC method. The values were expressed as GSH nmoles/mg protein, GSSG nmoles/mg protein and GSH/GSSG. The data are presented as average+ S.E.M. of n=8-9 mice per genotype per treatment group.

Results: We found that the intestine tissues from unirradiated *Cebpd*-KO mice showed a significantly reduced levels of GSH/GSSG suggestive of oxidative stress (Fig. 5). The elevated levels of 3-nitrotyrosine and S-

nitrosoglutathione which is indicative of nitrosative stress and correlated robust induction of Nos2 mRNA levels at early timepoints post-TBI (Fig. 5).

These data point to elevated oxidative and nitrosative stress in the intestine tissue of irradiated *Cebpd*-KO mice which may have implications for the alterations in tight junction proteins and increased intestinal permeability.

Aim 1.2 a. Determine whether IR-induced increased intestinal permeability in the *Cebpd*-KO mice.

We further examined whether the increased expression of inflammatory cytokines and chemokines as well as oxidative/nitrosative stress in the intestines of *Cebpd*-KO mice had a functional effect on the intestinal barrier function and whether it led to a disruption of the intestinal barrier function.

Methodology: Mice were exposed to 8.5 Gy TBI and on day 4 post-TBI, a midline laparotomy was performed, and the renal artery and vein were ligated bilaterally. A 10 cm small intestinal segment, located 5 cm distal to the ligament of Treitz was isolated and tied off. One hundred microliters of 4-kDa fluorescein isothiocyanate-conjugated dextran (FITC-dextran 25mg/ml in phosphate-buffered saline) was injected into the isolated intestine using a 30 Gauge needle followed by closure of the abdominal incision. After 90 min, blood was collected from the retro-orbital sinus and plasma separated by centrifuging at 4°C, 8000 rpm for 10 min. A group of unirradiated WT and KO mice were included as controls in this study. During the duration of the procedure, mice were under isoflurane anesthesia and the body temperatures were maintained by keeping them on heating pads warmed to 37°C. The mice were euthanized by cervical dislocation after collection of blood. The FITC-dextran concentrations in plasma were estimated based on a standard curve of pure FITC dextran solution.

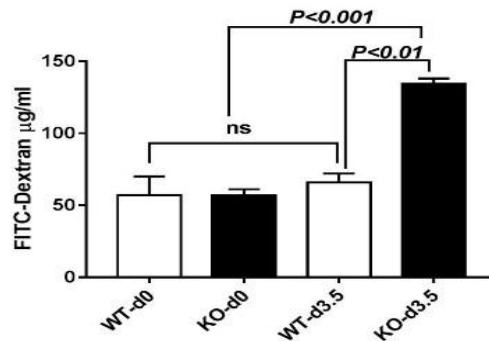


Fig. 6. *Cebpd*^{-/-} mice show increased intestinal barrier disruption after exposure to IR. Blood was collected at the indicated timepoints from *Cebpd*-WT and *Cebpd*-KO mice after exposure to IR. Intestinal permeability was measured by analyzing plasma samples for the presence of FITC-Dextran. Data are presented as average + S.E.M. of n = 7–9 samples per treatment group.

Results: *Cebpd*-KO mice showed a significant increase in intestinal permeability at day 4 post-irradiation compared to irradiated *Cebpd*-WT mice, as measured by the increased levels of FITC-Dextran in the plasma 90 minutes after injection into the ligated intestine.

Aim 1.2 b. Determine the expression of tight junction proteins in WT and KO mice before and after irradiation.

Next we determined the alterations in the expression of tight junction proteins, as they are known to be altered by elevated inflammatory cytokines as well as by oxidative stress.

Methodology: Mice were exposed to isoflurane intestine tissues from *Cebpd*-WT and KO mice (n=4-10/ timepoint/ genotype) were harvested at various timepoints (0h, 1h, 4h, 24h, 3.5d, 7d and 12d) after exposure to TBI (8.5 Gy). The gene expression for the tight junction proteins were measured by real-time PCR and

normalized to *Gapdh* as an endogenous reference. The data are presented as fold change normalized to unirradiated *Cebpd*-WT group.

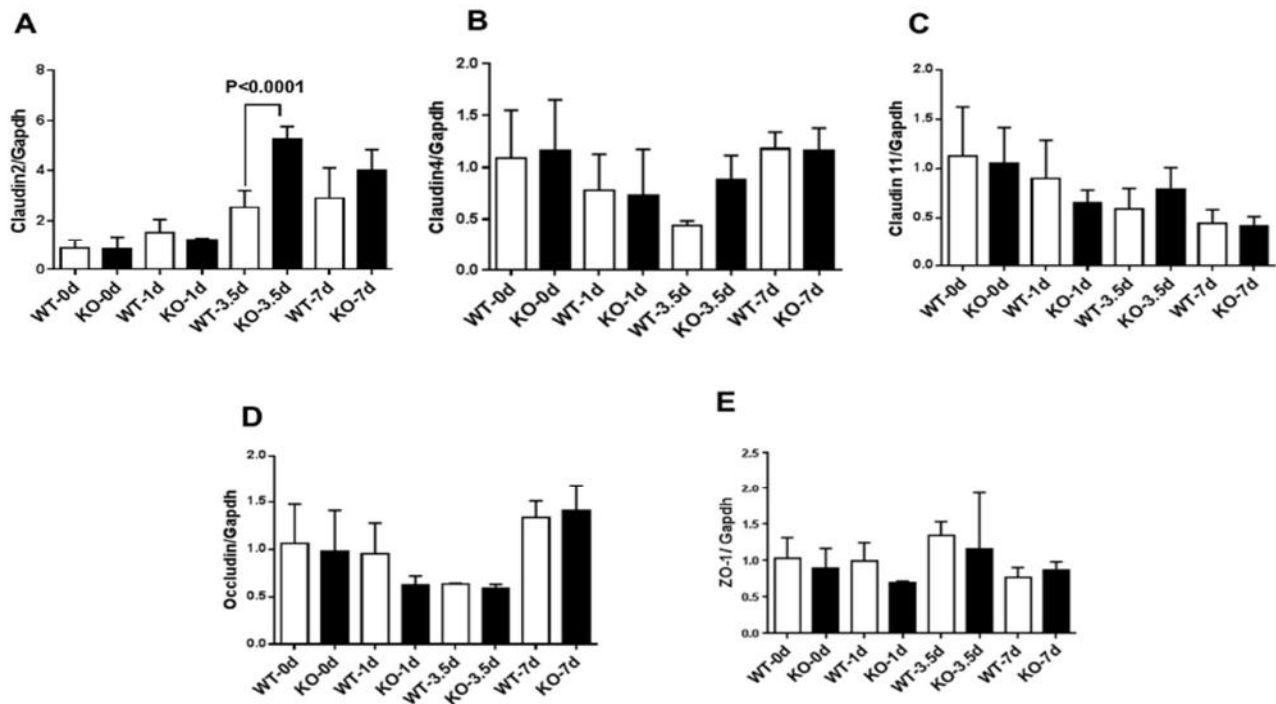


Fig. 7. Irradiated *Cebpd*-KO mice showed significant upregulation of Claudin-2, a marker of intestinal barrier disruption. The expression of various tight junction proteins such as Claudin-2, Claudin-4, Claudin-11, Occludin and ZO-1 were measured by real-time q-PCR and normalized to the endogenous

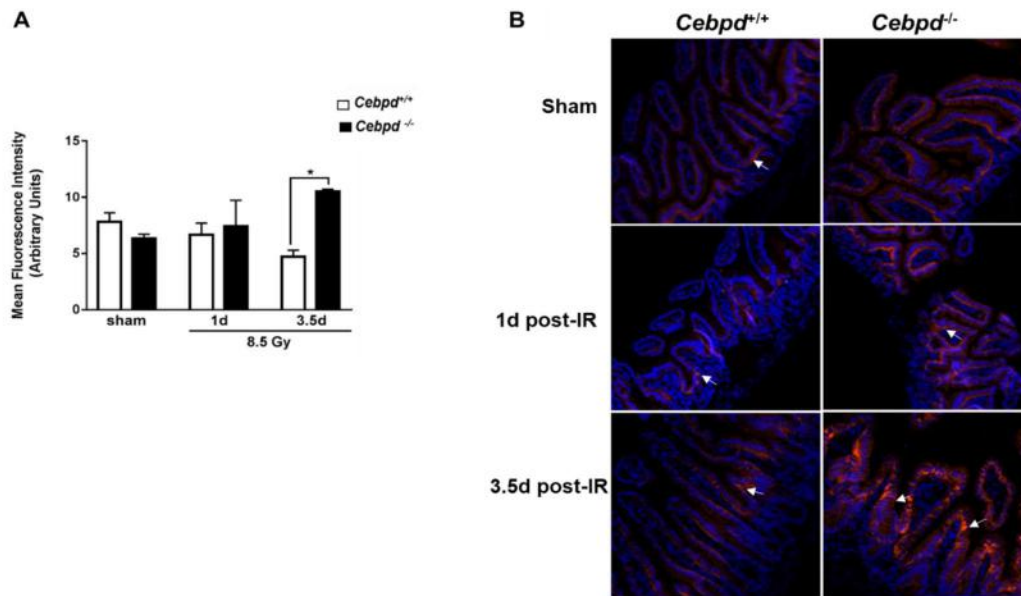


Fig. 8. Claudin-2 protein levels are elevated in intestines of irradiated *Cebpd*-KO mice. A) Quantitation of Claudin-2 expression shown in stained sections (B). Data are presented from intestine sections from n=3 mice per timepoint /genotype.

Results: Among all the Claudins and other tight junction proteins such as ZO-1 and Occludin that were tested, we found that only Claudin-2 was significantly elevated at day 3.5 post-irradiation in KO mice (**Fig. 7**). Claudin-2 is a protein involved in transcellular permeability and is known to be elevated by pro-inflammatory

cytokines such as IL-6 and TNF- α . Particularly in several intestinal inflammatory disorders, Claudin-2 upregulation is known to promote intestinal barrier disruption. Further we also confirmed the expression of Claudin-2 by immunofluorescence and found increased expression with altered localization (**Fig. 8**).

Aim 1.2 c Determine whether lack of *Cebpd* increased bacterial translocation post-TBI.

Next we assessed whether there was a functional consequence to the elevated expression of Claudin-2 in the intestinal function by measuring and measuring plasma levels of lipopolysaccharide binding protein (LBP) and (3) measuring bacterial translocation to the liver.

Methodology: Bacterial translocation was measured by amplification of the 16S rRNA specific product in the liver tissues by standard curve real-time PCR at various timepoints post-irradiation such 0, 3.5 and 7 day post-irradiation in WT and KO (n=8-9) liver tissues. The standard curve was generated using *E.coli* genomic DNA and absolute amounts of 16rRNA amplicon were measured from 20ng template DNA from each sample per treatment group and normalized to respective wet weight of liver tissue. The data are presented as ng per gm liver tissue and expressed as average + standard error mean (SEM). We also measured the plasma levels of lipopolysaccharide-binding protein, which is a marker of presence of bacteria in the blood using ELISA.

Results: We further confirmed 2-fold increase in the levels of the 16S rRNA amplicon in the irradiated KO mice compared to WT mice at day 3.5 post-irradiation, indicative of bacterial translocation to the liver (**Fig. 9**). In addition, using ELISA we showed that there was a robust increase in plasma LBP levels indicative of the presence of bacteremia and presence of endotoxin in systemic circulation.

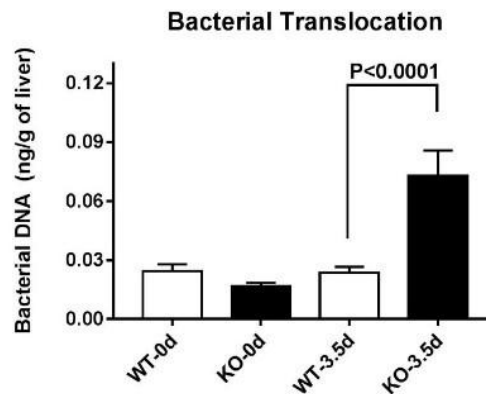


Fig. 9. Irradiated *Cebpd*-KO mice display increased bacterial translocation to the liver compared to irradiated *Cebpd* WT-mice.

Key Accomplishments: All the studies outlined in this aim were accomplished. The findings from the studies in Aim 1 were recently accepted for publication in the Scientific Reports Journal (1).

Additional data not directly related to the project:

To determine the gut microflora changes in response to TBI between *Cebpd*-WT and *Cebpd*-KO mice, feces were collected from harvested intestines and the fecal microbiome was analyzed by 16 S rRNA Next gen sequencing was carried out by Mr. DNA technologies, Dallas, TX..

Results: 1) Irradiated WT mice showed increases in family % of *Eubacteriaceae*, *Clostridiales family iii incertae sedis*, *Bacillales*, *Coriobacteriaceae*, and *Bifidobacteriaceae* (**Fig. 10**), while irradiated KO mice showed higher expression of *Staphylococcus*, *Oscillospiriae*, *Clostridiales*, *Porphyromonadaceae*, *Enterococcaceae*, *Sutterellaceae* and *Gloebacterales* in fecal samples (**Fig.11**).

Analysis of family % at d3.5

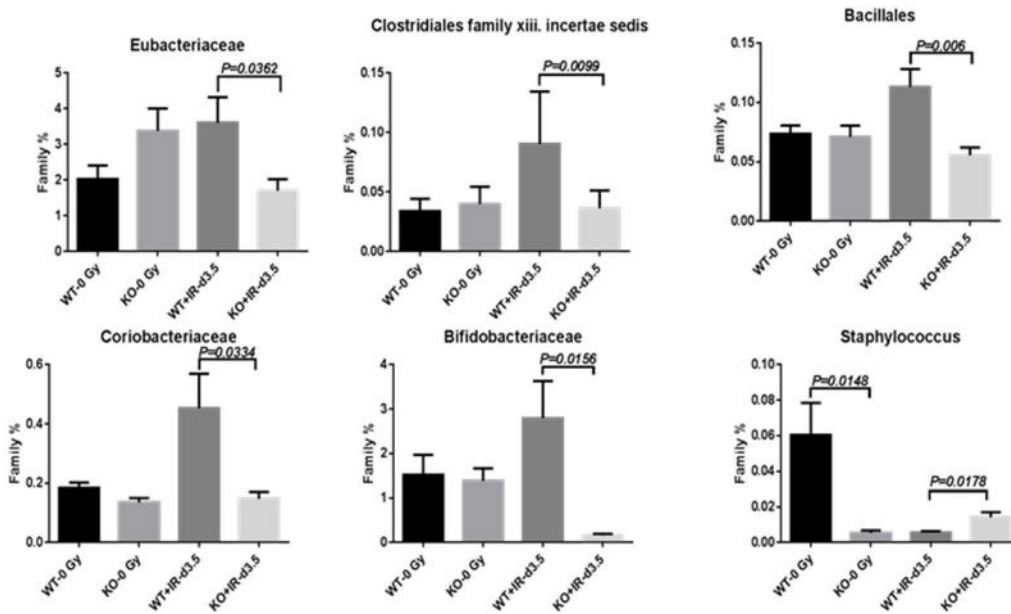


Fig. 10. Families that showed decrease in families of bacteria in irradiated *Cebpd*-KO mice compared to *Cebpd*-WT mice. Data were obtained n=8 mice per timepoint/genotype.

Analysis of family % which are upregulated in KO+ IR samples compared with WT+IR samples at d 1 and 3.5

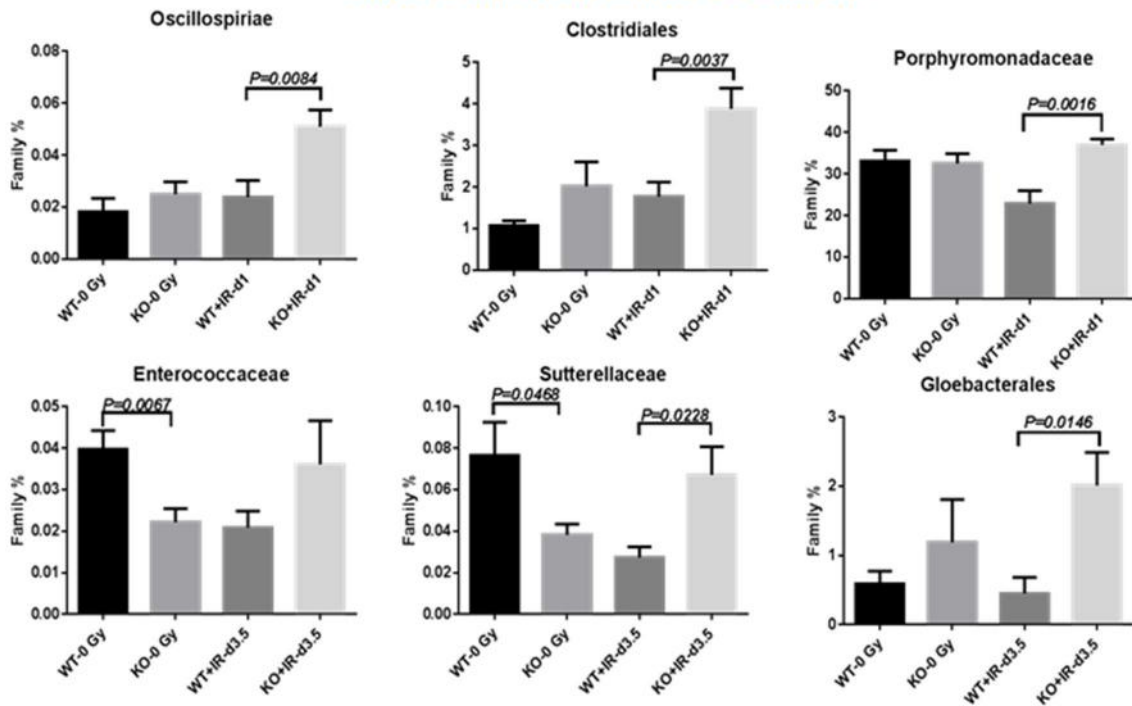


Fig. 11. Families that were upregulated in irradiated *Cebpd*-KO mice post-irradiation as well as those that were downregulated in unirradiated *Cebpd*-KO mice.

2) Analysis at the level of genus, WT mice showed increased expression of *Anaerobacterium*, *Bifidobacterium*, while KO mice showed decreased expression of *Parabacteroides* and *Calanoraerobacter* (Fig. 12).

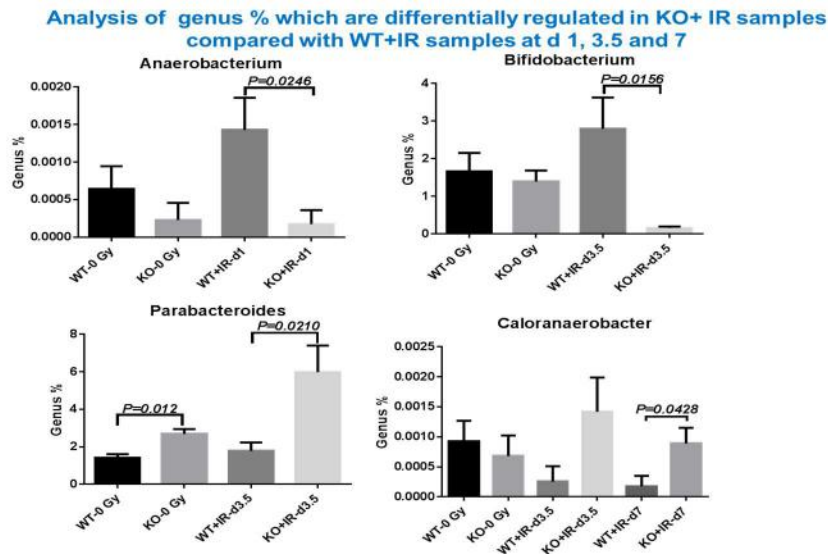


Fig.12. Genus of bacteria upregulated at absal as well as post-irradiation in feces of *Cebpd*-KO compared to that of *Cebpd*-WT mice.

Key Accomplishments: These studies are currently at the stage of manuscript preparation to be submitted to the Journal Microbiome.

1.3b: Determine the role of gamma-tocotrienol (GT3) in alleviating the TLR4-mediated inflammation and intestinal injury.

1.3b.1. Compare intestinal crypt colony survival in *Cebpd*-KO and WT mice at day 3.5 post-irradiation.

Methodology: *Cebpd*- WT and KO mice (n=8) were injected with GT3 (200mg/kg) or with respective vehicle controls 24h prior to exposure to 8.5 Gy TBI as described (3). This is the dose of TBI where we have observed 100% lethality and as well as a significant decrease in crypt colony survival in KO mice (4). The dose of GT3 is chosen based on previous studies which showed maximal protection against TBI (3). Mice were anesthetized by isoflurane inhalation and sacrificed at 3.5 days post-TBI dose of 8.5 Gy.

Results: We re-confirmed the protective effects of GT3 on intestinal crypt colony survival in *Cebpd*-WT mice, similar to studies reported by Ghosh *et al.*, 2009. In contrast, the intestinal crypt colony survival did not show any significant protection mediated by GT3 in irradiated *Cebpd*-KO mice (**Fig. 13**). These results suggest that GT3-mediated radioprotection occurs in a *Cebpd*-dependent manner.

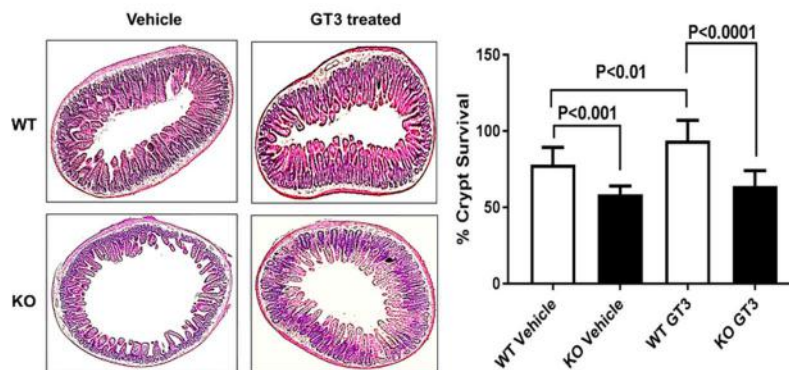


Fig. 13. GT3-mediated protection of intestinal crypt colony survival is occurs in a *Cebpd*-dependent manner.

1.3b.2 Compare the expression of G-CSF in *Cebpd*-WT and KO mice at various timepoints post-irradiation.

Methodology: *Cebpd*-WT and KO mice (n=4-8) were exposed to 8.5 Gy TBI as described (3,5). Mice were anesthetized by isoflurane inhalation and blood was collected by orbital puncture prior at various timepoints 0, 1, 3.5 and 7days post-TBI dose of 8.5 Gy. G-CSF levels were measured by ELISA using appropriate standards and absorbance was measured at 405nm by a spectrophotometer.

Results: We examined the expression of G-CSF, as it is known to be induced by IR and is essential for the recovery of the hematopoietic compartment after exposure to IR after GT3 treatment (6). The G-CSF promoter has C/EBP binding sites, so we examined whether G-CSF induction is dependent on the expression of *Cebpd*. Interestingly we found that the IR-inducible expression of G-CSF is not dependent on *Cebpd*, particularly at day 7 post-irradiation *Cebpd*-KO mice show an increased expression of G-CSF compared to that of *Cebpd*-WT mice (Fig. 14).

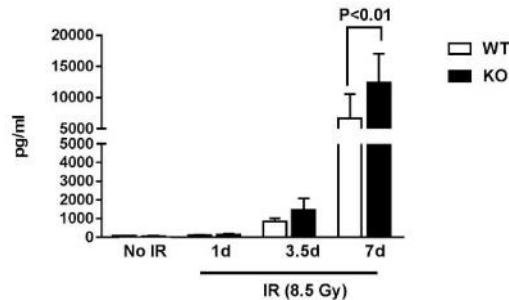


Fig. 14. G-CSF is significantly upregulated in *Cebpd*-KO mice at day 7 post-irradiation. Plasma levels of G-CSF in *Cebpd*^{+/+} and *Cebpd*^{-/-} mice at the indicated timepoints post-8.5 Gy (n = 5/timepoint/genotype).

1.3b.3. Determine whether GT3-mediate upregulation of G-CSF in a *Cebpd*-dependent manner at day 3.5 post-irradiation.

Methodology: GT3 is known to stimulate the IR-induced expression of G-CSF *Cebpd*-WT and KO mice (n=6-8) were injected with GT3 (200mg/kg) or with respective vehicle controls 24h prior to exposure to 8.5 Gy TBI. Mice were anesthetized by isoflurane inhalation and blood was collected by orbital puncture at 3.5 days post-TBI dose of 8.5 Gy. Plasma was isolated by centrifuging the blood samples at 2000rpm for 10min at 4°C. G-CSF levels were measured by ELISA using appropriate standards as described above.

Results: We found that G-CSF expression was induced to a similar extent in GT3-treated WT and KO mice. This suggests that GT3-mediated induction of G-CSF is not dependent on *Cebpd* and also did not show any protective effects in the intestinal crypt colony survival (Fig. 15).

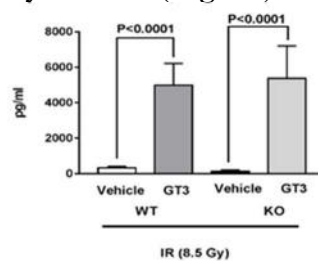


Fig. 15. GT3-mediated induction of G-CSF after TBI does not occur in a *Cebpd*-dependent manner. Plasma levels of G-CSF at the indicated timepoints post-8.5 Gy in vehicle- or GT3-treated *Cebpd*^{+/+} and *Cebpd*^{-/-} mice at day 3.5 post-8.5 Gy. The data are presented as mean \pm S.E.M. of n=8 mice per treatment per genotype.

1.3b.4. Compare the expression of *Cebpd* in response to GT3 and also measure the expression of pro-inflammatory cytokines and chemokines, and tight junction proteins in *Cebpd*-KO and WT mice at day 3.5 post-irradiation.

Methodology: *Cebpd*-WT and KO mice (n=8) were injected with GT3 (200mg/kg) or with respective vehicle controls 24h prior to exposure to 8.5 Gy TBI. Mice were anesthetized by isoflurane inhalation and sacrificed at 3.5 days post-TBI dose of 8.5 Gy and intestine tissue was harvested. The expression of pro-inflammatory cytokines *Il-6*, *Tnf- α* , and chemokines *Cxcl1*, *Mcp-1*, tight junction proteins, *Cebpd* and *Gapdh* were measured by real-time PCR.

Results:

1) We have shown that *Tlr4* expression is upregulated at early timepoints (1h, 4h) after TBI in *Cebpd*-KO mice. Here we found that while GT3 treatment led to decreased *Tlr4* expression in *Cebpd*-WT mice, KO mice showed increased *Tlr4* and *Tlr2* expression at day 3.5 post-irradiation. In contrast *Cebpd*-WT mice show a downregulation of *Tlr4* while change of *Tlr2* expression in GT3-treated groups (**Fig. 16**).

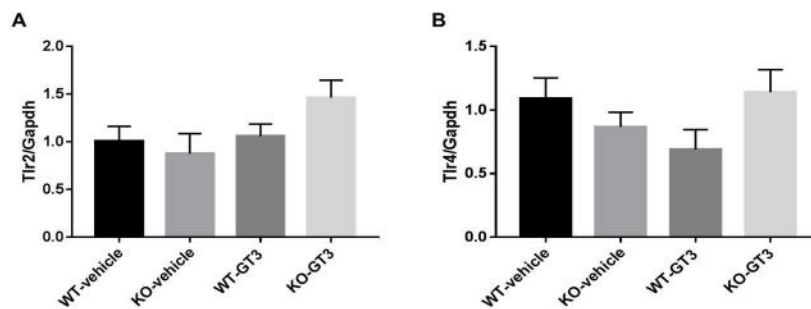


Fig. 16. GT3 pre-treatment prior to irradiation showed increased *Tlr2* and *Tlr4* expression in *Cebpd*-KO mice, but not in *Cebpd*-WT mice at 3.5 days after TBI (8.5 Gy).

2) In the last report, we showed that GT3 treatment did not protect crypt colony survival at day 3.5 post-irradiation in *Cebpd*-KO mice compared to *Cebpd*-WT mice. Here we show that GT3 treatment did not downregulate IR-induced *Il-6* (**Fig.17 B**) and *Tgf-beta* (**Fig. 17 C**) expression in *Cebpd*-KO mice at day 3.5 post-irradiation. GT3-treated *Cebpd*-KO mice also showed increased expression of *Cxcl1* (**Fig.17 D**) and *Mcp-1* (**Fig. 17 E**), while the expression of *Tnf- α* was not significantly changed between the vehicle and GT3-treated groups in both genotypes (**Fig.17 A**).

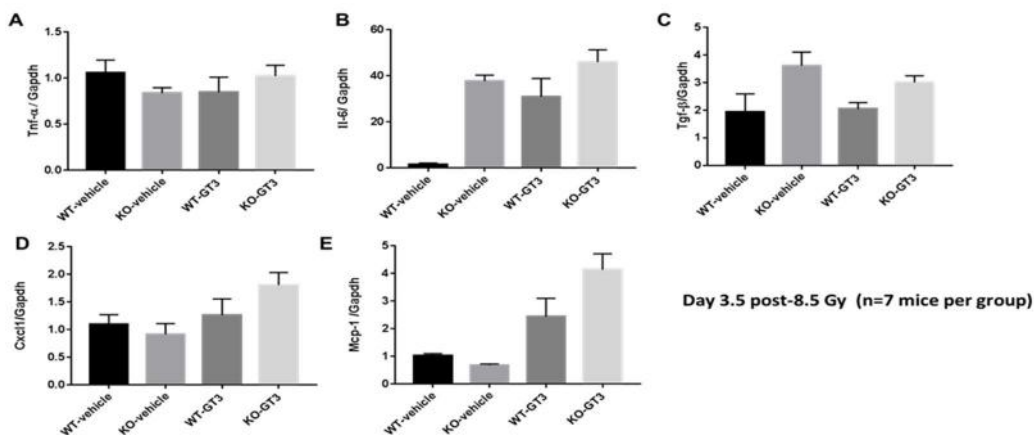


Fig. 17. GT3-treatment promoted increased expression of *Il-6*, *Cxcl1* & *Mcp-1* in *Cebpd*-KO mice at day 3.5 post-TBI.

3) At day 3.5 post-8.5 Gy, GT3-treated *Cebpd*-KO mice display increased expression of Claudin 2, a tight junction protein associated with transport of water and cations and its upregulation is correlated with intestinal barrier dysfunction (**Fig. 18 A**). While the expression of Claudin 4 was significantly downregulated in the GT3-treated groups, there was no significant change between the genotypes (**Fig. 18 B**). Occludin was downregulated in GT3-treated WT mice but not in KO mice at day 3.5 post-TBI (**Fig. 18 C**).

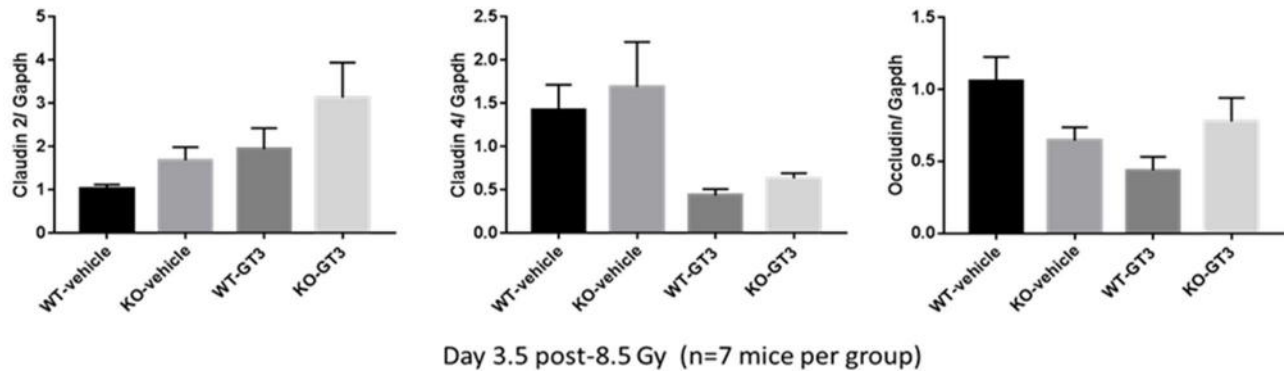


Fig. 18. GT3-treatment led to increased expression of *Claudin 2* in *Cebpd*-KO mice.

4) Since we did not observe a protective effect of GT3 on radiation-induced intestinal injury in *Cebpd*-KO mice. We investigated whether the expression of *Cebpd* was affected by GT3 treatment. While we observe increased 1.3-fold induction of *Cebpd* in vehicle treated group and found that GT3-treatment led to 2.3-fold increase in *Cebpd*-expression. Since we know that *Cebpd* is expressed at early timepoints post-irradiation, we plan to examine *Cebpd* expression at early timepoint post-irradiation in GT3-treated *Cebpd*-WT mice (**Fig. 19**).

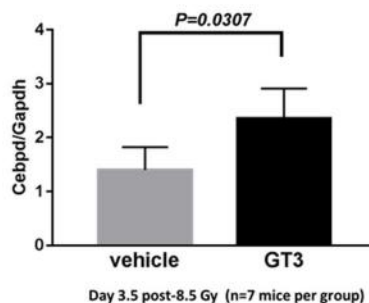


Fig. 19. GT3 stimulates the expression of *Cebpd* in intestine tissues.

1.3b.5 Determine whether GT3 treatment leads to downregulation of oxidative stress at day 3.5 post-irradiation in intestine tissue of *Cebpd*-KO and WT mice.

Methodology: Exposure to IR is known to induce increased oxidative stress and more recently we have shown that *Cebpd*-deficient mouse embryonic fibroblasts express increased IR-induced oxidative stress and mitochondrial dysfunction which is in part due to decreased GSH levels (7). Therefore we next examined whether GT3 treatment can alleviate the IR-induced oxidative and nitrosative stress in irradiated *Cebpd*-KO mice.

Results:

- 1) GT3 treatment exacerbated the expression of *Nos2* and *Hmox1* in *Cebpd*-KO mice but not *Cebpd*-WT mice. Increased *Nos2* expression is indicative of nitrosative stress (8), while increased *Hmox1* expression is a

response to increased oxidative stress (9). Thus our results reveal that GT3 treatment led to exacerbation of nitrosative and oxidative stress response in *Cebpd*-KO mice and did not exert any protective effects (Fig. 20).

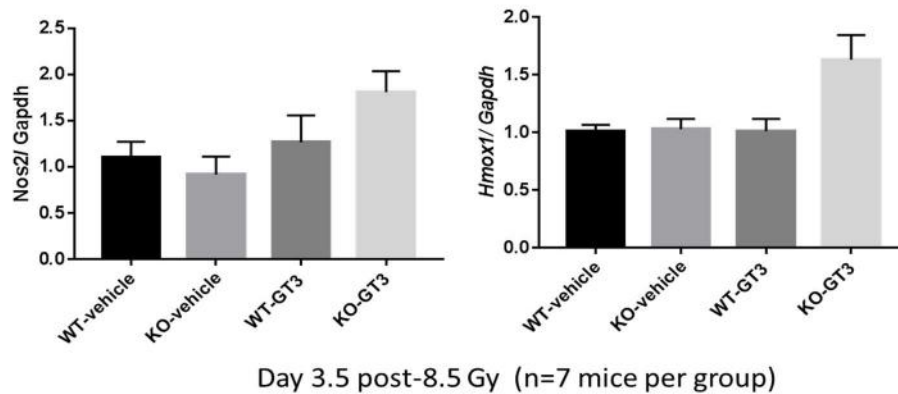


Fig. 20. GT3 pre-treatment increased expression of *Nos2* and *Hmox1* at day 3.5 post-irradiation in *Cebpd*-KO mice

2) In order to correlate the increased oxidative/nitrosative stress, we examined the levels of GSH, GSNO and 3-NT in the intestine tissues of GT3 and or vehicle-treated *Cebpd*-WT and KO mice at day 3.5 post-irradiation. While we did not observe any significant changes in GSH levels, *Cebpd*-KO mice showed increased levels of GSNO and 3 NT, however GT3 treatment did not decrease these levels. Thus the increased intestinal injury in GT3-treated mice could be due to high GSNO levels (Fig. 21).

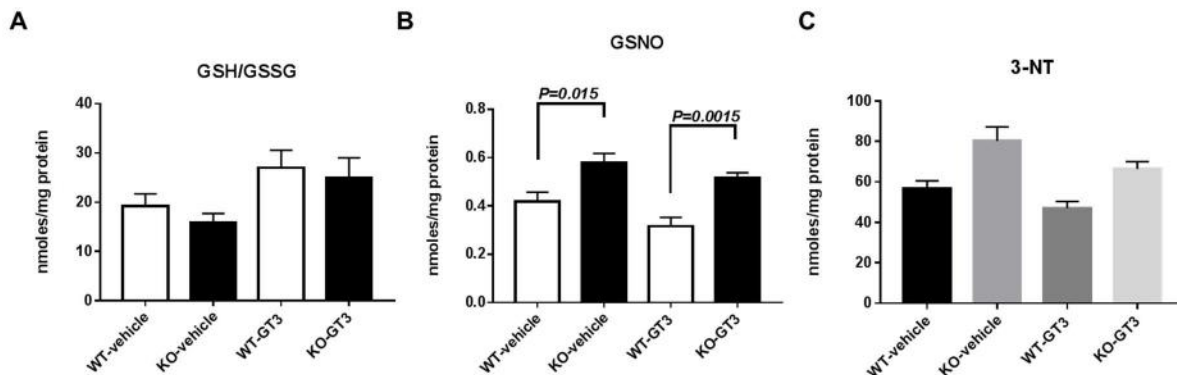


Fig. 21. GT3 treatment led to increased nitrosative and oxidative stress in *Cebpd*-KO mice.

1.3b.6. Determine whether GT3 protects *Cebpd*-KO mice from radiation-induced hematopoietic injury.

Methodology: *Cebpd*-WT and KO mice (n=5) were injected with GT3 (200mg/kg) or with respective vehicle controls 24h prior to exposure to 6 Gy TBI. This is a sublethal dose of TBI and WT mice are expected to recover from hematopoietic injury by day 14 post-irradiation (4). Mice were anesthetized by isoflurane inhalation and sacrificed at 2 weeks post-TBI dose of 6 Gy and the blood cell parameters were analyzed using Hemavet blood cell analyzer.

Results:

GT3 protects from radiation-induced lethality by protection from hematopoietic as well as intestinal injury, so we next examined whether GT3-treatment protects *Cebpd*-KO mice from radiation-induced hematopoietic injury. In the vehicle-treated group, *Cebpd*-KO mice showed significant decrease as reported previously (Pawar *et al.*, 2014, PLOS One). We found that while WBCs showed impaired recovery in *Cebpd*-KO mice, platelets and RBCs showed comparable recovery in the GT3-treated group (Fig. 22).

GT3-treatment led to a significant increase in the neutrophils in WT mice compared to *Cebpd*-KO mice (Fig. 23 A). While lymphocytes showed comparable recovery in both genotypes after GT3 treatment, monocytes clearly did not show any protective effects due to GT3 (Fig. 23 B).

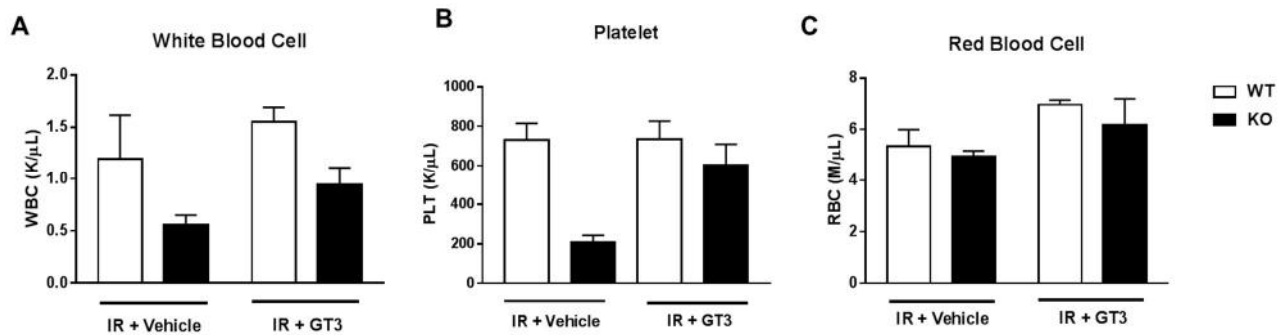


Fig. 22. Effect of GT3 pre-treatment 24h prior to sublethal-TBI. Blood cell parameters were analyzed at 2 weeks post-6 Gy in *Cebpd*-WT and KO mice, (A) WBCs, (B) platelets and (C) RBCs.

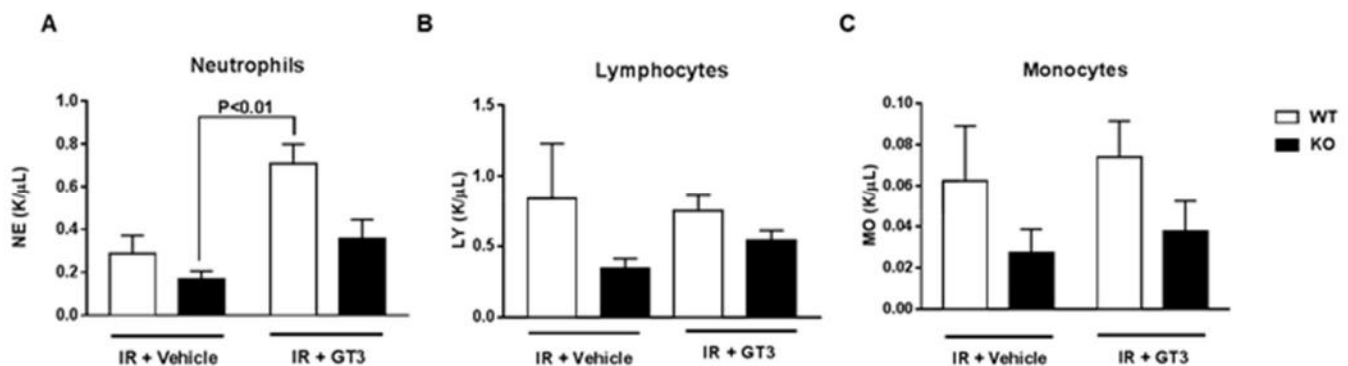


Fig. 23. Effect of GT3 pre-treatment 24h prior to sublethal-TBI. Blood cell parameters were analyzed at 2 weeks post-6 Gy in *Cebpd*-WT and KO mice, (A) neutrophils, (B) lymphocytes and (C) monocytes.

Key Accomplishments: All the studies outlined in this subaim were accomplished. These studies were published in the journal Antioxidants in 2018 (2).

1.3a: Determine the effect of TLR4 inhibitor in alleviating the TLR4-mediated inflammation and intestinal injury in WT and KO mice.

1.3a.1. Determine the expression of *Tlr4* at mRNA and protein levels in *Cebpd*-WT and KO mice at various timepoints post-TBI.

Methodology: WT and KO mice (n=4-6 per timepoint per group) were exposed to 8.5 Gy TBI and intestine tissues were harvested at 0, 4h and 3.5 days post-irradiation and processed for RNA and protein extracts

A) *Tlr4* expression was measured by real time PCR and normalized to *Gapdh* as an endogenous reference. The data are presented as fold change normalized to non-irradiated (0h) group analyzed by one-way ANOVA followed by Tukey's post-hoc analysis. **B)** Immunoblot of intestine (*jejunum*) tissue extracts were probed anti-TLR4 antibody showing increased expression of TLR4 protein levels. Densitometry of the images was done using NIH image.

Results: We confirmed that *Cebpd*-KO mice showed increased upregulation of TLR4 mRNA and protein levels at early timepoints post-irradiation (**Fig. 24 A**). Interestingly while TLR4 mRNA levels did not show any significant changes after irradiation at mRNA levels, but the protein levels were upregulated at 4h and 24h post-IR exposure. In contrast, the *Cebpd*-KO mice show increased mRNA levels at 1h and 4h post-irradiation which also correlated with increased expression of TLR4 protein levels at these timepoints. At 24h post-irradiation the TLR4 mRNA levels were not upregulated, but the protein levels of TLR4 were upregulated to a similar extent in both genotypes (**Fig. 24 B**).

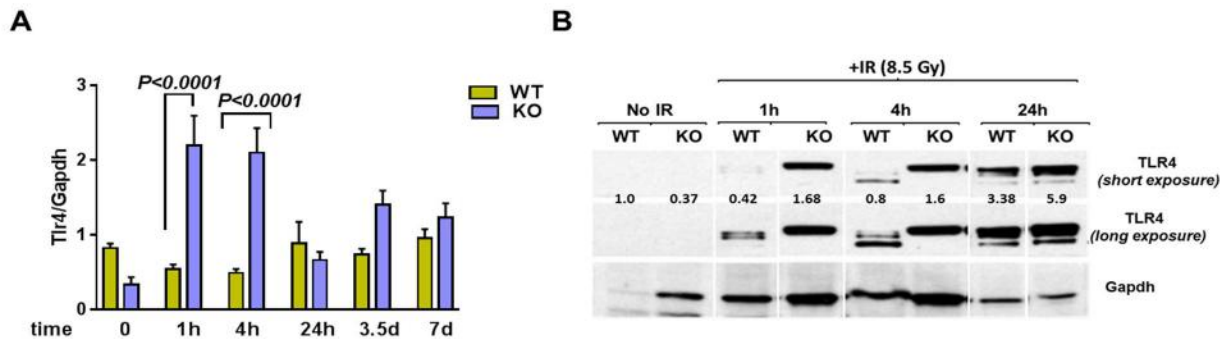


Fig. 24. *Cebpd*-KO mice show increased expression of TLR4 mRNA and protein in intestine tissues after exposure to IR. A) *Tlr4* mRNA levels; B) TLR4 protein levels.

1.3a.2. To develop an in vitro model of intestinal organoids and assess effects of IR on growth.

Methodology: Isolation and culture of intestinal crypts were done as described previously (10). Briefly, the small intestine of 4- to 6-week-old *Cebpd*-WT or *Cebpd*-KO mice was opened longitudinally and washed with PBS. The intestine was cut into 1–2 cm pieces, washed three times with cold PBS and incubated with 2 mM EDTA in PBS for 30 min at 4 °C on a rotating wheel. Residual villi were removed by gentle shaking, the villi containing supernatant was removed and replaced with cold PBS. This procedure was repeated until no villi could be observed. Crypts were then detached from the basal membrane by Cell dissociation reagent (StemCell technologies). The crypts enriched in the supernatant were passed through a 70- μ m cell strainer (Falcon, USA), centrifuged at 100 \times g (3 min, 4 °C) and resuspended in 10 ml PBS with 2% BSA for counting using microscopy. Pelleted crypts were resuspended in Matrigel (Corning, USA) at a desired crypt density. Two hundred to five hundred crypts in 7 μ l Matrigel were seeded per well on a pre-warmed 24-well flat-bottom plate and incubated for 15 min at 37 °C. Then, 50 μ l of complete crypt culture medium was added (DMEM/F12 containing 0.1% BSA, 2 mM L-glutamine, 10 mM HEPES, 100 U/ml penicillin, 100 μ g/ml streptomycin, 1 mM N-acetyl cysteine, 1 \times B27 supplement, 1 \times N2 supplement, 50 ng/ml mEGF, 100 ng/ml mNoggin, 500 ng/ml human R-spondin-1 (StemCell Technologies, Canada). Organoids were cultured at 37 °C in a 5% CO₂ atmosphere for at least 5 days.

Results: Intestinal organoids were successfully isolated as per the manufacturer's instructions (Stem Cell technologies). We found that *Cebpd*-KO intestinal organoids show decreased growth at day 5 post-irradiation compared to *Cebpd*-WT organoids, showing the inability of the intestinal stem cells to recover from IR-induced damage (**Fig. 25**).

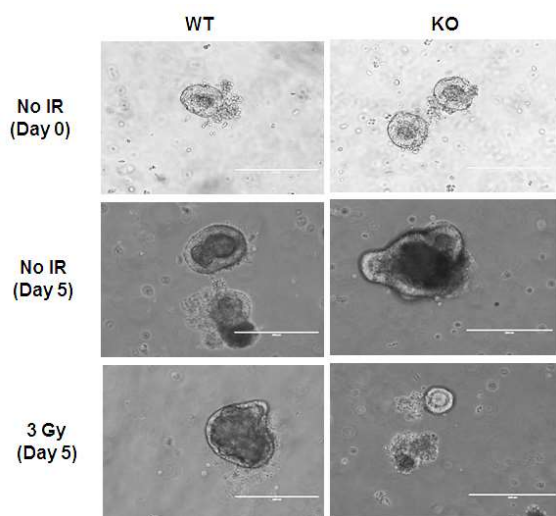


Fig. 25. Decreased growth of intestinal organoids from *Cebpd*-KO mice after irradiation.
Representative image of intestinal organoids at 10X magnification.

1.3a.3. Determine the effects of the TLR4 inhibitor in an *in vitro*-intestinal organoid assay.

Before initiating the studies with the TLR4 inhibitor *in vivo*, we utilized the intestinal organoids as a model system to screen the effects of the TLR4 inhibitor. Due to the delay in getting the MTA approval from Eisai Inc. for Eritoran tetrasodium, we utilized another TLR4 inhibitor C-34 (2-acetoamidopyranoside) available from Sigma. The compound C-34 docks to the hydrophobic internal pocket of the TLR4-co-receptor MD-2 and has been shown to inhibit TLR4 in enterocytes and macrophages and reduce systemic inflammation in mouse models of endotoxemia and necrotizing enterocolitis (11).

Methodology:

Isolation and culture of intestinal crypts were done as described previously (10). Intestinal organoids were cultured at 37 °C in a 5% CO₂ atmosphere for at least 5 days. Intestinal organoids were treated for 30 minutes with the TLR inhibitor C-34(10μM), and then treated with or without irradiation at 3 Gy and growth was analyzed at day 5 post-irradiation. Light microscopy images were captured at 4x magnification and compared. Quantitation and analysis of organoid growth was done by NIH image J analysis (12).100 organoids were counted for each group.

Results: We have shown that intestinal organoids obtained from *Cebpd*-KO mice display increased sensitivity to IR compared to the intestinal organoids from *Cebpd*-WT mice when exposed to 3 Gy. Here we report that pre-treatment with the TLR4 inhibitor antagonist C-34 for 30 mins did not have any significant effects on the growth of unirradiated intestinal organoids obtained from both *Cebpd*-WT and KO mice. However, 30 minutes pre-treatment with the TLR4 inhibitor prior to irradiation showed robust rescue of growth of the intestinal organoids of both *Cebpd*-KO and WT genotypes (**Fig. 26**).

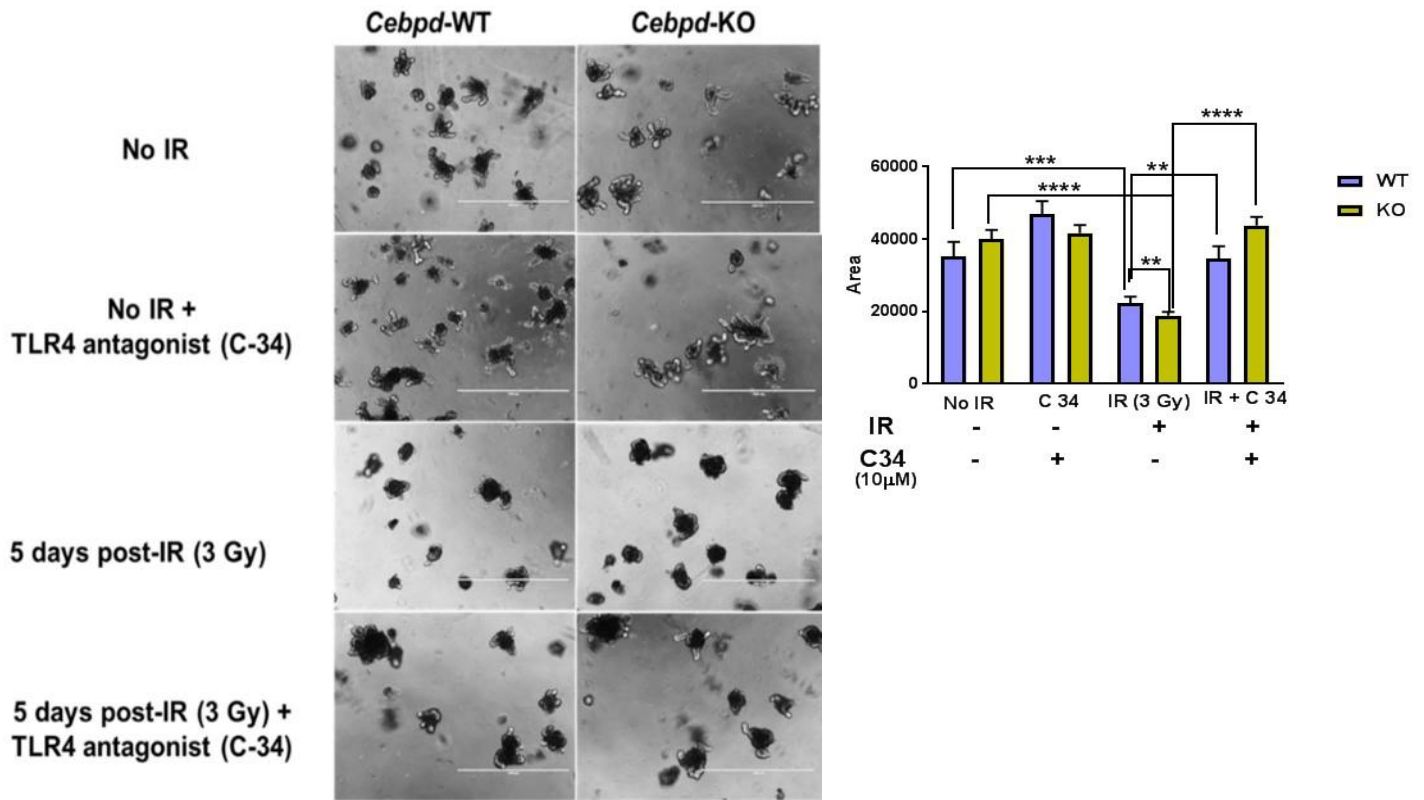


Fig. 26. TLR4 antagonist pre-treatment rescued the IR-induced growth inhibition of intestinal organoids from *Cebpd*-KO mice.

1.3a.4. Determine the effects of TLR4 inhibitor on inflammatory cytokines and *Nos-2* expression in irradiated WT and KO mice.

Methodology: Another study was done to examine *in vivo* effects of the TLR4 inhibitor C-34 (1mg/kg) at 1h post-irradiation in the intestine tissue. The TLR4 inhibitor was administered intraperitoneally immediately after the *Cebpd*-WT and KO mice (n=3-6 mice per genotype per group) were exposed to irradiation (8.5 Gy). The intestine tissue and blood was collected at 1h post-irradiation. We analyzed the gene expression of the *Tlr4*, *IL-6* & *Nos2*.

Results: The TLR4 inhibitor was able to downregulate the expression of inflammatory cytokines *Il-6* and *Tnf-α* which are robustly induced by ionizing radiation (IR). Similarly pre-treatment with the TLR4 inhibitor also downregulated the expression of *Nos2* (Fig. 27).

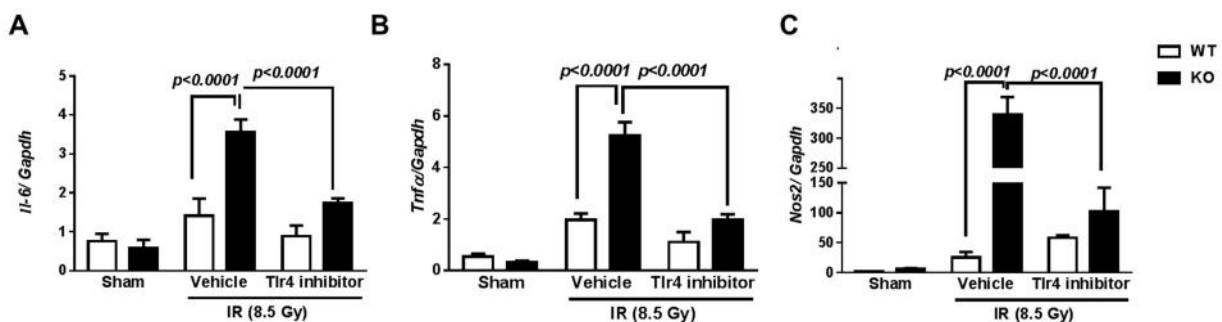


Fig. 27. *Cebpd*-KO mice show robust downregulation of Il-6, Tnf- α and Nos2 expression upon treatment with the TLR4 inhibitor immediately post-irradiation.

1.3a.5. Compare the effects of TLR4 inhibitor treatment on *Cebpd*-WT and KO mice at day 3.5 post-irradiation.

Methodology: *Cebpd*-WT and KO mice (n=8) were exposed to 8.5 Gy TBI. This is the dose of TBI where we have observed 100% lethality and as well as a significant decrease in crypt colony survival in KO mice (Pawar et al., 2014). The TLR4 inhibitor C34 (1mg/kg) dissolved in saline was administered intra-peritoneally immediately post-irradiation of mice. Mice were anesthetized by isoflurane inhalation and sacrificed at 3.5 days post-TBI. 4-5 transverse sections were used per mouse for the analysis. For the vehicle and TLR4 inhibitor treated groups n=3-4 mice were used, whereas for controls, n=6-7 were used.

Results:

We recapitulated our previous findings of decreased crypt survival in KO mice, when we compared irradiated KO+vehicle group to either unirradiated WT or KO mice (Pawar *et al.*, 2014, PLOS One). Additionally we also found that in the vehicle as well as TLR4 inhibitor-treated groups, KO mice showed significant decreases in crypt colony survival compared to respective WT groups (**Fig. 28 A, B**). Fig. 1 A shows the intestinal crypts residing at the base of the villi shown in blue color and the villi are stained in pink color. As expected post-TBI, we see that both WT and KO mice show a significant reduction in crypt colonies. Additionally when we compared WT vehicle to WT+TLR4 inhibitor treated group or KO vehicle to KO+TLR4 inhibitor treated groups, we found a significant increase in crypt colony survival, which is attributed to TLR4 inhibition. Interestingly the TLR4 inhibitor did not provide a complete rescue, which could be due to the fact that we gave only one injection of the inhibitor.

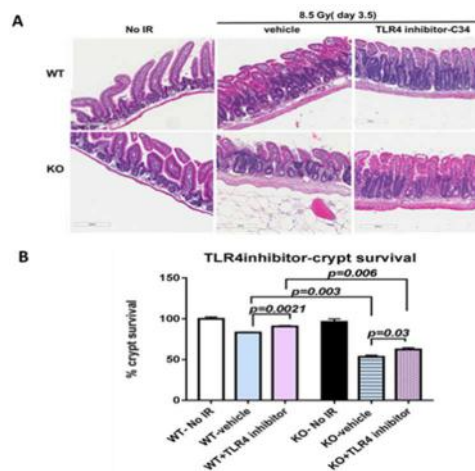


Fig. 28. TLR4 inhibitor (1mg/kg) treatment showed a modest protection of intestinal crypt colonies in both the genotypes.

1.3a.6. To examine whether TLR4 inhibitor can alleviate the intestinal injury at a dose that is known to induce lethality due to the GI syndrome.

Methodology:

Cebpd-WT and KO mice (n=8) were exposed to 10 Gy TBI. This is the dose of TBI where we have observed 100% lethality and as well as a significant decrease in crypt colony survival in KO mice (4). The TLR4 inhibitor C34 (5mg/kg) dissolved in saline was administered intra-peritoneally immediately post-irradiation of mice. Mice were anesthetized by isoflurane inhalation and sacrificed at 3.5 days post-TBI. 4-5 transverse sections were used

per mouse for the analysis. For the vehicle and TLR4 inhibitor treated groups n=3-4 mice were used, whereas for controls, n=6-7 were used.

Results:

We recapitulated our previous findings of decreased crypt survival in KO mice, when we compared mice from irradiated KO+vehicle group to either unirradiated WT or KO + vehicle group. We also included a sham group to see the effect of TLR4 inhibition on crypt colonies and found that there was a 0.25-fold decrease in crypt colonies, however there was no significant difference between WT and KO mice. Interestingly, TLR4 inhibitor treatment was able to alleviate IR-induced injury both in WT and KO mice. We found that WT+vehicle group showed 65% intestinal crypt colony survival which increased to 91% in the TLR4 treated group. On the other hand, KO=vehicle showed 22% survival of crypt colonies, while also found that in the vehicle as well as TLR4 inhibitor-treated groups, KO mice showed significant decreases in crypt colony survival compared to respective WT groups (Fig. 29).

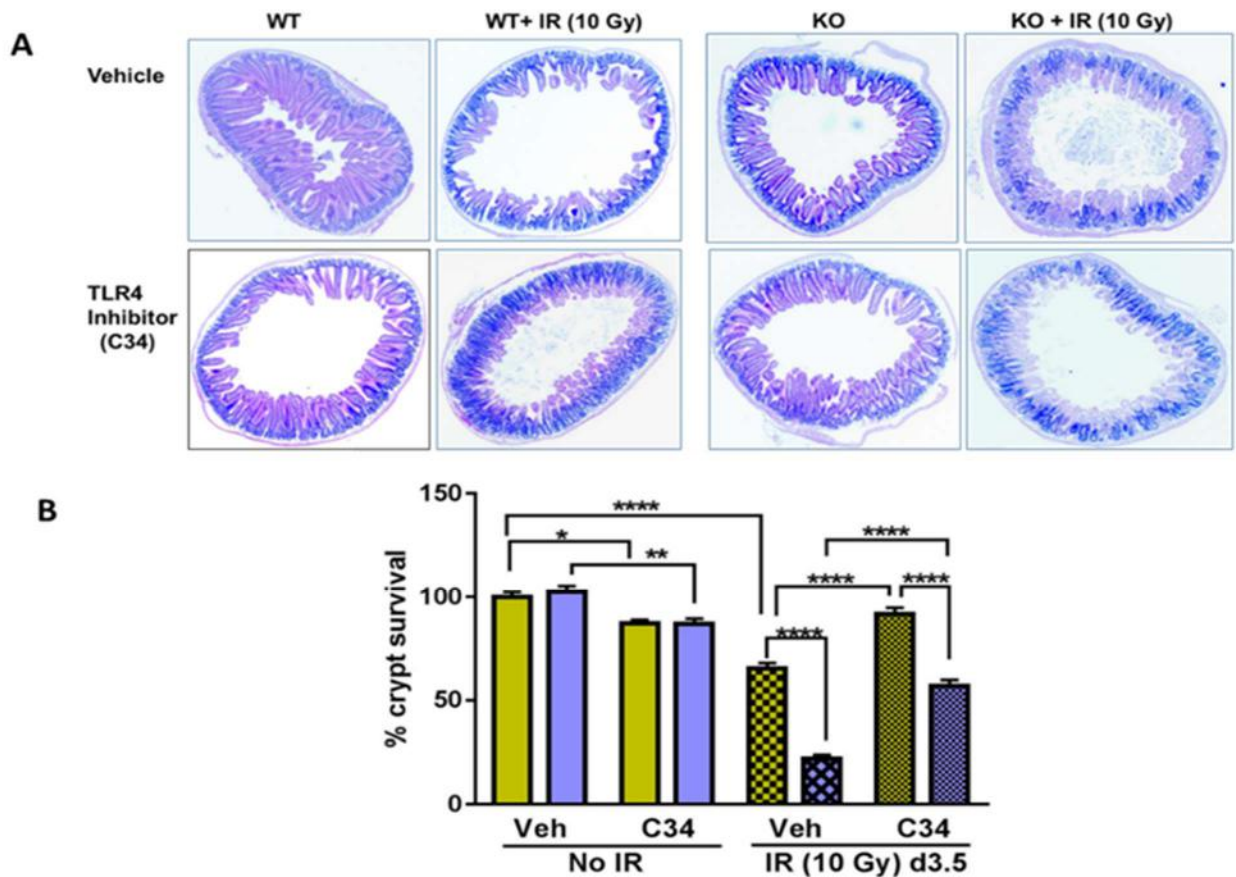


Fig. 29. Increasing TLR4 inhibitor concentration to 5mg/kg showed significant protection of not only KO intestinal crypts but also WT crypts at day 3.5 post-10 Gy TBI.

1.3a.7. Determine the effect of IR downstream target of TLR4 signaling in intestinal tissue extracts from Cebpd-WT and KO mice post-irradiation.

Methodology: *Cebpd*-WT and KO mice aged 10-12 weeks were exposed to 8.5 Gy TBI and intestine tissues (proximal jejunums) were harvested at 0 and 4h post irradiation. Tissue extracts were prepared and quantified by Bradford assay, approximately 40µg protein per loaded per lane and immunoblotted and probed with antibodies to TLR4, TRAF6, IRAK-m, TOLLIP, and GAPDH.

Results: Previously we have shown that *Cebpd*-KO mice express high levels of TLR4 at early timepoints post-irradiation (1h & 4h) (see 1.3a.1, Fig. 24). We did not observe any significant changes at early timepoints post-irradiation in the negative or positive regulators of TLR4 signaling pathway in the intestine tissue extracts of *Cebpd*-WT and *Cebpd*-KO mice.

At 24h post-IR, in addition to upregulation of TLR4, TRAF6-a positive regulator of TLR4 signaling was upregulated, while the negative regulator TOLLIP was downregulated in irradiated KO intestine tissues. In contrast, the TLR4 levels were lower in WT tissues and correlated with lower TRAF6 and higher expression of TOLLIP (Fig. 30).

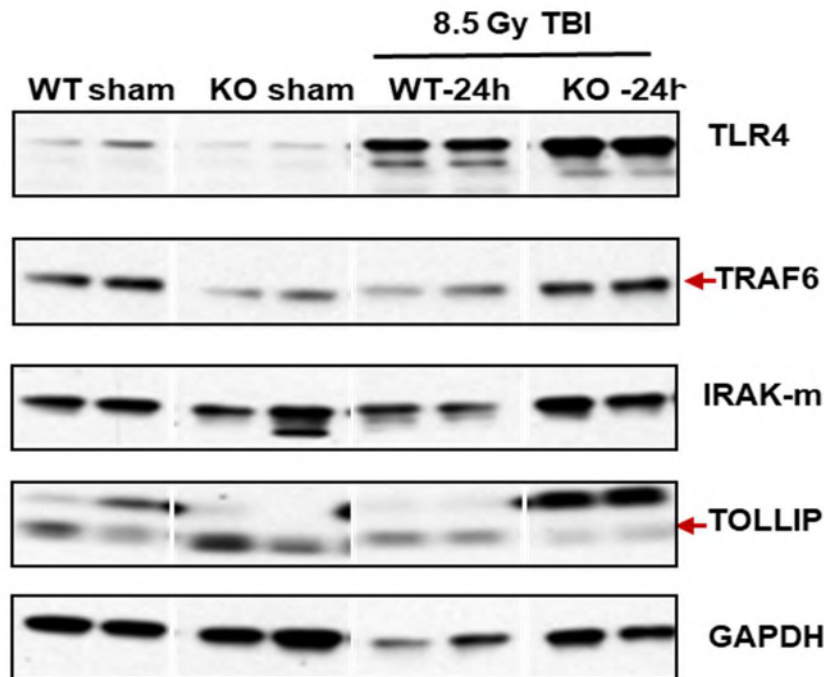


Fig. 30. TOLLIP-a negative regulator of TLR4 is decreased, while TRAF6 is increased in *Cebpd*-KO intestine at 24 h post-IR

Key Accomplishments: The overall objectives of the studies proposed in this aim were achieved. These findings will be submitted in the form of a manuscript that is currently under preparation.

Our results reveal that treatment with TLR4 inhibitor immediately post-irradiation showed a significant protection of intestinal crypts at day 3.5 post-10 Gy, however the effect on overall survival remain unexplored. Given that TLR4 does play an important role in intestinal homeostasis as well as in hematopoietic system, the time and dosing regimen will play a critical role. In this regards, the pharmacokinetics and pharmacodynamics of the TLR4 inhibitor C34 will need to be determined.

Specific Aim 2: Determine whether *Cebpd*-KO mice show perturbed macrophage response post-IR.

2.1. Determine whether *Cebpd*-deficient macrophages show increased pro-inflammatory cytokines and oxidative stress post-irradiation.

Methodology:

Cebpd-WT and KO mice (n=2) were anesthetized by isoflurane followed by cervical dislocation. Femurs and tibiae were harvested and bone marrow cells were flushed in 4% FBS in PBS, followed by lysis of red blood cells in hypotonic ACK lysis buffer. Cells were enumerated using a cell counter (Countess, Invitrogen).

Approximately 2×10^6 bone marrow cells were seeded in a 10cm dish in RPMI medium containing 10% fetal bovine serum and 10ng/ml M-CSF. The media was changed after 3-4 days. By day 5-7, once the dishes were confluent, BMDMs were exposed to 0 and or 4 Gy and cells were harvested at 0, 1h, 4h, and 24h post-irradiation. The expression of mRNA levels of Il-6, Tnf- α and Nos2 were measured and normalized to *Gapdh* as an endogenous reference and to unirradiated WT samples. The data presented below is from cells obtained from 1 mouse per genotype. RNA was isolated from cells followed by preparation of cDNA. Overall scheme of BMDM and underlying experiments is described in Fig. 31.

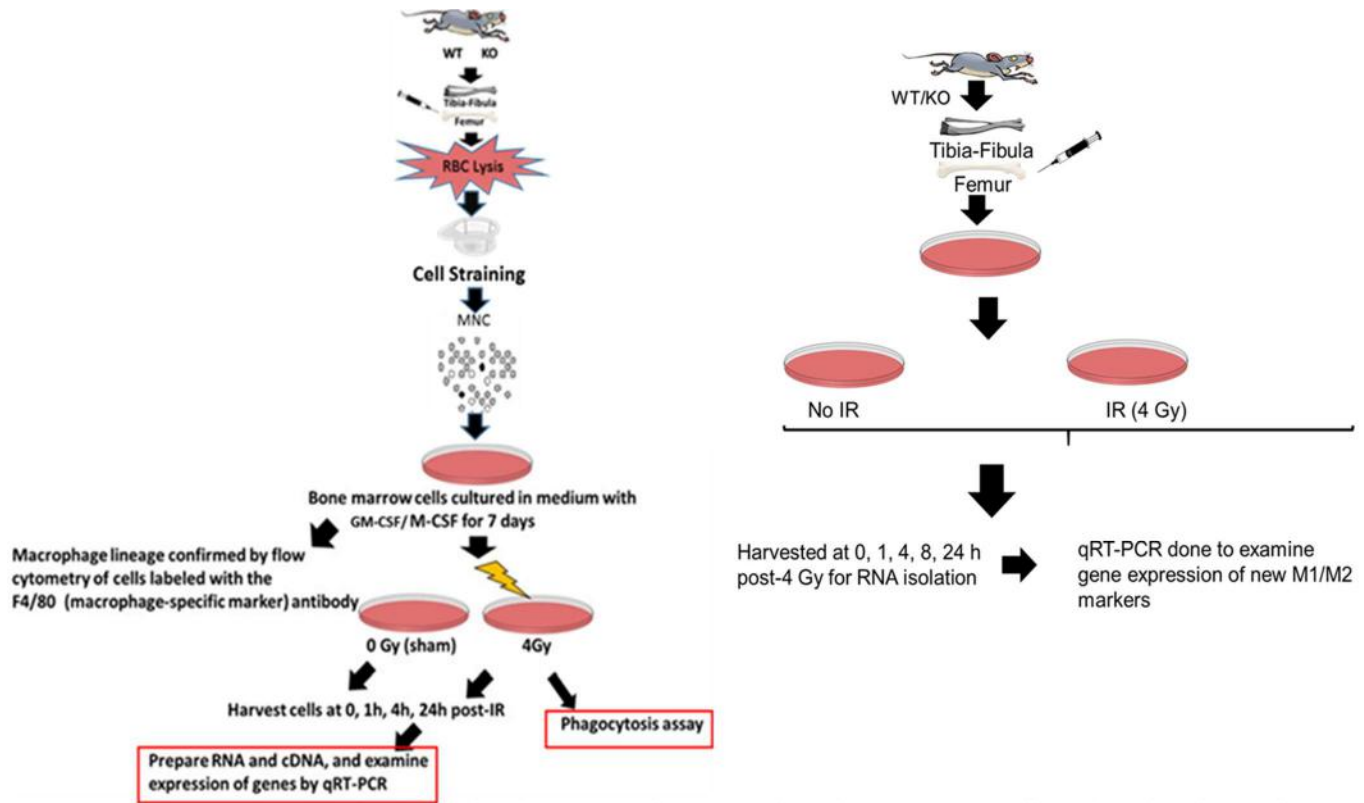


Fig.31. Overall scheme for derivation of BM-DMs from bone marrow cells and molecular analysis.

Results:

1) BMDMs were derived from bone marrow cells that were cultured in presence of M-CSF or GM-CSF. Typically M-CSF skew the macrophages to a M2-like phenotype, while GM-CSF skews to a M1-like phenotype. A representative picture of the BMDMS is shown in Fig. 32.

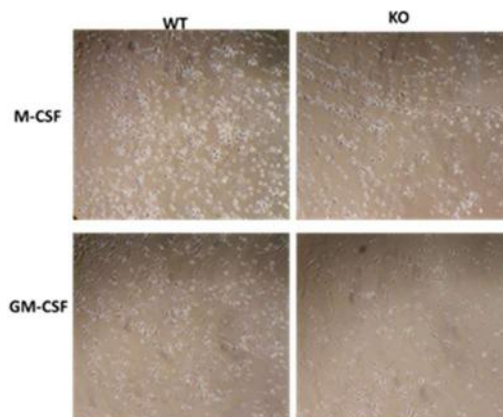


Fig.32. Derivation of bone marrow derived macrophages in presence of M-CSF and GM-CSF

- 2) Next, the identity of BMDMs were confirmed by labeling cells with an antibody specific to the F4/80 macrophage-specific marker (**Fig. 33**). We found that 94% of the cells expressed the F4/80 marker.

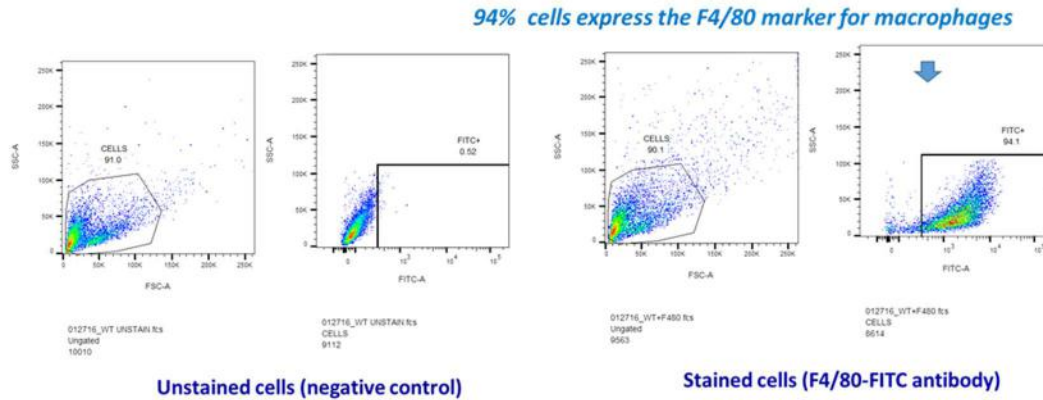


Fig. 33. BM-DMs were confirmed by labeling with a macrophage-specific marker F4/80.

- 3) We measured the expression of M1-specific markers *Il-6*, *Tnf- α* and *Nos2*. At baseline, there were no significant differences in the expression of *Il-6*, *Tnf- α* or *Nos2* between WT and KO BMDMs. We found that IL-6 levels were elevated at 1h post-IR exposure in BMDMs of both genotypes. Similarly the expression of *Tnf- α* showed induction at 1h post-IR in KO BMDMs compared to WT BMDMs, however this difference disappeared at later timepoints (**Fig. 34**) and was not significant. IR induced *Nos2* expression to a similar extent at 4h and 24h post-irradiation in both WT and KO BMDMs. Overall there were no significant differences in the expression of inflammatory cytokines such as *Il-6*, *Tnf- α* or *Nos2* between WT and KO BMDMs (**Fig. 34**).

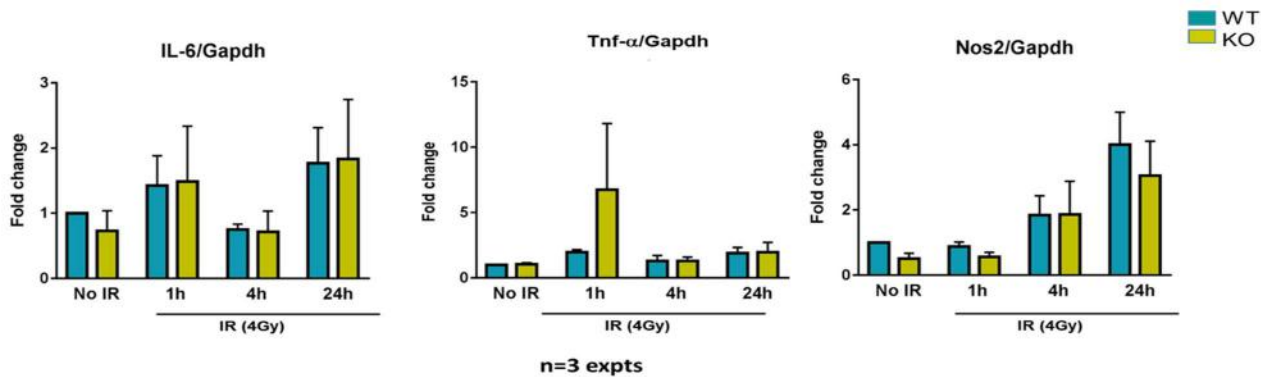


Fig. 34. No significant differences in the expression of classical M1 macrophage markers between *Cebpd*-WT and *Cebpd*-KO BMDMs before and after exposure to radiation.

- 4) Similarly the expression of M2-macrophage specific markers were measured. The expression of *Il-10* and *Arg-1* were measured. There were no significant differences between WT and KO BMDMs at baseline in the expression of either *Il-10* or *Arg-1*. Both WT and KO BMDMs showed increased expression of *Il-10* at 4h and 24h post-IR, compared to WT BMDMs. (**Fig. 35**).

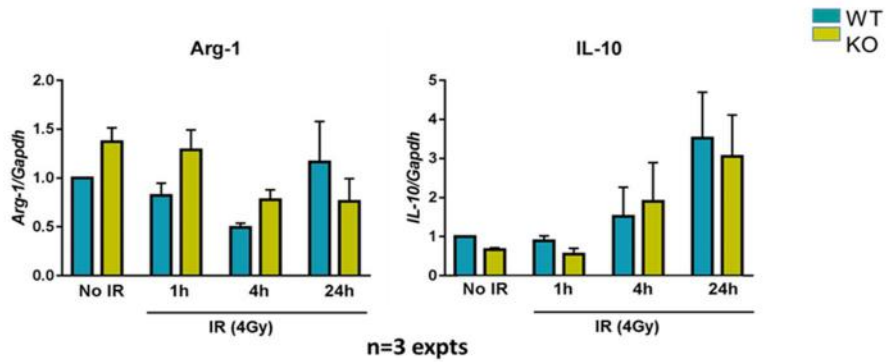
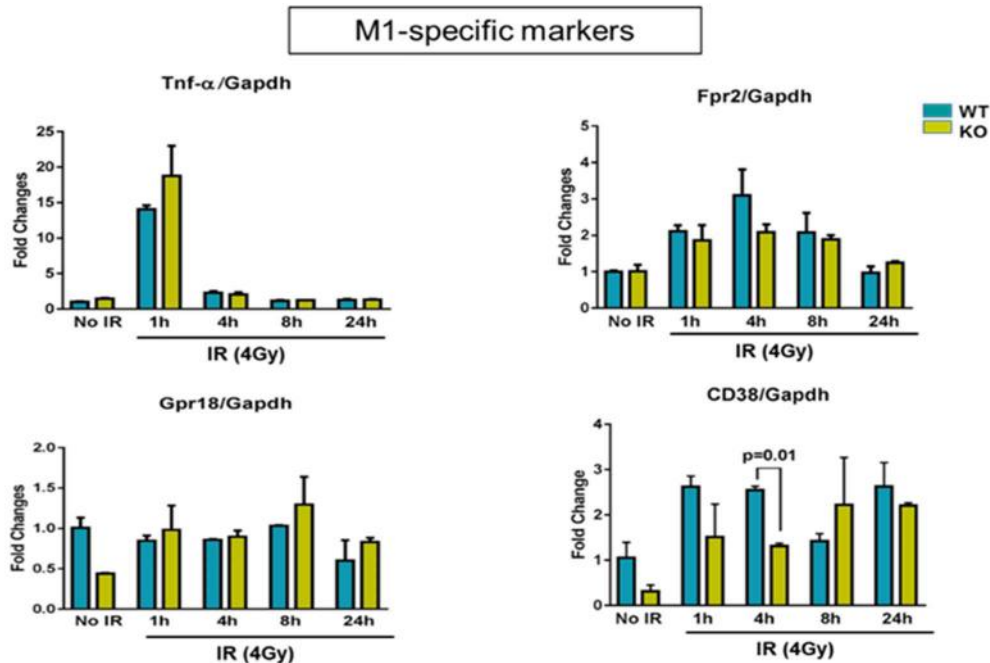


Fig. 35. No significant difference in M2 macrophage-specific markers between *Cebpd*-WT and *Cebpd*-KO BMDMs before and after exposure to radiation.

5) These results indicate that KO BMDMs did not any significant change in the expression of either the classical M1 and or alternative M2 markers, thus it was difficult to classify the macrophages as either M1 or M2 phenotype and additional markers needed to be explored.

A recent study by Jablonski et al., (PLOS One, 10, 1-25, 2015) identified novel M1 and M2 specific markers which were tested under the same conditions of radiation. We therefore analyzed the expression of novel M1-macrophage specific markers such as *Fpr2*, *Gpr18*, *CD38* and also included *Tnf-α* as one of the markers (Fig. 36). We also examined *c-Myc* and *Chil3* as a M2-specific novel markers. Of the M1-markers, only CD38 showed impaired expression at 4h post-irradiation, however at later timepoints, the expression was not significantly between the genotypes. With respect to the M2 markers, again there was no significant change in the expression between WT and KO BMDMs.

Since we did not observe any significant changes in the expression of either M1 or M2 –specific markers, we next investigated whether increasing the dose of IR exposure may skew the macrophages to a specific M1/M2 type.



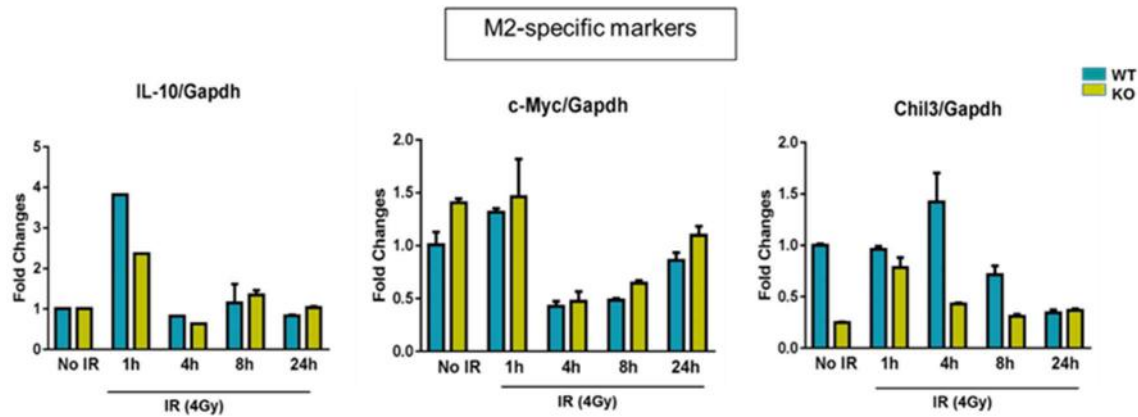


Fig. 36. Validation of new M1 and M2 macrophage-specific markers in *Cebpd*-WT and KO before and after exposure to IR

6) Expression of M1-specific markers post-10 Gy exposure. In contrast to our previous results with 4 Gy exposure, the expression of the inflammatory cytokine *Tnf- α* , did not show any significant differences in induction at 1h and 24h post-10 Gy exposure between *Cebpd*-KO and WT BMDMs (**Fig. 37 A**). Similarly, we also did not observe any significant differences in the expression of *Nos2*, which was induced by IR at 4h and 24h in both *Cebpd*-KO and WT BMDMs (**Fig. 37 B**). CD38 was induced at 24h post-10 Gy, interestingly KO BMDMs showed significant upregulation compared to WT BMDMs (**Fig. 37 C**).

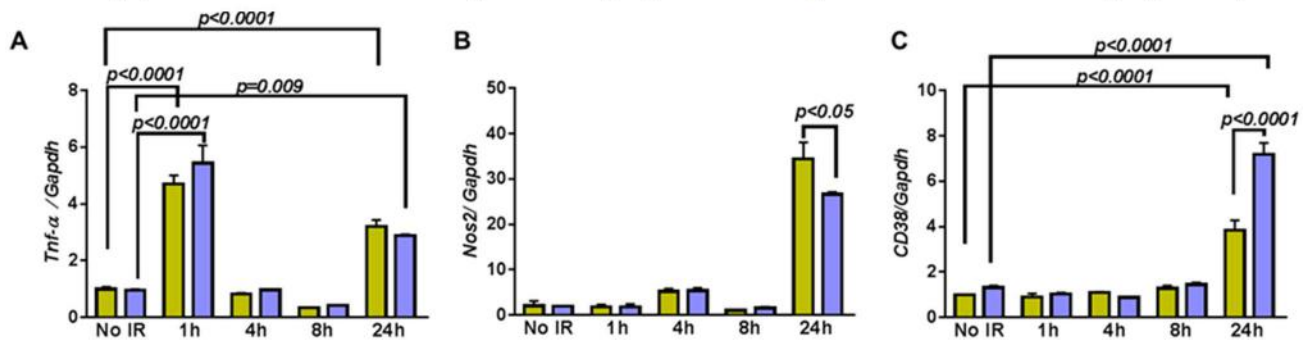


Fig. 37. Expression of M1 macrophage-specific markers in *Cebpd*-WT and KO BMDMs post-10 Gy exposure.

7) Expression of M2-specific markers post 10 Gy exposure. At 1h post-10 Gy, KO BMDMs showed 1.2-fold upregulation of *Arg-1*, but by 24h post-irradiation, *Arg-1* expression was downregulated by 1.4-fold, compared to WT BMDMs (**Fig. 38 A**). The anti-inflammatory cytokine *Il-10* was upregulated by 2.6-fold in WT and by 3.0-fold in KO BMDMs at 1h post-irradiation compared to respective unirradiated controls. *Il-10* expression was downregulated at 4h and 8h post-irradiation. At 24h post-irradiation, *Il-10* was upregulated by 1.3-fold in WT BMDMs compared to KO BMDMs. Compared to unirradiated controls, WT BMDMs showed 6.2-fold upregulation of *Il-10* and 4.7-fold in KO BMDMs. The new M2-specific marker *Chil3* was downregulated at 4h post-irradiation and further repressed below baseline in WT BMDMs, however KO BMDMs did not show significant downregulation at this timepoint compared to unirradiated controls. But by 8h and 24h post-irradiation, both KO and WT BMDMs, *Chil3* expression was significantly down-regulated.

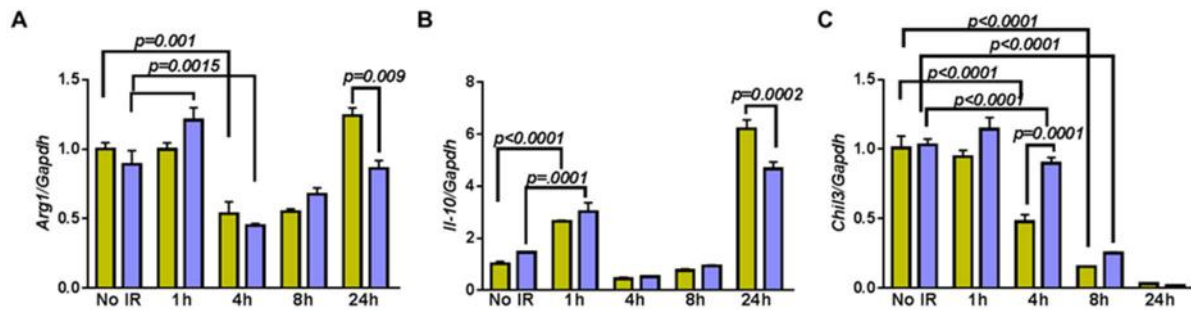


Fig. 38. Expression of M2 macrophage-specific markers in *Cebpd*-WT and KO BMDMs post-10 Gy exposure.

8) Expression of TLR4 post 10 Gy expression in WT and KO BMDMs. At early timepoints, there was no induction of TLR4, which showed about 3.17-fold induction in WT BMDMs, but only 1.976-fold induction in KO BMDMs compared to unirradiated controls (**Fig. 39**).

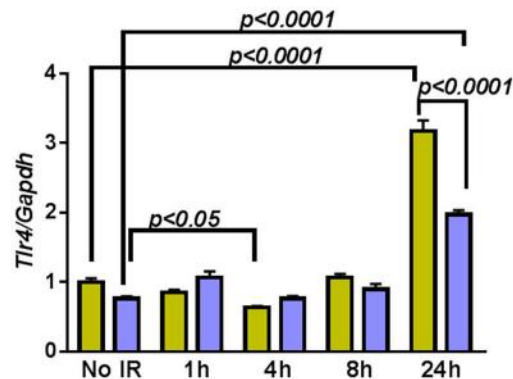


Fig. 39. KO BMDMs show decreased induction of *Tlr4* at 24h post-exposure to 10 Gy.

9) Expression of *Cebpd* in BMDMs after exposure to 10 Gy. Compared to our previous studies with 4 Gy, where we saw induction of *Cebpd* expression at 1h, 4h, 8h and 24h post-irradiation. The peak of *Cebpd* induction was observed at 4h post-4 Gy exposure. Interestingly, at 1h post-10 Gy, *Cebpd* was repressed by 8-fold. WT BMDMs showed robust induction at 4h (1.42-fold), 8h (2.5-fold) and the peak of induction by 24h (4.8-fold) post-10 Gy exposure. This induction at 24h correlates with some of the changes in the expression of *Nos2*, *CD38*, *Arg1*, *Il-10* and *Tlr4* which were significantly downregulated in KO BMDMs. Overall there was no clear indication in M1/M2 skewing from these studies.

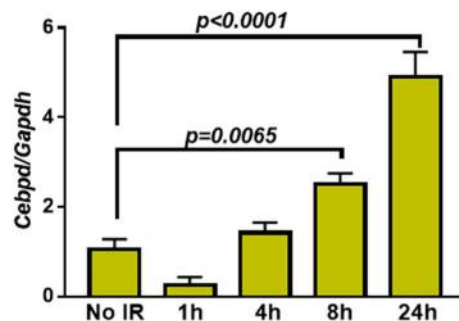


Fig.40. Kinetics of *Cebpd* induction by IR in WT BMDMs after exposure to 4 Gy.

10) We also examined the effect of LPS (promotes M1 macrophage activation) and IL-4 (skews macrophages to M2 phenotype) on *Cebpd*-WT and KO BMDMs.

Methodology: BMDMs were exposed to 0, 4 and 10 Gy or treated for 24 hours with LPS(10ng/ml) or IL-4 (10ng/ml) and cells were harvested at 0, 1h, 4h, and 24h post-irradiation. RNA was isolated from cells followed by preparation of cDNA and gene expression was measured by real-time PCR. The expression of markers specific to the M1- macrophages such as *Tnf- α* , *Fpr2*, *Gpr18*, *CD38* which are thought to play a role in inflammation and markers specific to a M2-phenotype such as *Il-10*, *Chil3* and *c-Myc* which play a role in anti-inflammation and tissue remodeling were measured by real-time PCR. The expression of mRNA levels of M1/M2 target genes and *Cebpd* were measured and normalized to *Gapdh* as an endogenous reference and to unirradiated WT samples.

Results: Similar to the results obtained with IR exposure, we again found that there was no significant differences between *Cebpd*-WT and KO BMDMs in terms of expression of either M1 or M2 markers in response to LPS (Fig. 41). Interestingly, only *Chil3* and *c-Myc* were upregulated in response to IL-4, while the M1 markers like *Tnf-a*, *Fpr2*, *CD38* and surprisingly *IL-10* were stimulated by LPS treatment. In conclusion, again, our results indicate that *Cebpd*-deficiency did not alter the macrophage to M1 or M2 phenotype.

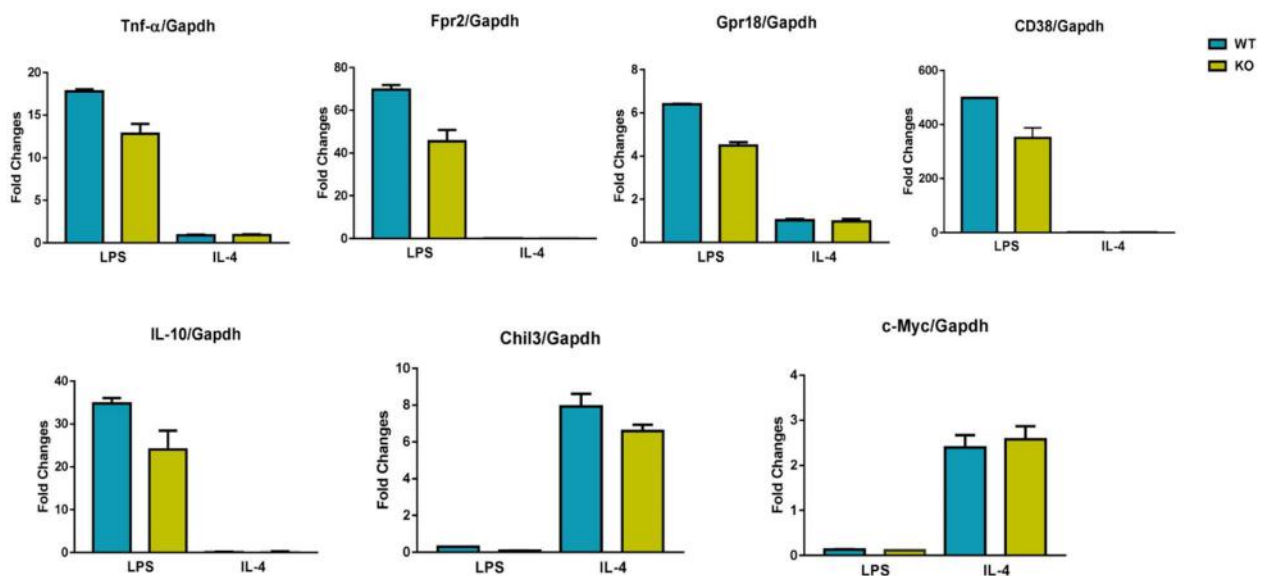


Fig. 41. *Cebpd*-KO mice show impaired expression of M1/M2 macrophage specific markers in response to IL-4, but robust stimulation with LPS treatment.

11) To further test whether *Cebpd* is induced differentially with radiation versus LPS and IL-4, we examined the expression of *Cebpd* in WT BMDMs. All these three treatments-radiation, LPS and IL-4 stimulated the expression of *Cebpd*, however the highest induction of 30-fold was observed with 24h LPS treatment, whereas radiation and IL-4 stimulated about 12-fold expression of *Cebpd*.

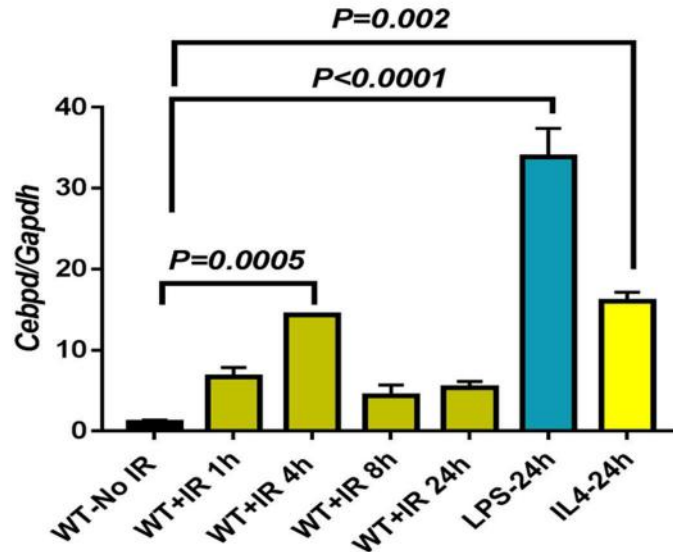


Fig. 42. *Cebpd* is induced by IR (10 Gy), LPS & IL-4 treatment in BMDMs

12) We compared the phagocytic activity of *Cebpd*-KO and WT macrophages under basal and post-irradiation.

Methodology: BMDMs were incubated with pHRhodo particles conjugated to Fluorescein dye, which fluoresces only when it is internalized by the macrophage. Cells were incubated with these particles at 4h post-irradiation or in untreated BMDMs and incubated for 30mins. After 30minutes the immunofluorescence images were taken. Cells were seeded in 6-well plates and treated similarly as described above were harvested for analysis by flow cytometry and mean fluorescence intensity was measured.

Results: Again we did not observe a significant difference in phagocytosis of pHRhodo particles at 4h post-irradiation, although KO BMDMs showed slightly lower phagocytosis activity, the difference was not statistically significant (**Fig. 43**)

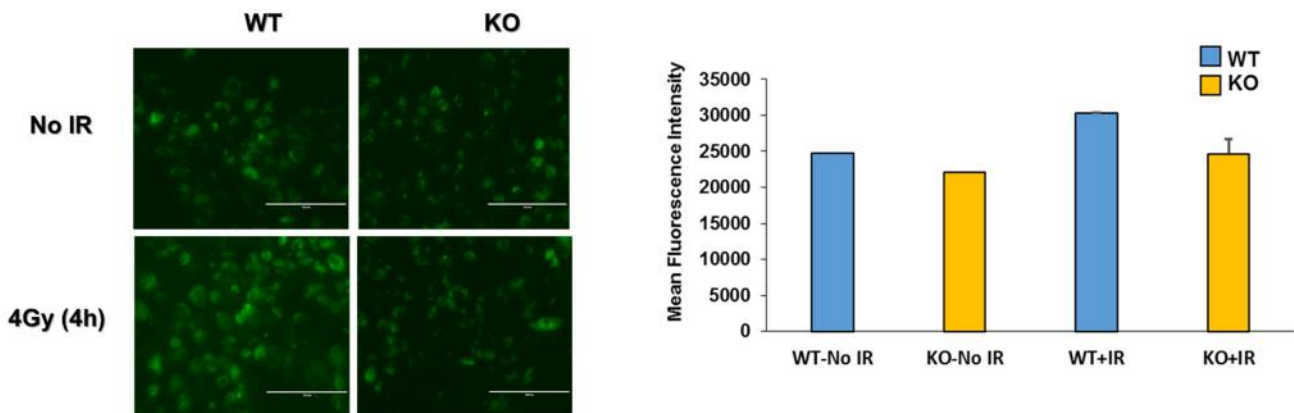


Fig. 43. *Cebpd*-KO-BMDMs do not show any significant difference in phagocytosis activity post-irradiation compared to *Cebpd*-WT BMDMs.

13) To further rule out that this lack of phenotype is possibly due to *in vitro* differentiation of the macrophages from the bone marrow cells, we performed bone marrow transplantation (BMT) experiments to test whether it could rescue the IR-induced lethality of KO mice.

Methodology: Bone marrow mononuclear cells were prepared from young (3 months) *Cebpd*-WT and KO mice. WT and KO mice received lethal irradiation dose of 11 Gy TBI. 24 h post-irradiation one WT and KO group received 1×10^6 cells in 100 μ l of sterile saline via tail vein injection. 3-5 transverse intestinal sections per mouse were generated and stained with hematoxylin and eosin. The surviving crypts were enumerated and data represents an average of 3-5 mice per group.

Results: In the irradiation alone group, *Cebpd*-KO mice showed fewer surviving crypts, as we have reported earlier (Fig. 43). Radiation alone treated *Cebpd*-WT mice showed 31% crypt survival while WT mice that received KO BMCs showed 48% crypt survival. Similarly in the KO group with radiation alone, there were only 6% of crypt colony survival, while KO mice that received WT BMCs showed about 18% survival of intestinal crypts. Clearly these results suggest that BMCs from unirradiated WT and KO mice can protect from radiation-induced loss of intestinal crypts.

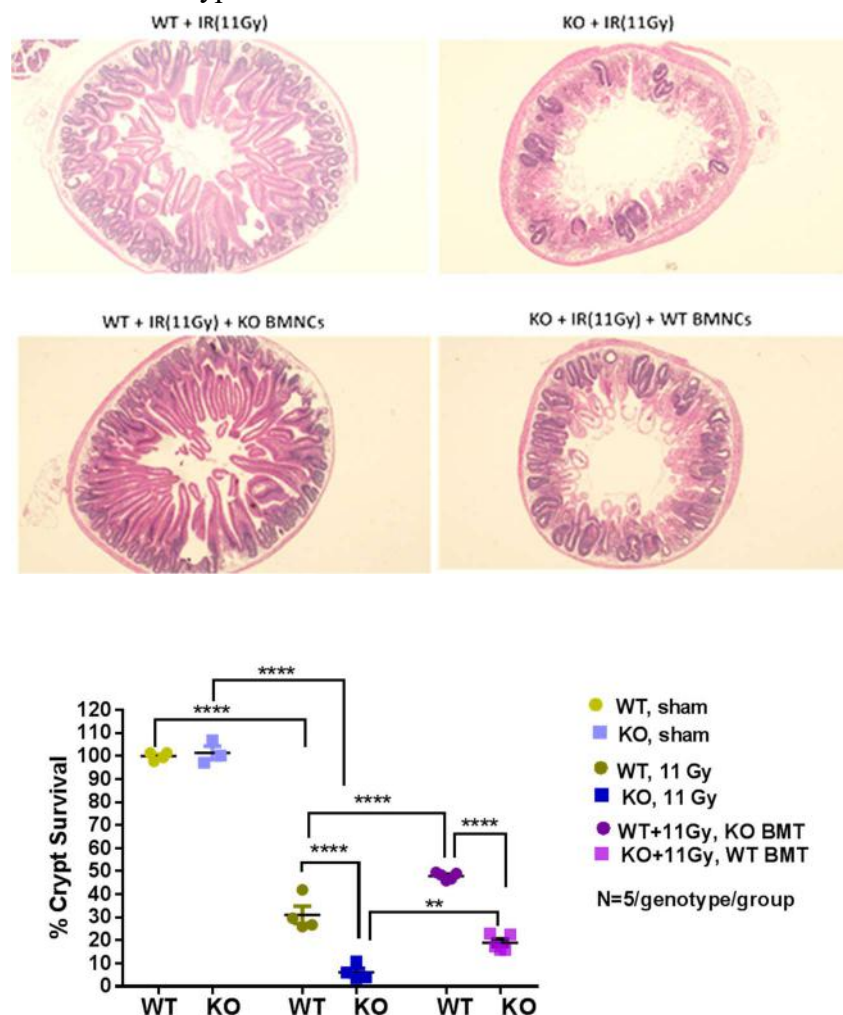


Fig.43. Bone marrow transplantation rescued the intestinal crypt colony survival at day 3.5 post-irradiation compared to radiation alone group independent of genotype.

Key accomplishments: The overall objective of Aim 2 was achieved. Our results suggest that *Cebpd*-deficiency does not perturb the response of KO macrophages to promote increased intestinal injury in response to TBI exposure. These findings are similar to a recent study examining the role of C/EBP delta in experimental colitis. In the mouse model of experimental colitis induced by DSS, it is reported that lack of *Cebpd* leads to increased apoptosis of intestinal epithelial cells, however independent of the role of macrophages, as *Cebpd*-KO macrophages did not show altered response in presence of LPS compared to *Cebpd*-WT macrophages (13).

c. What opportunities for training and professional development has the project provided?

During the funding period of this grant, all personnel (including postdoctoral fellows, graduate student, research assistant and undergraduate summer research fellows) were provided numerous opportunities to attend National/local Meetings and Conferences and present their research either in the form of oral presentations or poster presentations.

Participation of trainees/personnel in various professional development activities is listed below:

| | |
|-------------------------------|--|
| Sudip Banerjee, PhD | Received Scholar-in training travel award to present poster at Radiation Research Society Meeting, Weston, FL, Sep 19-22, 2015. |
| Debajyoti Majumdar, M. Pharm. | Received UAMS Graduate School travel award, 6 th Biennial NIH/NIGMS National IDeA Symposium for Biomedical Research Excellence meeting in Washington DC, June 26-28, 2016. |
| Sumit Shah, MBBS, MPH | Received 1 st prize in the student category (\$100 award), South Central Chapter of the Society of Toxicology, UAMS, Little Rock, AR, Oct 28, 2016. |
| Sudip Banerjee, PhD | Received 1 st prize non-student category (\$100 award), South Central Chapter of the Society of Toxicology Meeting, UAMS, Little Rock, AR, Oct 28, 2016. |
| Robin Raley | Selected for NIH- Summer Internship Program Fellowship, May-August 2017, based on her research project in my laboratory. |
| Sudip Banerjee, PhD | Selected for oral presentation, Drug Discovery and Development Colloquium, UAMS, Little Rock, AR, June 15-17, 2017. |
| Debajyoti Majumdar, M. Pharm | Received 3 rd prize for poster presentation in graduate student category (\$100 award), Drug Discovery and Development Colloquium, UAMS, Little Rock, AR, June 15-17, 2017. |
| Jessica Orton | Selected for the Graduate Student Boot Camp, Pratt School of engineering at Duke University, based on her summer research project done in my laboratory, Sep15, 2017. |
| Jessica Orton | Received Arkansas INBRE travel award, to present her summer research at the Southeast IDeA Meeting, Morgantown, WV, Oct 11-13, 2017. |
| Sudip Banerjee, PhD | Selected for oral presentation at the Conference on Normal Tissue Radiation Effects and Countermeasures, Morrilton, AR, May 14-17, 2018. |
| Sudip Banerjee, PhD | Received Scholar-in training travel award & selected for oral presentation at the 64 th Annual meeting of the Radiation Research Society, Chicago, IL, Sep 23-26, 2018. |

| | |
|-------------------------------|---|
| Jessica Orton | Selected for Duke University's Pratt School of Engineering Summer REU Program, based on her previous summer research experience in my lab. |
| Sudip Banerjee, PhD | Received Scholar-in training travel award, selected for oral presentation at the 65 th Annual meeting of the Radiation Research Society, San Diego, CA, Nov 3-6, 2019. |
| Debajyoti Majumdar, M. Pharm. | Nominated as one of the top 10 submitted abstracts, received Scholar-in training travel award to present his poster at the 65 th Annual meeting of the Radiation Research Society, San Diego, CA, Nov 3-6, 2019. |

d. How were the results disseminated to communities of interest?

"Nothing to Report"

e. What do you plan to do during the next reporting period to accomplish the goals?

"Nothing to Report"

4. IMPACT:

a. What was the impact on the development of the principal discipline(s) of the project?

"Nothing to Report"

b. What was the impact on other disciplines?

"Nothing to Report"

c. What was the impact on technology transfer?

"Nothing to Report"

d. What was the impact on society beyond science and technology?

"Nothing to Report"

5. CHANGES/PROBLEMS:

a. Changes in approach and reasons for change

"Nothing to Report"

b. Actual or anticipated problems or delays and actions or plans to resolve them

Due to the extended delay in the Material transfer Agreement process to procure Eritoran (Eisai Inc), another TLR4 inhibitor-C34 that was readily obtained from Sigma was used for the experiments described in Aim 1.3a. These changes were done with approval from the Science Officer Mrs. Sandy Snyder.

c. Changes that had a significant impact on expenditures

"Nothing to Report"

- d. **Significant changes in use or care of human subjects, vertebrate animals, biohazards, and/or select agents**

"Nothing to Report"

- e. **Significant changes in use or care of human subjects**

“Not applicable”

- f. **Significant changes in use or care of vertebrate animals.**

"Nothing to Report"

- g. **Significant changes in use of biohazards and/or select agents**

"Nothing to Report"

6. PRODUCTS:

- a. **Publications, conference papers, and presentations**

Report only the major publication(s) resulting from the work under this award.

i.1 Journal publications

- 1) Banerjee S, Shah, SK, Melnyk SB, Pathak R, Hauer-Jensen and **Pawar SA***. C/EBP δ is essential for gamma tocotrienol-mediated protection against radiation-induced hematopoietic and intestinal injury. **Antioxidants**, **7: 55, 2018**, *acknowledgement of federal support (yes)*.
- 2) Banerjee S, Fu Q, Melnyk SB, Shah SK, Sterneck E, Hauer-Jensen M, **Pawar SA***. C/EBP δ protects from radiation-induced intestinal injury and sepsis by suppression of inflammatory and nitrosative stress. **Sci. Rep.**, **9:13953, 2019**. <https://doi.org/10.1038/s41598-019-49437-x>, *acknowledgement of federal support (yes)*.

i.2 Manuscripts related to the current project to be submitted/in preparation

- 3) Banerjee S, Shah SK, Hauer-Jensen M and **Pawar SA***. Impaired TLR4 signaling promotes radiation-induced intestinal injury in *Cebpd*-deficient mice. **Innate Immunity**, *acknowledgement of federal support (yes)*.
- 4) **Pawar SA***, Banerjee S, Gill K and Cheema AK. C/EBP δ -deficiency promotes gut dysbiosis after radiation exposure and correlates with metabolomics changes. **Journal of Proteome Research**. *acknowledgement of federal support (yes)*.
- 5) Majumdar D and **Pawar SA***. C/EBP δ -deficiency does not alter the radiation response of M1 and M2 genes in bone marrow derived macrophages. **Journal of Immunology**. *acknowledgement of federal support (yes)*.

i.3 Invited Talks by PI related to current project

- 1) C/EBP δ protects from radiation-induced intestinal injury by downregulation of inflammation, COBRE New Investigator Research Forum, UAMS, UAMS, Little Rock, AR, January 12, 2016. *acknowledgement of federal support (yes)*.
- 2) C/EBP δ - a novel player in radiation-induced normal tissue injury, Winthrop P. Rockefeller Cancer Research Forum Seminar, UAMS, Little Rock, AR, April 25, 2016. *acknowledgement of federal support (yes)*.
- 3) C/EBP δ - a novel player in radiation response, National Cancer Institute, Frederick, MD, June 29, 2016. *acknowledgement of federal support (yes)*.
- 4) C/EBP δ - a novel player in radiation response, Armed Forces Research in Radiobiology Institute, Bethesda, MD, June 30, 2016. *acknowledgement of federal support (yes)*.
- 5) Molecular mechanism of C/EBP δ in ionizing radiation response, Center for Biomedical Research Excellence External Advisory Committee Meeting, UAMS, Little Rock, AR, November 3, 2016. *acknowledgement of federal support (yes)*.
- 6) C/EBP δ - A Novel Player in Ionizing Radiation Response, Free Radical and Radiation Biology Division, Department of Radiation Oncology, University of Iowa, Iowa City, IA, April 3, 2017. *acknowledgement of federal support (yes)*.
- 7) Targeting the C/EBP δ /TLR4 nexus protects from radiation-induced gut injury, Department of Physiology & Biophysics, UAMS, Little Rock, AR, October 26, 2017.
- 8) Molecular mechanism of C/EBP δ in ionizing radiation response, Center for Biomedical Research Excellence External Advisory Committee Meeting, UAMS, Little Rock, AR, November 6, 2017. *acknowledgement of federal support (yes)*.
- 9) C/EBP δ : A Novel Player in Normal Tissue Responses to Ionizing Radiation, Division of Radiation Research, Department of Radiology, Rutgers New Jersey Medical School, Newark, NJ, April 10, 2018. *acknowledgement of federal support (yes)*.
- 10) C/EBP δ : A Novel Target to Alleviate Radiation-induced Normal Tissue Toxicity, Masonic Medical Research Institute, Utica, NY, May 21, 2019. *acknowledgement of federal support (yes)*.
- 11) C/EBP δ : A Novel Player in Normal Tissue Responses to Ionizing Radiation, Department of Radiation Oncology, Upstate Medical University, Syracuse, NY, May 23, 2019. *acknowledgement of federal support (yes)*.

i.4 Invited Oral presentations at National Meetings

- 1) Banerjee S, Fu Q, Shah SK, Melnyk SB, Hauer-Jensen M and **Pawar SA***. Aberrant TLR4 signaling promotes radiation-induced intestinal injury in *Cebpd*-deficient mice. Conference on Normal Tissue Radiation Effects and Countermeasures (CONTREC), Morrilton, AR, May 14-17, 2018. *acknowledgement of federal support (yes)*.
- 2) Gorantla A[#], Banerjee S, Tyler A, Chokhani P, Groves T, Allen AR and **Pawar SA**. Investigating the role of C/EBP δ in inflammaging and oxidative stress in the aging brain. Center for Diversity Affairs Summer Research Internship presentation, UAMS, Little Rock, AR, July 23, 2018. *acknowledgement of federal support (yes)*.
- 3) Banerjee S*, Fu Q, Shah SK, Melnyk SB, Hauer-Jensen M and **Pawar SA[#]**. TLR4 inhibition attenuates radiation-induced inflammation and oxidative stress to protect mice from gastrointestinal injury. 64th Annual meeting of the Radiation Research Society, Chicago, IL, September 14-17, 2018. (*acknowledgement of federal support (yes)*).

- 4) Banerjee S*, Krager K, Majumdar D, Boerma M, Hauer-Jensen M and **Pawar SA**. C/EBP δ protects from radiation-induced gastrointestinal injury. 65th Annual meeting of the Radiation Research Society, San Diego, CA, Nov 3-6, 2019. *acknowledgement of federal support (yes)*.

(* presenter & recipient of travel award/# presenter)

i.5 Poster presentations

- 1) Majumdar D*, Banerjee S, Hauer-Jensen M, and **Pawar SA**. C/EBP δ -deficient macrophages display altered inflammatory response to ionizing radiation. 6th Biennial NIH/NIGMS National IDeA Symposium for Biomedical Research Excellence, Washington, DC, June 26-28, 2016. *acknowledgement of federal support (yes)*.
- 2) Banerjee S, Fu Q, Ponnappan U, Melnyk SB, Hauer-Jensen M and **Pawar SA**. Radiation-induced intestinal injury in *Cebpd*-knockout mice occurs due to aberrant inflammatory and oxidative stress response. Gordon Research Conference, "Extracellular vesicles": Biologic Effects and Therapeutic Potential of Extracellular Vesicles, Newry, ME, August 21-26, 2016. *acknowledgement of federal support (yes)*!
- 3) Banerjee S, Fu Q, Ponnappan U, Melnyk SB, Hauer-Jensen M and **Pawar SA**. Radiation-induced intestinal injury in *Cebpd*-knockout mice occurs due to aberrant inflammatory and oxidative stress response. Arkansas Biosciences Institute Symposium, Stephens Spine Institute, UAMS, Little Rock, AR, September 13, 2016. *acknowledgement of federal support (yes)*!
- 4) Banerjee S, Fu Q, Ponnappan U, Melnyk SB, Hauer-Jensen M and **Pawar SA**. Radiation-induced intestinal injury in *Cebpd*-knockout mice occurs due to aberrant inflammatory and oxidative stress response. Annual Meeting of the South Central Chapter of Society of Toxicology, UAMS, Little Rock, AR, October 27-28, 2016. *acknowledgement of federal support (yes)*.
- 5) Majumdar D, Banerjee S, Hauer-Jensen M, and **Pawar SA**. C/EBP δ -deficient macrophages display altered inflammatory response to ionizing radiation. Annual Meeting of the South Central Chapter of Society of Toxicology, UAMS, Little Rock, AR, October 27-28, 2016. *acknowledgement of federal support (yes)*.
- 6) Banerjee S, Fu Q, Ponnappan U, Melnyk SB, Hauer-Jensen M and **Pawar SA**. Radiation-induced intestinal injury in *Cebpd*-knockout mice occurs due to aberrant inflammatory and oxidative stress response. Basic Subcellular Mechanisms, Showcase of Medical Discoveries, UAMS, Little Rock, AR, November 9, 2016.!
- 7) Banerjee S, Fu Q, Ponnappan U, Melnyk SB, Hauer-Jensen M and **Pawar SA**. Role of TLR4 in promoting radiation-induced intestinal injury. 40th Annual Conference of Shock Society, Fort Lauderdale, FL, June 3-6, 2017. *acknowledgement of federal support (yes)*.
- 8) Majumdar D*, Chang J, Zhou D, Banerjee S, Hauer-Jensen M and **Pawar SA**. C/EBP δ -deficiency alters radiation-induced myeloid responses. Drug Discovery and Development Colloquium, UAMS, Little Rock, AR, June 15-17, 2017. *acknowledgement of federal support (yes)*.
- 9) Banerjee S, Shah SK, Pathak R, Melnyk SB, Hauer-Jensen M and **Pawar SA**. Gamma-tocotrienol-mediated protection against radiation-induced injury is dependent on C/EBP δ . Drug Discovery and Development Colloquium, UAMS, Little Rock, AR, June 15-17, 2017. *acknowledgement of federal support (yes)*!
- 10) Murdock S, Majumdar D, Banerjee S, Hauer-Jensen M and **Pawar SA**. Investigating the role of C/EBP δ in macrophage response to ionizing radiation. Center for Diversity Affairs

- Summer Research Internship presentation, UAMS, Little Rock, AR, July 25, 2017. *acknowledgement of federal support (yes).*
- 11) Banerjee S, Fu Q, Ponnappan U, Melnyk SB, Hauer-Jensen M and **Pawar SA**. Impaired TLR4 signaling promotes radiation-induced intestinal injury in *Cebpd*-deficient mice. 2017 Southeast IDeA Regional Meeting, Morgantown, WV, October 11-13, 2017. *acknowledgement of federal support (yes).*
 - 12) Majumdar D, Banerjee S, Hauer-Jensen M and **Pawar SA**. C/EBP δ -deficiency results in impaired phagocytic response to ionizing radiation. 2017 Southeast IDeA meeting, Morgantown, WV, October 11-13, 2017. *acknowledgement of federal support (yes).*
 - 13) Banerjee S, Fu Q, Ponnappan U, Melnyk SB, Hauer-Jensen M and **Pawar SA**. Impaired TLR4 signaling promotes radiation-induced intestinal injury in *Cebpd*-deficient mice. 63rd Annual International meeting of the Radiation Research Society, Cancun, Mexico, October 15-18, 2017. *acknowledgement of federal support (yes).!*
 - 14) Majumdar D, Banerjee S, Hauer-Jensen M and **Pawar SA**. C/EBP δ -deficiency results in impaired phagocytic response to ionizing radiation. 4th Annual Graduate Student Association Fall Symposium, UAMS, Little Rock, AR, Oct 27, 2017. *acknowledgement of federal support (yes).*
 - 15) Majumdar D, Wang X, Zhou D, Hauer-Jensen M, and **Pawar SA**. Role of C/EBP δ in radiation-induced hematopoietic injury. Student Research Day, UAMS, Little Rock, AR, March 6, 2018. *acknowledgement of federal support (yes).*
 - 16) Banerjee S, Shah SK, Melnyk SB, Hauer-Jensen M and **Pawar SA**. *Cebpd* is essential for gamma-tocotrienol mediated protection against radiation-induced hematopoietic and intestinal injury. Military Health System Research Symposium, Kissimmee, FL, Aug 20-23, 2018. *acknowledgement of federal support (yes).!*
 - 17) Banerjee S, Fu Q, Shah SK, Melnyk SB, Hauer-Jensen M and **Pawar SA**. TLR4 inhibition alleviates IR-induced intestinal injury and underlying sepsis in C/EBP δ -deficient mice. Military Health System Research Symposium, Kissimmee, FL, Aug 20-23, 2018. *acknowledgement of federal support (yes).!*
 - 18) Majumdar D, Stumhofer J, Pietras E, and **Pawar SA**. C/EBP δ protects hematopoietic stem cells and myeloid progenitor cells from radiation-induced injury. 64th Annual meeting of the Radiation Research Society, Chicago, IL, September 14-17, 2018. *acknowledgement of federal support (yes).*
 - 19) Banerjee S, Shah SK, Melnyk SB, Hauer-Jensen M and **Pawar SA**. *Cebpd* is essential for gamma-tocotrienol mediated protection against radiation-induced hematopoietic and intestinal injury. 64th Annual meeting of the Radiation Research Society, Chicago, IL, September 14-17, 2018. *acknowledgement of federal support (yes).!*
 - 20) Majumdar D, Stumhofer J, Pietras E, and **Pawar SA**. Investigating the role of C/EBP δ -deficiency in radiation-induced bone marrow failure. 60th American Society of Hematology Annual Meeting & Exposition, San Diego, CA, Dec 1-4, 2018. *acknowledgement of federal support (yes).*
 - 21) Majumdar D*, Banerjee S, Pietras EM and **Pawar SA**. C/EBP δ promotes post-radiation recovery of hematopoietic stem cells by downregulating oxidative stress and DNA damage. 65th Annual meeting of the Radiation Research Society, San Diego, CA, Nov 3-6, 2019. *acknowledgement of federal support (yes).*

ii. **Books or other non-periodical, one-time publications.**

"Nothing to Report"

iii. Other publications, conference papers, and presentations.

iii.1 Other publications:

- 1) Banerjee S, Aykin-Burns N, Krager KJ, Shah SK, Melnyk SB, Hauer-Jensen M, **Pawar SA***. Loss of C/EBP δ enhances IR-induced cell death by promoting oxidative stress and mitochondrial dysfunction. **Free Radical Biology and Medicine**, **99:296-307, 2016**. *acknowledgement of federal support (yes)*.
- 2) Garg S, Sadhukhan R, Banerjee S, Savenka AL, Basnakian AG, McHargue V, Wang J, **Pawar SA**, Ghosh SP, Ware J, Hauer-Jensen M, Pathak R*. Gamma-tocotrienol protects the intestine from radiation potentially by accelerating mesenchymal immune cell recovery. **Antioxidants**. **8 (3), 2019. pii: E57**. *acknowledgement of federal support (yes)*.
- 3) Banerjee S, Tyler A, Majumdar D, Groves T, Wang J, Gorantla A, Allen AR* and **Pawar SA***. Loss of C/EBP δ exacerbates radiation-induced neurocognitive decline by suppression of oxidative stress in aged mice. **Int. J. Mol. Sci.**, **20, 885, 2019**. *acknowledgement of federal support (yes)*.

iii.2 Manuscripts related to the current project to be submitted/in preparation

- 1) Shah SK[#], Banerjee S[#], Ponnappan U, Stumhofer J, Hauer-Jensen M and **Pawar SA***. IL17A does not play a role in radiation-induced intestinal injury. **Int. J. Mol. Sci.** *acknowledgement of federal support (yes)*.
- 2) Byrum SD, Banerjee S, Orr L, Ponnappan U, Tackett AJ and **Pawar SA***. Identification of C/EBP δ -targets involved in regulation of radiation response utilizing a proteomics approach. **Journal of Proteomics & Bioinformatics**. *acknowledgement of federal support (yes)*.
- 3) Orton J[#], Raley R[#], Vue S[#], Coates C, Banerjee S, Kuppasamy B, Sterneck E and **Pawar SA***. C/EBP δ -deficiency sensitizes cells to etoposide-induced cytotoxicity due to impaired DNA damage response. **Cell Death & Disease**. *acknowledgement of federal support (yes)*.
- 4) Majumdar D, Chavez JC, Pietras EM, and **Pawar SA***. C/EBP δ protects from radiation-induced bone marrow failure by suppression of ROS-induced DNA damage and cell cycle proliferation. **Hematologica**. *acknowledgement of federal support (yes)*.
- 5) Chavez JC[#], Majumdar D, **Pawar SA*** and Pietras EM*. C/EBP δ -deficiency promotes impaired myeloid differentiation in response to chronic inflammation. **Blood**. *acknowledgement of federal support (yes)*.
- 6) Majumdar D, **Pawar SA**, Chowdhury P, Griffin R, Narayanasamy G, Dobretsov M, Hauer-Jensen M and Pathak R*. Simultaneous exposure to chronic low-grade irradiation and simulated microgravity promotes increased oxidative stress in hematopoietic stem cells. **Scientific Reports**. *acknowledgement of federal support (yes)*.
- 7) **Pawar SA***, Banerjee S, Majumdar D and Hauer-Jensen M. C/EBP δ -deficiency in aged mice promotes increased radiation-induced intestinal injury. **PLOS One**. *acknowledgement of federal support (yes)*.

iii.2 Oral presentations:

- 1) **Pawar SA***, Banerjee S, Byrum SD, Orr L, Tackett AJ, Ponnappan U and Hauer-Jensen M. A proteomics approach to delineate the role of C/EBP δ in ionizing radiation-induced oxidative stress. Southeast Regional IDEa Conference, Cell signaling session, Biloxi, MS, November 11-13, 2015. *acknowledgement of federal support (yes)*.

- 2) Banerjee S, Byrum SD, Orr L, Tackett A, Ponnappan U, Hauer-Jensen M and **Pawar SA***. Identification of C/EBP δ targets involved in regulation or IR-induced oxidative stress. National IDeA Symposium for Biomedical Research Excellence, Washington, DC, June 26-28, 2016. *acknowledgement of federal support (yes)*.

iii.3 Other Poster presentations

- 1) **Pawar SA**, Banerjee S, Aykin-Burns N, Krager KJ, Melnyk SB, and Hauer-Jensen M. C/EBP δ modulates oxidative stress and mitochondrial dysfunction to promote post-radiation survival. Society for Redox Biology and Medicine, Boston, MA, November 18-22, 2015. *acknowledgement of federal support (yes)!*
- 2) LoBianco FV, **Pawar SA**, Krager KJ, Breen PJ, Compadre CM, Hauer-Jensen M and Aykin-Burns N. Tocotrienol-rich DG3 as a therapeutic agent protects against ionizing radiation-induced intestinal injury. Student Research Day, UAMS, Little Rock, AR, April 13, 2016. *acknowledgement of federal support (yes)*.
- 3) Shah SK, Banerjee S, Majumdar D, Ponnappan U, Stumhofer J, Hauer-Jensen M, and **Pawar SA**. IL-17 signaling may be dispensable for promoting radiation-induced intestinal injury. 6th Biennial NIH/NIGMS National IDeA Symposium for Biomedical Research Excellence, Washington, DC, June 26-28, 2016. *acknowledgement of federal support (yes)*.
- 4) Shah SK, Banerjee S, Majumdar D, Ponnappan U, Stumhofer J, Hauer-Jensen M, and **Pawar SA**. IL-17 signaling may be dispensable for promoting radiation-induced intestinal injury. Arkansas Biosciences Institute Symposium, Stephens Spine Institute, UAMS, Little Rock, AR, September 13, 2016. *acknowledgement of federal support (yes)*.
- 5) Banerjee S, Byrum S, Orr L, Tackett AJ, Ponnappan U, Hauer-Jensen M and **Pawar SA**. Identification of C/EBP δ -targets involved in regulation of radiation-induced oxidative stress utilizing a proteomics approach. 62nd Annual Meeting Radiation Research Society, Maui, HI, October 16-19, 2016. *acknowledgement of federal support (yes)*.
- 6) LoBianco FV, **Pawar SA**, Krager KJ Breen PJ, Compadre CM, Hauer-Jensen M, Aykin-Burns N. Tocotrienol-rich DG3 as a therapeutic agent protects against ionizing radiation-induced intestinal injury. 62nd Annual Meeting Radiation Research Society, Maui, HI, October 16-19, 2016. *acknowledgement of federal support (yes)*.
- 7) Shah SK*, Banerjee S, Majumdar D, Ponnappan U, Stumhofer J, Hauer-Jensen M, and **Pawar SA**. IL-17 signaling may be dispensable for promoting radiation-induced intestinal injury. Annual Meeting of the South Central Chapter of Society of Toxicology, UAMS, Little Rock, AR, October 27-28, 2016. *acknowledgement of federal support (yes)*.
- 8) Orton J, Raley R, Banerjee S, Eldred C, Hauer-Jensen M and **Pawar SA**. Investigating the role of C/EBP δ in etoposide-mediated cytotoxicity. Central Arkansas Undergraduate Summer Research Conference, UAMS, Little Rock, AR, July 26, 2017. *acknowledgement of federal support (yes)*.
- 9) Eldred C, Orton J, Raley R, Banerjee S, Hauer-Jensen M and **Pawar SA**. C/EBP δ -deficiency promotes doxorubicin-induced cytotoxicity due to increased mitochondrial damage and dysfunction. 51st Fall Annual Seminar, Arkansas Association for Health Systems Pharmacists, Little Rock, AR, October 5-6, 2017. *acknowledgement of federal support (yes)*.
- 10) Orton J, Raley R, Banerjee S, Eldred C, Krager KJ, Aykin-Burns N and **Pawar SA**. C/EBP δ -deficient cells show increased toxicity to etoposide due to impaired DNA damage response, increased oxidative stress response and mitochondrial damage. 2017 Southeast

IDEA Regional Meeting, Morgantown, WV, October 11-13, 2017. *acknowledgement of federal support (yes).*

- 11) Orton J, Raley R, Banerjee S, Eldred C, Hauer-Jensen M and **Pawar SA**. C/EBP δ -deficient cells show increased toxicity to etoposide due to impaired DNA damage response, increased oxidative stress response and mitochondrial damage. Annual INBRE conference, University of Arkansas-Fayetteville, AR, Oct 27-28, 2017. *acknowledgement of federal support (yes).*
- 12) Coates C, Banerjee S, Orton J, Hauer-Jensen M and **Pawar SA**. C/EBP δ protects cells from Doxorubicin cytotoxicity by suppression of DNA damage and mitochondrial dysfunction. Student Research Day, UAMS, Little Rock, AR, March 6, 2018. *acknowledgement of federal support (yes).*
- 13) Pathak R, Sadhukhan R, Garg S, **Pawar SA**, Boerma M, Ware J and Hauer-Jensen M. Kruppel-like factor 2 (KLF2): A novel radiation target is suppressed in the mouse intestine. Conference on Normal Tissue Radiation Effects and Countermeasures (CONTREC), Morrilton, AR, May 14-17, 2018. *acknowledgement of federal support (yes).*
- 14) Gorantla A, Banerjee S, Tyler A, Chokhani P, Groves T, Allen AR and **Pawar SA**. Investigating the role of C/EBP δ in inflammaging and oxidative stress in the aging brain. Center for Diversity Affairs Summer Research Internship presentation, UAMS, Little Rock, AR, July 23, 2018. *acknowledgement of federal support (yes).*
- 15) Pathak R, Sadhukhan R, Garg S, **Pawar SA**, Boerma M, Ware J and Hauer-Jensen M. Kruppel-like factor 2 (KLF2): A novel radiation target, shear-responsive KLF2, is suppressed in the mouse intestine. 64th Annual meeting of the Radiation Research Society, Chicago, IL, September 14-17, 2018. *acknowledgement of federal support (yes).*
- 16) Sadhukhan R, Majumdar D, Garg S, **Pawar SA**, Chowdhury P, Griffin R, Narayanasamy G, Dobretsov M, Hauer-Jensen M and Pathak R. Simultaneous exposure to chronic low-grade irradiation and simulated microgravity alter immune cells phenotype in mice thymus and spleen. 65th Annual meeting of the Radiation Research Society, San Diego, CA, Nov 3-6, 2019. *acknowledgement of federal support (yes).*

b. Website(s) or other Internet site(s)

"Nothing to Report"

c. Technologies or techniques

"Nothing to Report"

d. Inventions, patent applications, and/or licenses

"Nothing to Report"

e. Other Products

"Nothing to Report"

7. PARTICIPANTS & OTHER COLLABORATING ORGANIZATIONS

a. What individuals have worked on the project?

| | |
|--|---|
| Name: | Snehalata Pawar, PhD |
| Project Role: | Principal Investigator |
| Researcher Identifier (e.g. ORCID ID): | 0000-0003-3992-2494 |
| Nearest person month worked: | 4.8 cal mths |
| Contribution to Project: | Dr. Pawar designed and supervised the experimental studies to carry out experimental aims, supervised the studies, analysis and interpretation of results, results, wrote the manuscripts, presented research findings in form of invited talks/oral presentations to scientific community etc. |
| Funding Support: | |

| | |
|--|--|
| Name: | Usha Ponnappan, PhD |
| Project Role: | Co-Investigator |
| Researcher Identifier (e.g. ORCID ID): | |
| Nearest person month worked: | 0.5 cal mths |
| Contribution to Project: | Helped with intellectual directions to the projects. |
| Funding Support: | |

| | |
|--|---|
| Name: | Martin Hauer-Jensen, MD, PhD |
| Project Role: | Co-Investigator |
| Researcher Identifier (e.g. ORCID ID): | |
| Nearest person month worked: | 0.5 cal mths |
| Contribution to Project: | Helped with intellectual directions to the projects and review of manuscripts |
| Funding Support: | |

| | |
|--|---|
| Name: | Daohong Zhou, MD |
| Project Role: | Co-Investigator |
| Researcher Identifier (e.g. ORCID ID): | |
| Nearest person month worked: | 0.1 cal mths |
| Contribution to Project: | Helped with intellectual directions to the projects |
| Funding Support: | |

| | |
|--|---------------------|
| Name: | Qiang Fu, MD, PhD |
| Project Role: | Co-Investigator |
| Researcher Identifier (e.g. ORCID ID): | 0000-0003-2700-4231 |

| | |
|------------------------------|---|
| Nearest person month worked: | 2.4 cal mths |
| Contribution to Project: | Performed tissue harvests, <i>in vivo</i> intestinal permeability experiments |
| Funding Support: | |

| | |
|--|--|
| Name: | Sudip Banerjee, PhD |
| Project Role: | Postdoctoral Fellow |
| Researcher Identifier (e.g. ORCID ID): | 0000-0002-0522-3479 |
| Nearest person month worked: | 12.0 cal mth |
| Contribution to Project: | Assisted with studies in Aims 1 and 2, namely blood collection, tissue harvest, ELISA for inflammatory cytokines and chemokines, immunoblotting etc. |
| Funding Support: | NIH/NIGMS |

| | |
|--|--|
| Name: | Debajyoti Majumdar |
| Project Role: | Graduate Research Assistant |
| Researcher Identifier (e.g. ORCID ID): | 0000-0001-8025-3857 |
| Nearest person month worked: | 4.0 cal mths |
| Contribution to Project: | Assisted with blood collection, tissue harvest, ELISA for inflammatory cytokines and chemokines, studies in Aim 2. |
| Funding Support: | NIH/NIGMS |

| | |
|--|--|
| Name: | Sumit Shah |
| Project Role: | Research Assistant |
| Researcher Identifier (e.g. ORCID ID): | 0000-0003-2916-8045 |
| Nearest person month worked: | 0.1 cal mths |
| Contribution to Project: | Assisted with genotyping of <i>Cebpd</i> -mice and preparation of plasma, immunohistology stainings for Claudin-2, myeloperoxidase and intestinal crypt survival assays. |
| Funding Support: | |

b. **Has there been a change in the active other support of the PD/PI(s) or senior/key personnel since the last reporting period?**

"Nothing to Report"

- c. **What other organizations were involved as partners?**
“Nothing to Report”

2. **SPECIAL REPORTING REQUIREMENTS**

- a. **COLLABORATIVE AWARDS:** “Nothing to Report”
- b. **QUAD CHARTS:** Submitted as a separate attachment

3. **APPENDICES:**

- 1. Bibliography
- 2. Original copies of articles
- 3. Invited talks-slides
- 4. Oral presentation-slides
- 5. Poster presentation
- 6. Curriculum vitae

3.1. BIBLIOGRAPHY

1. Banerjee, S., Fu, Q., Shah, S. K., Melnyk, S. B., Sterneck, E., Hauer-Jensen, M., and Pawar, S. A. (2019) C/EBPdelta protects from radiation-induced intestinal injury and sepsis by suppression of inflammatory and nitrosative stress. *Scientific reports* **9**, 13953
2. Banerjee, S., Shah, S., Melnyk, S., Pathak, R., Hauer-Jensen, M., and Pawar, S. (2018) Cebpδ Is Essential for Gamma-Tocotrienol Mediated Protection against Radiation-Induced Hematopoietic and Intestinal Injury. *Antioxidants* **7**, 55
3. Ghosh, S. P., Kulkarni, S., Hieber, K., Toles, R., Romanyukha, L., Kao, T. C., Hauer-Jensen, M., and Kumar, K. S. (2009) Gamma-tocotrienol, a tocol antioxidant as a potent radioprotector. *Int J Radiat Biol* **85**, 598-606
4. Pawar, S. A., Shao, L., Chang, J., Wang, W., Pathak, R., Zhu, X., Wang, J., Hendrickson, H., Boerma, M., Sterneck, E., Zhou, D., and Hauer-Jensen, M. (2014) C/EBP delta Deficiency Sensitizes Mice to Ionizing Radiation-Induced Hematopoietic and Intestinal Injury. *PLoS ONE* **9**, e94967
5. Berbee, M., Fu, Q., Boerma, M., Wang, J., Kumar, K. S., and Hauer-Jensen, M. (2009) gamma-Tocotrienol ameliorates intestinal radiation injury and reduces vascular oxidative stress after total-body irradiation by an HMG-CoA reductase-dependent mechanism. *Radiat Res* **171**, 596-605
6. Kulkarni, S. S., Cary, L. H., Gambles, K., Hauer-Jensen, M., Kumar, K. S., and Ghosh, S. P. (2012) Gamma-tocotrienol, a radiation prophylaxis agent, induces high levels of granulocyte colony-stimulating factor. *International immunopharmacology* **14**, 495-503
7. Banerjee, S., Aykin-Burns, N., Krager, K. J., Shah, S. K., Melnyk, S. B., Hauer-Jensen, M., and Pawar, S. A. (2016) Loss of C/EBPδ enhances IR-induced cell death by promoting oxidative stress and mitochondrial dysfunction. *Free Radical Biology and Medicine* **99**, 296-307
8. McKinney, L. C., Aquilla, E. M., Coffin, D., Wink, D. A., and Vodovotz, Y. (2000) Ionizing radiation potentiates the induction of nitric oxide synthase by interferon-gamma and/or lipopolysaccharide in murine macrophage cell lines: Role of tumor necrosis factor-alpha. *Annals of the New York Academy of Sciences* **899**, 61-68
9. Loboda, A., Damulewicz, M., Pyza, E., Jozkowicz, A., and Dulak, J. (2016) Role of Nrf2/HO-1 system in development, oxidative stress response and diseases: an evolutionarily conserved mechanism. *Cellular and molecular life sciences : CMLS* **73**, 3221-3247
10. Sato, T., and Clevers, H. (2013) Primary mouse small intestinal epithelial cell cultures. *Methods Mol Biol* **945**, 319-328
11. Neal, M. D., Jia, H., Eyer, B., Good, M., Guerriero, C. J., Sodhi, C. P., Afrazi, A., Prindle, T., Jr., Ma, C., Branca, M., Ozolek, J., Brodsky, J. L., Wipf, P., and Hackam, D. J. (2013) Discovery and Validation of a New Class of Small Molecule Toll-Like Receptor 4 (TLR4) Inhibitors. *PLOS ONE* **8**, e65779
12. Imada, S., Murata, Y., Kotani, T., Hatano, M., Sun, C., Konno, T., Park, J.-h., Kitamura, Y., Saito, Y., Ohdan, H., and Matozaki, T. (2016) Role of Src Family Kinases in Regulation of Intestinal Epithelial Homeostasis. *Molecular and Cellular Biology* **36**, 2811-2823
13. Jozawa, H., Inoue-Yamauchi, A., Arimura, S., and Yamanashi, Y. (2019) Loss of C/EBPdelta enhances apoptosis of intestinal epithelial cells and exacerbates experimental colitis in mice. *Genes to cells : devoted to molecular & cellular mechanisms*

OPEN

C/EBP δ protects from radiation-induced intestinal injury and sepsis by suppression of inflammatory and nitrosative stress

Sudip Banerjee¹, Qiang Fu¹, Sumit K. Shah¹, Stepan B Melnyk², Esta Sterneck³, Martin Hauer-Jensen¹ & Snehalata A. Pawar¹

Ionizing radiation (IR)-induced intestinal damage is characterized by a loss of intestinal crypt cells, intestinal barrier disruption and translocation of intestinal microflora resulting in sepsis-mediated lethality. We have shown that mice lacking C/EBP δ display IR-induced intestinal and hematopoietic injury and lethality. The purpose of this study was to investigate whether increased IR-induced inflammatory, oxidative and nitrosative stress promote intestinal injury and sepsis-mediated lethality in *Cebpd*^{-/-} mice. We found that irradiated *Cebpd*^{-/-} mice show decreased villous height, crypt depth, crypt to villi ratio and expression of the proliferation marker, proliferating cell nuclear antigen, indicative of intestinal injury. *Cebpd*^{-/-} mice show increased expression of the pro-inflammatory cytokines (*Il-6*, *Tnf- α*) and chemokines (*Cxcl1*, *Mcp-1*, *Mif-1 α*) and *Nos2* in the intestinal tissues compared to *Cebpd*^{+/+} mice after exposure to TBI. *Cebpd*^{-/-} mice show decreased GSH/GSSG ratio, increased S-nitrosoglutathione and 3-nitrotyrosine in the intestine indicative of basal oxidative and nitrosative stress, which was exacerbated by IR. Irradiated *Cebpd*-deficient mice showed upregulation of Claudin-2 that correlated with increased intestinal permeability, presence of plasma endotoxin and bacterial translocation to the liver. Overall these results uncover a novel role for C/EBP δ in protection against IR-induced intestinal injury by suppressing inflammation and nitrosative stress and underlying sepsis-induced lethality.

The likelihood of civilians as well as military forces encountering radiological hazard has increased many folds with proliferation of radioactive material, nuclear weapons and nuclear power facilities¹⁻³. A major side-effect of exposure to whole body radiation such as explosion of a nuclear bomb or during a nuclear accident or during abdominal radiotherapy is the acute toxicity of IR to the rapidly renewing cell systems such as the bone marrow and gastrointestinal tract mucosa³⁻⁵. There is a paucity of safe and effective interventions to treat or prevent IR-induced gut-associated sepsis⁶⁻⁸. In order to develop therapeutic interventions, therefore it is essential to understand the molecular underpinnings of IR-induced GI syndrome and associated lethality.

The gut mucosa is particularly radiation sensitive because of a high mucosal turnover rate⁹. The production of reactive oxygen species (ROS) and reactive nitrogen species (RNS), induced by IR promotes the induction of apoptosis and clonogenic cell death, which leads to mucosal breakdown¹⁰⁻¹⁵. It is known that exposure to IR leads to increased inflammation and that uncontrolled inflammation is known to exacerbate damage/injury to the tissues¹³⁻¹⁵. The process of inflammation is amplified by recruitment of neutrophils and transmigration of monocytes and activation of resident mast cells producing pro-inflammatory mediators like IL-1 β , IL-6, CXCL1 and TNF- α ¹¹⁻¹⁴. This leads to the upregulation of pro-inflammatory cytokines, chemokines, and growth factors in the microvascular and mucosal compartments, presumably not only by recruited immune cells but also by enterocytes, depending on the severity of tissue trauma^{14,15}.

¹Division of Radiation Health, Department of Pharmaceutical Sciences, College of Pharmacy, University of Arkansas for Medical Sciences, Little Rock, AR, 72205, USA. ²Arkansas Children's Research Institute, Little Rock, AR, 72202, USA. ³Laboratory of Cell and Developmental Signaling, Center for Cancer Research, National Cancer Institute, Frederick, MD, 21702, USA. Correspondence and requests for materials should be addressed to S.A.P. (email: SAPawar@uams.edu)

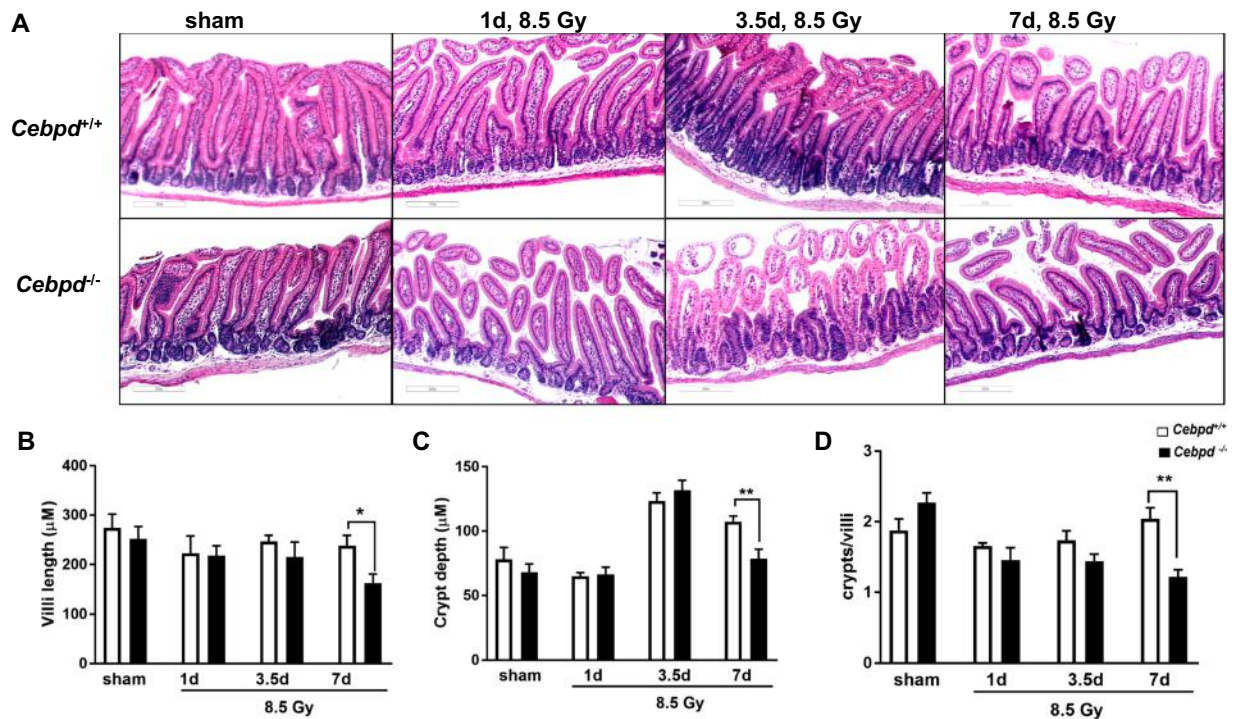


Figure 1. *Cebpd*^{-/-} mice show increased damage to intestinal crypts and villi after exposure to IR. (A) Representative images showing the cross sections of the small intestine from *Cebpd*^{+/+} and *Cebpd*^{-/-} mice exposed to 0 and 8.5 Gy and harvested at indicated timepoints. Histograms showing the measurements of intestinal injury parameters such as (B) villous height, (C) crypt depth and (D) crypt to villous ratio. The data are presented as average + standard error mean (S.E.M.) of n = 4–5 mice per genotype per group.

Exposure to high doses of IR causes damage to the intestinal epithelial barrier, vascular leakage and translocation of the intestinal microflora in the blood leading to an inflammatory cascade resulting in sepsis-induced mortality and is a hallmark of the GI syndrome¹⁶. Although the GI syndrome and associated sepsis have been extensively characterized^{17,18}, the key signaling factors that modulate IR-induced intestinal injury are not well understood.

C/EBP δ is a basic leucine zipper transcription factor that is shown to regulate target genes involved in diverse biological functions such as apoptosis, genomic instability, cell cycle, oxidative stress, stem cell self-renewal and tumor suppression^{19–27}. C/EBP δ also plays an important role in regulation of the inflammatory and stress responses as well as in innate and adaptive immune response^{28–31}.

We have previously shown that C/EBP δ -deficiency in mice leads to IR-induced lethality due to the underlying injury to the intestine and hematopoietic tissues³². Our recent studies revealed that the increased sensitivity of *Cebpd*^{-/-} mouse embryonic fibroblasts (MEFs) to IR occurs due to an impaired ability to modulate IR-induced oxidative stress and mitochondrial dysfunction³³. Interestingly, very little is known about the exact mechanism via which C/EBP δ protects from IR-induced intestinal injury and underlying sepsis. In this study, we further investigated whether the increased IR-induced intestinal injury in *Cebpd*^{-/-} mice occurs due to an impaired ability to regulate inflammation and oxidative as well as nitrosative stress responses.

Results

***Cebpd*^{-/-} mice show increased intestinal injury in response to increasing doses of IR.** We have previously shown that compared to 40% mortality in *Cebpd*^{+/+} mice, 100% of *Cebpd*^{-/-} mice die by day 9–13 after exposure to a TBI dose of 8.5 Gy, which occurs due to the increased cell death of the intestinal stem cells of the crypts as well as injury to the bone marrow³². We further characterized the effects of IR exposure on the intestinal injury parameters such as villous height, crypt depth and crypt to villous ratio in the sham and irradiated *Cebpd*^{+/+} and *Cebpd*^{-/-} intestines at 1, 3.5 and 7 days post exposure to a dose of 8.5 Gy. There were no significant differences between *Cebpd*^{+/+} and *Cebpd*^{-/-} mice with respect to villous height, crypt depth and or crypts to villi ratio in the sham group and in the irradiated groups at days 1 and 3.5 post-8.5 Gy exposure. However, at day 7 post-irradiation, *Cebpd*^{-/-} mice showed significant decreases in villous height, crypt depth as well as crypt to villi ratio compared to respective *Cebpd*^{+/+} mice (Fig. 1A–C). Further, analysis of the proliferation marker -proliferating cell nuclear antigen (PCNA) revealed no significant difference between *Cebpd*^{+/+} and *Cebpd*^{-/-} intestines in the sham group. However, *Cebpd*^{-/-} mice showed fewer PCNA-positive proliferating crypts compared to *Cebpd*^{+/+} mice at day 3.5 post-irradiation doses of 7.4 (sublethal dose), 8.5 (LD_{50/30} dose) and 10 Gy (Fig. 2). These results suggest C/EBP δ may have a protective function in the intestinal epithelial and crypt cells in the context of radiation-induced damage.

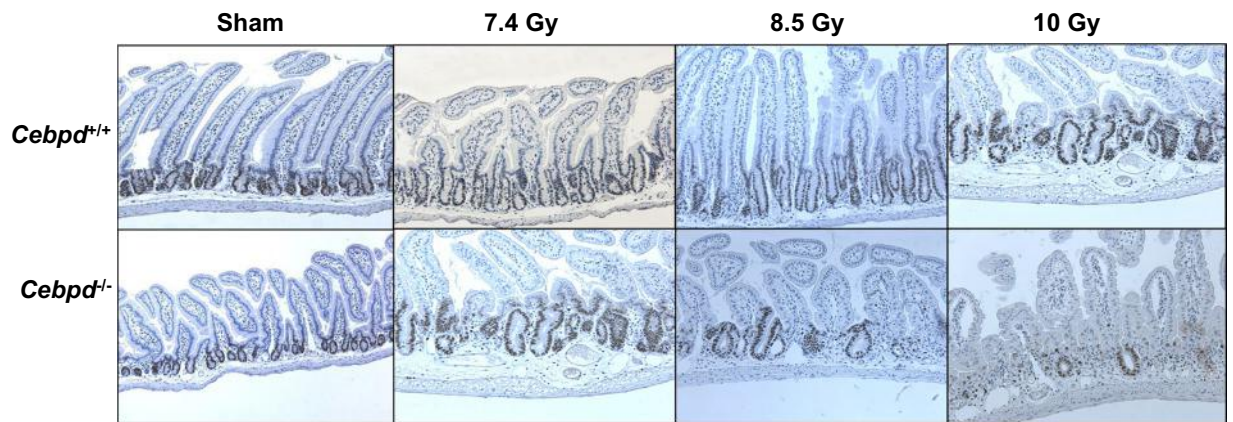


Figure 2. *Cebpd*^{-/-} crypts show decreased proliferation of intestinal crypts with increasing doses of radiation. Representative images showing the expression of PCNA in cross sections of the small intestine from *Cebpd*^{+/+} and *Cebpd*^{-/-} mice exposed to 0, 7.4, 8.5 and 10 Gy and harvested at day 3.5 post-irradiation.

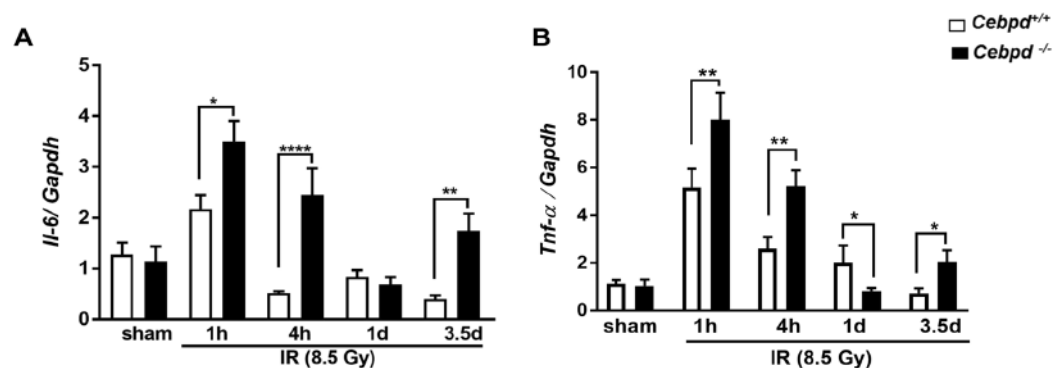


Figure 3. *Cebpd*^{-/-} mice display increased pro-inflammatory cytokines and chemokine expression in intestine tissues after exposure to IR. The mRNA expression of (A) *Il-6* and (B) *Tnf-α*, were analyzed in the intestines of *Cebpd*^{+/+} and *Cebpd*^{-/-} mice and expressed as fold change relative to unirradiated *Cebpd*^{+/+} mice at the indicated timepoints post-irradiation. The data are presented as average + standard error mean (S.E.M.) of n = 3–8 mice per treatment per genotype.

***Cebpd*^{-/-} mice display upregulation of pro-inflammatory cytokines in intestine tissues at early timepoints after exposure to IR.** It is known that exposure to IR leads to increased inflammation and that uncontrolled inflammation exacerbates damage/injury to the tissues^{11,12}. We therefore compared the changes in expression of pro-inflammatory cytokines in the intestine tissues of *Cebpd*^{-/-} and *Cebpd*^{+/+} mice at various timepoints after exposure to IR.

We found that both *Cebpd*^{+/+} mice and *Cebpd*^{-/-} mice showed IR-induced upregulation of *Il-6*. However, *Cebpd*^{-/-} mice showed significantly elevated expression of *Il-6* at 1 h (3.5-fold) and 4 h (2.4-fold) post-irradiation compared to *Cebpd*^{+/+} mice (Fig. 3A). The expression of *Il-6* was downregulated in both genotypes by day 1 post-irradiation. By day 3.5 post-irradiation, the expression of *Il-6* was 1.5-fold in *Cebpd*^{-/-} mice, while it was further downregulated in *Cebpd*^{+/+} mice, compared to respective sham controls (Fig. 3A).

Similarly, we did not find any changes in the expression of *Tnf-α* in sham mice of both genotypes, however post-irradiation there was a robust induction of *Tnf-α* in both *Cebpd*^{+/+} and *Cebpd*^{-/-} mice at 1 h and 4 h post-irradiation. *Cebpd*^{+/+} mice showed a 5-fold induction, while *Cebpd*^{-/-} mice showed 8-fold induction of *Tnf-α* at 1 h post-irradiation compared to respective sham groups. *Cebpd*^{+/+} mice showed 2.5-fold induction at 4 h post-irradiation and about 2-fold at day 1 post-irradiation. In contrast, while *Cebpd*^{-/-} mice showed 5-fold induction of *Tnf-α* at 4 h post-irradiation, but was rapidly downregulated to about 0.5-fold compared to the respective sham group at day 1 post-irradiation (Fig. 3B). Overall, these results indicate elevated expression of the inflammatory cytokines *Il-6* and *Tnf-α* in *Cebpd*^{-/-} mice compared to *Cebpd*^{+/+} mice.

***Cebpd*^{-/-} showed elevated expression of chemokines post-irradiation compared to *Cebpd*^{+/+} mice.**

Next, we examined the expression levels of chemokines, which play a prominent role in the recruitment of inflammatory cells to damaged tissues. Monocyte chemoattractant protein-1 (*Mcp-1*) is a chemokine that recruits monocytes and macrophages to the sites of inflammation³⁴. The expression of *Mcp-1* was upregulated in both *Cebpd*^{+/+} and *Cebpd*^{-/-} mice at day 1 post-irradiation by about 2-fold compared to respective shams. However, by day 3.5 post-irradiation, *Cebpd*^{-/-} mice showed a 6-fold increase in the expression of *Mcp-1* compared

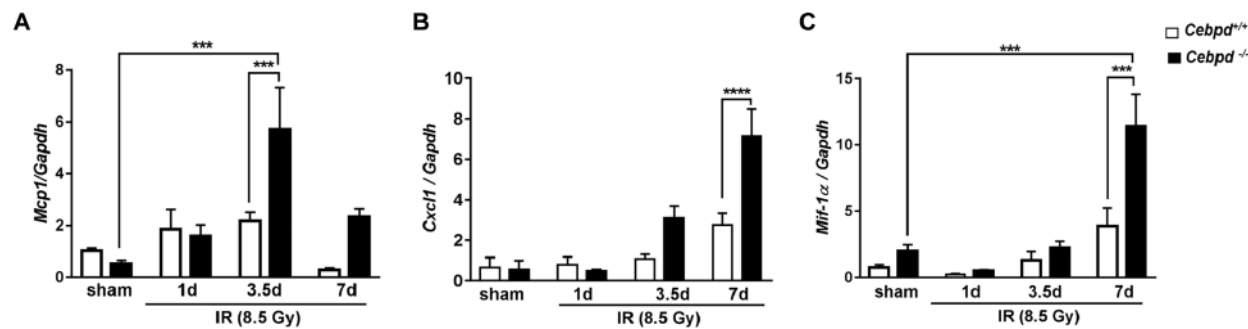


Figure 4. *Cebpd*^{-/-} mice increased intestinal expression of chemokines after exposure to IR. The mRNA expression of (A) *Mcp-1*, (B) *Cxcl1* and (C) *Mif-1-α*, were analyzed in the intestines of *Cebpd*^{+/+} and *Cebpd*^{-/-} mice and expressed as fold change relative to unirradiated *Cebpd*^{+/+} mice at the indicated timepoints post-irradiation. The data are presented as average + S.E.M. of n = 3–8 mice per treatment per genotype.

to *Cebpd*^{+/+} mice (Fig. 4A). In contrast, at day 7 post-irradiation *Cebpd*^{-/-} mice showed a 1.8-fold increase, while *Cebpd*^{+/+} mice showed a dramatic decrease to 0.24-fold when compared with the respective sham groups (Fig. 4A).

Cxcl1 {Chemokine (C-X-C motif) ligand 1} also known as KC is another chemokine expressed by macrophages, neutrophils and epithelial cells and has neutrophil chemoattractant activity³⁵. There were no significant differences in the intestinal expression of *Cxcl1* between both the genotypes in unirradiated mice. At day 7 post-irradiation, *Cebpd*^{-/-} mice showed a 7-fold increase, while *Cebpd*^{+/+} mice showed a 2-fold increase in the expression of *Cxcl1* in the intestine tissues (Fig. 4B).

Macrophage migration inhibitory factor (*Mif-1α*), a pro-inflammatory cytokine which is upregulated by IR and oxidative stress³⁶. MIF also has a chemokine-like function and promotes the directed migration and recruitment of leukocytes into infectious and inflammatory sites^{37,38}. Unirradiated *Cebpd*^{-/-} mice showed slightly higher expression of *Mif-1α*, however this difference was not significant when compared with unirradiated *Cebpd*^{+/+} mice. Interestingly at day 7 post-irradiation, *Cebpd*^{+/+} mice showed a 2-fold induction, while *Cebpd*^{-/-} mice showed a robust upregulation of *Mif-1α* by almost 10-fold (Fig. 4C).

These results indicate that the elevated expression of chemokines may promote the increased recruitment of neutrophils and macrophages, in the intestine tissues of *Cebpd*^{-/-} mice compared to that of *Cebpd*^{+/+} mice after exposure to IR.

***Cebpd*-deficiency promotes increased nitrosative stress in the intestine prior to and post-irradiation.**

iNOS (inducible nitric oxide synthase) or *Nos2* is involved in immune response and is known to be significantly induced by exposure of cells/tissues to IR^{39–42}. *Cebpd*^{-/-} mice showed robust induction of *Nos2* expression in intestine by 10-fold, which is significant compared to respective *Cebpd*^{+/+} mice at 1 h post-irradiation. Both *Cebpd*^{+/+} and *Cebpd*^{-/-} showed elevated expression of *Nos2*, however it reduced about 25- and 22-fold at 4 h and to 2.4-fold and 1.6-fold at 1 day post-irradiation respectively. At day 3.5 post-irradiation, the *Nos2* transcript was induced by 2.6-fold *Cebpd*^{-/-} mice compared to 3-fold in *Cebpd*^{+/+} mice and was not significant (Fig. 5A).

This post-irradiation induction of *Nos2* results in increased nitric oxide levels, which react with the oxygen free radicals produced in the cells as a consequence of radiation-induced oxidative stress to form peroxynitrite, which causes nitrosylation of the cellular proteins^{43,44}. The intestine tissues of *Cebpd*^{+/+} and *Cebpd*^{-/-} mice were compared for the expression levels of 3-nitrotyrosine (3-NT) by HPLC. In the sham group, the intestinal tissue extracts of *Cebpd*^{-/-} mice showed a 1.7-fold increase compared to *Cebpd*^{+/+} mice. Exposure to IR further showed significant increase in the 3-NT expression in the intestinal tissues of *Cebpd*^{-/-} mice compared to *Cebpd*^{+/+} mice and with respect to the sham controls (Fig. 5B).

***Cebpd*-deficiency results in basal and IR-induced oxidative stress.**

Glutathione (GSH) is the global antioxidant which plays a critical role in maintaining the redox state of cells and detoxification of IR-induced oxidative stress^{45,46}. We therefore examined the expression of GSH and its oxidized dimer glutathione disulfide (GSSG) in intestine tissues. The levels of GSH and GSSG were decreased by IR and were not significantly different between both genotypes (Supplementary Fig. 1). A decrease in the ratio of GSH/GSSG is considered a measure of oxidative stress. Interestingly, we found that in the sham group, *Cebpd*^{-/-} mice displayed a significant decrease in the GSH/GSSG compared to *Cebpd*^{+/+} mice (Fig. 6A). At days 1 and 3.5 post-irradiation, although there was a decrease in the GSH/GSSG ratio in both the genotypes, however these differences were not significant. In addition, GSH also acts a scavenger of nitric oxide to form S-nitrosoglutathione (GSNO)^{47,48}. We examined in both *Cebpd*^{+/+} and *Cebpd*^{-/-} intestinal tissues and found that the GSNO levels were significantly elevated at basal levels as well as post-irradiation in *Cebpd*^{-/-} mice compared to *Cebpd*^{+/+} mice (Fig. 6B).

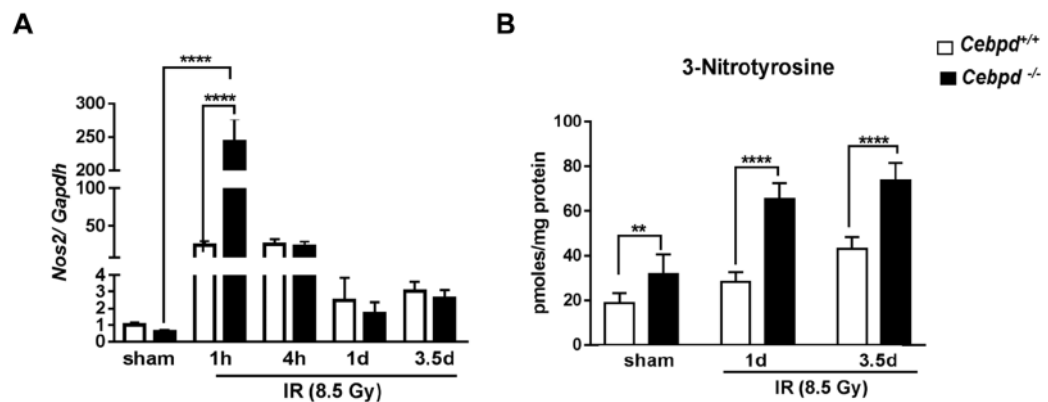


Figure 5. *Cebpd*^{-/-} mice show increased nitrosative stress prior to and after exposure to IR. (A) The mRNA expression of *Nos2* was analyzed and expressed as fold changes relative to that of unirradiated *Cebpd*^{+/+} mice and presented as an average + S.E.M. of n = 4–9 mice per treatment per genotype. (B) The intestine tissue were harvested at indicated timepoints from *Cebpd*^{+/+} and *Cebpd*^{-/-} mice and analyzed for 3-NT. The data are presented as average + S.E.M. of n = 7–9 mice per treatment per genotype.

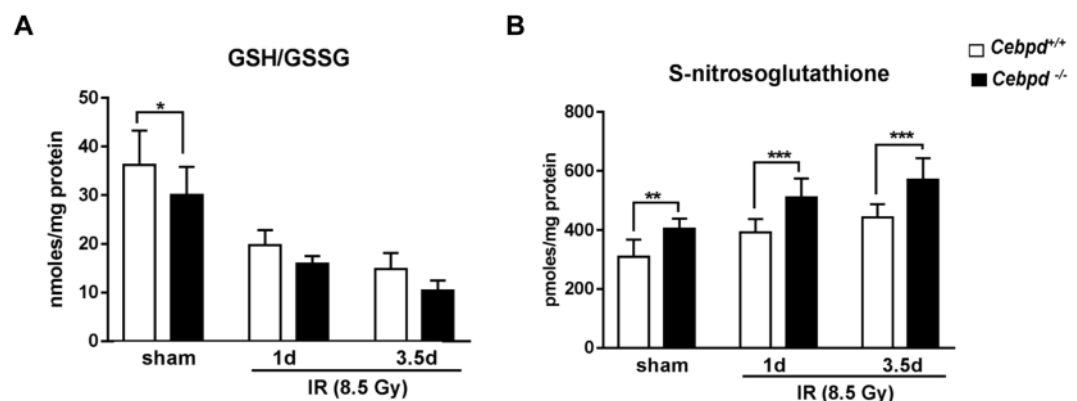


Figure 6. *Cebpd*^{-/-} mice display increased oxidation and nitrosylation of GSH. (A) The levels of oxidized to reduced GSH and (B) GSNO were measured in intestine tissues of *Cebpd*^{+/+} and *Cebpd*^{-/-} mice at indicated timepoints post-irradiation

***Cebpd*-deficient mice show IR-inducible upregulation of Claudin-2 and altered localization in intestine tissue.** There were no significant changes between both the genotypes in the expression of *Cldn-2* in sham unirradiated controls and at day 1 post-irradiation. However at day 3.5 post-irradiation, *Cldn2* mRNA and protein levels were upregulated by 2-fold in the intestine tissues of *Cebpd*^{-/-} mice compared to that of *Cebpd*^{+/+} mice (Fig. 7A,C). Some of the other genes such as *Cldn4*, *Cldn11*, *Ocln* and *Zo-1* did not any significant differences between both the genotypes either in the sham or at day 1 and 3.5 post-irradiation (Supplementary Fig. 2). Further immunofluorescence staining of intestine sections revealed that there were no significant differences in the expression of Claudin-2 in the sham or at day 1 post-irradiation in both the genotypes. The Claudin-2 expression was localized on the basal surface of the epithelial cells in the sham group and at day 1 post-irradiation in both *Cebpd*^{-/-} and *Cebpd*^{+/+} mice. At day 3.5 post-irradiation, the localization of Claudin-2 was found in the tight junctions between the epithelial cells as well on the luminal surface in *Cebpd*^{-/-} mice. In contrast the *Cebpd*^{+/+} mice showed the Claudin-2 expression on the basal surface of the epithelial cells (Fig. 7B).

***Cebpd*-deficient mice show increased IR-induced *in vivo* intestinal permeability, increased endotoxemia and bacterial translocation.** As a functional consequence of Claudin-2 upregulation, next we determined whether irradiated *Cebpd*^{-/-} mice showed alterations in intestinal permeability. *Cebpd*^{-/-} mice showed a 2-fold increase in FITC-dextran levels in plasma compared to *Cebpd*^{+/+} mice at day 3.5 post-irradiation indicative of increased intestinal permeability (Fig. 8A). We further confirmed whether increased intestinal permeability led to a significant increase in the lipopolysaccharide-binding protein (LBP) in *Cebpd*^{-/-} mice after exposure to IR. There were no differences between both genotypes in the sham controls. However, at days 3.5 and 7 post-irradiation, compared to *Cebpd*^{+/+} mice, there was a 5-fold and a 3.7-fold increase in the plasma levels of LBP in *Cebpd*^{-/-} mice, indicative of bacteria in systemic circulation (Fig. 8B). These results correlated with a 2-fold increase in the amplification of 16S rRNA in liver tissues at day 3.5 post-irradiation in *Cebpd*^{-/-} mice compared to that of *Cebpd*^{+/+} mice, indicating translocation of bacteria from the intestine (Fig. 8C). All these results

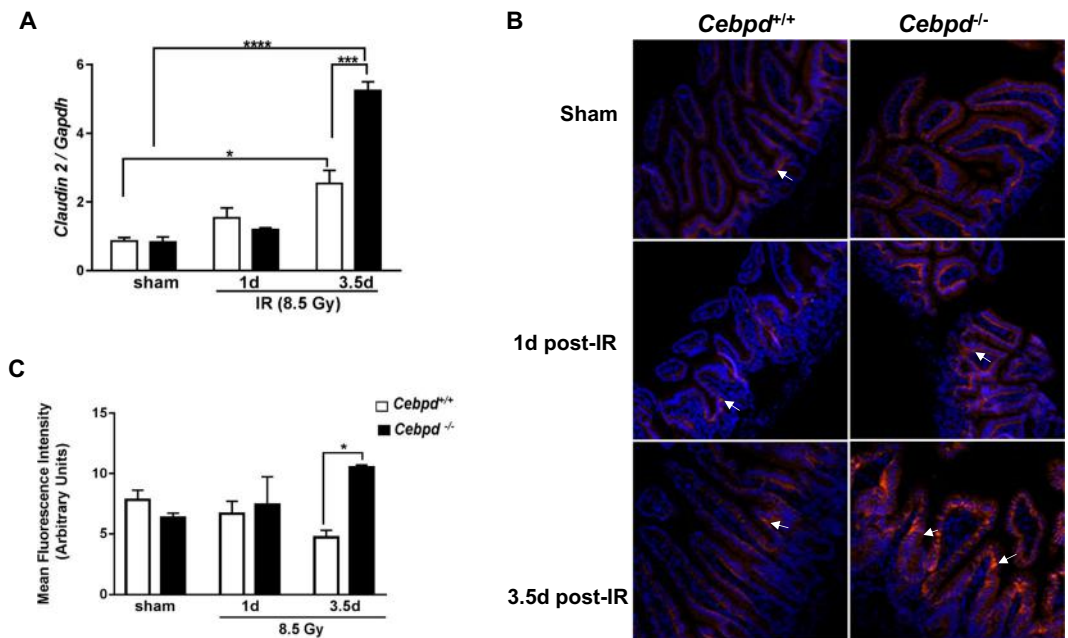


Figure 7. *Cebpd*^{-/-} mice show radiation-induced upregulation of Claudin-2 in the intestine. (A) The expression of *Cldn2* was analyzed in intestine tissues of *Cebpd*^{+/+} and *Cebpd*^{-/-} mice harvested at indicated timepoints post-irradiation. The values are expressed as fold changes normalized to unirradiated *Cebpd*^{+/+} control mice. The data are presented as average + S.E.M. of n = 7–9 mice per treatment per genotype. (B) Representative images of immunofluorescence staining of Claudin 2 in cross sections of the small intestine of *Cebpd*^{+/+} and *Cebpd*^{-/-} mice harvested at indicated timepoints post-8.5 Gy. (C) Quantification of Claudin-2 expression levels in intestinal crypts and villi at indicated time-points after exposure to IR. Values are presented as mean + SEM, n = 3 per genotype per group.

demonstrate that the increased leakiness of the gut in the *Cebpd*^{-/-} mice at day 3.5 post-irradiation leads to the onset of sepsis-like sequelae.

Discussion

Exposure to the whole or substantial parts of the body to IR often result in life-threatening injuries, primarily to self-renewing tissues such as the hematopoietic and GI^{1,3,6,7}. The main cause of lethality after exposure to IR is due to the intestinal bacteria that penetrate the defective mucosal barrier and are an important source of bacteremia. An increase in mucosal permeability occurs through a combination of disruption of epithelial tight junctions and insufficient replacement of the villus epithelium, due to cell death of intestinal progenitor cells in the crypts. Enhanced intestinal permeability, leading to bacterial and lipopolysaccharide translocation are characteristics of IR-induced multiple organ dysfunction syndrome^{16,49}.

Previously, we reported that the increased lethality to IR exposure observed in *Cebpd*^{-/-} mice occurred due to increased thrombocytopenia, neutropenia and loss of intestinal crypts³². These very same processes are implicated as key hallmarks of sepsis^{16,49}. In this study we show that *Cebpd*^{-/-} mice show increased damage to the intestinal villi and crypts at day 7 post 8.5 Gy. Further the loss of intestinal crypts at a dose of 10 Gy suggests a direct role for C/EBP δ in protection of intestinal crypt epithelial cells.

The IR-induced inflammatory response is initiated by the production of ROS/RNS that promote the induction of apoptosis and clonogenic cell death, activation of the transcription of several pro-inflammatory cytokines, chemokines, and growth factors in the microvascular and mucosal compartments, by the recruited immune cells and by enterocytes and residing cells, depending on the severity of tissue trauma^{10,15,50,51}. The production of cytokines such as *Il-6* and *Tnf- α* is time-dependent usually peaking between 4–24 h post-irradiation with subsequent decrease to basal levels with 24 h to few days⁵⁰. It is now realized that sepsis is associated with an “inflammatory storm”, which results in multi-organ damage/failure^{16–18}. *Mcp-1* is one of the key chemokines that regulates migration and infiltration of monocytes/macrophages³⁴, while *Cxcl1* is implicated in recruiting neutrophils that are frequently the first immune cells to enter an inflamed or infected tissue³⁵. *Mif-1 α* is an integral component of host inflammatory responses and is known to be induced by IR and is positively associated with sepsis^{36–38}. In the present study, we found that intestines of *Cebpd*^{-/-} mice showed rapid upregulation of the pro-inflammatory cytokines, *Il-6* and *Tnf- α* at early timepoints post-irradiation. In contrast, the expression of chemokines such as *Mcp-1*, *Cxcl1* and *Mif1- α* were upregulated by days 3.5 and 7 post-irradiation compared to *Cebpd*^{+/+} mice.

Inducible nitric oxide synthase (iNOS) is expressed by infiltrating as well as resident activated macrophages in inflamed gastrointestinal tissue and is also stimulated by pro-inflammatory cytokines like *Il-6* and *Tnf- α* as well as by IR⁴². In response to IR exposure, the increased nitric oxide reacts with superoxide formed by the mitochondria to form peroxynitrite (ONOO⁻) which is a prooxidant. Peroxynitrite reacts with the tyrosine residues in the

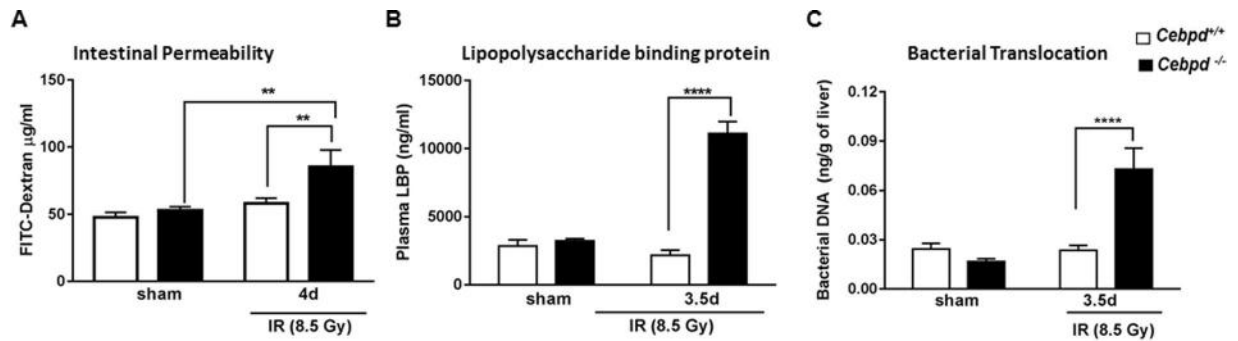


Figure 8. *Cebpd*^{-/-} mice show increased intestinal barrier disruption and bacterial translocation after exposure to IR. Blood, intestine and liver tissues were harvested at the indicated timepoints from *Cebpd*^{+/+} and *Cebpd*^{-/-} mice after exposure to IR. (A) Intestinal permeability was measured by analyzing plasma samples for the presence of FITC-Dextran, (B) Bacterial translocation was measured by amplification of 16S rRNA in liver tissues by real-time PCR and (C) LBP was measured in plasma samples by ELISA. All the data are presented as average + S.E.M. of n = 7–9 samples per treatment group.

cellular proteins and forms 3-NT^{43,44}. Increased 3-NT causes increased radiation-induced intestinal toxicity and blocking or reducing 3-NT protects against radiation injury. In the present study, *Cebpd*^{-/-} mice show elevated levels of 3-NT at basal as well as post-irradiation compared to *Cebpd*^{+/+} mice.

GSH is the first line of defense for oxidative stress⁴⁵. Decreased levels of GSH indicate decrease capacity to remove free radicals. The ratio of GSH/GSSG is a measure of redox state of the cell or tissue⁴⁶. Interestingly, the expression of GSH/GSSG in the intestine tissues of *Cebpd*^{-/-} mice were significantly lower than that of *Cebpd*^{+/+} mice indicative of increased oxidative stress in the sham controls.

The elevated levels of NO produced are scavenged by the cellular antioxidant, GSH, resulting in the formation of GSNO^{47,48}. GSNO is the nitrosylated form of reduced glutathione (GSH), responsible for its antioxidant cytoprotective action⁴⁷. Although GSNO is shown to have a protective function in maintaining the epithelial barrier function⁴⁸, we found that *Cebpd*^{-/-} mice expressed significantly elevated GSNO levels in the sham as well irradiated group. At very high concentrations, GSNO is converted to GSSG and NO and the released NO can react with superoxide present in the cell and generate increased peroxynitrite as described previously⁴³. This could be a plausible mechanism for the increased 3-NT levels, as we have previously shown evidence for basal as well as IR-induced oxidative stress and mitochondrial dysfunction via reduced expression of GSH levels in *Cebpd*-deficient MEFs³³. The increased mRNA levels of iNOS and increased expression of 3-NT and GSNO are indicative of overall increased nitrosative stress in the intestines of *Cebpd*^{-/-} mice compared to that of *Cebpd*^{+/+} mice.

The epithelial tight junctions form a barrier to the entry of allergens, toxins and pathogens across the epithelium into the interstitial tissue. The tight junction proteins, adherens junction and desmosomes seal the intercellular junctions of intestinal epithelial cells^{52,53}. While the tight junctions function as a barrier from noxious molecules and a pore for the permeation of ions, solutes and water, the adherence junctions and desmosomes provide a strong adhesive bond between cells and in intercellular communication. One of the mechanisms via which inflammation promotes intestinal permeability is via the downregulation of tight junction proteins such as Occludin, junctional adhesion molecules (JAM), ZO-1, Claudins etc.^{54–60}. In addition, ROS and RNS can promote the disruption of tight junctions and promote intestinal permeability^{56,57}. Studies have shown that radiation injury led to downregulation of the tight junction proteins in the intestinal mucosa^{54,55}. The upregulation of Claudin2 by IL-6 as well as TNF- α are known to cause an increase in intestinal permeability^{60,61}. Similarly in this study, we found significantly elevated expression of *Il-6* and *Tnf- α* , which correlated with the upregulation of *Cldn2* in *Cebpd*^{-/-} mice at day 3.5 post-irradiation. Further studies in other inflammatory intestinal disorders have reported altered localization of Claudin 2 similar to that observed in irradiated *Cebpd*^{-/-} mice^{62,63}. These results correlated with the increased *in vivo* intestinal permeability and elevated plasma LBP levels as well as bacterial translocation observed in irradiated *Cebpd*^{-/-} mice. *Cebpd*^{-/-} mice show increased inflammatory, oxidative and nitrosative stress that leads to increased intestinal permeability and bacterial translocation at day 3.5 post-irradiation, thus confirming that the increased mortality to radiation occurs due to underlying sepsis.

The present study uncovers a novel role for C/EBP δ in protection from IR-induced gut injury and underlying sepsis-mediated lethality by downregulating the IR-induced oxidative/nitrosative stress and inflammatory responses (Fig. 9). Further studies are warranted to elucidate whether blocking the IR-induced inflammation and oxidative/nitrosative stress can alleviate the lethality of *Cebpd*-deficient mice to IR. Overall these results may have relevance in terms of human exposure to IR either in accidental exposure or in the clinical setting. Recently we have described that C/EBP δ is essential to mediate the radioprotective functions of the potent radioprotector gamma-tocotrienol (GT3)⁶⁴. We found that GT3 induces the C/EBP δ expression in the intestine and helps protect the *Cebpd*-WT mice, but was unable to impart protection to *Cebpd*-KO mice from radiation induced injury to the intestinal and hematopoietic systems. Therefore it can be speculated that agents that induce C/EBP δ expression may have the potential to protect normal tissue from radiation-induced damage to the intestine tissues in the clinical setting as well.

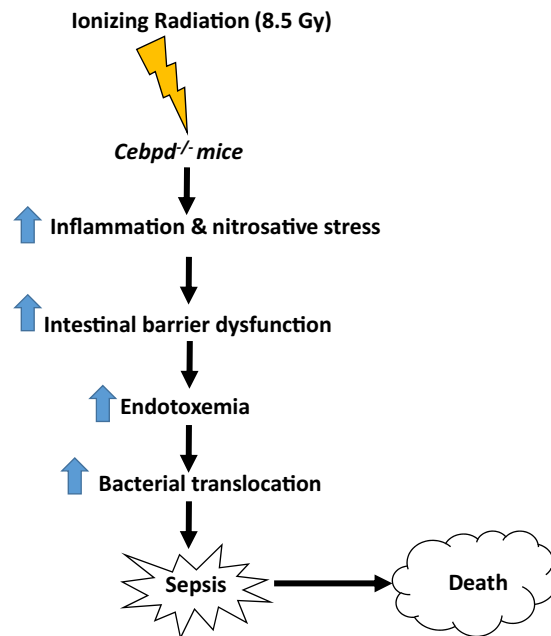


Figure 9. Schematic model depicting IR-induced increased inflammation and nitrosative stress that leads to increased intestinal permeability and bacterial translocation in *Cebpd*^{-/-} mice.

Materials and Methods

Ethics statement. This study was carried out in strict accordance with the recommendations in the Guide for the Care and Use of Laboratory Animals of the National Institutes of Health and approved by the Institutional Animal Care and Use Committee of the University of Arkansas for Medical Sciences.

Animals. *Cebpd*-heterozygous breeder mice were backcrossed for more than 20 generations to the C57BL/6 strain background. Genotyping was done as described previously⁶⁵. In all the studies, 10–12 weeks old subjects derived from heterozygous mating pairs and litter mate controls were used whenever possible. The animals were housed in the Division of Laboratory Medicine (DLAM, University of Arkansas for Medical Sciences, Little Rock, AR) under standardized conditions with controlled temperature and humidity and a 12 h day, 12 h night light cycle. Blood, intestine and liver tissues were harvested following isoflurane inhalation to minimize suffering and the animals were euthanized by cervical dislocation.

Irradiation of mice. Irradiation was administered in a Mark I irradiator (J. L. Shepherd). Dose uniformity was assessed by an independent company (Ashland Specialty Ingredients) with radiographic film and alanine tablets. Alanine tables were analyzed by the National Institute of Standards and Technology (Gaithersburg, MD, USA) and demonstrated a dose rate of 1.14 Gy/min at 21 cm from the source. For each experiment the dose rate was corrected for decay.

Assessment of villus height and crypt depth. Intestinal tissue sections stained with hematoxylin and eosin (H&E) were used to measure villus height and crypt depth using a computer-assisted image analysis platform (ImageScope ver 12.2.2.5, Leica Biosystems, e, MD, USA). Intestinal tissues fixed in Methyl-Carnoy's fixed and embedded in paraffin were cut into 2–4 μm sections with a microtome. The slides with tissue sections were de-waxed by placing in an incubator overnight set at 60 °C, cooled down to room temperature, dipped into hematoxylin solution for 30 s, washed with deionized water, stained with 1% eosin solution, dehydrated with two changes in 95% and 100% alcohol for 30 s each, washed with xylene, and finally mounted with low viscosity Permount™ mounting media (Thermo Fisher Scientific, Grand Island, NY, USA). Mucosal villus height was measured from the tip to the base of each villus, and crypt depth was measured from the crypt base to the top opening. Images captured at 4x magnification were analyzed for crypt to villus measurements. 20 villi and crypts were respectively analyzed for villous height and crypt depth measurements on images at 20x magnification.

Immunohistochemical staining for PCNA. Jejunums were collected from *Cebpd*^{+/+} and *Cebpd*^{-/-} mice 0 and 3.5 days post-TBI (0, 7.4, 8.5 and 10 Gy), after isoflurane anesthesia. The intestine tissues were fixed with methanol carnoy's fixative (methanol: chloroform: acetic acid, 6:3:1) for 24 h, dehydrated, were embedded in paraffin in cross-sectional orientation. For staining, sections of 5-μm thickness were cut, dewaxed, rehydrated in PBS (10 mM sodium phosphate, pH 7.4; 140 mM NaCl).

Samples were probed with antibody to PCNA (FL-261)-sc7907 (Santa Cruz Biotechnology Inc., Dallas, TX) at 1:100 dilution in blocking buffer (2% goat serum, PBS). For control sections, blocking buffer contained blocking

solution only (no primary antibody). The PCNA expression was detected with biotinylated anti-rabbit IgG (Vector Laboratories, BA-1000) at 1:400 dilution and developed with 3, 3' diaminobenzidine tetrahydrochloride. Images for PCNA were captured at 20X magnification.

Immunofluorescence staining for Claudin-2. The intestine tissues were fixed with methanol carnoy's fixative (methanol: chloroform: acetic acid, 6:3:1) for 24 h, dehydrated, were embedded in paraffin in cross-sectional orientation. Sections were stained with rabbit anti-Claudin-2 (ab53032) (Abcam) at 1:50 dilution in blocking buffer (0.5% BSA, 0.05% Tween-20, PBS). Each section was probed and goat anti-rabbit IgG-AlexaFluor 594 (Invitrogen) at 1:400 dilution for 1 h at 37°C and then rinsed three times with 0.05% Tween-20 in PBS. After staining, sections were counterstained with 4',6-diamidino-2-phenylindol to visualize cell nuclei and were mounted under cover slips with Prolong Antifade kit (Invitrogen). Images for Claudin-2 and DAPI staining were acquired with an Olympus IX-51 inverted microscope (Olympus America) with a 10× objective, equipped with Hamamatsu ORCA-ER monochrome camera (Hamamatsu Photonics K.K.). For claudin-2 staining, a total of 5 fields of view per tissue section (10× objective), and the mean intensity was measured in each compartment. The average mean intensity of the field of view per tissue section was considered as a datapoint for statistical analysis. The data are presented as mean fluorescence intensity per field in $n = 4$ animals per timepoint. Slidebook 4.2 software (Intelligent Imaging Innovations, Inc.) was used for image capturing and analysis.

Real-time PCR. Total RNA was purified from frozen tissue using RNeasy Plus Mini Kit (Qiagen, Valencia, CA, USA) as instructed by the manufacturer after homogenizing the samples in TRIzol® Reagent (Life Technologies, Grand Island, NY, USA). cDNA was synthesized using a cDNA reverse transcription kit (Life Technologies, Grand Island, NY, USA) after treating the RNA samples with DNase I (Qiagen, Valencia, CA, USA). Predesigned Taqman assay for mouse genes: *Il-6*, Mm00446190_m1; *Tnf-α* Mm00443258_m1; *Cxcl1*, Mm04207460_m1; *Mcp-1*, Mm00441242_m1; *Mif-1α*, Mm01611157_m1; *Nos2*, Mm00440502_m1; *Cldn2*, Mm00516703_s1; *Cldn4*, Mm00515514_s1; *Cldn11*, Mm00500915_m1; *Ocln*, Mm00500912_m1; *Zo-1*, Mm00493699_m1 and *Gapdh*, Mm99999915_g1 were obtained from (Life Technologies, Grand Island, NY, USA). *Gapdh* was used as an endogenous reference gene. Fold changes were calculated by normalizing to unirradiated WT sample using the standard $2^{-\Delta\Delta Ct}$ method as described previously²³.

HPLC assays. High-performance liquid chromatography (HPLC) was used to quantify the reduced as well as oxidized glutathione (GSH, GSSG), S-nitrosoglutathione (GSNO) and 3-nitrotyrosine (3-NT). Approximately 20 mg of intestine tissue were homogenized in ice-cold phosphate-buffered saline. To precipitate proteins, 10% metaphosphoric acid was added to the homogenate and incubated for 30 min on ice. The samples were then centrifuged at 18,000 g at 4°C for 15 min, and 20 μl of the resulting supernatants were injected into the HPLC column for metabolite quantification, while the pellet was used for protein analysis using BCA protein assay. The details for HPLC elution and electrochemical detection of free unbound GSH, GSSG, GSNO and 3-NT in proteins (hydrolyzed by 6 N HCl treatment) have been described previously described⁶⁶.

In vivo intestinal permeability assay. Intestinal permeability was measured in 20 mice (5 per group) as described by Biju *et al.*⁶⁷. Briefly, 4 days after exposure to 0 and 8.5 Gy irradiation, the mice were anesthetized with isoflurane inhalation, a midline laparotomy was performed, and the renal artery and vein were ligated bilaterally. A 10 cm small intestinal segment, located 5 cm distal to the ligament of Treitz was isolated and tied off. One hundred microliters of 4-kDa fluorescein isothiocyanate conjugated dextran (FITC-dextran 25 mg/ml in phosphate-buffered saline) was injected into the isolated intestine using a 30 Gauge needle and the abdominal incision was closed. After 90 min, blood was collected from the retro-orbital sinus and plasma was separated by centrifuging at 4°C, 8000 rpm for 10 min. The concentration of FITC-dextran was determined with a fluorescence spectrophotometer SpectraMax M2^e (Molecular Devices, CA, USA) at an excitation wavelength of 480 nm and an emission wavelength of 520 nm. Standard curves were prepared from dilutions of FITC-dextran in PBS to calculate FITC-dextran concentration in the plasma samples.

ELISA assay. Plasma LBP level was measured using the mouse LBP ELISA kit (HK205) from Hycult Biotech, Uden, Netherlands. Briefly, blood was collected in EDTA coated tubes, centrifuged at 2000 rpm at 4°C for 15 min and plasma samples were snap frozen and stored at -80°C. One hundred μl of standard and plasma samples were loaded onto pre-coated 96-well plates, incubated for 2 h at room temperature. Biotinylated tracer antibody was incubated for 1 h at room temperature, developed against a streptavidin-peroxidase conjugate, and absorbance was measured at 450 nm. The concentration of LBP was determined against the standard curve. Values are expressed as nanogram LBP protein per ml plasma.

Bacterial translocation. Bacterial translocation was determined as bacterial load in liver tissue and was quantified by real time PCR using the 16S rRNA gene consensus sequence. The total load of bacteria in the liver was determined using primer sequences to amplify the highly conserved sequence for a broad species consensus as reported elsewhere⁶⁷. Livers were removed aseptically and homogenized immediately. Bacterial translocation was quantified by real-time PCR. Briefly, DNA was isolated from sterile livers harvested at baseline and at day 3.5 post-exposure to 8.5 Gy using a DNA purification kit (Promega, Madison, WI). Real-time PCR was performed using PowerUp SYBR green PCR master mix (Applied Biosystems, Foster City, CA) and 16S rRNA gene targeted primers, forward (5'-ACTCCTACGGGAGGCAGCAGT-3') and reverse (5'-TATTACCGCGGCTGCTGGC-3'). Serially diluted bacterial genomic DNA was used to generate the standard curve. PCR-derived bacterial counts were expressed as nanogram bacterial DNA per gram mouse liver tissue.

Statistical analyses. Statistical analysis was performed using GraphPad Prism 7.0 (GraphPad Software, San Diego, California). Data were expressed as mean \pm S.E.M. unless otherwise specified. One-way ANOVA analysis with Tukey's post analysis was used to study the differences among 3 or more means. Significance was determined at 95% confidence interval and $p < 0.05$ was considered statistically significant.

Data Availability

Data or reagent described in this study will be made available upon request.

References

- Hatchett, R. J. M. Slow progress in preparing for radiological and nuclear emergencies. [Editorial]. *Disaster Medicine & Public Health Preparedness* **5**, 180–182 (2011).
- Moulder, J. E. 2013 Dade W. Moeller Lecture: Medical Countermeasures Against Radiological Terrorism. [Article]. *Health Physics* **107**, 164–171 (2014).
- Williams, J. P. *et al.* Addressing the Symptoms or Fixing the Problem? Developing Countermeasures against Normal Tissue Radiation Injury. *Radiation Research* **186**, 1–16 (2016).
- Shadad, A. K., Sullivan, F. J., Martin, J. D. & Egan, L. J. Gastrointestinal radiation injury: Symptoms, risk factors and mechanisms. *World Journal of Gastroenterology: WJG* **19**, 185–198 (2013).
- Shadad, A. K., Sullivan, F. J., Martin, J. D. & Egan, L. J. Gastrointestinal radiation injury: Prevention and treatment. *World Journal of Gastroenterology: WJG* **19**, 199–208 (2013).
- Dainiak, N. M. *et al.* Literature review and global consensus on management of acute radiation syndrome affecting nonhematopoietic organ systems. [Review]. *Disaster Medicine & Public Health Preparedness* **5**, 183–201 (2011).
- Singh, V. K., Romaine, P. L. & Seed, T. M. Medical Countermeasures for Radiation Exposure and Related Injuries: Characterization of Medicines, FDA Approval Status and Inclusion into the Strategic National Stockpile. *Health Physics* **108**, 607–630 (2015).
- Rosen, E. M., Day, R. & Singh, V. K. New approaches to radiation protection. *Front Oncol* **4**, 381 (2014).
- Potten, C. S. Extreme sensitivity of some intestinal crypt cells to X and gamma irradiation. *Nature* **269**, 518–521 (1977).
- Francois, A., Milliat, F., Guipaud, O. & Benderitter, M. Inflammation and immunity in radiation damage to the gut mucosa. *Biomed Res Int* **2013**, 123241 (2013).
- Schaeue, D. M. *et al.* Radiation and inflammation. *Semin Radiat Oncol* **25**, 4–10 (2015).
- Di Maggio, F. M. *et al.* Portrait of inflammatory response to ionizing radiation treatment. *Journal of Inflammation* **12**, 1–11 (2015).
- Mollà, M. & Panés, J. Radiation-induced intestinal inflammation. *World Journal of Gastroenterology: WJG* **13**, 3043–3046 (2007).
- Ong, Z. Y. *et al.* Pro-inflammatory cytokines play a key role in the development of radiotherapy-induced gastrointestinal mucositis. *Radiat Oncol* **5**, 22 (2010).
- Polistena, A. *et al.* Local radiotherapy of exposed murine small bowel: apoptosis and inflammation. *BMC Surg* **8**, 1 (2008).
- Monti, P., Wysocki, J., van der Meeren, A. & Griffiths, N. M. The contribution of radiation-induced injury to the gastrointestinal tract in the development of multi-organ dysfunction syndrome or failure. In *The British Journal of Radiology*, **78**, 89–94 (The British Institute of Radiology, 2005).
- Alverdy, J. C. & Chang, E. B. The re-emerging role of the intestinal microflora in critical illness and inflammation: why the gut hypothesis of sepsis syndrome will not go away. *Journal of leukocyte biology* **83**, 461–466 (2008).
- Brown, M. What causes the radiation gastrointestinal syndrome?: overview. *International Journal of Radiation Oncology, Biology, Physics* **70**, 799–800 (2008).
- O'Rourke, J. P., Newbound, G. C., Hutt, J. A. & Dewille, J. CCAAT/enhancer-binding protein delta regulates mammary epithelial cell G0 growth arrest and apoptosis. *Journal of Biological Chemistry* **274**, 16582–16589 (1999).
- Gery, S., Tanosaki, S., Hofmann, W. K., Koppel, A. & Koeffler, H. P. C/EBP[delta] expression in a BCR-ABL-positive cell line induces growth arrest and myeloid differentiation. [Article]. *Oncogene* **24**, 1589–1597 (2005).
- Huang, A. M. *et al.* Loss of CCAAT/enhancer binding protein delta promotes chromosomal instability. *Oncogene* **23**, 1549–1557 (2004).
- Wang, J. *et al.* CCAAT/enhancer binding protein delta (C/EBPdelta, CEBPD)-mediated nuclear import of FANCD2 by IPO4 augments cellular response to DNA damage. *Proceedings of the National Academy of Sciences* **107**, 16131–16136 (2010).
- Pawar, S. A. *et al.* C/EBP delta targets cyclin D1 for proteasome-mediated degradation via induction of CDC27/APC3 expression. *Proceedings of the National Academy of Sciences of the United States of America* **107**, 9210–9215 (2010).
- Hour, T. C. *et al.* Transcriptional up-regulation of SOD1 by CEBPD: a potential target for cisplatin resistant human urothelial carcinoma cells. *Biochemical Pharmacology* **80**, 325–334 (2010).
- Barbaro, V. *et al.* C/EBPdelta regulates cell cycle and self-renewal of human limbal stem cells. *Journal of Cell Biology* **177**, 1037–1049 (2007).
- Porter, D. *et al.* Molecular markers in ductal carcinoma *in situ* of the breast. *Mol Cancer Res* **1**, 362–375 (2003).
- Sarkar, T. R. *et al.* Identification of a Src tyrosine kinase/SIAH2 E3 ubiquitin ligase pathway that regulates C/EBPdelta expression and contributes to transformation of breast tumor cells. *Mol Cell Biol* **32**, 320–332 (2012).
- Alam, T., An, M. R. & Papaconstantinou, J. Differential expression of three C/EBP isoforms in multiple tissues during the acute phase response. *Journal of Biological Chemistry* **267**, 5021–5024 (1992).
- Poli, V. The role of C/EBP isoforms in the control of inflammatory and native immunity functions. *Journal of Biological Chemistry* **273**, 29279–29282 (1998).
- Lu, Y. C. *et al.* Differential role for c-Rel and C/EBPbeta/delta in TLR-mediated induction of proinflammatory cytokines. *Journal of Immunology* **182**, 7212–7221 (2009).
- Balamurugan, K. & Sterneck, E. The many faces of C/EBPdelta and their relevance for inflammation and cancer. *Int J Biol Sci* **9**, 917–933 (2013).
- Pawar, S. A. *et al.* C/EBP delta deficiency sensitizes mice to ionizing radiation-induced hematopoietic and intestinal injury. *PLoS ONE* **9**, e94967 (2014).
- Banerjee, S. *et al.* Loss of C/EBPδ enhances IR-induced cell death by promoting oxidative stress and mitochondrial dysfunction. *Free Radical Biology and Medicine* **99**, 296–307 (2016).
- Deshmane, S. L., Kremlev, S., Amini, S. & Sawaya, B. E. Monocyte chemoattractant protein-1 (MCP-1): an overview. *J Interferon Cytokine Res* **29**, 313–326 (2009).
- De Filippo, K. *et al.* Mast cell and macrophage chemokines CXCL1/CXCL2 control the early stage of neutrophil recruitment during tissue inflammation. *Blood* **121**, 4930–4937 (2013).
- Gupta, Y., Pasupuleti, V., Du, W. & Welford, S. M. Macrophage migration inhibitory factor secretion is induced by ionizing radiation and oxidative stress in cancer cells. *PLoS One* **11**, e0146482 (2016).
- Bernhagen, J. *et al.* MIF is a noncognate ligand of CXC chemokine receptors in inflammatory and atherogenic cell recruitment. *Nat Med* **13**, 587–596 (2007).

38. Gando, S. *et al.* High macrophage migration inhibitory factor levels in disseminated intravascular coagulation patients with systemic inflammation. *Inflammation* **30**, 118–124 (2007).
39. Davies, M. G., Fulton, G. J. & Hagen, P. O. Clinical biology of nitric oxide. *British Journal of Surgery* **82**, 1598–1610 (1995).
40. Kobayashi, Y. The regulatory role of nitric oxide in proinflammatory cytokine expression during the induction and resolution of inflammation. *Journal of Leukocyte Biology* **88**, 1157–1162 (2010).
41. McKinney, L. C., Aquilla, E. M., Coffin, D., Wink, D. A. & Vodovotz, Y. Ionizing radiation potentiates the induction of nitric oxide synthase by interferon-gamma and/or lipopolysaccharide in murine macrophage cell lines: Role of tumor necrosis factor- α . *Annals of the New York Academy of Sciences* **899**, 61–68 (2000).
42. MacNaughton, W. K., Aurora, A. R., Bhamra, J., Sharkey, K. A. & Miller, M. J. Expression, activity and cellular localization of inducible nitric oxide synthase in rat ileum and colon post-irradiation. *Int J Radiat Biol* **74**, 255–264 (1998).
43. Dijkstra, G. *et al.* Expression of nitric oxide synthase and formation of nitrotyrosine and reactive oxygen species in inflammatory bowel disease. *Journal of Pathology* **186**, 416–421 (1998).
44. Banerjee, S. *et al.* The neuronal nitric oxide synthase inhibitor NANT blocks acetaminophen toxicity and protein nitration in freshly isolated hepatocytes. *Free Radical Biology & Medicine* **89**, 750–757 (2015).
45. Chatterjee, A. *et al.* Reduced glutathione: a radioprotector or a modulator of DNA-repair activity? *Nutrients* **5**, 525–542 (2013).
46. Lushchak, V. I. Glutathione homeostasis and functions: Potential targets for medical interventions. *Journal of Amino Acids* **736837**, 1–27 (2012).
47. Broniowska, K. A., Diers, A. R. & Hogg, N. S-Nitrosoglutathione. *Biochimica et Biophysica Acta* **1830**, 3173–3181 (2013).
48. Constantini, T. W. *et al.* Vagal nerve stimulation protects against burn-induced intestinal injury through activation of enteric glial cells. *American Journal of Physiology, Gastrointestinal and Liver Physiology* **299**, G1308–G1318 (2010).
49. Cohen, J. The immunopathogenesis of sepsis. *Nature* **420**, 885–891 (2002).
50. Hong, J. H. *et al.* Induction of acute phase gene expression by brain irradiation. *International Journal of Radiation Oncology, Biology, Physics* **33**, 619–626 (1995).
51. Mittal, M. *et al.* Reactive oxygen species in inflammation and tissue injury. *Antioxidants & Redox Signaling* **20**, 1126–1167 (2014).
52. Suzuki, T. Regulation of intestinal epithelial permeability by tight junctions. In *Cell. Mol. Life Sci* **70**, 631–659 (2013).
53. Rowlands, B. J., Soong, C. V. & Gardiner, K. R. The gastrointestinal tract as a barrier in sepsis. *British Medical Bulletin* **55**, 196–211 (1999).
54. Garg, S. *et al.* Segmental Differences in Radiation-Induced Alterations of Tight Junction-Related Proteins in Non-Human Primate Jejunum, Ileum and Colon. *Radiation research* **185**, 50–59 (2016).
55. Shukla, P. K. *et al.* Rapid disruption of intestinal epithelial tight junction and barrier dysfunction by ionizing radiation in mouse colon in vivo: protection by N acetyl-L-cysteine. *American Journal of Physiology - Gastrointestinal and Liver Physiology* **310**, G705–G715 (2016).
56. Ara, N. *et al.* Disruption of gastric barrier function by luminal nitrosative stress: a potential chemical insult to the human gastro-oesophageal junction. *Gut* **57**, 306–313 (2008).
57. Bhattacharyya, A., Chattopadhyay, R., Mitra, S. & Crowe, S. E. Oxidative stress: an essential factor in the pathogenesis of gastrointestinal mucosal diseases. *Physiol Rev* **94**, 329–354 (2014).
58. Tang, Y. *et al.* Nitric oxide-mediated intestinal injury is required for alcohol-induced gut leakiness and liver damage. *Alcoholism, Clinical and Experimental Research* **33**, 1220–1230 (2009).
59. Al-Sadi, R. *et al.* Interleukin-6 modulation of intestinal epithelial tight junction permeability is mediated by JNK pathway activation of Claudin-2 gene. *PLoS ONE* **9**, e85345 (2014).
60. Suzuki, T., Yoshinaga, N. & Tanabe, S. Interleukin-6 (IL-6) regulates Claudin-2 expression and tight junction permeability in intestinal epithelium. *Journal of Biological Chemistry* **286**, 31263–31271 (2011).
61. Mankertz, J. *et al.* TNF α up-regulates Claudin-2 expression in epithelial HT-29/B6 cells via phosphatidylinositol-3-kinase signaling. *Cell and Tissue Research* **336**, 67–77 (2009).
62. Kusugami, K. *et al.* Elevation of interleukin-6 in inflammatory bowel disease is macrophage- and epithelial cell-dependent. *Dig Dis Sci* **40**, 949–959 (1995).
63. Ares, G. *et al.* Caveolin 1 is associated with upregulated Claudin 2 in Necrotizing Enterocolitis. *Scientific Reports* **9**, 4982 (2019).
64. Banerjee, S. *et al.* *Cebpd* is essential for Gamma-Tocotrienol mediated protection against radiation-induced hematopoietic and intestinal injury. *Antioxidants* **7**, 55 (2018).
65. Sterneck *et al.* Selectively enhanced contextual fear conditioning in mice lacking the transcriptional regulator CCAAT/enhancer binding protein delta. *Proceedings of the National Academy of Sciences of the United States of America* **95**, 10908–10913 (1998).
66. Melnyk, S., Pogribna, M., Pogribny, L., Hine, R. J. & James, S. J. A new HPLC method for the simultaneous determination of oxidized and reduced plasma aminothiols using coulometric electrochemical detection. *The Journal of Nutritional Biochemistry* **10**, 490–497 (1999).
67. Biju, P. G. *et al.* Procalcitonin as a predictive biomarker for total body irradiation-induced bacterial load and lethality in mice. *Shock* **38**, 170–176 (2012).

Acknowledgements

The authors acknowledge Dr. Randolph Mildred, Gail Wagoner, Bianca Schutte, Erika Nicholson, Rebecca Mitchell, Jeannie Holland and Bridgette Angie for excellent animal care. Grant support by the Center for Host Responses to Cancer therapy COBRE Grant P20GM109005 (S.A.P. and M.H.J.); CDMRP-Department of Defense (PR140967) W81XWH-15-1-0489 (S.A.P. and M.H.J.); and the Arkansas Bioscience Institute (S.A.P. and S.B.M.) is gratefully acknowledged.

Author Contributions

S.B., Q.F., S.A.P., conceived and designed the experiments; S.B., Q.F., S.K.S., S.B.M. performed the experiments; S.B., S.A.P. analyzed the data and prepared the figures; S.B., E.S., M.H.J. and S.A.P. wrote the paper.

Additional Information

Supplementary information accompanies this paper at <https://doi.org/10.1038/s41598-019-49437-x>.

Competing Interests: The authors declare no competing interests.

Publisher's note: Springer Nature remains neutral with regard to jurisdictional claims in published maps and institutional affiliations.



Open Access This article is licensed under a Creative Commons Attribution 4.0 International License, which permits use, sharing, adaptation, distribution and reproduction in any medium or format, as long as you give appropriate credit to the original author(s) and the source, provide a link to the Creative Commons license, and indicate if changes were made. The images or other third party material in this article are included in the article's Creative Commons license, unless indicated otherwise in a credit line to the material. If material is not included in the article's Creative Commons license and your intended use is not permitted by statutory regulation or exceeds the permitted use, you will need to obtain permission directly from the copyright holder. To view a copy of this license, visit <http://creativecommons.org/licenses/by/4.0/>.

© The Author(s) 2019



Article

Cebpd Is Essential for Gamma-Tocotrienol Mediated Protection against Radiation-Induced Hematopoietic and Intestinal Injury

Sudip Banerjee ¹, Sumit K. Shah ¹, Stepan B. Melnyk ², Rupak Pathak ¹ , Martin Hauer-Jensen ¹ and Snehalata A. Pawar ^{1,*}

¹ Division of Radiation Health, University of Arkansas for Medical Sciences, Little Rock, AR 72205, USA; SBanerjee@uams.edu (S.B.); SSHAH3@uams.edu (S.K.S.); RPathak@uams.edu (R.P.); mhjensen@uams.edu (M.H.-J.)

² Arkansas Children's Hospital Research Institute, Little Rock, AR 72205, USA; MelnykStepanB@uams.edu

* Correspondence: SAPawar@uams.edu; Tel.: +1-501-686-5784

Received: 6 March 2018; Accepted: 3 April 2018; Published: 6 April 2018



Abstract: Gamma-tocotrienol (GT3) confers protection against ionizing radiation (IR)-induced injury. However, the molecular targets that underlie the protective functions of GT3 are not yet known. We have reported that mice lacking CCAAT enhancer binding protein delta (*Cebpd*^{-/-}) display increased mortality to IR due to injury to the hematopoietic and intestinal tissues and that *Cebpd* protects from IR-induced oxidative stress and cell death. The purpose of this study was to investigate whether *Cebpd* mediates the radio protective functions of GT3. We found that GT3-treated *Cebpd*^{-/-} mice showed partial recovery of white blood cells compared to GT3-treated *Cebpd*^{+/+} mice at 2 weeks post-IR. GT3-treated *Cebpd*^{-/-} mice showed an increased loss of intestinal crypt colonies, which correlated with increased expression of inflammatory cytokines and chemokines, increased levels of oxidized glutathione (GSSG), S-nitrosoglutathione (GSNO) and 3-nitrotyrosine (3-NT) after exposure to IR compared to GT3-treated *Cebpd*^{+/+} mice. *Cebpd* is induced by IR as well as a combination of IR and GT3 in the intestine. Studies have shown that granulocyte-colony stimulating factor (G-CSF), mediates the radioprotective functions of GT3. Interestingly, we found that IR alone as well as the combination of IR and GT3 caused robust augmentation of plasma G-CSF in both *Cebpd*^{+/+} and *Cebpd*^{-/-} mice. These results identify a novel role for *Cebpd* in GT3-mediated protection against IR-induced injury, in part via modulation of IR-induced inflammation and oxidative/nitrosative stress, which is independent of G-CSF.

Keywords: *Cebpd*; gamma tocotrienol; granulocyte-colony stimulating factor; intestinal injury; hematopoietic injury; ionizing radiation; GSNO; GSH

1. Introduction

The health benefits of Vitamin E are mediated through its inherent antioxidant, neuroprotective, anti-inflammatory and stress/damage response properties [1–3]. The Vitamin E family comprises of a set of related tocopherols and tocotrienols, collectively called tocols. The naturally occurring tocols encompass α -, β -, γ - and δ -tocopherol and α -, β -, γ - and δ -tocotrienol. Tocols and their derivatives have been extensively investigated as radiation countermeasure agents [4–7]. A number of studies have shown that tocotrienols are superior antioxidants compared to tocopherols and protect mice against radiation injury and promote post-radiation survival [8–12]. Several studies have shown that GT3 protects against gastrointestinal injury as well as hematopoietic injury [10,12]. The radioprotective efficacy of GT3 is mediated largely through G-CSF and helps to mobilize the progenitor cells and

protects from both gastrointestinal injury as well as hematopoietic injury [13–18]. GT3 treatment is shown to suppress radiation-induced cytogenetic damage by inducing RAD50 in HUVEC cells [19]. GT3 affects the expression of a number of radiation-modulated miRNAs that are known to be involved in hematopoiesis and lymphogenesis [20]. GT3 pretreatment suppressed the upregulation of radiation-induced p53, suggesting a role in the prevention of radiation-induced damage to the spleen [20]. GT3 modulates the expression of pro-apoptotic and anti-apoptotic genes to promote intestinal stem cells and thus confer protection from radiation-induced intestinal injury [21]. However, the molecular targets of GT3 that mediate its radioprotective functions have not been elucidated.

The transcription factor CCAAT enhancer binding protein delta (*Cebpd*, C/EBP δ) is a basic leucine zipper transcription factor that is shown to regulate inflammation, oxidative stress and DNA damage response as well as innate and adaptive immune responses [22–28]. We have previously shown that *Cebpd*-deficiency in mice leads to IR-induced lethality to total body irradiation (TBI) [29]. Specifically, we showed that *Cebpd*^{-/-} mice display impaired recovery of hematopoietic stem and progenitor cells as well as decreased white blood cells, platelets and myeloid cells, while un-irradiated mice did not show any significant phenotypic differences in these parameters [29]. We also reported that *Cebpd*^{-/-} mice show decreased crypt colonies in response to 7.4 Gy, 8.5 Gy and 10 Gy TBI doses. The increased sensitivity of *Cebpd*^{-/-} mouse embryonic fibroblasts (MEFs) to IR occurs due to an impaired ability to modulate IR-induced oxidative stress and mitochondrial dysfunction [28].

In this study, we investigated whether *Cebpd* mediates the radioprotective functions of GT3. Here, we report that GT3 treatment enhanced the recovery of platelets but not WBCs and neutrophils in *Cebpd*^{-/-} mice. *Cebpd* is dispensable for both the IR-inducible and combination of IR and GT3-mediated induction of G-CSF. GT3 did not alleviate IR-induced oxidative/nitrosative stress and underlying intestinal injury in *Cebpd*^{-/-} mice. Lastly, we also reported that the *Cebpd* gene is induced by IR, as well as by the combination of IR and GT3.

2. Materials and Methods

2.1. Animals

Cebpd^{-/-} and *Cebpd*^{+/+} mice (C57BL/6 background) were generated as described [29,30]. *Cebpd* heterozygous mice were kindly provided by Dr. Esta Sterneck (National Cancer Institute, Frederick, MD, USA) to establish a breeding colony at UAMS. 10–12-week-old male and female littermate mice, derived from heterozygous mating pairs, were used in this study. Genotyping was done as described previously [29]. The animals were housed in the Division of Laboratory Animal Medicine (University of Arkansas for Medical Sciences, Little Rock, AR, USA) under standardized conditions with controlled temperature, humidity, 12 h day and 12 h night light cycle. This study was carried out in strict accordance with the recommendations in the Guide for the Care and Use of Laboratory Animals of the National Institutes of Health. Mouse experiments were approved by the Institutional Animal Care and Use Committee. The experiments were performed under an approved protocol AUP#3611. Mice were anesthetized by isoflurane inhalation and tissues such as small intestine (proximal jejunum), femurs and tibiae and blood were harvested.

2.2. Irradiation and GT3 Treatment

Un-anesthetized mice were placed in mouse holders and exposed to a TBI dose of 6 Gy or 8.5 Gy in a Mark I irradiator (JL Shepherd and Associates, San Fernando, CA, USA). Dose uniformity was assessed by an independent company (Ashland Specialty Ingredients, Wilmington, DE, USA) with radiographic film and alanine tablets. Alanine tablets were analyzed by the National Institute of Standards and Technology (Gaithersburg, MD, USA) and demonstrated a dose rate of 1.09 Gy/min at 21 cm from the source. For each experiment, the dose rate was corrected for decay. GT3 was obtained from Yasoo Health Inc. (Johnson City, TN, USA).

24 h prior to radiation exposure to 6 Gy or 8.5 Gy, *Cebpd*^{+/+} and *Cebpd*^{-/-} mice were injected subcutaneously either with vehicle (5% Tween-80 in normal saline), or GT3 (200 mg/kg body weight). The dose of 200 mg/kg body weight was chosen based on a previous study where it has been shown to confer 100% survival after exposure to a TBI dose of 10.5 Gy [10]. Doses higher than 200 mg/kg are shown to have a mild to moderately severe dermatitis that can be observed clinically and microscopically in animals at the injection site [31]. Intestine (proximal jejunum) and blood samples were collected at 0, 1 h, 4 h, 24 h and 3.5 days post-irradiation.

2.3. Blood Parameters

For the bone marrow injury studies, blood parameters were measured at 2 weeks post-exposure to a sublethal TBI dose of 6 Gy. Blood was collected at 0, 1, 3.5 and 7 days post-irradiation by orbital puncture, following isoflurane inhalation from untreated *Cebpd*^{+/+} and *Cebpd*^{-/-} mice. Blood samples were also collected from vehicle and or GT3-treated *Cebpd*^{+/+} and *Cebpd*^{-/-} mice at day 3.5 post-exposure to 8.5 Gy. Blood was collected in EDTA-coated tubes and blood cell parameters were determined by a Hemavet Instrument (Drew Scientific, Inc. Miami, FL, USA). Plasma samples were prepared by centrifugation at 14,000 rpm at 4 °C for 15 min and used for enzyme linked immunosorbent assay (ELISA) as described below in Section 2.7.

2.4. Intestinal Crypt Colony Assay

Previous studies with a LD₅₀ dose of 8.5 Gy (for C57BL/6 mice) revealed that *Cebpd*^{-/-} mice showed increased loss of intestinal crypt colonies at day 3.5 post-TBI and 100% mortality in the thirty-day survival study [29]. Hence in the present study, we utilized 8.5 Gy TBI to study the intestinal injury. Intestinal micro colony crypt survival assays were performed as described previously [29]. Briefly, *Cebpd*^{+/+} and *Cebpd*^{-/-} mice (*n* = 7–8 per group) were sacrificed 3.5 days post-TBI dose of 8.5 Gy and segments of proximal jejunum were obtained, fixed, embedded (4–5 transverse sections per specimen), cut into 3–5- μ m slices and stained with hematoxylin and eosin. A group of untreated mice of both genotypes were used as controls. The surviving crypts (those with ≥ 10 adjacent, chromophilic, non-Paneth cells) were counted. Four to five circumferences of proximal jejunum were scored per mouse and micro colony survival was expressed as the average number of surviving crypts per circumference. The average from each mouse was considered a single value for statistical purposes. Percent survival was calculated by normalizing to un-irradiated *Cebpd*^{+/+} crypts as described previously [29].

2.5. Real-Time PCR

Total RNA was purified from frozen tissue using the RNeasy Plus Mini Kit (Qiagen, Valencia, CA, USA), as instructed by the manufacturer, after homogenizing the samples in TRIzol[®] Reagent (Life Technologies, Grand Island, NY, USA). cDNA was synthesized using a cDNA reverse transcription kit (Life Technologies, Grand Island, NY, USA) after treating the RNA samples with DNase I (Qiagen, Valencia, CA, USA). Taqman assays for *Il-6* Mm00446190_m1; *Tnf- α* Mm00443258_m1; *Tgf- β* Mm01178820_m1; *Mcp-1* (Ccl2), Mm00441242_m1; *Cxcl1* Mm04207460_m1; *Hmox1* Mm00516005_m1; *Nos2* Mm00440502_m1 and *Gapdh* Mm01178820_m1 were used. For *Cebpd* expression, we utilized Sybr Green-based assays. RT-PCR primers for *Cebpd* [(GAACCCGCGGCCCTTCTA (F), TGTTGAAGAGGTC-GGCCA (R)] were obtained from Integrated DNA Technologies and RT² PCR Primer Set mouse *Gapdh* from Applied Biosystems (Cat # 4331182, Foster City, CA, USA). The PCR conditions followed were as described by Power Sybr Green (Cat # 1601040, Life Technologies, Austin, TX, USA) as per manufacturer's instructions. Fold changes were calculated by normalizing to un-irradiated *Cebpd*^{+/+} samples, using the standard $2^{\Delta\Delta C_t}$ method as described previously [32].

2.6. HPLC Assays for Detection of GSH, GSSG, GSNO and 3-NT

Aliquots of intestine tissue obtained from vehicle- and or GT3-treated *Cebpd*^{+/+} and *Cebpd*^{-/-} mice collected at day 3.5 post 8.5 Gy were processed and analyzed by high-performance liquid

chromatography (HPLC-ECD) to quantify reduced glutathione (GSH), GSSG, GSNO and 3-NT as described previously [28]. Approximately 20 mg of intestine tissue were homogenized in ice-cold phosphate-buffered saline. 10% metaphosphoric acid was added to the homogenate, incubated for 30 min on ice to precipitate the proteins. The samples were then centrifuged at $18,000\times g$ at $4\text{ }^{\circ}\text{C}$ for 15 min and 20 μL of the resulting supernatants were injected into the HPLC column for metabolite quantification, while the pellet was used for protein analysis using bicinchoninic acid protein assay. The details for HPLC elution and electrochemical detection of free unbound GSH, GSSG, GSNO and 3-NT in proteins (hydrolyzed by 6N HCl treatment) have been described previously [28,33].

2.7. ELISA

Plasma G-CSF was measured using the mouse G-CSF ELISA kit (Ray Biotech, GA, USA). For plasma G-CSF, the 96 well pre-coated plates were loaded with 100 μL of standard and plasma samples and processed as per the manufacturer's instructions and absorbance was measured at 450 nm. The concentration of G-CSF in each sample was quantified against the standard curve. Values are expressed as pg/mL plasma.

2.8. Statistical Analyses

Statistical analyses were performed with the Graphpad prism, version 7.0 (Graphpad Software, La Jolla, CA, USA). Data are presented as mean \pm S.E.M. and analyzed by one-way ANOVA followed by post-hoc analysis (*Tukey's analysis*) or as student's two-tailed *t* test for independent comparisons between vehicle and treated groups or between genotypes. A value of $p < 0.05$ was considered a significant difference.

3. Results

3.1. GT3-Pretreatment Showed an Impaired Recovery of WBCs, Specifically Neutrophils in Irradiated *Cebpd*^{-/-} Mice

First, we investigated whether GT3 can alleviate the IR-induced hematopoietic injury in *Cebpd*^{-/-} mice. Analysis of peripheral blood cells at 2 weeks post sublethal irradiation (6 Gy) revealed that the vehicle-treated *Cebpd*^{-/-} mice displayed significantly reduced numbers of white blood cells (WBCs) and platelets compared to vehicle-treated *Cebpd*^{+/+} mice (Figure 1A–C), similar to our previously published study [29]. In the vehicle-treated groups, although the *Cebpd*^{-/-} mice showed fewer lymphocytes and monocytes compared to *Cebpd*^{+/+} mice, these differences were not significant (Figure 1C–D).

GT3-treated *Cebpd*^{+/+} mice showed a significant increase in absolute numbers of WBCs, neutrophils, lymphocytes and platelets compared to respective vehicle-treated mice at 2 weeks post-6 Gy (Figure 1A–D). Although GT3-treatment of *Cebpd*^{-/-} mice resulted in a significant increase in WBCs compared to respective vehicle-treated mice, it was significantly lower than the GT3-treated *Cebpd*^{+/+} mice. In contrast, GT3-treated *Cebpd*^{-/-} mice showed a robust recovery of platelets comparable to that of GT3-treated *Cebpd*^{+/+} mice. (Figure 1E). In both vehicle- and GT3-treated groups, the numbers of RBCs were similar in both genotypes (Figure 1F). Thus, our results indicate that GT3 could rescue platelets but only provide a partial recovery of WBCs and specifically neutrophils in *Cebpd*^{-/-} mice post-sublethal irradiation.

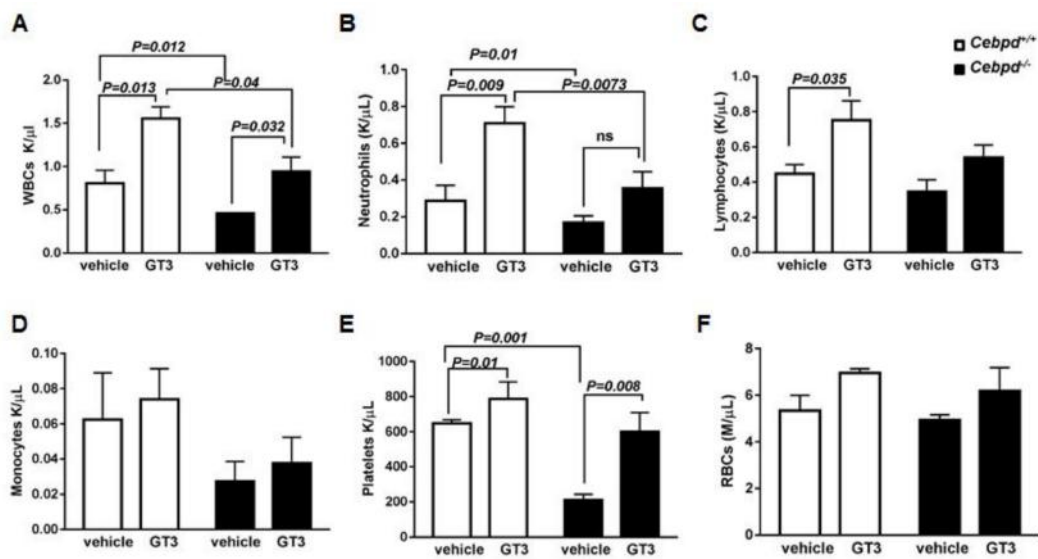


Figure 1. GT3 pre-treatment showed partial rescue of the blood cells in irradiated *Cebpd*^{-/-} mice. Peripheral blood cell counts (A) WBCs, (B) Neutrophils, (C) Lymphocytes, (D) Monocytes, (E) platelets and (F) RBCs from vehicle- and GT3-treated *Cebpd*^{+/+} and *Cebpd*^{-/-} mice at 2 weeks after exposure to 6 Gy. Data are expressed as mean + standard error mean (S.E.M.) and obtained from $n = 4-5$ mice/genotype/group. $p < 0.05$ was considered statistically significant.

3.2. GT3-Treatment Protected Intestinal Crypt Colony Survival of *Cebpd*^{+/+} Mice but Not *Cebpd*^{-/-} Mice Post-TBI Exposure

Exposure of mice to TBI results in damage to the intestinal crypt stem cells [34,35]. After exposure of mice to doses in the sublethal to LD₅₀ dose range of 8.5 Gy (for C57BL/6 mice), the intestinal crypt stem cells can repopulate the injured tissue. However, at doses higher than the LD₅₀ dose of 8.5 Gy (9 Gy–15 Gy), there is damage to the intestinal stem cells residing in the crypts. This results in lethality primarily due to an inability to repopulate the damaged villi, which results in breakdown of the intestinal barrier leading to bacterial translocation. Intestinal stem cells are quiescent and relatively resistant to radiation; however, after radiation injury (usually 3–4 days post-irradiation), they are stimulated to enter a proliferative phase to repopulate the injured tissue and maintain tissue integrity and function and is the basis for the intestinal crypt colony survival assay [34,35]. GT3 pre-treatment has been shown to increase the intestinal crypt colony survival and protection from vascular oxidative stress and protect from acute GI syndrome [12].

Here we investigated whether GT3 protects *Cebpd*^{+/+} and *Cebpd*^{-/-} mice from radiation-induced intestinal injury, by examining the survival of intestinal crypt colonies at day 3.5 post-TBI. The number of surviving crypts were enumerated in GT3- and vehicle-treated *Cebpd*^{+/+} and *Cebpd*^{-/-} mice. We found that vehicle-treated *Cebpd*^{-/-} mice display a significant decrease in intestinal crypt colony survival when compared to respective *Cebpd*^{+/+} mice at day 3.5 post-TBI, as shown previously [29]. *Cebpd*^{+/+} mice treated with GT3 displayed a significant increase in intestinal crypt survival compared to respective vehicle-treated mice at day 3.5 post-TBI (Figure 2A,B). However, GT3 treatment did not confer any significant improvement of intestinal crypt survival of *Cebpd*^{-/-} mice when compared to respective irradiated vehicle-treated group.

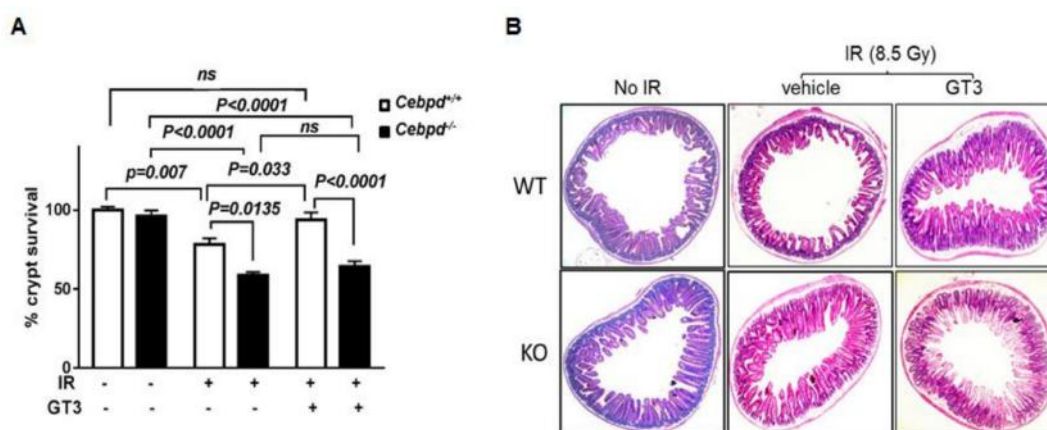


Figure 2. GT3 treatment did not rescue *Cebpd*^{-/-} mice from radiation-induced loss of intestinal crypts. (A) Surviving crypts were scored in *Cebpd*^{+/+} and *Cebpd*^{-/-} mice that were un-irradiated and or vehicle- and or GT3-treated 24 h prior to exposure to 8.5 Gy. Data are expressed as mean + S.E.M. and obtained from $n = 7-8$ mice/genotype/group. $p < 0.05$ was considered statistically significant; *ns*, not significant (B) Representative hematoxylin and eosin stained transverse sections of small intestine (jejunum) showing the crypts and villi harvested at day 3.5 post 8.5 Gy TBI.

3.3. GT3 Promotes IR-Induced Inflammatory and Oxidative Stress Markers in *Cebpd*^{-/-} Mice

We further examined markers of inflammatory and oxidative stress in the intestine at early and late time points post-irradiation in vehicle- and GT3-treated *Cebpd*^{+/+} and *Cebpd*^{-/-} mice. GT3-treated *Cebpd*^{-/-} mice showed a 2-fold increase in *Il-6* at 4 h, which decreased to basal levels comparable to the vehicle-treated controls of both genotypes at later time points (Figure 3A). While other cytokines such as *Tnf- α* and *Tgf- β* did not show any significant differences between both the genotypes in either vehicle or GT3-treated groups (Supplementary Materials Figure S1). *Tgf- β* was upregulated at day 3.5 post-TBI in vehicle- and GT3-treated mice of both genotypes (Supplementary Materials Figure S1).

Next, we examined the expression levels of chemokines, which play a prominent role in the recruitment of inflammatory cells to damaged tissues. Monocyte chemoattractant protein-1 (*Mcp-1*) is a chemokine that recruits monocytes and macrophages to the sites of inflammation [36]. GT3-treated *Cebpd*^{-/-} mice showed a 4-fold induction of the chemokine *Mcp-1* expression compared to 2-fold induction in GT3-treated *Cebpd*^{+/+} mice at day 3.5 day post-TBI. *Cxcl1* {Chemokine (C-X-C motif) ligand 1} also known as KC is another chemokine expressed by macrophages, neutrophils and epithelial cells and has neutrophil chemoattractant activity [37]. *Cxcl1* was upregulated to 1.9-fold in *Cebpd*^{-/-} compared to 1.3-fold in *Cebpd*^{+/+} mice (Figure 3B,C).

Inducible nitric oxide synthase (*Nos2*) is a gene that is known to be induced by IR [38]. There were no significant changes in the IR-induced expression of *Nos2* in either vehicle- or GT3-treated *Cebpd*^{+/+} mice. On the other hand, GT3-treated *Cebpd*^{-/-} mice showed a 10-fold induction of *Nos2* at 4 h post-irradiation, which was downregulated to basal levels by days 1 and 3.5 post-TBI (Figure 3D).

We examined the expression of heme oxygenase-1 (*Hmox1*), a well-known marker of oxidative stress [39]. GT3-treated *Cebpd*^{+/+} mice showed a 1.2-fold induction, while *Cebpd*^{-/-} mice showed about a 2.3-fold induction compared to vehicle-treated *Cebpd*^{+/+} mice at 4h post-TBI (Figure 3E). The expression of *Hmox1* in the GT3 as well as vehicle-treated *Cebpd*^{+/+} mice returned to basal levels by day 1 post-TBI. In contrast compared to the vehicle-treated mice of both genotypes, we found that GT3-treated *Cebpd*^{-/-} mice showed 1.6-fold upregulation compared to *Cebpd*^{+/+} mice at day 3.5 post-TBI (Figure 3E). Overall these results suggest that GT3 treatment promoted increased inflammatory and oxidative stress in *Cebpd*^{-/-} mice compared to *Cebpd*^{+/+} mice in response to IR.

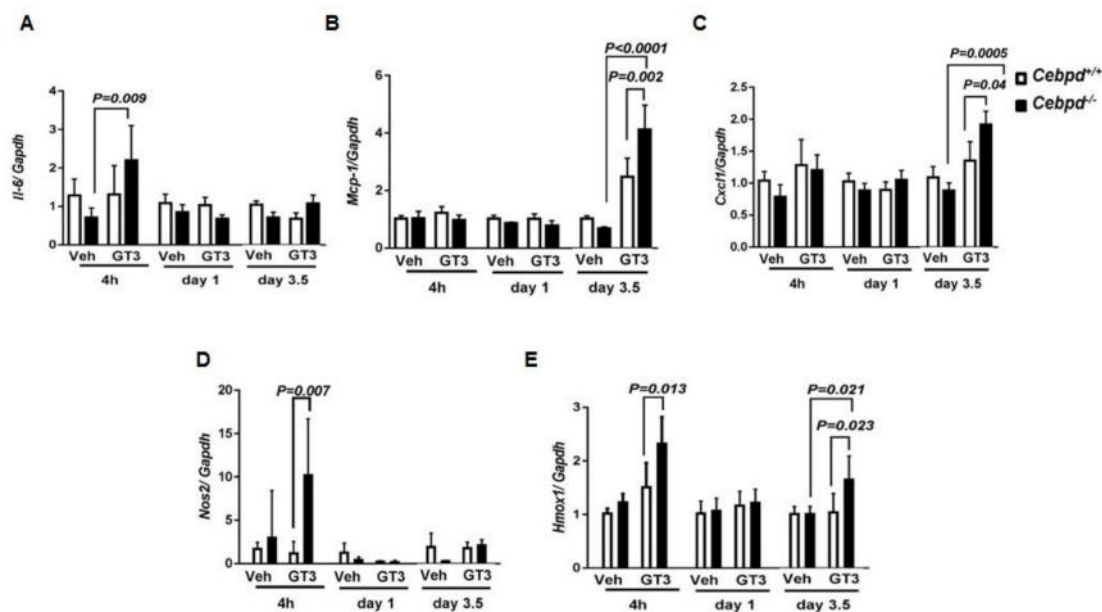


Figure 3. GT3 treatment promotes IR-induced inflammation and oxidative stress in *Cebpd*^{-/-} mice compared to *Cebpd*^{+/+} mice. The intestinal expression of (A) *Il-6*, (B) *Mcp-1*, (C) *Cxcl1*, (D) *Nos2* and (E) *Hmox1* transcripts were analyzed at indicated time points in vehicle- and or GT3-treated *Cebpd*^{+/+} and *Cebpd*^{-/-} mice exposed to 8.5 Gy. The data are expressed as fold change relative to vehicle treated *Cebpd*^{+/+} mice. The data are presented as mean + S.E.M. of $n = 4-8$ mice per treatment per genotype/time point. $p < 0.05$ was considered statistically significant.

3.4. GT3-Treatment Did Not Attenuate IR-Induced Oxidative and Nitrosative Stress in Irradiated *Cebpd*^{-/-} Mice

Next, we examined the tissue levels of the global cellular antioxidant GSH. It is known that decreased GSH is indicative of cellular oxidative stress [40,41]. The intestinal tissues from vehicle-treated *Cebpd*^{-/-} mice contained 12.4 nmoles/mg protein compared to 20.96 nmoles/mg protein of GSH from respective *Cebpd*^{+/+} mice at day 3.5 post-TBI (Figure 4A). The intestinal tissues from GT3-treated *Cebpd*^{+/+} mice contained showed 18.5 nmoles/mg protein, while *Cebpd*^{-/-} mice showed 15.24 nmoles/mg protein of GSH. However, these differences were not significant when compared between the genotypes. Overall, GT3 treatment did not improve GSH levels in the intestine tissues in response to IR in both the genotypes.

In contrast, GT3-treatment showed a significant decrease in GSSG compared to vehicle-treatment in *Cebpd*^{+/+} mice at day 3.5 post-TBI. However, *Cebpd*^{-/-} mice did not show any significant effects on GSSG levels between the vehicle- and GT3-treated groups (Figure 4B).

GSH acts as a scavenger of NO, especially when the NO levels are high enough to be detrimental to cells/tissues and forms GSNO [42]. This is particularly relevant to cells/organisms exposed to IR. GSNO is known to play a role in various inflammatory disease conditions and potentiates tissue damage [42–44]. Interestingly in our studies, we found a significant increase in the GSNO levels in intestines of vehicle-treated *Cebpd*^{-/-} mice compared to respective *Cebpd*^{+/+} at day 3.5 post-TBI (Figure 4C). The levels of GSNO were significantly reduced in GT3-treated *Cebpd*^{+/+} mice when compared with respective vehicle-treated group at day 3.5 post-TBI. In contrast, GT3-treatment of *Cebpd*^{-/-} mice did not significantly reduce the GSNO levels compared to the vehicle-treated mice (Figure 4C).

3-NT is a product of tyrosine nitration mediated by reactive nitrogen species such as peroxynitrite anion. We measured 3-NT in the intestine and found that vehicle-treated *Cebpd*^{-/-} mice showed significantly increased levels compared to vehicle-treated *Cebpd*^{+/+} mice (Figure 4D). GT3-treated *Cebpd*^{-/-} mice showed a significant decrease in 3-NT levels compared to respective vehicle treated

group. However, GT3-treated *Cebpd*^{-/-} mice showed elevated intestinal levels of 3-NT compared to respective *Cebpd*^{+/+} mice (Figure 4D). Overall these results showed that GT3 treatment led to elevated levels of GSSG, GSNO and 3-NT, which promoted the intestinal injury in irradiated *Cebpd*^{-/-} mice.

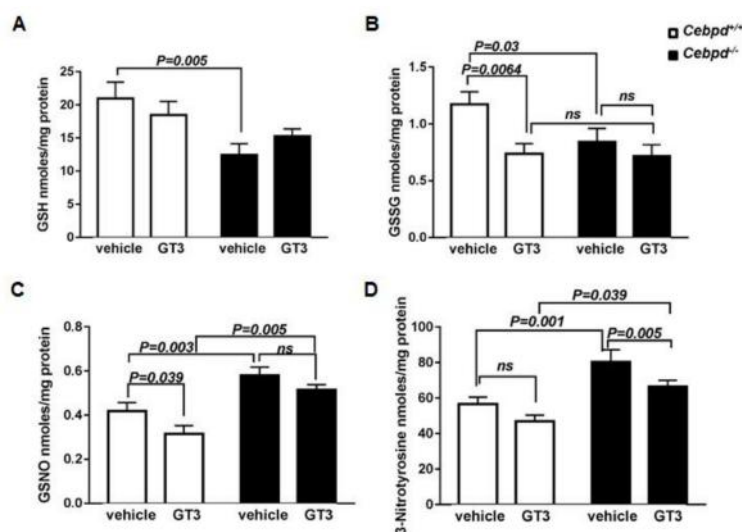


Figure 4. GT3 treatment promotes increased IR-induced oxidative and nitrosative stress in *Cebpd*^{-/-} mice compared to *Cebpd*^{+/+} mice. The intestinal levels of (A) GSH; (B) GSSG, (C) GSNO and (D) 3-NT were measured in intestine tissues of vehicle- or GT3-treated *Cebpd*^{+/+} and *Cebpd*^{-/-} mice at day 3.5 post-exposure to 8.5 Gy ($n = 7-8$ mice/genotype/group). All the data are presented as mean + S.E.M. of $n = 3-8$ mice per treatment per genotype. $p < 0.05$ was considered statistically significant.

3.5. *Cebpd* Is Upregulated by IR and a Combination of IR and GT3 in Intestine Tissue

We next addressed whether IR and or GT3 stimulates the expression of *Cebpd*, which may thus play a protective role against radiation-induced intestinal injury. Here we compared the expression of *Cebpd* in intestine tissues of irradiated *Cebpd*^{+/+} mice harvested at various time points post-irradiation in vehicle- and GT3-treated mice. The expression of *Cebpd* was induced up to 1.4-fold in vehicle-treated mice and by 2.3-fold in GT3-treated mice (Figure 5). These results suggest that both IR as well as the combination of IR and GT3 stimulated the expression of *Cebpd* at day 3.5 post-TBI.

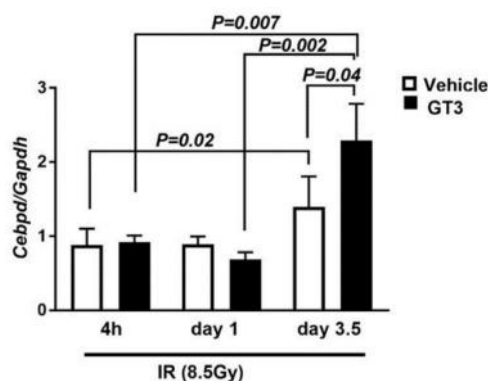


Figure 5. *Cebpd* is upregulated by IR and combination of IR and GT3 in the intestine tissues. The intestinal expression of *Cebpd* and *Gapdh* transcripts were analyzed in *Cebpd*^{+/+} mice at 4 h, 1 day and 3.5 days post-exposure to 8.5 Gy. The data are expressed as fold change relative to 4 h vehicle-treated *Cebpd*^{+/+} mice. The data are presented as mean + S.E.M. of $n = 4-8$ mice per treatment per genotype.

3.6. G-CSF Induction by IR and Combination of IR and GT3 Is Independent of *Cebpd*

Since GT3-mediated radiation protection has been shown to be dependent on G-CSF induction [13,14], we first examined whether impaired G-CSF induction by GT3 led to the increased IR-induced injury to hematopoietic and intestinal tissues observed in *Cebpd*^{-/-} mice. Therefore, we first compared plasma G-CSF levels in *Cebpd*^{+/+} and *Cebpd*^{-/-} mice at various time points post-irradiation.

We did not find any significant differences in G-CSF levels at early time points (0–24 h) post-irradiation between both the genotypes (Supplementary Materials Figure S2). We therefore examined plasma G-CSF levels at the later time points of days 1, 3.5 and 7 post-irradiation. There were no significant differences in the plasma levels of G-CSF at day 1 post-TBI between the genotypes compared to the un-irradiated group. There was a 10.8-fold and 21.3-fold induction in the G-CSF levels in *Cebpd*^{+/+} and *Cebpd*^{-/-} mice compared to the respective un-irradiated mice at day 3.5 post-8.5 Gy. *Cebpd*^{-/-} mice express a further 180-fold increase in plasma levels of G-CSF compared to that of an 85-fold increase in *Cebpd*^{+/+} mice at day 7 post-8.5 Gy compared to the respective un-irradiated control mice (Figure 6A). Contrary to our expectation, these results indicate that G-CSF is robustly induced in both genotypes and that *Cebpd* is not essential for the IR-induced upregulation of G-CSF.

Next, we investigated whether *Cebpd* is essential for the GT3-mediated induction of G-CSF, therefore plasma G-CSF levels in vehicle- and GT3-treated *Cebpd*^{+/+} and *Cebpd*^{-/-} mice at day 3.5 post-irradiation were measured. While we found that *Cebpd*^{-/-} mice express lower plasma levels of G-CSF compared to the respective vehicle-treated *Cebpd*^{+/+} mice, however this difference was not significant (Figure 6B). In the GT3-treated groups, we found a robust 14.5-fold and 39-fold induction of G-CSF in both *Cebpd*^{+/+} and *Cebpd*^{-/-} mice compared to respective vehicle-treated mice (Figure 6B). These results indicate that *Cebpd* may be dispensable for the combination of IR and GT3-mediated induction of G-CSF.

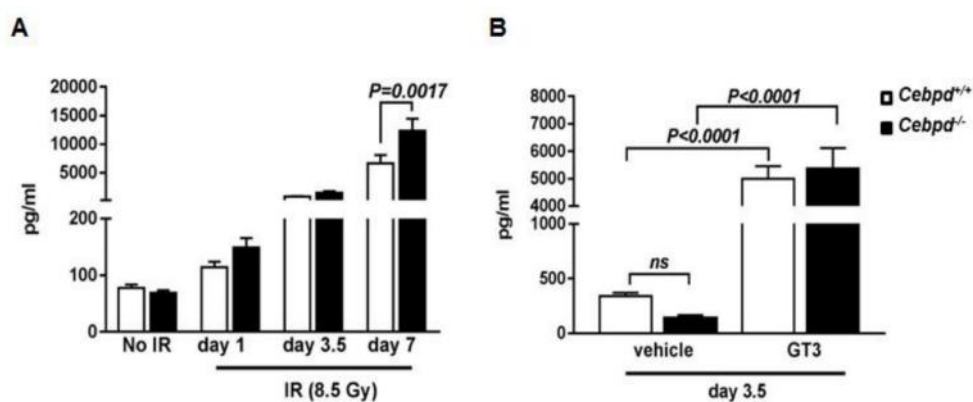


Figure 6. G-CSF induction by IR and combination of IR and GT3 is independent of *Cebpd*. (A) Plasma levels of G-CSF in *Cebpd*^{+/+} and *Cebpd*^{-/-} mice at the indicated time points post-8.5 Gy ($n = 5$ /time point/genotype); and (B) vehicle- or GT3-treated *Cebpd*^{+/+} and *Cebpd*^{-/-} mice at day 3.5 post-8.5 Gy ($n = 7$ – 8 /genotype/group). The data are presented as mean + S.E.M. of $n = 6$ – 8 mice per treatment per genotype. $p < 0.05$ was considered statistically significant.

4. Discussion

The vitamin E analog GT3 has shown promise as a radioprotector in mice and in primates [10,11]. However, the molecular targets that play a role in the radioprotective functions of GT3 remain to be elucidated. A single dose administration of GT3 24 h prior to irradiation leads to decreased radiation injury in organ systems like the bone marrow by stimulating the proliferation and differentiation of hematopoietic progenitors and intestine and vascular systems in part via reduction of vascular oxidative stress [10,12]. We found that GT3-treated *Cebpd*^{+/+} mice showed a robust rescue of WBCs, neutrophils, lymphocytes and platelets compared to vehicle-treated *Cebpd*^{+/+} mice as described

previously [10]. In contrast, GT3-treated *Cebpd*^{-/-} mice showed a robust rescue of platelets and WBCs but not of neutrophils compared with vehicle-treated *Cebpd*^{-/-} mice. Interestingly, our previous studies had reported increased sensitivity of hematopoietic stem and progenitor cells and impaired recovery of myeloid cells in *Cebpd*^{-/-} mice 2 weeks after exposure to 6 Gy, while there were no significant differences between un-irradiated *Cebpd*^{+/+} and *Cebpd*^{-/-} mice [29].

Depletion of intestinal stem cells (ISCs) located at or near the base of intestinal crypts post irradiation is one of the main cause of gastrointestinal syndrome [34,35,45,46]. As apical cells are shed and ISCs die or enter the cell cycle arrest due to DNA damage, the crypts become progressively denuded leading to decreased villus length, number of villi per circumference and decreased number of crypts starting about four days post-irradiation [34,35,46]. We have shown in our previous study that *Cebpd*^{-/-} mice show 100% mortality after exposure to 8.5 Gy and in addition to hematopoietic injury, we also showed decreased intestinal crypt survival in the dose range of 7.4 Gy to 10 Gy [29]. GT3-treatment resulted in increased intestinal crypt colony survival of *Cebpd*^{+/+} mice compared to respective vehicle-treated mice, which is similar to a previous study [12]. However, GT3 treatment did not confer any such protective effects on crypt survival of *Cebpd*^{-/-} mice. These results suggest that the protective effect of GT3 for crypt survival is dependent on *Cebpd*. Recent studies have shown that GT3 promotes intestinal cell survival via upregulation of expression of anti-apoptotic genes and downregulation of pro-apoptotic genes [21]. Our results therefore suggest that *Cebpd* may perhaps regulate GT3 mediated upregulation of anti-apoptotic genes or downregulation of pro-apoptotic genes to protect the intestinal cells in response to IR.

IR induces an inflammatory response that recruits neutrophils and macrophages to eliminate the damaged cells in the tissue and allow for tissue regeneration. Several studies have reported a role for the anti-inflammatory and antioxidant functions of GT3 [47–49]. We found that GT3 treatment stimulated significant increases in the expression of *Il-6* and chemokines *Cxcl1* and *Mcp-1* in *Cebpd*^{-/-} mice compared to *Cebpd*^{+/+} mice, indicative of increased inflammatory stress. The main source of nitric oxide (NO) during stress conditions such as inflammation is *Nos2* and is a key player in oxidative stress [38]. We found that the elevated levels of *Nos2* expression in the intestines of irradiated *Cebpd*^{-/-} mice, indicative of increased oxidative/nitrosative stress, were not alleviated by GT3. Another important marker of cellular oxidative stress is *Hmox1* [39,50,51]. In our studies GT3 treatment led to increased *Hmox1* expression in *Cebpd*^{-/-} mice but not in *Cebpd*^{+/+} mice. *Hmox1* induction may protect cells by augmenting catabolism of pro-oxidant heme and heme proteins by the free radical scavengers under oxidative stress conditions [50]. Work by other groups has shown that GT3 downregulates both inflammation by the inhibition of NF-κB and oxidative stress by scavenging reactive oxygen species or by stabilizing Nrf2 [3,47–49]. Perhaps GT3-mediated *Cebpd* may modulate the IR-induced inflammation and oxidative stress, which is lacking in *Cebpd*^{-/-} mice and therefore resulting in increased inflammation and oxidative stress.

GSH is known to play a key role in maintaining the redox state as well as the cellular antioxidant that imparts protection against radiation-induced oxidative stress [40,41,52]. We have earlier shown that *Cebpd* deficient mouse embryonic fibroblasts show increased basal oxidative stress due to decreased GSH levels [28]. This oxidative stress is further exacerbated by IR and is also associated with increased mitochondrial dysfunction in the cells [28]. GT3 prevented the oxidation of GSH in *Cebpd*^{+/+} mice but not in the *Cebpd*^{-/-} mice which showed a significant increase in the GSSG levels in the intestine tissues. These results implicate *Cebpd* as a key player in GT3-mediated GSH regeneration.

Another important player in the response of cells to IR is the reactive nitrogen species such as peroxynitrite (ONOO⁻), a product of superoxide and nitric oxide which is both reducing as well as oxidizing agent and has a very short half-life [53,54]. Several studies have implicated a role for reactive nitrogen species (RNS) in promoting radiation-induced normal tissue injury [55–60]. Various agents such as GSH, metalloporphyrins, selenium compounds, uric acid, β-carotene and vitamin E provide non-enzymatic protection against RNS [53]. Peroxynitrite reacts with GSH to form the nitric oxide donor GSNO [42,61]. The levels of GSNO in vehicle-treated *Cebpd*^{-/-} mice were significantly higher

than that in the vehicle-treated *Cebpd*^{+/+} mice and were not attenuated by GT3-treatment. Overall our results indicate that GT3 was unable to protect *Cebpd*^{-/-} mice from the nitrosative stress by decreasing GSNO levels. Although GT3 treatment resulted in a modest decrease in 3-NT levels but compared to GT3-treated *Cebpd*^{+/+} mice, these levels were still significantly higher. Studies have shown that exogenous GSNO promotes radio sensitization [61] and this may perhaps explain the loss of intestinal crypts in *Cebpd*^{-/-} mice post-irradiation.

Our studies also revealed that *Cebpd* is an IR-inducible gene that is further upregulated by combination of IR and GT3 in the intestine tissue and may perhaps explain the protective effects in *Cebpd*^{+/+} mice but not in the *Cebpd*^{-/-} mice. This is supported by our own studies, which reveal that *Cebpd* is induced by IR in bone marrow mononuclear cells, spleen, thymus and intestine tissues (Pawar et al., unpublished results).

Radiation is known to suppress blood neutrophil counts. G-CSF regulates the production of neutrophils within the bone marrow and stimulates neutrophil progenitor cell proliferation, differentiation and activation [62–65]. Several studies have shown that GT3 upregulates G-CSF and plays a key role in the recovery of the IR-induced bone marrow injury via mobilization of the hematopoietic progenitors in blood [13,14,17,18]. Pre-clinical studies by Kulkarni et al. (2013) demonstrated that neutralization of G-CSF abrogates GT3-mediated radiation protection, suggesting that GT3 confers radiation protection via G-CSF induction [14]. Additionally exogenous G-CSF alleviates IR-induced injury to the intestine [15,16]. In 2015, FDA approved the use of human G-CSF or filgrastim (Neupogen is the trade mark of filgrastim) as the only radiation countermeasure agent to accelerate the recovery of blood neutrophil levels after radiation exposure [64,65].

In the present study, we found that G-CSF was induced to similar levels in both *Cebpd*^{+/+} and *Cebpd*^{-/-} mice post-irradiation. Interestingly, our results reveal a G-CSF independent pathway in the radioprotection of hematopoietic and intestinal injury by GT3 that may be mediated by *Cebpd*. Similar to our findings, a recent study revealed increased bone marrow injury and lethality in *TM*^{Pro/-} mice, despite the expression of high G-CSF levels in response to IR and GT3 in combination [66]. There is no evidence in the literature for G-CSF as an inducer of *Cebpd*, although other family members, such as *Cebpa* and *Cebpe*, are known to be induced by G-CSF that drives myeloid differentiation [62,67]. Alternatively, it is plausible that GT3-mediated G-CSF may stimulate *Cebpd* expression cannot be ruled out. However this would need to be further confirmed by studies in G-CSF deficient mice, which is beyond the scope of the current study.

5. Conclusions

Overall, these studies identify *Cebpd* as a novel molecular target of GT3 that participates in its radioprotective functions via modulating IR-induced oxidative and nitrosative stress albeit in a G-CSF independent manner. The exact mechanism of *Cebpd* upregulation by GT3 and IR remains unclear.

Future studies will delineate whether GT3 induces these changes via G-CSF or via the NF-κB and ATF3 which are modulated by GT3 [3,48,68] and are known to have binding sites in the *Cebpd* promoter region [23,69]. The expression of *Cebpd* is modulated through its 3'UTR region [70], therefore it could be plausible that GT3 mediated miRNAs could modulate the regulation of *Cebpd*. Further studies will be needed to delineate into the exact mechanism.

Supplementary Materials: The following are available online at <http://www.mdpi.com/2076-3921/7/4/55/s1>, Figure S1: No significant changes in the expression of *Tnf-α* and *Tgf-β* between vehicle- and GT3-treated *Cebpd*^{-/-} and *Cebpd*^{+/+} mice post-irradiation. Figure S2: No significant changes in G-CSF induction by IR at early timepoint post-irradiation.

Acknowledgments: The authors acknowledge Randolph Mildred, Gail Wagoner, Bianca Schutte and Bridgette Angie for excellent animal care. Grant support by the Center for Host Responses to Cancer therapy COBRE Grant P20GM109005 (SAP, MHJ); Department of Defense W81XWH-15-1-0489 (SAP, MHJ); and the Arkansas Bioscience Institute (SAP, SBM) is gratefully acknowledged.

Author Contributions: Sudip Banerjee, Sumit K. Shah, Snehalata A. Pawar conceived and designed the experiments; Sudip Banerjee, Sumit K. Shah, Stepan B. Melnyk, Rupak Pathak, Snehalata A. Pawar performed the experiments and analyzed the data, Sudip Banerjee, Sumit K. Shah, Snehalata A. Pawar, Martin Hauer-Jensen; contributed reagents/materials/analysis tools, Sudip Banerjee, Snehalata A. Pawar, Rupak Pathak, Martin Hauer-Jensen wrote the paper.

Conflicts of Interest: The authors declare no conflict of interest. The funding sponsors had no role in the design of the study; in the collection, analyses, or interpretation of data; in the writing of the manuscript and in the decision to publish the results.

References

1. Nesaretnam, K. Multitargeted therapy of cancer by tocotrienols. *Cancer Lett.* **2008**, *269*, 388–395. [[CrossRef](#)] [[PubMed](#)]
2. Sailo, B.L.; Banik, K.; Padmavathi, G.; Javadi, M.; Bordoloi, D.; Kunnumakkara, A.B. Tocotrienols: The promising analogues of vitamin E for cancer therapeutics. *Pharmacol. Res.* **2018**. [[CrossRef](#)] [[PubMed](#)]
3. Zhou, C.; Tabb, M.M.; Sadatrafiei, A.; Grun, F.; Blumberg, B. Tocotrienols activate the steroid and xenobiotic receptor, SXR, and selectively regulate expression of its target genes. *Drug Metab. Dispos.* **2004**, *32*, 1075–1082. [[CrossRef](#)] [[PubMed](#)]
4. Singh, V.K.; Beattie, L.A.; Seed, T.M. Vitamin E: Tocopherols and tocotrienols as potential radiation countermeasures. *J. Radiat. Res.* **2013**, *54*, 973–988. [[CrossRef](#)] [[PubMed](#)]
5. Singh, V.K.; Ducey, E.J.; Brown, D.S.; Whitnall, M.H. A review of radiation countermeasure work ongoing at the Armed Forces Radiobiology Research Institute. *Int. J. Radiat. Biol.* **2012**, *88*, 296–310. [[CrossRef](#)] [[PubMed](#)]
6. Singh, V.K.; Hauer-Jensen, M. Gamma-tocotrienol as a promising countermeasure for acute radiation syndrome: Current Status. *Int. J. Mol. Sci.* **2016**, *17*, 663. [[CrossRef](#)] [[PubMed](#)]
7. Berbee, M.; Hauer-Jensen, M. Novel drugs to ameliorate gastrointestinal normal tissue radiation toxicity in clinical practice: What is emerging from the laboratory? *Curr. Opin. Support. Palliat. Care* **2012**, *6*, 54–59. [[CrossRef](#)] [[PubMed](#)]
8. Li, X.H.; Fu, D.; Latif, N.H.; Mullaney, C.P.; Ney, P.H.; Mog, S.R.; Whitnall, M.H.; Srinivasan, V.; Xiao, M. Delta-tocotrienol protects mouse and human hematopoietic progenitors from gamma-irradiation through extracellular signal-regulated kinase/mammalian target of rapamycin signaling. *Haematologica* **2010**, *95*, 1996–2004. [[CrossRef](#)] [[PubMed](#)]
9. Li, X.H.; Ghosh, S.P.; Ha, C.T.; Fu, D.; Elliott, T.B.; Bolduc, D.L.; Villa, V.; Whitnall, M.H.; Landauer, M.R.; Xiao, M. Delta-tocotrienol protects mice from radiation-induced gastrointestinal injury. *Radiat. Res.* **2013**, *180*, 649–657. [[CrossRef](#)] [[PubMed](#)]
10. Ghosh, S.P.; Kulkarni, S.; Hieber, K.; Toles, R.; Romanyukha, L.; Kao, T.C.; Hauer-Jensen, M.; Kumar, K.S. Gamma-tocotrienol, a tocol antioxidant as a potent radioprotector. *Int. J. Radiat. Biol.* **2009**, *85*, 598–606. [[CrossRef](#)] [[PubMed](#)]
11. Singh, V.K.; Kulkarni, S.; Fatanmi, O.O.; Wise, S.Y.; Newman, V.L.; Romaine, P.L.; Hendrickson, H.; Gulani, J.; Ghosh, S.P.; Kumar, K.S.; et al. Radioprotective efficacy of gamma-tocotrienol in nonhuman primates. *Radiat. Res.* **2016**, *185*, 285–298. [[CrossRef](#)] [[PubMed](#)]
12. Berbee, M.; Fu, Q.; Boerma, M.; Wang, J.; Kumar, K.S.; Hauer-Jensen, M. gamma-Tocotrienol ameliorates intestinal radiation injury and reduces vascular oxidative stress after total-body irradiation by an HMG-CoA reductase-dependent mechanism. *Radiat. Res.* **2009**, *171*, 596–605. [[CrossRef](#)] [[PubMed](#)]
13. Kulkarni, S.S.; Cary, L.H.; Gambles, K.; Hauer-Jensen, M.; Kumar, K.S.; Ghosh, S.P. Gamma-tocotrienol, a radiation prophylaxis agent, induces high levels of granulocyte colony-stimulating factor. *Int. Immunopharmacol.* **2012**, *14*, 495–503. [[CrossRef](#)] [[PubMed](#)]
14. Kulkarni, S.; Singh, P.K.; Ghosh, S.P.; Posarac, A.; Singh, V.K. Granulocyte colony-stimulating factor antibody abrogates radioprotective efficacy of gamma-tocotrienol, a promising radiation countermeasure. *Cytokine* **2013**, *62*, 278–285. [[CrossRef](#)] [[PubMed](#)]
15. Kim, J.S.; Ryoo, S.B.; Heo, K.; Kim, J.G.; Son, T.G.; Moon, C.; Yang, K. Attenuating effects of granulocyte-colony stimulating factor (G-CSF) in radiation induced intestinal injury in mice. *Food Chem. Toxicol.* **2012**, *50*, 3174–3180. [[CrossRef](#)] [[PubMed](#)]

16. Kim, J.S.; Yang, M.; Lee, C.G.; Kim, S.D.; Kim, J.K.; Yang, K. *In vitro* and *in vivo* protective effects of granulocyte colony-stimulating factor against radiation-induced intestinal injury. *Arch. Pharm. Res.* **2013**, *36*, 1252–1261. [[CrossRef](#)] [[PubMed](#)]
17. Ray, S.; Kulkarni, S.S.; Chakraborty, K.; Pessu, R.; Hauer-Jensen, M.; Kumar, K.S.; Kumar, K.S.; Ghosh, S.P. Mobilization of progenitor cells into peripheral blood by gamma-tocotrienol: A promising radiation countermeasure. *Int. Immunopharmacol.* **2013**, *15*, 557–564. [[CrossRef](#)] [[PubMed](#)]
18. Singh, V.K.; Wise, S.Y.; Fatanmi, O.O.; Scott, J.; Romaine, P.L.; Newman, V.L.; Verma, A.; Elliott, T.B.; Seed, T.M. Progenitors mobilized by gamma-tocotrienol as an effective radiation countermeasure. *PLoS ONE* **2014**, *9*, e114078. [[CrossRef](#)] [[PubMed](#)]
19. Pathak, R.; Bachri, A.; Ghosh, S.P.; Koturbash, I.; Boerma, M.; Binz, R.K.; Sawyer, J.R.; Hauer-Jensen, M. The Vitamin E analog gamma-tocotrienol (GT3) suppresses radiation-induced cytogenetic damage. *Pharm. Res.* **2016**, *33*, 2117–2125. [[CrossRef](#)] [[PubMed](#)]
20. Ghosh, S.P.; Pathak, R.; Kumar, P.; Biswas, S.; Bhattacharyya, S.; Kumar, V.P.; Hauer-Jensen, M.; Biswas, R. Gamma-tocotrienol modulates radiation-induced microRNA expression in mouse spleen. *Radiat. Res.* **2016**, *185*, 485–495. [[CrossRef](#)] [[PubMed](#)]
21. Suman, S.; Datta, K.; Chakraborty, K.; Kulkarni, S.S.; Doiron, K.; Fornace, A.J., Jr.; Sree Kumar, K.; Hauer-Jensen, M.; Ghosh, S.P. Gamma tocotrienol, a potent radioprotector, preferentially upregulates expression of anti-apoptotic genes to promote intestinal cell survival. *Food Chem. Toxicol.* **2013**, *60*, 488–496. [[CrossRef](#)] [[PubMed](#)]
22. Alam, T.; An, M.R.; Papaconstantinou, J. Differential expression of three C/EBP isoforms in multiple tissues during the acute phase response. *J. Biol. Chem.* **1992**, *267*, 5021–5024. [[PubMed](#)]
23. Poli, V. The Role of C/EBP isoforms in the control of inflammatory and native immunity functions. *J. Biol. Chem.* **1998**, *273*, 29279–29282. [[CrossRef](#)] [[PubMed](#)]
24. Lu, Y.C.; Kim, I.; Lye, E.; Shen, F.; Suzuki, N.; Suzuki, S.; Gerondakis, S.; Akira, S.; Gaffen, S.L.; Yeh, W.C.; et al. Differential role for c-Rel and C/EBPbeta/delta in TLR-mediated induction of proinflammatory cytokines. *J. Immunol.* **2009**, *182*, 7212–7221. [[CrossRef](#)] [[PubMed](#)]
25. Balamurugan, K.; Sterneck, E. The many faces of C/EBPdelta and their relevance for inflammation and cancer. *Int. J. Biol. Sci.* **2013**, *9*, 917–933. [[CrossRef](#)] [[PubMed](#)]
26. Wang, J.; Sarkar, T.R.; Zhou, M.; Sharan, S.; Ritt, D.A.; Veenstra, T.D.; Morrison, D.K.; Huang, A.M.; Sterneck, E. CCAAT/enhancer binding protein delta (C/EBPdelta, CEBPD)-mediated nuclear import of FANCD2 by IPO4 augments cellular response to DNA damage. *Proc. Natl. Acad. Sci. USA* **2010**, *107*, 16131–16136. [[CrossRef](#)] [[PubMed](#)]
27. Hour, T.C.; Lai, Y.L.; Kuan, C.I.; Chou, C.K.; Wang, J.M.; Tu, H.Y.; Hu, H.T.; Lin, C.S.; Wu, W.J.; Pu, Y.S.; et al. Transcriptional up-regulation of SOD1 by CEBPD: A potential target for cisplatin resistant human urothelial carcinoma cells. *Biochem. Pharmacol.* **2010**, *80*, 325–334. [[CrossRef](#)] [[PubMed](#)]
28. Banerjee, S.; Aykin-Burns, N.; Krager, K.J.; Shah, S.K.; Melnyk, S.B.; Hauer-Jensen, M.; Pawar, S.A. Loss of C/EBPdelta enhances IR-induced cell death by promoting oxidative stress and mitochondrial dysfunction. *Free Radic. Biol. Med.* **2016**, *99*, 296–307. [[CrossRef](#)] [[PubMed](#)]
29. Pawar, S.A.; Shao, L.; Chang, J.; Wang, W.; Pathak, R.; Zhu, X.; Wang, J.; Hendrickson, H.; Boerma, M.; Sterneck, E.; et al. C/EBP delta deficiency sensitizes mice to ionizing radiation-induced hematopoietic and intestinal injury. *PLoS ONE* **2014**, *9*, e94967. [[CrossRef](#)] [[PubMed](#)]
30. Sterneck, E.; Paylor, R.; Jackson-Lewis, V.; Libbey, M.; Przedborski, S.; Tessarollo, L.; Crawley, J.N.; Johnson, P.F. Selectively enhanced contextual fear conditioning in mice lacking the transcriptional regulator CCAAT/enhancer binding protein delta. *Proc. Natl. Acad. Sci. USA* **1998**, *95*, 10908–10913. [[CrossRef](#)] [[PubMed](#)]
31. Swift, S.N.; Pessu, R.L.; Chakraborty, K.; Villa, V.; Lombardini, E.; Ghosh, S.P. Acute toxicity of subcutaneously administered vitamin E isomers delta- and gamma-tocotrienol in mice. *Int. J. Toxicol.* **2014**, *33*, 450–458. [[CrossRef](#)] [[PubMed](#)]
32. Pawar, S.A.; Sarkar, T.R.; Balamurugan, K.; Sharan, S.; Wang, J.; Zhang, Y.; Dowdy, S.F.; Huang, A.M.; Sterneck, E. C/EBP delta targets cyclin D1 for proteasome-mediated degradation via induction of CDC27/APC3 expression. *Proc. Natl. Acad. Sci. USA* **2010**, *107*, 9210–9215. [[CrossRef](#)] [[PubMed](#)]

33. Melnyk, S.; Pogribna, M.; Pogribny, I.; Hine, R.J.; James, S.J. A new HPLC method for the simultaneous determination of oxidized and reduced plasma amino thiols using coulometric electrochemical detection. *J. Nutr. Biochem.* **1999**, *10*, 490–497. [[CrossRef](#)]
34. Potten, C.S. Extreme sensitivity of some intestinal crypt cells to X and gamma irradiation. *Nature* **1977**, *269*, 518–521. [[CrossRef](#)] [[PubMed](#)]
35. Potten, C.S. Stem cells in gastrointestinal epithelium: Numbers, characteristics and death. *Phil. Trans. R. Soc. Lond. Ser. B Biol. Sci.* **1998**, *353*, 821–830. [[CrossRef](#)] [[PubMed](#)]
36. Deshmane, S.L.; Kremlev, S.; Amini, S.; Sawaya, B.E. Monocyte chemoattractant protein-1 (MCP-1): An overview. *J. Interferon Cytokine Res.* **2009**, *29*, 313–326. [[CrossRef](#)] [[PubMed](#)]
37. De Filippo, K.; Dudeck, A.; Hasenberg, M.; Nye, E.; van Rooijen, N.; Hartmann, K.; Gunzer, M.; Roers, A.; Hogg, N. Mast cell and macrophage chemokines CXCL1/CXCL2 control the early stage of neutrophil recruitment during tissue inflammation. *Blood* **2013**, *121*, 4930–4937. [[CrossRef](#)] [[PubMed](#)]
38. Gorbunov, N.V.; Pogue-Geile, K.L.; Epperly, M.W.; Bigbee, W.L.; Draviam, R.; Day, B.W.; Wald, N.; Watkins, S.C.; Greenberger, J.S. Activation of the nitric oxide synthase 2 pathway in the response of bone marrow stromal cells to high doses of ionizing radiation. *Radiat. Res.* **2000**, *154*, 73–86. [[CrossRef](#)]
39. Chang, M.; Xue, J.; Sharma, V.; Habtezion, A. Protective role of hemeoxygenase-1 in gastrointestinal diseases. *Cell. Mol. Life Sci.* **2015**, *72*, 1161–1173. [[CrossRef](#)] [[PubMed](#)]
40. Dickinson, D.A.; Forman, H.J. Glutathione in defense and signaling: Lessons from a small thiol. *Ann. N. Y. Acad. Sci.* **2002**, *973*, 488–504. [[CrossRef](#)] [[PubMed](#)]
41. Dickinson, D.A.; Forman, H.J. Cellular glutathione and thiols metabolism. *Biochem. Pharmacol.* **2002**, *64*, 1019–1026. [[CrossRef](#)]
42. Broniowska, K.A.; Diers, A.R.; Hogg, N. S-Nitrosoglutathione. *Biochim. Biophys. Acta* **2013**, *1830*, 3173–3181. [[CrossRef](#)] [[PubMed](#)]
43. Cheng, Q.; Nabor, D.; Stowe, D.; Bienengraeber, M.; Lazar, J.; Riess, M. Deleterious effect of acute administration of nitric oxide donor GSNO on cardiac ischemia reperfusion injury in a consomic rat model. *FASEB J.* **2013**, *27*, 682–689.
44. Mikhailenko, V.M.; Muzalov, I.I. Exogenous nitric oxide potentiate DNA damage and alter DNA repair in cells exposed to ionising radiation. *Exp. Oncol.* **2013**, *35*, 318–324. [[PubMed](#)]
45. Yu, J. Intestinal stem cell injury and protection during cancer therapy. *Transl. Cancer Res.* **2013**, *2*, 384–396. [[PubMed](#)]
46. Potten, C.S. Radiation, the ideal cytotoxic agent for studying the cell biology of tissues such as the small intestine. *Radiat. Res.* **2004**, *161*, 123–136. [[CrossRef](#)] [[PubMed](#)]
47. Muid, S.; Froemming, G.R.; Rahman, T.; Ali, A.M.; Nawawi, H.M. Delta- and gamma-tocotrienol isomers are potent in inhibiting inflammation and endothelial activation in stimulated human endothelial cells. *Food Nutr. Res.* **2016**, *60*, 31526. [[CrossRef](#)] [[PubMed](#)]
48. Wang, Y.; Jiang, Q. gamma-Tocotrienol inhibits lipopolysaccharide-induced interleukin-6 and granulocyte colony-stimulating factor by suppressing C/EBPbeta and NF-kappaB in macrophages. *J. Nutr. Biochem.* **2013**, *24*, 1146–1152. [[CrossRef](#)] [[PubMed](#)]
49. Wang, Y.; Park, N.Y.; Jang, Y.; Ma, A.; Jiang, Q. Vitamin E Gamma-tocotrienol inhibits cytokine-stimulated NF-kappaB activation by induction of anti-inflammatory A20 via stress adaptive response due to modulation of sphingolipids. *J. Immunol.* **2015**, *195*, 126–133. [[CrossRef](#)] [[PubMed](#)]
50. Kamalvand, G.; Pinard, G.; Ali-Khan, Z. Heme-oxygenase-1 response, a marker of oxidative stress, in a mouse model of AA amyloidosis. *Amyloid* **2003**, *10*, 151–159. [[CrossRef](#)] [[PubMed](#)]
51. Lin, S.H.; Song, W.; Cressatti, M.; Zukor, H.; Wang, E.; Schipper, H.M. Heme oxygenase-1 modulates microRNA expression in cultured astroglia: Implications for chronic brain disorders. *Glia* **2015**, *63*, 1270–1284. [[CrossRef](#)] [[PubMed](#)]
52. Chatterjee, A. Reduced glutathione: A radioprotector or a modulator of DNA-repair activity? *Nutrients* **2013**, *5*, 525–542. [[CrossRef](#)] [[PubMed](#)]
53. Roberts, R.A.; Laskin, D.L.; Smith, C.V.; Robertson, F.M.; Allen, E.M.G.; Doorn, J.A.; Slikker, W. Nitrate and oxidative stress in toxicology and disease. *Toxicol. Sci.* **2009**, *112*, 4–16. [[CrossRef](#)] [[PubMed](#)]
54. Beckman, J.S.; Koppenol, W.H. Nitric oxide, superoxide and peroxynitrite: The good, the bad, and ugly. *Am. J. Physiol.* **1996**, *271*, C1424–C1437. [[CrossRef](#)] [[PubMed](#)]

55. Banerjee, S.; Melnyk, S.B.; Krager, K.J.; Aykin-Burns, N.; Letzig, L.G.; James, L.P.; Hinson, J.A. The neuronal nitric oxide synthase inhibitor NANT blocks acetaminophen toxicity and protein nitration in freshly isolated hepatocytes. *Free Radic. Biol. Med.* **2015**, *89*, 750–757. [[CrossRef](#)] [[PubMed](#)]
56. Ducrocq, C.; Blanchard, B.; Pignatelli, B.; Ohshima, H. Peroxynitrite: An endogenous oxidizing and nitrating agent. *Cell. Mol. Life Sci.* **1999**, *55*, 1068–1077. [[CrossRef](#)] [[PubMed](#)]
57. Kiang, J.G.; Agravante, N.G.; Smith, J.T.; Bowman, P.D. 17-DMAG diminishes hemorrhage-induced small intestine injury by elevating Bcl-2 protein and inhibiting iNOS pathway, TNF-alpha increase, and caspase-3 activation. *Cell Biosci.* **2011**, *1*, 21. [[CrossRef](#)] [[PubMed](#)]
58. Ohta, S.; Matsuda, S.; Gunji, M.; Kamogawa, A. The role of nitric oxide in radiation damage. *Biol. Pharm. Bull.* **2007**, *30*, 1102–1107. [[CrossRef](#)] [[PubMed](#)]
59. McKinney, L.C.; Aquilla, E.M.; Coffin, D.; Wink, D.A.; Vodovotz, Y. Ionizing radiation potentiates the induction of nitric oxide synthase by interferon-gamma and/or lipopolysaccharide in murine macrophage cell lines. Role of tumor necrosis factor-alpha. *Ann. N. Y. Acad. Sci.* **2000**, *899*, 61–68. [[CrossRef](#)] [[PubMed](#)]
60. Malaviya, R.; Gow, A.J.; Francis, M.; Abramova, E.V.; Laskin, J.D.; Laskin, D.L. Radiation-induced lung injury and inflammation in mice: Role of inducible nitric oxide synthase and surfactant protein, D. *Toxicol. Sci.* **2015**, *144*, 27–38. [[CrossRef](#)] [[PubMed](#)]
61. Mitchell, J.B.; Cook, J.A.; Krishna, M.C.; DeGraff, W.; Gamson, J.; Fisher, J.; Christodoulou, D.; Wink, D.A. Radiation sensitisation by nitric oxide releasing agents. *Br. J. Cancer Suppl.* **1996**, *27*, S181–S184. [[PubMed](#)]
62. Nakajima, H.; Ihle, J.N. Granulocyte colony-stimulating factor regulates myeloid differentiation through CCAAT/enhancer-binding protein epsilon. *Blood* **2001**, *98*, 897–905. [[CrossRef](#)] [[PubMed](#)]
63. Richards, M.K.; Liu, F.; Iwasaki, H.; Akashi, K.; Link, D.C. Pivotal role of granulocyte colony-stimulating factor in the development of progenitors in the common myeloid pathway. *Blood* **2003**, *102*, 3562–3568. [[CrossRef](#)] [[PubMed](#)]
64. Singh, V.K.; Romaine, P.L.; Seed, T.M. Medical countermeasures for radiation exposure and related injuries: Characterization of medicines, FDA-approval status and inclusion into the strategic national stockpile. *Health Phys.* **2015**, *108*, 607–630. [[CrossRef](#)] [[PubMed](#)]
65. Singh, V.K.; Romaine, P.L.; Newman, V.L.; Seed, T.M. Medical countermeasures for unwanted CBRN exposures: Part II radiological and nuclear threats with review of recent countermeasure patents. *Expert Opin. Ther. Pat.* **2016**, *26*, 1399–1408. [[CrossRef](#)] [[PubMed](#)]
66. Pathak, R.; Shao, L.; Ghosh, S.P.; Zhou, D.; Boerma, M.; Weiler, H.; Hauer-Jensen, M. Thrombomodulin contributes to gamma tocotrienol-mediated lethality protection and hematopoietic cell recovery in irradiated mice. *PLoS ONE* **2015**, *10*, e0122511. [[CrossRef](#)] [[PubMed](#)]
67. Iida, S.; Watanabe-Fukunaga, R.; Nagata, S.; Fukunaga, R. Essential role of C/EBPalpha in G-CSF-induced transcriptional activation and chromatin modification of myeloid-specific genes. *Genes Cells* **2008**, *13*, 313–327. [[CrossRef](#)] [[PubMed](#)]
68. Patacsil, D.; Tran, A.T.; Cho, Y.S.; Suy, S.; Saenz, F.; Malyukova, I.; Ressom, H.; Collins, S.P.; Clarke, R.; Kumar, D. Gamma-tocotrienol induced apoptosis is associated with unfolded protein response in human breast cancer cells. *J. Nutr. Biochem.* **2012**, *23*, 93–100. [[CrossRef](#)] [[PubMed](#)]
69. Litvak, V.; Ramsey, S.A.; Rust, A.G.; Zak, D.E.; Kennedy, K.A.; Lampano, A.E.; Nykter, M.; Shmulevich, I.; Aderem, A. Function of C/EBPdelta in a regulatory circuit that discriminates between transient and persistent TLR4-induced signals. *Nat. Immunol.* **2009**, *10*, 437–443. [[CrossRef](#)] [[PubMed](#)]
70. Dearth, L.R.; Dewille, J. An AU-rich element in the 3' untranslated region of the C/EBP delta mRNA is important for protein binding during G0 growth arrest. *Biochem. Biophys. Res. Commun.* **2003**, *304*, 344–350. [[CrossRef](#)]





Article

Gamma-Tocotrienol Protects the Intestine from Radiation Potentially by Accelerating Mesenchymal Immune Cell Recovery

Sarita Garg ¹, Ratan Sadhukhan ¹, Sudip Banerjee ¹, Alena V. Savenka ²,
Alexei G. Basnakian ^{2,3}, Victoria McHargue ¹, Junru Wang ¹, Snehalata A. Pawar ¹,
Sanchita P. Ghosh ⁴, Jerry Ware ⁵, Martin Hauer-Jensen ¹ and Rupak Pathak ^{1,*}

¹ Division of Radiation Health, Department of Pharmaceutical Sciences, College of Pharmacy, University of Arkansas for Medical Sciences, Little Rock, AR 72205, USA; GargSarita@uams.edu (S.G.); RSadhukhan@uams.edu (R.S.); SBanerjee@uams.edu (S.B.); vymchargue@ualr.edu (V.M.); WangJunru@uams.edu (J.W.); SAPawar@uams.edu (S.A.P.); mhjensen@uams.edu (M.H.-J.)

² Department of Pharmacology and Toxicology, University of Arkansas for Medical Sciences, Little Rock, AR 72205, USA; SavenkaAlenaV@uams.edu (A.V.S.); BasnakianAlexeiG@uams.edu (A.G.B.)

³ Central Arkansas Veterans Healthcare System, Little Rock, AR 72205, USA

⁴ Armed Forces Radiobiology Research Institute, USUHS, Bethesda, MD 20814, USA; sanchita.ghosh@usuhs.edu

⁵ Department of Physiology and Biophysics, College of Medicine, University of Arkansas for Medical Sciences, Little Rock, AR 72205, USA; JWare@uams.edu

* Correspondence: rpathak@uams.edu; Tel.: +1-501-603-1472

Received: 31 January 2019; Accepted: 28 February 2019; Published: 6 March 2019



Abstract: Natural antioxidant gamma-tocotrienol (GT3), a vitamin E family member, provides intestinal radiation protection. We seek to understand whether this protection is mediated via mucosal epithelial stem cells or sub-mucosal mesenchymal immune cells. Vehicle- or GT3-treated male CD2F1 mice were exposed to total body irradiation (TBI). Cell death was determined by terminal deoxynucleotidyl transferase dUTP nick end labeling (TUNEL) assay. Villus height and crypt depth were measured with computer-assisted software in tissue sections. Functional activity was determined with an intestinal permeability assay. Immune cell recovery was measured with immunohistochemistry and Western blot, and the regeneration of intestinal crypts was assessed with ex vivo organoid culture. A single dose of GT3 (200 mg/kg body weight (bwt)) administered 24 h before TBI suppressed cell death, prevented a decrease in villus height, increased crypt depth, attenuated intestinal permeability, and upregulated occludin level in the intestine compared to the vehicle treated group. GT3 accelerated mesenchymal immune cell recovery after irradiation, but it did not promote ex vivo organoid formation and failed to enhance the expression of stem cell markers. Finally, GT3 significantly upregulated protein kinase B or AKT phosphorylation after TBI. Pretreatment with GT3 attenuates TBI-induced structural and functional damage to the intestine, potentially by facilitating intestinal immune cell recovery. Thus, GT3 could be used as an intestinal radioprotector.

Keywords: radiation; immune cells; intestine; organoid; vitamin E

1. Introduction

Ionizing radiation (IR)-induced gastrointestinal damage during radiotherapy or due to accidental overexposure can produce significant morbidity and mortality. IR inflicts adverse effects by impairing cellular function and signaling and/or by inducing the death of various populations of cells in the irradiated intestinal microenvironment. This microenvironment contains epithelial stem and

progenitor cells and underlying non-epithelial mesenchymal cells, such as immune cells (neutrophils, lymphocytes, and macrophages), stromal cells (fibroblasts, myofibroblasts, and smooth-muscle cells), endothelial cells, and neuronal cells [1]. The impaired function or loss of these cells after irradiation collectively contributes to the development of intestinal toxicity. Importantly, the extent of intestinal damage depends on various factors, including dose, dose rate, and the quality of radiation [2]. In addition, the surface area of exposed tissue, individual radio-sensitivity, and the general health and genetic makeup of an individual determine the magnitude of gut injury [2].

Continually proliferating intestinal epithelial cells are highly sensitive to IR, and exposure to radiation induces apoptosis, characterized by DNA fragmentation [3]. The loss of epithelial cells causes villi to shorten, compromising the structural integrity of the intestine. In addition, damage to the epithelial layer disrupts barrier integrity and enhances intestinal permeability, allowing luminal bacteria to invade the damaged tissue. IR also alters the level of tight junction-related proteins, which are known to maintain barrier integrity [4]. Bacterial invasion due to the loss of barrier function eventually triggers inflammation and sepsis.

Immune cells such as macrophages, neutrophils, and lymphocytes play a critical role in neutralizing invading luminal pathogens [5]. Upon breakdown of the mucosal barrier, intestinal tissue-resident macrophages are activated and liberate pro-inflammatory cytokines and chemokines that attract neutrophils and monocytes. Immune cells also release soluble regenerative mediators to restore barrier integrity after intestinal injury [6–8]. A study by Lindemans et al. showed that innate and adaptive lymphoid cells promote intestinal stem cell regeneration by releasing IL-22 [9]. Macrophage-derived Wingless/Integrated (WNT) ligands, which are highly hydrophobic cysteine rich secreted proteins, were shown to protect intestinal epithelial cells after exposure to radiation [7], and neutrophils have been shown to promote intestinal mucosal barrier function and tissue repair by producing amphiregulin, a member of the EGFR ligand family, in a mouse model of colitis [10]. These data clearly indicate that different types of immune cells are critical for restoring intestinal homeostasis after injury. However, exposure to total body irradiation (TBI) significantly decreases the levels of various immune cells in the damaged gut and in the blood [11]. When fewer immune cells are present after irradiation, they cannot effectively eliminate bacteria that invade from the gut lumen by way of the compromised mucosal epithelial barrier, and they likely produce fewer epithelial regenerative signals. This, in turn, triggers acute inflammation, which is considered one of the critical early effects of radiation [12]. Early symptoms can produce delayed fibrotic changes and tissue remodeling. Therefore, developing strategies to minimize the loss of immune cells after TBI will not only help remove invading microbes, but such strategies could restore barrier integrity by inducing epithelial regenerative signals.

The vitamin E family member gamma-tocotrienol (GT3) is a natural antioxidant and potent radioprotector [13]; it has been shown to suppress IR-induced hematopoietic, vascular, and intestinal structural damage after TBI [14–16]. Although the exact mechanisms of GT3-mediated intestinal radiation protection are not clear, previous studies demonstrated that GT3 pretreatment preferentially upregulates the expression of anti-apoptotic genes and downregulates pro-apoptotic factors in irradiated intestinal tissue [17]. The same study also showed that there was significantly less TBI-induced DNA fragmentation in crypt cells from GT3-treated animals relative to vehicle-treated ones [17]. In addition, GT3 also improved endothelial cell activity by inducing the thrombomodulin-activated protein C axis [18,19], which is known to play a critical role in limiting radiation-induced intestinal damage [20,21]. These findings suggest that GT3 has the ability to protect intestinal epithelial and non-epithelial cells following irradiation. However, the role of GT3 in modulating the recovery of intestinal immune cells and barrier function after TBI is not known. Here, we report that a single dose of GT3 administered 24 h before TBI suppresses cell death, accelerates the recovery of intestinal immune cells, and augments barrier function.

2. Materials and Methods

2.1. Experimental Model, GT3 Treatment, Irradiation, Tissue Procurement, and Euthanasia

All animal studies were carried out in strict accordance with the recommendations in the Guide for the Care and Use of Laboratory Animals of the National Institutes of Health. The animal protocol (AUP #3823) was approved by the Institutional Animal Care and Use Committee of the University of Arkansas for Medical Sciences (UAMS). Male CD2F1 mice were obtained from Charles River Laboratories (Houston, TX); mice between 8 and 12 weeks of age were used for experiments. They were housed in conventional cages in a pathogen-free environment with controlled humidity, temperature, and a 12–12 light–dark cycle with free access to drinking water and standard chow (Teklad, Madison, WI, USA).

GT3 was prepared freshly before administration with 5% Tween-80 (Fisher Scientific, Waltham, MA, USA) in saline. A single dose of 100 μ L vehicle or GT3 (200 mg/kg body weight (bwt)) was administered subcutaneously 24 h before TBI.

Mice (not anesthetized) were exposed to a single TBI dose in a Shepherd Mark I 137Cs irradiator (model 25, J. L. Shepherd & Associates, San Fernando, CA, USA). During irradiation, the mice were placed in a custom-made, well-ventilated aluminum chamber with a Plexiglas lid (J.L. Shepherd & Associates). The chamber was divided into eight equal “pie slice” compartments by dividers made of T-6061 aluminum with a gold anodized coating. One mouse per compartment was placed to provide ample space to move. The chamber was placed on a turntable rotating at six revolutions per minute to assure uniform irradiation. The average dose rate was 1.01 Gy per min and was corrected for decay each day. A total dose in the range of 8 to 12 Gy was delivered depending on the endpoint assessed. For example, the mice were exposed to 8 Gy to measure apoptosis of epithelial cells and recovery of the immune cells, since these cells are highly sensitive to radiation, while we used relatively higher radiation dose (10 Gy and 12 Gy) for the intestinal permeability assay to induce enough damage in the intestine. The dose for the intestinal permeability assay was selected based on our previous experience. All radiation experiments were performed in the morning to minimize possible diurnal effects.

For tissue harvest, mice were anesthetized with 60 mg/kg sodium pentobarbital (Abbott Laboratories, Chicago, IL, USA) administered intraperitoneally. Samples of the intestine from irradiated and un-irradiated mice were procured and fixed in methanol–Carnoy’s solution for histological and immunohistochemical studies or snap-frozen in liquid nitrogen for molecular analysis. After tissue harvest, mice were euthanized by CO₂ asphyxiation followed by cervical dislocation to eliminate any reasonable doubt of survival.

2.2. TUNEL Assay

TUNEL assays were performed as described previously [22]. Tissue samples were fixed, dehydrated, and embedded in paraffin. 4 μ m thick tissue sections were cut using microtome, dewaxed, rehydrated in phosphate-buffered saline (PBS). TUNEL assay was performed using a In Situ Cell Death Detection Kit (Roche Diagnostics, Indianapolis, IN, USA) following the manufacturer’s instructions. Intestinal tissue sections were incubated with a reaction mixture of terminal deoxynucleotidyl transferase (TdT) and fluorescein (FITC)-labeled precursor in cacodylate-based buffer for 1 h at 37 °C, rinsed three times with 0.05% Tween-20 in PBS, and mounted under a ProLong[®] Antifade medium containing 4',6-diamidino-2-phenylindole dihydrochloride (DAPI) (Invitrogen, Carlsbad, CA, USA). TUNEL specificity was controlled by substituting the mixture of TdT and probe with the cacodylate buffer. The green spectrum (FITC) and blue spectrum (DAPI) were used to detect TUNEL-positive cells and nuclei, respectively. Images were captured with an Olympus IX-81 microscope (Olympus America Inc., Center Valley, PA, USA) equipped with a digital Hamamatsu ORCA-ER camera (Hamamatsu Photonics K.K., Hamamatsu City, Japan) under 63 \times magnification. Slidebook 6.2 software (SciTech Pty Ltd., Preston, Australia) was used for image capture. The results were presented as the frequency of

the area of TUNEL-positive nuclear DNA in the total DAPI-positive area of nuclear DNA calculated for individual cells.

2.3. Assessment of Villus Height and Crypt Depth

Intestinal tissue sections stained with hematoxylin and eosin (H&E) were used to measure villus height and crypt depth using a computer-assisted image analysis platform (Image-Pro Premier, Rockville, MD, USA). Intestinal tissues fixed in Methyl-Carnoy's fixed and embedded in paraffin were cut into 2–4 μm sections with a microtome. The slides with tissue sections were de-waxed by placing in an incubator overnight set at 60 °C, cooled down to room temperature, dipped into hematoxylin solution for 30 s, washed with deionized water, stained with 1% eosin solution, dehydrated with two changes in 95% and 100% alcohol for 30 s each, washed with xylene, and finally mounted with low viscosity Permout™ mounting media (Thermo Fisher Scientific, Grand Island, NY, USA). Mucosal villus height was measured from the tip to the base of each villus, and crypt depth was measured from the crypt base to the top opening. All measurements were done with a 10 \times objective lens, and a total of five areas were measured for each sample.

2.4. In Vivo Intestinal Permeability Assay

Intestinal permeability was assessed using an *in vivo* FITC-labeled dextran method after 4 days of total body exposure to 10 Gy or 12 Gy in mice pre-treated with or without GT3. After anesthetizing the mice by isoflurane inhalation, a midline laparotomy was performed, and the renal artery and vein were ligated bilaterally. A 10 cm segment of the small intestine, located 5 cm distal to the ligament of Treitz, was isolated and tied off. One hundred microliters of 4 kDa FITC-dextran (25 mg/mL in PBS) was injected into the isolated intestine using a 30 gauge needle, and the abdominal incision was closed. The renal artery and vein were ligated to prevent loss of FITC-dextran via urine. Blood samples were collected retro-orbitally 90 min after infusion of FITC-dextran into the intestinal lumen. Plasma sample was separated from whole blood by centrifugation (8000 rpm, 10 min, 4 °C) and the FITC-dextran content was measured with a fluorescence spectrophotometer (Synergy HT, Bio-Tek Instruments, Winooski, VT, USA) at an excitation wavelength of 480 nm and an emission wavelength of 520 nm. Standard curves were prepared to determine the concentration of FITC-dextran in plasma samples taking into account the dilution factor.

2.5. Immunoblotting

Protein lysates were prepared from intestinal tissue as described previously [23]. Primary antibodies to β -actin (Cell Signaling Technology; Danvers, MA), p-AKT (Cell Signaling Technology), CD2 (Santa Cruz Biotechnology; Dallas, TX), and occludin (Abcam; Cambridge, MA, USA) were used at a 1:1000 dilution for overnight incubation at 4 °C. Goat anti-rabbit IgG-HRP (Cell Signaling Technology, Danvers, MA, USA) and goat anti-mouse IgG-HRP (Santa Cruz Biotechnology, Dallas, TX, USA) secondary antibodies were used at a 1:5000 dilution for 2 h incubation at room temperature. Western blots were developed on autoradiography film (GeneMate, Kaysville, UT, USA) using chemiluminescent substrate (Thermo Fisher Scientific, Grand Island, NY, USA). Densitometry analyses were performed with ImageJ software available at NIH website, and β -actin was used as the loading control.

2.6. Intestinal Crypt Isolation and Organoid Culture in Matrigel

Small intestines were dissected and opened longitudinally, scraped gently to eliminate intestinal villi, and washed with cold PBS. The intestines were cut into 5 mm pieces and further washed three times with cold PBS to remove all visible debris. The tissue fragments were kept in 2.5 mM EDTA-PBS and incubated for 1 h on ice. After that, the tissue fragments were washed and re-suspended in cold PBS containing 5% fetal bovine serum (FBS). Then, fragments were gently mixed up and down with a 10 mL pipette and allowed to settle down for 5 min. The supernatant was enriched with crypts. The crypts were collected by passing through a 70 μm cell strainer (Fisher Scientific). Then, the fractions

were centrifuged at 250 g to remove individual cells. Isolated crypts were counted and pelleted; 150–300 crypts were mixed with 40 μ L Matrigel (Corning, Tewksbury, MA, USA) and dropped into the center of a well in a 24-well plate. After the Matrigel polymerized, 500 μ L of crypt culture medium (Stemcell Technologies, Vancouver, BC, USA) was added into each well of the 24-well plate and kept in a CO₂ incubator for 7 days.

2.7. Immunohistochemistry

Immunohistochemical staining was performed with standard techniques using an avidin–biotin complex, diaminobenzidine chromogen, and hematoxylin counterstaining. Appropriate positive and negative controls were included. Immunohistochemical staining for myeloperoxidase (MPO, for neutrophils) and macrophages was performed, as described previously [11], on proximal segments of the jejunum obtained at 0 h, 4 days, 7 days, and 21 days (with and without GT3). Tissue sections were incubated with primary rabbit anti-MPO (1:100, Dako, Glostrup, Denmark) or monoclonal rat anti-macrophage antibodies (RM0029-11H3, 1:100, Abcam) for 2 hours at room temperature. This was followed by a 30 min incubation with biotinylated secondary goat anti-rabbit IgG (MPO) and rabbit anti-rat IgG (macrophage) antibodies, with specificity for respective primary antibodies, at a 1:400 dilution (Vector laboratories, Burlingame, CA, USA). The slides were further incubated with the horseradish peroxidase (HRP) labelled avidin–biotin complex (Vector Laboratories) at a 1:100 dilution for 45 min. The HRP activity was measured with 0.5 mg/ml 3,3-diaminobenzidine tetrahydrochloride (DAB-HCl) solution (Sigma-Aldrich, St. Louis, MO, USA) and 0.003% H₂O₂ in Tris-buffered saline (TBS; Cell Signaling Technology) that enables developing the color. DAB solution was prepared immediately prior to use by dissolving 10 mg of DAB-HCl in 15 mL of TBS. Immunoreactivity was quantified using a computerized image analysis software, called Image-Pro Premier (Media Cybernetics; Rockville, MD, USA) as described elsewhere [24]. Cells positive for MPO and macrophages were identified after setting the color thresholding. The number of positive cells per 10 fields at 40 \times magnification was considered as a single value for statistical analysis.

2.8. RNA Extraction, cDNA Preparation, and Quantitative Reverse-Transcription PCR (qRT-PCR)

Total RNA was purified from frozen tissue with the RNeasy Plus Mini Kit (Qiagen, Valencia, CA, USA), according to the manufacturer's instructions, after homogenizing the samples in TRIzol[®] Reagent (Life Technologies, Grand Island, NY, USA). cDNA was synthesized with a cDNA reverse-transcription kit (Applied Biosystems, Foster City, CA, USA) after treating with RQ-DNase I (Promega, Madison, WI, USA). Predesigned Taqman assays (Applied Biosystems) for the following mouse genes were used: *Lgr5*, Mm00438890_m1; *Msi1*, Mm01203522_m1; *Bmi1*, Mm03053308_g1; and 18S rRNA, Hs99999901_s1. The mRNA levels were normalized to eukaryotic 18S rRNA and calculated relative to control mice with the standard $\Delta\Delta$ Ct method.

2.9. Statistical Analysis

Results are expressed as means \pm the standard error of the mean (SEM). Data were analyzed with Prism software (version 4.0; GraphPad, San Diego, CA). Multiple means were compared by ANOVA and pairwise comparisons were analyzed with the Student's t-test. A two-sided value of $p < 0.05$ was considered statistically significant. We followed the Guide for the Use of the International System of Units (SI) as recommend by National Institute of Standards and Technology (<https://physics.nist.gov/cuu/pdf/sp811.pdf>).

3. Results

3.1. GT3 Pretreatment Attenuated Intestinal Cell Death, Maintained Villus Height, and Enhanced Crypt Depth in Irradiated Mice

Radiation-induced intestinal cell death, characterized by DNA fragmentation, is an important contributor to acute radiation syndrome and determines survivability. We used the TUNEL assay to measure irreversible cell death in mice 24 h after they were irradiated in the presence or absence of GT3. A representative image of TUNEL-positive cells in the intestine is shown in Figure 1A. We observed no difference in the frequency of TUNEL-positive cells in vehicle- or GT3-treated groups before irradiation (Figure 1B). However, there were significantly more TUNEL-positive cells after irradiation (frequency of TUNEL positive cells in sham-irradiated vehicle, 0.04 ± 0.01 vs. irradiated vehicle, 0.72 ± 0.09 ; $p = 0.0004$) (Figure 1B). Interestingly, treating the mice with GT3 before irradiation suppressed intestinal cell death relative to vehicle treatment (frequency of TUNEL positive cells in irradiated GT3, 0.16 ± 0.04 vs. irradiated vehicle, 0.72 ± 0.09 ; $p < 0.0001$) (Figure 1B).

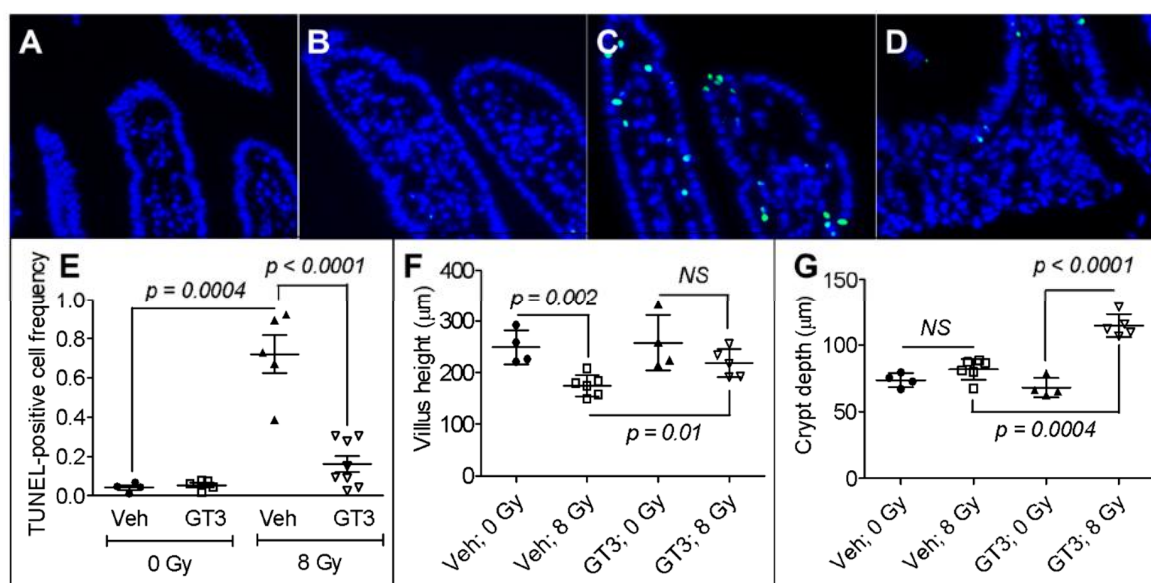


Figure 1. Effects of gamma-tocotrienol (GT3) pretreatment on total body irradiation (TBI)-induced intestinal damage. Representative photomicrograph of TUNEL-positive cells (green) in (A) vehicle (veh) un-irradiated, (B) GT3 un-irradiated, (C) vehicle irradiated, and (D) GT3 irradiated groups. (E) Frequency of TUNEL-positive cells in the intestine of sham-irradiated or irradiated mice, with or without GT3 pretreatment, TUNEL-positive cells were counted 24 h after 8 Gy TBI; (F) Villus height measured 4 d after 8 Gy TBI in sham-irradiated or irradiated groups, with or without GT3 pretreatment; (G) Crypt depth measured 4 d after 8 Gy TBI in sham-irradiated or irradiated groups, with or without GT3 pretreatment. Data represent the mean \pm standard error of the mean (SEM). NS = not significant.

The loss of epithelial cells after irradiation shortens the villi, disrupting the structural integrity of the intestine. We found no difference in villus height between the sham-irradiated vehicle- and GT3-treated groups (Figure 1C). However, exposure to 8 Gy TBI on day 4 significantly decreased the height of villi in vehicle-treated animals (sham-irradiated vehicle, $248.87 \pm 16.40 \mu\text{m}$ vs. irradiated vehicle, $174.84 \pm 8.41 \mu\text{m}$; $p = 0.002$) (Figure 1C). GT3 administration 24 h before 8 Gy TBI attenuated this decrease in villus height (irradiated vehicle, $174.84 \pm 8.41 \mu\text{m}$ vs. irradiated GT3, $217.90 \pm 12.28 \mu\text{m}$; $p = 0.01$) (Figure 1C).

An increase in crypt depth is associated with the survival and a higher proliferation rate of stem cells after intestinal injury. Here, we measured crypt depth 4 days after 8 Gy TBI. In the sham-irradiated groups, we observed no difference in crypt depth after vehicle- or GT3-treatment

(Figure 1D). However, in the irradiated animals, GT3-treatment significantly increased crypt depth compared to vehicle-treatment (GT3-treated group, $114.69 \pm 3.83 \mu\text{m}$ vs. vehicle-treated group, $81.89 \pm 3.23 \mu\text{m}$; $p = 0.0004$) (Figure 1D).

3.2. GT3 Pretreatment Restored the Intestinal Barrier and Upregulated the Level of Occludin Protein in Irradiated Intestinal Tissue

Disrupting the structural integrity of the intestine impairs its barrier function, making it permeable to luminal contents. We measured intestinal barrier function with a permeability assay 4 days after exposure to 10 Gy or 12 Gy TBI; permeability was quantified as the optical density of FITC-labeled dextran in the blood following administration in the intestinal lumen (Figure 2A). The rationale for using a relatively higher dose of radiation for this study is to make sure the barrier integrity is lost. In vehicle-treated mice, 10 Gy TBI significantly increased intestinal permeability (sham-irradiated vehicle, $4266.70 \pm 220.62 \text{ ng/mL}$ vs. 10 Gy vehicle, $11,463.72 \pm 2176.74 \text{ ng/mL}$; $p = 0.01$), as did 12 Gy TBI (sham-irradiated vehicle, $4266.70 \pm 220.62 \text{ ng/mL}$ vs. 12 Gy vehicle, $15,996.03 \pm 2665.01 \text{ ng/mL}$; $p = 0.006$) (Figure 2A). However, pretreating the animals with GT3 significantly attenuated this increase in permeability compared to vehicle-treatment after both 10 Gy TBI (10 Gy vehicle, $11,463.72 \pm 2176.74 \text{ ng/mL}$ vs. 10 Gy GT3, $5188.08 \pm 154.39 \text{ ng/mL}$; $p = 0.009$) and 12 Gy TBI (12 Gy vehicle, $15,996.03 \pm 2665.01 \text{ ng/mL}$ vs. 12 Gy GT3, $7285.45 \pm 1291.09 \text{ ng/mL}$; $p = 0.02$) (Figure 2A).

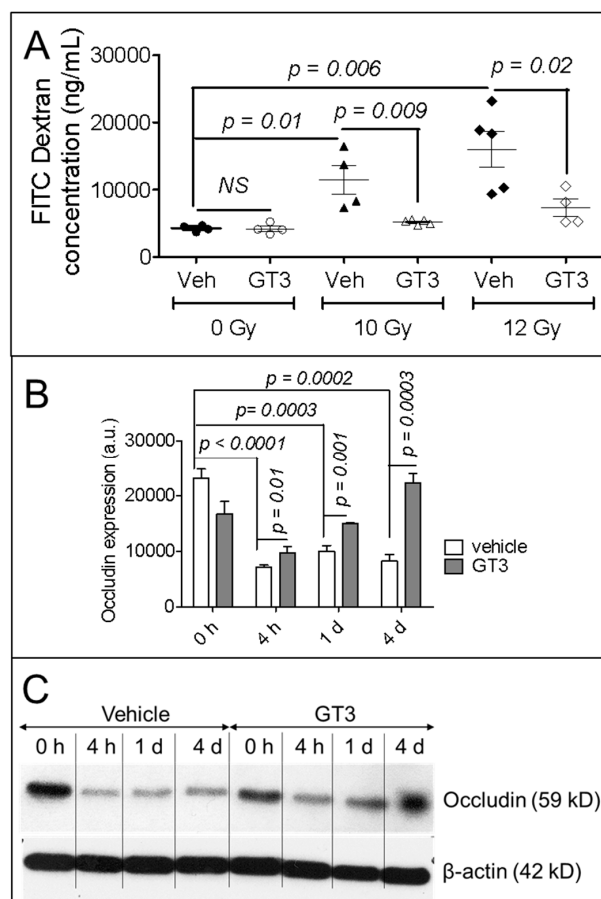


Figure 2. Effects of GT3 pretreatment on intestinal function. (A) Functional activity was measured on day 4 after 10 Gy or 12 Gy TBI with an intestinal permeability assay, as described in the Methods; (B) Densitometry of immunoblot showing time-dependent change in occludin in intestinal tissue from irradiated or sham-irradiated mice, with or without GT3 pretreatment 24 h before exposure to TBI; (C) Representative immunoblot of occludin at different time points. Data represent the mean \pm SEM.

Because radiation-induced changes in the level of tight junction-related proteins also play a critical role in intestinal permeability, we measured occludin protein level in the intestines of mice irradiated with or without GT3 pretreatment. Occludin level was measured at 4 h, 1 d, and 4 d after 8 Gy TBI. Compared to sham-irradiated animals (0 h), TBI significantly down-regulated occludin level at 4 h ($p < 0.0001$), 1 d ($p = 0.0003$), and 4 d ($p = 0.0002$) after vehicle treatment. However, compared to vehicle-treated irradiated groups, GT3 pretreatment significantly upregulated occludin level at 4 h ($p = 0.01$), 1 d ($p = 0.001$), and 4 d ($p = 0.0003$) (Figure 2B); at day 4, the level of occludin level reached that of the sham-irradiated group (Figure 2B). Figure 2C shows representative immunoblot data of occludin level at different time points in intestinal tissue before and after TBI and with or without GT3 pretreatment.

3.3. GT3 Pretreatment Rescued Populations of Intestinal Neutrophils, Macrophages, and Lymphocytes

TBI is known to deplete immune cells in the intestine. Neutrophil and macrophage levels in the intestine were measured at 4 d, 7 d, and 21 d by immunohistochemistry after exposure to 8 Gy TBI; lymphocyte levels were measured at 4 h, 1 d, and 4 d by immunoblot after exposure to 8 Gy TBI (Figure 3). Because lymphocytes are highly sensitive to radiation, we measured them at earlier time points. Compared to the sham-irradiated group, TBI significantly decreased the population of neutrophils at 4 d ($p = 0.0002$), 7 d ($p = 0.002$), and 21 d ($p = 0.03$) (Figure 3A–E). Importantly, pretreating the animals with GT3 significantly increased the neutrophil population at 4 d ($p < 0.0001$), 7 d ($p = 0.005$), and 21 d ($p = 0.0009$) compared to vehicle-treatment (Figure 3E).

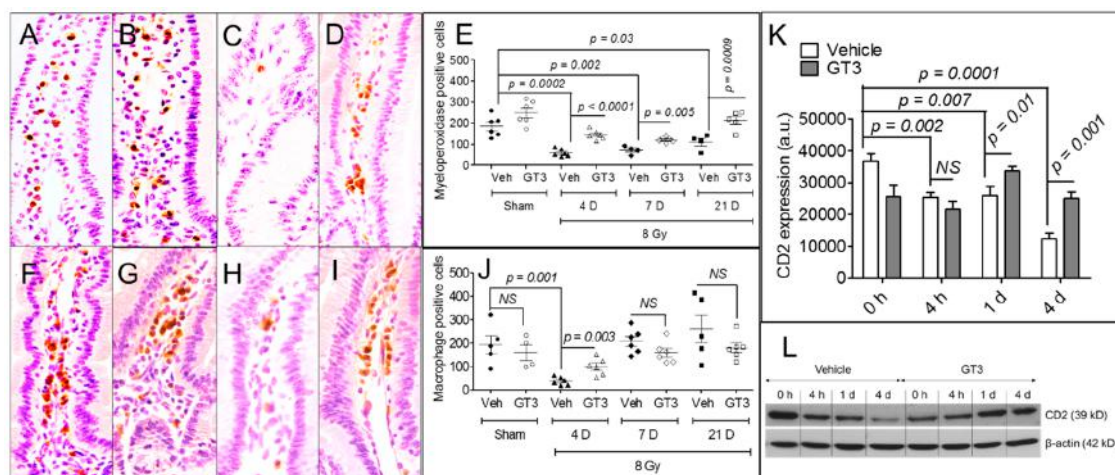


Figure 3. Effects of GT3 pretreatment on intestinal mesenchymal immune cells. (A–D) Representative photomicrographs (40 \times magnification) of myeloperoxidase immunostaining in samples from sham-irradiated vehicle, sham-irradiated GT3, irradiated vehicle, and irradiated GT3 groups on day 4 post-irradiation; (E) Myeloperoxidase-positive cells in immunostained tissue at different time points; (F–I) Representative photomicrographs (40 \times magnification) of macrophage immunostaining in samples from sham-irradiated vehicle, sham-irradiated GT3, irradiated vehicle, and irradiated GT3 groups on day 4 post-irradiation; (J) Cells with positive macrophage immunostaining at different time points; (K) Densitometry of immunoblot showing time-dependent change in CD2 in intestinal tissue of irradiated or sham-irradiated mice, with or without GT3 pretreatment 24 h before TBI; (L) Representative immunoblot of CD2 level at different time points. Data represent the mean \pm SEM. NS = not significant.

Compared to the sham-irradiated group, TBI significantly decreased the population of macrophages at 4 d in the vehicle-treated group (frequency of sham-irradiated vehicle, 193.8 ± 38.16 cells vs. irradiated vehicle, 37.83 ± 6.99 cells; $p = 0.001$) (Figure 3F–J); however, the macrophage population recovered at days 7 and 21, resembling that of the sham-irradiated group (Figure 3J). Pretreating the animals with GT3

significantly increased the macrophage population in the intestine on day 4 compared to vehicle-treatment (frequency of irradiated vehicle, 37.83 ± 6.99 cells vs. irradiated GT3, 100.17 ± 14.96 cells; $p = 0.003$) (Figure 3J).

Next, we assayed lymphocytes by immunoblotting for CD2 (a lymphocyte marker) in the intestinal tissue of sham-irradiated and irradiated animals pretreated with or without GT3 (Figure 3K–L). We observed a significant decrease in lymphocytes in vehicle-treated animals after TBI relative to the sham-irradiated group at 4 h ($p = 0.002$), 1 d ($p = 0.007$), and 4 d ($p = 0.0001$) (Figure 3K). However, pretreating the animals with GT3 significantly increased the lymphocyte population compared to vehicle-treatment at 1 d ($p = 0.01$) and 4 d ($p = 0.001$) after TBI, but no difference in lymphocyte level was observed at 4 h (Figure 3K). Figure 3L shows a representative immunoblot of CD2 at different time intervals.

3.4. GT3 Pretreatment Failed to Promote Ex Vivo Intestinal Organoid Formation after TBI

Next, we investigated whether pretreating animals with GT3 before irradiation enhanced the ability of crypt cells to form intestinal organoids ex vivo, to determine whether GT3 can protect epithelial cells in absence of underlying mesenchymal cells. Figure 4A,B show a representative spheroid and an organoid formed from intestinal crypt cells. Although GT3 pretreatment significantly enhanced spheroid formation, there were significantly fewer organoids in the GT3-treated group than the vehicle-treated group (Figure 4C). Overall, there was no difference between the vehicle- and GT3-treated groups for the total count of organoids and spheroids (Figure 4C). In addition, GT3 pretreatment did not affect the expression of various stem cell markers, including Lgr5, Msi1, and Bmi1, in the intestinal tissue of sham-irradiated or irradiated mice (Figure S1A–C).

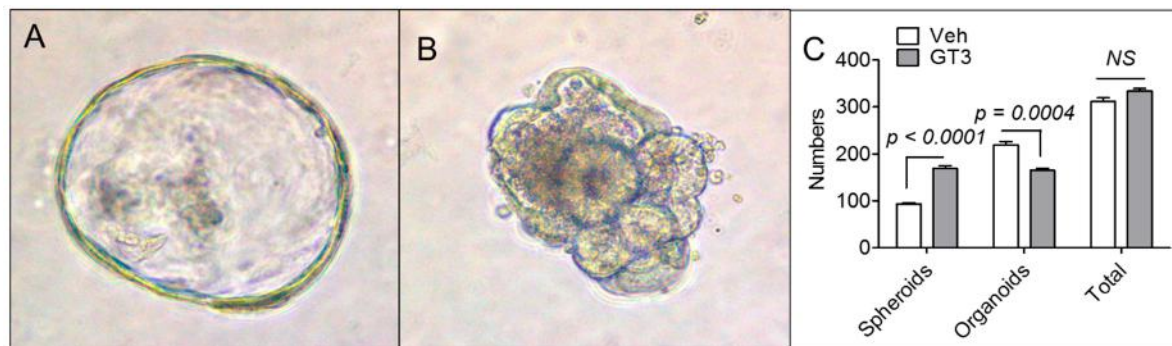


Figure 4. Effects of GT3 pretreatment on ex vivo intestinal organoid formation. (A) Representative photomicrograph of spheroid formed from intestinal crypt cells; (B) Representative photomicrograph of organoid formed from intestinal crypt cells; (C) Number of spheroids or organoids formed 7 days after exposure to 8 Gy TBI. Data represent the mean \pm SEM. NS = not significant.

3.5. GT3 Pretreatment Enhanced AKT Phosphorylation on Day 4 after Irradiation

Immune cells, particularly neutrophils and lymphocytes, are capable of activating the β -catenin pathway, which enhances epithelial cell proliferation through AKT phosphorylation. Thus, we assayed AKT phosphorylation on day 4 after TBI in the intestinal tissue of sham-irradiated or irradiated mice with or without GT3 pretreatment. In the vehicle-treated groups, TBI induced a significant decrease in AKT phosphorylation compared to sham-irradiation (Figure 5A). However, GT3 significantly upregulated AKT phosphorylation in irradiated animals compared to sham-irradiated ones (Figure 5A). Figure 5B shows a representative immunoblot for phosphorylated AKT in the intestinal tissue.

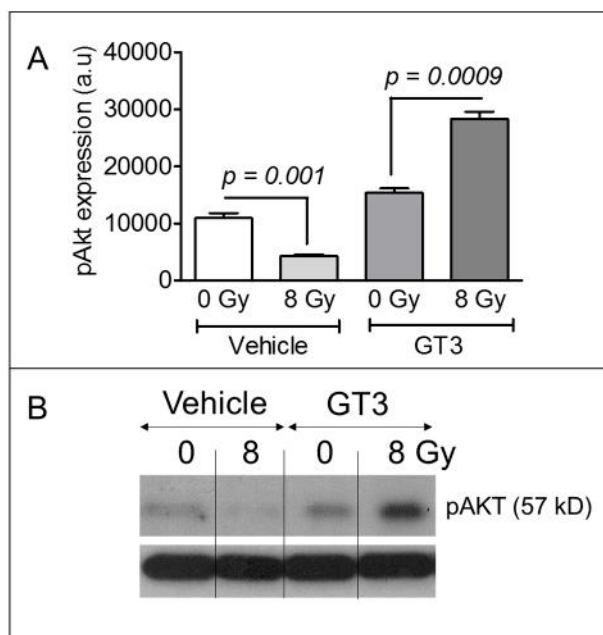


Figure 5. Effects of GT3 pretreatment on AKT phosphorylation in intestinal tissue. (A) Densitometry of an immunoblot showing change in AKT phosphorylation in intestinal tissue from irradiated or sham-irradiated mice, given either vehicle or GT3 24 h before exposure to TBI; (B) Representative immunoblot of phosphorylated AKT (pAKT) in intestinal tissue 4 d after 8 Gy TBI. Data represent the mean \pm SEM.

4. Discussion

TBI is used to treat hematopoietic malignancies and solid tumors. Further, TBI and chemotherapeutic drugs are routinely used to prepare patients for hematopoietic stem cell transplants [25–29]. In addition, astronauts are continuously exposed to chronic doses of TBI during their entire period of a space mission. Finally, the risk of exposure to TBI during radiological warfare is unavoidable. Under any of these circumstances, TBI can adversely affect various organs [30,31], especially the intestine [32], which is highly sensitive to IR.

The pathogenesis of IR-induced intestinal damage is an exceedingly complex process, involving the elimination, aberrant interaction, or functional dysregulation of various cell types present at the damaged site. IR disrupts cellular redox homeostasis, induces the generation of reactive oxygen species, and enhances oxidative stress, which may trigger apoptotic or non-apoptotic cell death, characterized by DNA fragmentation [17,33]. Fragmented DNA is the hallmark of irreversible cell death and can be detected by TUNEL assay. The loss of mucosal epithelial cells disrupts the structural integrity of the intestine, characterized by villus blunting and a decrease in mucosal length. We observed a statistically significant decrease in villus height on day 4 after 8 Gy TBI in vehicle-treated animals relative to un-irradiated controls, suggesting that the structural integrity of the intestine was compromised. Similar to our current findings, various groups have demonstrated that 8 Gy TBI adversely affects the structural integrity of the intestine [15,34,35]. However, we did not observe a decrease in villus height if the mice received a single dose of subcutaneous GT3 24 h before TBI. One explanation is that GT3 suppresses radiation-induced apoptosis. Suman et al. (2013) demonstrated that administration of GT3 (200 mg/kg bwt) significantly suppressed apoptotic cell death in the intestine relative to controls after 11 Gy TBI [17]. They also showed that GT3 pretreatment upregulated an array of anti-apoptotic genes and downregulated pro-apoptotic ones [17]. We found that treating animals with GT3 24 h before TBI significantly reduced intestinal cell death. Moreover, GT3 pretreatment increased the average crypt depth (crypts contain intestinal stem cells), suggesting that more stem cells could have survived and proliferated after TBI. Indeed, Liu et al. (2016) identified a strong positive correlation between crypt

depth and stem cell survival after irradiation [36]. These findings clearly suggest that GT3 has the potential to suppress structural damage to the intestines after TBI.

The radiation-induced apoptotic death of epithelial cells reduces the mucosal surface area, disrupts barrier integrity, increases intestinal permeability, and facilitates the invasion of luminal microbes to the intestinal tissue. Epithelial cells, specifically Lgr5-positive, crypt-base columnar epithelial stem cells and their progenitors, are highly sensitive to IR and rapidly undergo apoptotic and mitotic death after exposure, reducing the integrity of the mucosal barrier. We observed a dose-dependent increase in intestinal permeability after exposure to 10 Gy or 12 Gy TBI. Importantly, pretreating animals with GT3 significantly decreased this radiation-induced intestinal permeability. Radiation-induced changes at the level of tight junction-related proteins play a critical role in enhancing intestinal permeability [4,37,38]. Occludin is a major constituent of tight junction-related proteins and is critical for maintaining the integrity of the intestinal epithelial barrier. Occludin-deficient mice exhibit increased colonic mucosal barrier dysfunction after ethanol challenge [39]. Moreover, genetic knockdown of occludin in human colon cancer cells (Caco-2) promote the disruption of tight junctions and barrier dysfunction after exposure to acetaldehyde [39]. All of these data indicate that suppressing occludin increases intestinal permeability. Our present study demonstrated a significant decrease in occludin level in the intestinal tissue, and this likely increased intestinal permeability after irradiation. A similar decrease in occludin level has also been noted in the intestines of non-human primates after radiation exposure [4]. Interestingly, pretreating our mice with GT3 significantly upregulated occludin level, relative to vehicle treatment, 4 days after TBI, suggesting that GT3 helps restore barrier integrity, potentially by upregulating occludin. All of these data clearly indicate that GT3 pretreatment plays a critical role in reinstating both the structural and functional integrity of the intestine after irradiation. However, we do not know how GT3 exerts its positive effects in the intestinal mucosa and on stem cells.

After irradiation, the crosstalk between epithelial stem cells and immune cells at the damaged site is critical for restoring intestinal homeostasis and modulating radio-sensitivity [7,9]. For example, depleting macrophages enhances radiation lethality in mice [40]. Moreover, macrophages play important roles in the repair and regeneration of damaged intestinal tissue [41], potentially by: (1) modulating inflammatory responses, (2) neutralizing invading microbes, and (3) releasing regenerative signals to activate intestinal stem cells [7]. IR not only eliminates intestinal stem cells, but significantly depletes immune cell populations at the damaged site. We found that TBI substantially reduces, in a time-dependent manner, the levels of neutrophils, lymphocytes, and macrophages in the intestinal stroma after exposure to 8 Gy TBI, and this is in agreement with findings by Garg et al. (2010) [11]. The greatest decrease in immune cells was observed on day 4 after TBI. This loss could be the result of apoptotic or mitotic death due to irreparable radiation-induced DNA damage. However, GT3 treatment enhanced the recovery of immune cells in the intestine after irradiation, potentially restoring epithelial homeostasis.

When the intestines are damaged, immune cells, specifically neutrophils and lymphocytes, promote the growth and differentiation of crypt epithelial cells via AKT phosphorylation, which in turn activates the regenerative β -catenin pathway [42,43]. Sumagin et al. (2016) showed that neutrophils activate the β -catenin pathway, through AKT phosphorylation, in mucosal epithelial cells to promote wound healing [42]. Using a co-culture model, Dahan et al. (2008) demonstrated that lymphocytes induce AKT phosphorylation in intestinal epithelial cells within 30 min [43]. Indeed, we observed a significant increase in AKT phosphorylation in intestinal samples from the GT3 group, relative to the vehicle-treated group, and this could be a major mechanism by which GT3 protects the intestines from radiation damage.

Similarly, Saha et al. (2016) showed that macrophage-derived Wnt ligands suppress radiation damage in epithelial cells in mice by activating the β -catenin pathway [7]. We found that GT3 accelerated the recovery of macrophages in the intestine after irradiation. This increase in the macrophage population could exert positive effects on intestinal epithelial cells by releasing

regenerative signals. All of these data suggest that the GT3-mediated recovery of mesenchymal immune cells may play a critical role in protecting the intestine from radiation damage.

To further investigate the ability of GT3 to enhance stem cell proliferation in the absence of mesenchymal cells, crypts were cultured *ex vivo* in intestinal organoid culture medium. Interestingly, GT3 failed to promote intestinal organoid formation, suggesting that GT3 protects the intestine potentially by modulating mesenchymal immune cells, not by exerting positive effects directly on epithelial cells. Previous studies demonstrated that immune cells promote the proliferation of intestinal epithelial cells and recovery after injury by activating the β -catenin pathway via AKT phosphorylation [42,43]. Indeed, we found that GT3 significantly upregulated post-irradiation AKT-phosphorylation in the intestine. These data suggest that GT3 could alter AKT phosphorylation to protect the intestines from radiation damage.

5. Conclusions

In conclusion, we found that GT3 suppresses radiation-induced structural and functional damage in the intestine, potentially by upregulating occludin level and by facilitating the recovery of mesenchymal immune cells after TBI. Thus, GT3 has the potential to be a non-toxic medical countermeasure to protect the intestines from radiation damage.

Supplementary Materials: The following are available online at <http://www.mdpi.com/2076-3921/8/3/57/s1>, Figure S1: Effects of GT3 pretreatment on TBI-induced intestinal stem cell markers.

Author Contributions: S.G., R.S., S.B., A.V.S., V.M., and R.P. designed and performed experiments and collected data. S.G., J.W., M.H.-J., A.G.B., S.P.G., S.A.P., and R.P. planned experiments, analyzed and interpreted data, and edited the manuscript. R.P. conceived of and directed the study and wrote the manuscript.

Funding: This study was supported by Arkansas Space Grant Consortium grant NNX15AR71H (RP); an Institutional Development Award (IDeA) from the NIGMS of the National Institutes of Health under grant number P20 GM109005 (RP, AGB, SAP, and MHJ); NIFA-USDA grant ARKW-2017-07886 (AGB); and VA Merit Review grant I01 BX002425 (AGB); Peer Reviewed Medical Research Program award from Department of Defense (SAP).

Acknowledgments: This manuscript was edited by the Science Communication Group at the University of Arkansas for Medical Sciences (UAMS). The authors acknowledge Gail Wagoner and the staff members of the UAMS Department of Laboratory Animal Medicine for excellent animal care. The opinions contained herein are the views of the authors and are not necessarily those of Armed Forces Radiobiology Research Institute, the Uniformed Services of the University of the Health Sciences, or the Department of Defense.

Conflicts of Interest: It is hereby confirmed that no actual or potential conflicts of interest exist in relation to this article. The funders had no role in the design of the study; in the collection, analyses, or interpretation of data; in the writing of the manuscript, or in the decision to publish the results.

References

1. Gehart, H.; Clevers, H. Tales from the crypt: New insights into intestinal stem cells. *Nat. Rev. Gastroenterol. Hepatol.* **2019**, *16*, 19–34. [[CrossRef](#)] [[PubMed](#)]
2. Shadad, A.K.; Sullivan, F.J.; Martin, J.D.; Egan, L.J. Gastrointestinal radiation injury: symptoms, risk factors and mechanisms. *World J. Gastroenterol.* **2013**, *19*, 185–198. [[CrossRef](#)] [[PubMed](#)]
3. Inagaki-Ohara, K.; Takamura, N.; Yada, S.; Alnadjim, Z.; Liu, E.; Yu, X.; Yoshida, H.; Lin, T. Radiation-induced crypt intestinal epithelial cell apoptosis *in vivo* involves both caspase-3-dependent and -independent pathways. *Dig. Dis. Sci.* **2002**, *47*, 2823–2830. [[CrossRef](#)] [[PubMed](#)]
4. Garg, S.; Zheng, J.; Wang, J.; Authier, S.; Pouliot, M.; Hauer-Jensen, M. Segmental Differences in Radiation-Induced Alterations of Tight Junction-Related Proteins in Non-Human Primate Jejunum, Ileum and Colon. *Radiat. Res.* **2016**, *185*, 50–59. [[CrossRef](#)] [[PubMed](#)]
5. Liang, S.C.; Tan, X.-Y.; Luxenberg, D.P.; Karim, R.; Dunussi-Joannopoulos, K.; Collins, M.; Fouser, L.A. Interleukin (IL)-22 and IL-17 are coexpressed by Th17 cells and cooperatively enhance expression of antimicrobial peptides. *J. Exp. Med.* **2006**, *203*, 2271–2279. [[CrossRef](#)] [[PubMed](#)]

6. Pull, S.L.; Doherty, J.M.; Mills, J.C.; Gordon, J.I.; Stappenbeck, T.S. Activated macrophages are an adaptive element of the colonic epithelial progenitor niche necessary for regenerative responses to injury. *Proc. Natl. Acad. Sci. USA* **2005**, *102*, 99–104. [[CrossRef](#)] [[PubMed](#)]
7. Saha, S.; Aranda, E.; Hayakawa, Y.; Bhanja, P.; Atay, S.; Brodin, N.P.; Li, J.; Asfaha, S.; Liu, L.; Tailor, Y.; et al. Macrophage-derived extracellular vesicle-packaged WNTs rescue intestinal stem cells and enhance survival after radiation injury. *Nat. Commun.* **2016**, *7*, 13096. [[CrossRef](#)] [[PubMed](#)]
8. Serhan, C.N.; Chiang, N.; van Dyke, T.E. Resolving inflammation: Dual anti-inflammatory and pro-resolution lipid mediators. *Nat. Rev. Immunol.* **2008**, *8*, 349–361. [[CrossRef](#)] [[PubMed](#)]
9. Lindemans, C.A.; Calafiore, M.; Mertelsmann, A.M.; O'Connor, M.H.; Dudakov, J.A.; Jenq, R.R.; Velardi, E.; Young, L.F.; Smith, O.M.; Lawrence, G.; et al. Interleukin-22 promotes intestinal-stem-cell-mediated epithelial regeneration. *Nature* **2015**, *528*, 560–564. [[CrossRef](#)] [[PubMed](#)]
10. Chen, F.; Yang, W.; Huang, X.; Cao, A.T.; Bilotta, A.J.; Xiao, Y.; Sun, M.; Chen, L.; Ma, C.; Liu, X.; et al. Neutrophils Promote Amphiregulin Production in Intestinal Epithelial Cells through TGF- β and Contribute to Intestinal Homeostasis. *J. Immunol.* **2018**, *201*, 2492–2501. [[CrossRef](#)] [[PubMed](#)]
11. Garg, S.; Boerma, M.; Wang, J.; Fu, Q.; Loose, D.S.; Kumar, K.S.; Hauer-Jensen, M. Influence of sublethal total-body irradiation on immune cell populations in the intestinal mucosa. *Radiat. Res.* **2010**, *173*, 469–478. [[CrossRef](#)] [[PubMed](#)]
12. Hauer-Jensen, M.; Denham, J.W.; Andreyev, H.J.N. Radiation enteropathy—pathogenesis, treatment and prevention. *Nat. Rev. Gastroenterol. Hepatol.* **2014**, *11*, 470–479. [[CrossRef](#)] [[PubMed](#)]
13. Ghosh, S.P.; Kulkarni, S.; Hieber, K.; Toles, R.; Romanyukha, L.; Kao, T.-C.; Hauer-Jensen, M.; Kumar, K.S. Gamma-tocotrienol, a tocol antioxidant as a potent radioprotector. *Int. J. Radiat. Biol.* **2009**, *85*, 598–606. [[CrossRef](#)] [[PubMed](#)]
14. Kulkarni, S.; Ghosh, S.P.; Satyamitra, M.; Mog, S.; Hieber, K.; Romanyukha, L.; Gambles, K.; Toles, R.; Kao, T.-C.; Hauer-Jensen, M.; et al. Gamma-tocotrienol protects hematopoietic stem and progenitor cells in mice after total-body irradiation. *Radiat. Res.* **2010**, *173*, 738–747. [[CrossRef](#)] [[PubMed](#)]
15. Berbée, M.; Fu, Q.; Boerma, M.; Wang, J.; Kumar, K.S.; Hauer-Jensen, M. gamma-Tocotrienol ameliorates intestinal radiation injury and reduces vascular oxidative stress after total-body irradiation by an HMG-CoA reductase-dependent mechanism. *Radiat. Res.* **2009**, *171*, 596–605. [[CrossRef](#)] [[PubMed](#)]
16. Berbee, M.; Fu, Q.; Boerma, M.; Pathak, R.; Zhou, D.; Kumar, K.S.; Hauer-Jensen, M. Reduction of radiation-induced vascular nitrosative stress by the vitamin E analog γ -tocotrienol: evidence of a role for tetrahydrobiopterin. *Int. J. Radiat. Oncol. Biol. Phys.* **2011**, *79*, 884–891. [[CrossRef](#)] [[PubMed](#)]
17. Suman, S.; Datta, K.; Chakraborty, K.; Kulkarni, S.S.; Doiron, K.; Fornace, A.J.; Sree Kumar, K.; Hauer-Jensen, M.; Ghosh, S.P. Gamma tocotrienol, a potent radioprotector, preferentially upregulates expression of anti-apoptotic genes to promote intestinal cell survival. *Food Chem. Toxicol.* **2013**, *60*, 488–496. [[CrossRef](#)] [[PubMed](#)]
18. Pathak, R.; Shao, L.; Ghosh, S.P.; Zhou, D.; Boerma, M.; Weiler, H.; Hauer-Jensen, M. Thrombomodulin contributes to gamma tocotrienol-mediated lethality protection and hematopoietic cell recovery in irradiated mice. *PLoS ONE* **2015**, *10*, e0122511. [[CrossRef](#)] [[PubMed](#)]
19. Pathak, R.; Ghosh, S.P.; Zhou, D.; Hauer-Jensen, M. The Vitamin E Analog Gamma-Tocotrienol (GT3) and Statins Synergistically Up-Regulate Endothelial Thrombomodulin (TM). *Int. J. Mol. Sci.* **2016**, *17*, 1937. [[CrossRef](#)] [[PubMed](#)]
20. Geiger, H.; Pawar, S.A.; Kerschen, E.J.; Nattamai, K.J.; Hernandez, I.; Liang, H.P.H.; Fernández, J.Á.; Cancelas, J.A.; Ryan, M.A.; Kustikova, O.; et al. Pharmacological targeting of the thrombomodulin-activated protein C pathway mitigates radiation toxicity. *Nat. Med.* **2012**, *18*, 1123–1129. [[CrossRef](#)] [[PubMed](#)]
21. Pathak, R.; Wang, J.; Garg, S.; Aykin-Burns, N.; Petersen, K.-U.; Hauer-Jensen, M. Recombinant Thrombomodulin (Solulin) Ameliorates Early Intestinal Radiation Toxicity in a Preclinical Rat Model. *Radiat. Res.* **2016**, *186*, 112–120. [[CrossRef](#)] [[PubMed](#)]
22. Apostolov, E.O.; Soultanova, I.; Savenka, A.; Bagandov, O.O.; Yin, X.; Stewart, A.G.; Walker, R.B.; Basnakian, A.G. Deoxyribonuclease I is essential for DNA fragmentation induced by gamma radiation in mice. *Radiat. Res.* **2009**, *172*, 481–492. [[CrossRef](#)] [[PubMed](#)]
23. Alegria-Schaffer, A.; Lodge, A.; Vattem, K. Performing and optimizing Western blots with an emphasis on chemiluminescent detection. *Methods Enzymol.* **2009**, *463*, 573–599. [[CrossRef](#)] [[PubMed](#)]

24. Wang, J.; Zheng, H.; Sung, C.C.; Richter, K.K.; Hauer-Jensen, M. Cellular sources of transforming growth factor-beta isoforms in early and chronic radiation enteropathy. *Am. J. Pathol.* **1998**, *153*, 1531–1540. [[CrossRef](#)]
25. Van Bekkum, D.W. Effectiveness and risks of total body irradiation for conditioning in the treatment of autoimmune disease with autologous bone marrow transplantation. *Rheumatology* **1999**, *38*, 757–761. [[CrossRef](#)] [[PubMed](#)]
26. Deeg, H.J.; Amylon, I.D.; Harris, R.E.; Collins, R.; Beatty, P.G.; Feig, S.; Ramsay, N.; Territo, M.; Khan, S.P.; Pamphilon, D.; et al. Marrow transplants from unrelated donors for patients with aplastic anemia: Minimum effective dose of total body irradiation. *Biol. Blood Marrow Transplant.* **2001**, *7*, 208–215. [[CrossRef](#)] [[PubMed](#)]
27. Geller, R.B.; Devine, S.M.; O'Toole, K.; Persons, L.; Keller, J.; Mauer, D.; Holland, H.K.; Dix, S.P.; Piotti, M.; Redei, I.; et al. Allogeneic bone marrow transplantation with matched unrelated donors for patients with hematologic malignancies using a preparative regimen of high-dose cyclophosphamide and fractionated total body irradiation. *Bone Marrow Transplant.* **1997**, *20*, 219–225. [[CrossRef](#)] [[PubMed](#)]
28. Soni, S.; Abdel-Azim, H.; McManus, M.; Nemecek, E.; Sposto, R.; Woolfrey, A.; Frangoul, H. Phase I Study of Clofarabine and 2-Gy Total Body Irradiation as a Nonmyeloablative Preparative Regimen for Hematopoietic Stem Cell Transplantation in Pediatric Patients with Hematologic Malignancies: A Therapeutic Advances in Childhood Leukemia Consortium Study. *Biol. Blood Marrow Transplantat.* **2017**, *23*, 1134–1141. [[CrossRef](#)]
29. Wei, C.; Candler, T.; Davis, N.; Elson, R.; Crabtree, N.; Stevens, M.; Crowne, E. Bone Mineral Density Corrected for Size in Childhood Leukaemia Survivors Treated with Haematopoietic Stem Cell Transplantation and Total Body Irradiation. *Horm. Res. Paediatr.* **2018**, *89*, 246–254. [[CrossRef](#)] [[PubMed](#)]
30. Thomas, O.; Mahé, M.; Campion, L.; Bourdin, S.; Milpied, N.; Brunet, G.; Lisbona, A.; Le Mevel, A.; Moreau, P.; Harousseau, J.; et al. Long-term complications of total body irradiation in adults. *Int. J. Radiat. Oncol. Biol. Phys.* **2001**, *49*, 125–131. [[CrossRef](#)]
31. Gopal, R.; Ha, C.S.; Tucker, S.L.; Khouri, I.F.; Giralt, S.A.; Gajewski, J.L.; Andersson, B.S.; Cox, J.D.; Champlin, R.E. Comparison of two total body irradiation fractionation regimens with respect to acute and late pulmonary toxicity. *Cancer* **2001**, *92*, 1949–1958. [[CrossRef](#)]
32. Lutgens, L.C.H.W.; Blijlevens, N.M.A.; Deutz, N.E.P.; Donnelly, J.P.; Lambin, P.; de Pauw, B.E. Monitoring myeloablative therapy-induced small bowel toxicity by serum citrulline concentration: A comparison with sugar permeability tests. *Cancer* **2005**, *103*, 191–199. [[CrossRef](#)] [[PubMed](#)]
33. Zheng, K.; Wu, W.; Yang, S.; Huang, L.; Chen, J.; Gong, C.; Fu, Z.; Lin, R.; Tan, J. Treatment of radiation-induced acute intestinal injury with bone marrow-derived mesenchymal stem cells. *Expe. Ther. Med.* **2016**, *11*, 2425–2431. [[CrossRef](#)] [[PubMed](#)]
34. Pawar, S.A.; Shao, L.; Chang, J.; Wang, W.; Pathak, R.; Zhu, X.; Wang, J.; Hendrickson, H.; Boerma, M.; Sterneck, E.; et al. C/EBP δ deficiency sensitizes mice to ionizing radiation-induced hematopoietic and intestinal injury. *PLoS ONE* **2014**, *9*, e94967. [[CrossRef](#)] [[PubMed](#)]
35. Son, T.G.; Gong, E.J.; Bae, M.J.; Kim, S.D.; Heo, K.; Moon, C.; Yang, K.; Kim, J.S. Protective effect of genistein on radiation-induced intestinal injury in tumor bearing mice. *BMC Complementary Alternative Med.* **2013**, *13*, 103. [[CrossRef](#)] [[PubMed](#)]
36. Liu, Z.; Tian, H.; Jiang, J.; Yang, Y.; Tan, S.; Lin, X.; Liu, H.; Wu, B. β -Arrestin-2 modulates radiation-induced intestinal crypt progenitor/stem cell injury. *Cell Death Differ.* **2016**, *23*, 1529–1541. [[CrossRef](#)] [[PubMed](#)]
37. Shukla, P.K.; Gangwar, R.; Manda, B.; Meena, A.S.; Yadav, N.; Szabo, E.; Balogh, A.; Lee, S.C.; Tigyi, G.; Rao, R. Rapid disruption of intestinal epithelial tight junction and barrier dysfunction by ionizing radiation in mouse colon in vivo: protection by N-acetyl-L-cysteine. *Am. J. Physiol. Gastrointest. Liver Physiol.* **2016**, *310*, G705–15. [[CrossRef](#)] [[PubMed](#)]
38. Wei, L.; Leibowitz, B.J.; Epperly, M.; Bi, C.; Li, A.; Steinman, J.; Wipf, P.; Li, S.; Zhang, L.; Greenberger, J.; et al. The GS-nitroxide JP4-039 improves intestinal barrier and stem cell recovery in irradiated mice. *Sci. Rep.* **2018**, *8*, 2072. [[CrossRef](#)] [[PubMed](#)]
39. Mir, H.; Meena, A.S.; Chaudhry, K.K.; Shukla, P.K.; Gangwar, R.; Manda, B.; Padala, M.K.; Shen, L.; Turner, J.R.; Dietrich, P.; et al. Occludin deficiency promotes ethanol-induced disruption of colonic epithelial junctions, gut barrier dysfunction and liver damage in mice. *Biochim. Biophys Acta* **2016**, *1860*, 765–774. [[CrossRef](#)] [[PubMed](#)]

40. Saha, S.; Bhanja, P.; Kabarriti, R.; Liu, L.; Alfieri, A.A.; Guha, C. Bone marrow stromal cell transplantation mitigates radiation-induced gastrointestinal syndrome in mice. *PLoS ONE* **2011**, *6*, e24072. [[CrossRef](#)] [[PubMed](#)]
41. Wynn, T.A.; Vannella, K.M. Macrophages in Tissue Repair, Regeneration, and Fibrosis. *Immunity* **2016**, *44*, 450–462. [[CrossRef](#)] [[PubMed](#)]
42. Sumagin, R.; Brazil, J.C.; Nava, P.; Nishio, H.; Alam, A.; Luissint, A.C.; Weber, D.A.; Neish, A.S.; Nusrat, A.; Parkos, C.A. Neutrophil interactions with epithelial-expressed ICAM-1 enhances intestinal mucosal wound healing. *Mucosal Immunol.* **2016**, *9*, 1151–1162. [[CrossRef](#)] [[PubMed](#)]
43. Dahan, S.; Roda, G.; Pinn, D.; Roth-Walter, F.; Kamalu, O.; Martin, A.P.; Mayer, L. Epithelial: Lamina propria lymphocyte interactions promote epithelial cell differentiation. *Gastroenterology* **2008**, *134*, 192–203. [[CrossRef](#)] [[PubMed](#)]



© 2019 by the authors. Licensee MDPI, Basel, Switzerland. This article is an open access article distributed under the terms and conditions of the Creative Commons Attribution (CC BY) license (<http://creativecommons.org/licenses/by/4.0/>).



Article

Loss of C/EBP δ Exacerbates Radiation-Induced Cognitive Decline in Aged Mice due to Impaired Oxidative Stress Response

Sudip Banerjee , Tyler Alexander, Debajyoti Majumdar, Thomas Groves, Frederico Kiffer, Jing Wang, Akshita Gorantla, Antiño R. Allen * and Snehalata A. Pawar *

Division of Radiation Health, Department of Pharmaceutical Sciences, College of Pharmacy, University of Arkansas for Medical Sciences, Little Rock, AR 72205, USA; SBanerjee@uams.edu (S.B.); Tyler.alexander@stjude.org (T.A.); DMajumdar@uams.edu (D.M.); tuk52207@temple.edu (T.G.); FCKiffer@uams.edu (F.K.); JWang2@uams.edu (J.W.); akshitagorantla@gmail.com (A.G.)

* Correspondence: ARAllen@uams.edu (A.R.A.); SAPawar@uams.edu (S.A.P.); Tel.: +1-501-686-7553 (A.R.A.); +1-501-686-5784 (S.A.P.); Fax: +1-501-686-6057 (A.R.A.); +1-501-686-6057 (S.A.P.)

Received: 18 December 2018; Accepted: 11 February 2019; Published: 18 February 2019



Abstract: Aging is characterized by increased inflammation and deterioration of the cellular stress responses such as the oxidant/antioxidant equilibrium, DNA damage repair fidelity, and telomeric attrition. All these factors contribute to the increased radiation sensitivity in the elderly as shown by epidemiological studies of the Japanese atomic bomb survivors. There is a global increase in the aging population, who may be at increased risk of exposure to ionizing radiation (IR) as part of cancer therapy or accidental exposure. Therefore, it is critical to delineate the factors that exacerbate age-related radiation sensitivity and neurocognitive decline. The transcription factor CCAAT enhancer binding protein delta (C/EBP δ) is implicated with regulatory roles in neuroinflammation, learning, and memory, however its role in IR-induced neurocognitive decline and aging is not known. The purpose of this study was to delineate the role of C/EBP δ in IR-induced neurocognitive decline in aged mice. We report that aged *Cebpd*^{-/-} mice exposed to acute IR exposure display impairment in short-term memory and spatial memory that correlated with significant alterations in the morphology of neurons in the dentate gyrus (DG) and CA1 apical and basal regions. There were no significant changes in the expression of inflammatory markers. However, the expression of superoxide dismutase 2 (SOD2) and catalase (CAT) were altered post-IR in the hippocampus of aged *Cebpd*^{-/-} mice. These results suggest that *Cebpd* may protect from IR-induced neurocognitive dysfunction by suppressing oxidative stress in aged mice.

Keywords: *Cebpd*; C/EBP δ ; ionizing radiation; hippocampus; behavior; novel object recognition; spatial learning; short-term memory; oxidative stress; reactive oxygen species

1. Introduction

There is strong evidence for multifaceted damage to the brain after IR exposure provided by epidemiological studies on the atomic bomb survivors, cancer survivors, and occupational cohorts [1]. The advent of modern medicine has led to a substantial increase in human lifespan and the number of older people among the global population is currently higher and still expanding. The hallmarks of aging are characterized by increased inflammation and deterioration of the cellular stress responses such as the oxidant/antioxidant equilibrium, DNA damage repair fidelity, and telomeric attrition [2]. All these factors contribute to the increased radiation sensitivity in the elderly [2]. Therefore, understanding the mechanistic processes involved in age-related radiation sensitivity is of utmost relevance, particularly in view of the increasing aging population who may be exposed to IR as part

of cancer therapy or accidental exposure to IR. However, very little is known about the molecular mechanism of increased sensitivity to radiation during aging.

Exposure to IR leads to the expression of pro-inflammatory cytokines and reactive oxygen species (ROS) in the brain areas [3–7]. Loss of verbal memory, spatial memory, attention, and novel problem-solving ability are the hallmarks of radiation-induced cognitive impairment [8–13]. A major role in learning, consolidation, and retrieval of information is done by the hippocampus [13,14]. Hippocampus, the main region of the brain where neurogenesis occurs throughout one's lifetime, is highly susceptible to radiation-induced damage [15]. An important player in neurogenesis is the identification of mitochondrial function and, together with observations that mitochondria are targets for ionizing radiation effects, potentially implied mitochondrial dysfunction in radiation-induced deficit of hippocampal neurogenesis-dependent cognition [4,15,16]. Regulation of adult neurogenesis depends on the metabolic status of the animal [17]. Previous studies have reported that exposure to total body irradiation (TBI) induces acute alterations in neuronal structure and early cognitive changes [18,19]. Data from us and others show that doses of high linear energy transfer radiation from 0.1–1 Gy cause significant, dose-responsive reductions in hippocampal dendritic complexity and spine density, which last for up to nine months post-irradiation [20–23]. Therefore, the purpose of this study was to investigate the early effects of TBI on neurocognitive functions in *Cebpd*^{+/+} and *Cebpd*^{-/-} mice. In susceptibility to radiation, age also plays a major role [2,15,24]. Although much is known about the late effects of radiation on neurocognitive deficits, very little is known about the molecular markers and morphological changes that occur in the brain in response to acute effects of IR exposure on neurocognitive functions in the context of aging. Understanding these molecular mechanisms of IR's early effects on neurocognitive dysfunction would enable the development of novel interventions to alleviate the adverse effects due to accidental exposure or as part of radiotherapy to the brain.

The transcription factor CCAAT enhancer binding protein delta (C/EBP δ) is implicated in having a regulatory role in diverse biological functions such as acute-phase response (reaction to inflammation), growth arrest, apoptosis, differentiation, stem cell self-renewal, and tumor suppression [25]. Work by us and others has shown a role for C/EBP δ in maintaining genomic stability, cell cycle arrest, DNA damage repair, and oxidative stress [26–31]. There are several compelling studies that point to a role of C/EBP δ in neuroinflammation in diseases such as Alzheimer's, where the ablation of C/EBP δ is shown to confer a protective role [32,33]. We have previously shown a role for C/EBP δ in radiation response, in promoting post-radiation survival by protection against radiation-induced hematopoietic and intestinal injury, and in modulating basal as well as IR-induced oxidative stress and mitochondrial dysfunction [34,35]. In the present study, we investigated whether the loss of *Cebpd* exacerbates radiation-induced cognitive deficits due to an impaired ability to detoxify IR-induced ROS and/or inflammation.

2. Results

2.1. Irradiation Impairs Short-Term Memory during Y-Maze Test in *Cebpd*^{-/-} Mice

The Y-maze is an established behavioral assay for short-term spatial memory [36]. The amount of time a mouse spends exploring a novel arm relative to the familiar arm in the testing phase is indicative of its ability to retain the spatial memory encoded during familiarization. We observed that *Cebpd*^{+/+}-sham, *Cebpd*^{+/+}-IR, and *Cebpd*^{-/-}-sham groups displayed significant differences in exploration between the maze arms during the testing phase (*Cebpd*^{+/+}-sham: $F_{(2, 12)} = 8.16, p < 0.01$; *Cebpd*^{+/+}-IR: $F_{(2, 18)} = 16.21; p < 0.001$; *Cebpd*^{-/-}-sham: $F_{(2, 12)} = 6.56; p < 0.05$). Post-hoc tests indicate that *Cebpd*^{+/+}-sham animals spent significantly more time exploring the novel than the familiar ($p < 0.05$) or start ($p < 0.01$; Figure 1A) arms. Similarly, the *Cebpd*^{+/+}-IR treatment group also spent significantly more time exploring the novel than the familiar ($p < 0.001$) or start ($p < 0.001$; Figure 1B) arms. Next, the *Cebpd*^{-/-}-sham group was also successful in exploring the novel arm for longer periods of time than the familiar or start arms ($p < 0.05$; Figure 1C). However, the *Cebpd*^{-/-}-IR animals

displayed impaired short-term memory ($F_{(2, 12)} = 1.25$; $p = 0.32$; Figure 1D) spending equal amounts of time exploring the novel and start arms.

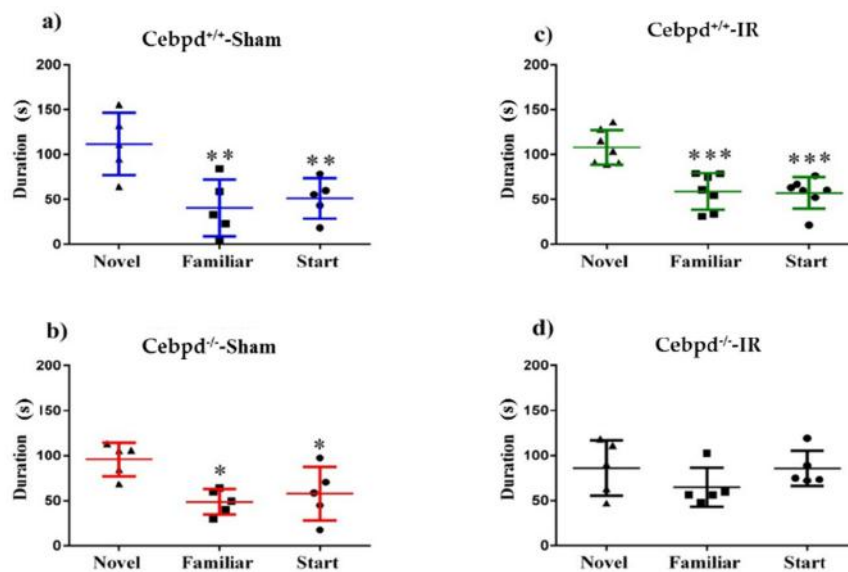


Figure 1. Short-term memory analyzed by Y-maze test in sham and irradiated aged *Cebpd*^{+/+} and *Cebpd*^{-/-} mice. (A–C) *Cebpd*^{+/+}-sham, *Cebpd*^{+/+}-IR, and *Cebpd*^{-/-}-sham mice were able to successfully distinguish the novel arm, by spending significantly more time exploring it. (D) *Cebpd*^{-/-}-IR mice were not able to distinguish between the three Y-maze arms, and spent an approximately equal time exploring all arms failing to recognize the novel environment when exposed to it 4 h later. N = 5/7 mice/treatment, Average \pm SEM; * $p < 0.05$, ** $p < 0.01$, *** $p < 0.001$.

2.2. Irradiation Impairs Spatial Memory in Aged *Cebpd*^{-/-} Mice

We used the novel object recognition (NOR) task to assess non-spatial declarative memory [37]. Rodents naturally orient their head toward novel stimuli, behavior that provides a simple and effective method for quantifying visual recognition [38]. Visuospatial orientation toward an object will attenuate with arena exposure time (habituation), and contrasting exploration of a novel versus a familiar object provides an index of object recognition and discrimination. Habituation learning occurs when animals' response to a stimulus lowers with increased exposure. Locomotor activity was tracked on the two empty arena habituation days, and the difference between total distances moved between open arena days 1 and 2 serve as a metric for habituation learning. There was no significant difference in distance moved day 1 ($F_{(3, 18)} = 0.73$; $p = 0.55$) nor day 2 ($F_{(3, 18)} = 1.79$; $p = 0.18$). During familiarization (day 3), mice were placed in the open field box with two identical objects. On day 4, one of the objects (henceforth "familiar") was replaced with a novel object. Statistical analysis of total object exploration in test sessions revealed that *Cebpd*^{+/+}-sham ($t = 5.33$, $p = 0.007$; Figure 2A), *Cebpd*^{+/+}-IR ($t = 3.40$, $p = 0.005$; Figure 2B) and *Cebpd*^{-/-}-sham ($t = 2.85$, $p = 0.02$; Figure 2C) mice showed novel object recognition and visited the novel object significantly more than the familiar object. However, radiation exposure significantly impaired *Cebpd*^{-/-} mice (Figure 2D) as they did not show any preferences for the novel object. Discrimination ratios provide a basis for interpreting animals' ability to remember or forget a novel arm or object. A positive ratio can be interpreted as animals successfully discriminating between two objects, and a negative ratio implies "forgetting" an object [39]. Radiation resulted in a negative discrimination ratio for *Cebpd*^{-/-}-IR mice ($F_{(3, 17)} = 4.42$; $p < 0.05$; Figure S1, Supplementary Materials).

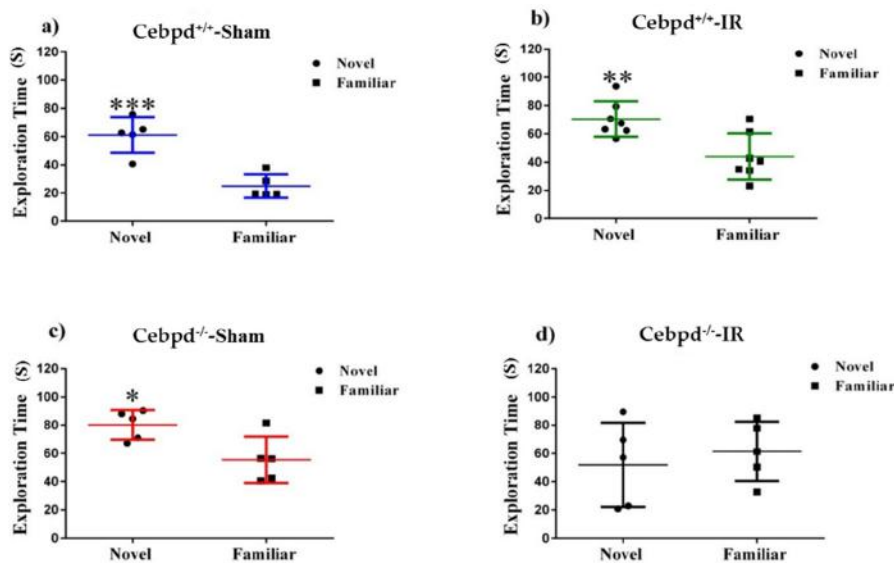


Figure 2. NOR of sham-irradiated and irradiated aged *Cebpd*^{+/+} and *Cebpd*^{-/-} mice. (A) *Cebpd*^{+/+}-sham, (B) *Cebpd*^{+/+}-IR, and (C) *Cebpd*^{-/-}-sham irradiated mice showed novel object recognition and spent more time exploring the novel than the familiar object. However, *Cebpd*^{-/-}-IR (D) mice did not show any preference for the novel object. N = 5/7 mice/treatment. Average \pm SEM; * $p < 0.05$, ** $p < 0.01$, *** $p < 0.001$.

2.2.1. Dendritic Morphology of Dentate Gyrus Granule Neurons is Significantly Altered in Irradiated *Cebpd*^{-/-} Mice

For morphological quantification of hippocampal neurons, we measured length and branching of the granule cells in the dentate gyrus (DG) and pyramidal neurons in the CA1 region from 5 *Cebpd*^{-/-} and 7 *Cebpd*^{+/+} mice. First, we examined dendritic complexity in the DG between treatment groups. An ANOVA found differences in dendritic complexity ($F_{(3,12)} = 9.81$; $p < 0.001$). Multiple comparisons show a marked decrease in complexity between *Cebpd*^{-/-}-sham compared to *Cebpd*^{-/-}-IR ($p < 0.01$; see Table 1). There were no significant differences between *Cebpd*^{+/+}-sham compared to *Cebpd*^{-/-}-sham nor between *Cebpd*^{+/+}-sham compared to *Cebpd*^{+/+}-IR. The variables that define dendritic complexity changed due to irradiation to similar extents as compared to sham. We observed decreases in dendritic length ($F_{(3,12)} = 11.78$; $p < 0.001$) and total branch points ($F_{(3,12)} = 19.88$; $p < 0.0001$; see Table 1).

Table 1. Analysis of dendritic morphology of dentate gyrus (DG) granule neurons in aged *Cebpd*^{+/+} and *Cebpd*^{-/-} mice. **** Bold figures represent significant compared to *Cebpd*^{-/-}-IR.

| Cell Type and Measurements | <i>Cebpd</i> ^{+/+} -Sham (mean \pm SEM) | <i>Cebpd</i> ^{-/-} -Sham (mean \pm SEM) | <i>Cebpd</i> ^{+/+} -IR (mean \pm SEM) | <i>Cebpd</i> ^{-/-} -IR (mean \pm SEM) |
|-------------------------------|---|---|---|---|
| DG | | | | |
| Total Dendritic Length | 1224 \pm 77.77 | 1313 \pm 86.06 | 987.4 \pm 144.5 | 587.7 \pm 36.45 |
| Total Number of Branch Points | 8.92 \pm 0.57 | 8.08 \pm 0.57 | 5.8 \pm 0.72 | 3.8 \pm 0.21 |
| Complexity | 30796 \pm 6401 | 38947 \pm 3424 | 15985 \pm 5436 | 7050 \pm 1350 |

The effect of irradiation was found to be associated with a different distribution of dendritic branches over the entire tree in the DG, as determined by ANOVA. We detected significant interactions between treatment and dendritic length ($F_{(89,348)} = 12.83$; $p < 0.0001$). We also found significant main effects of Sholl dendritic length ($F_{(29,348)} = 110.4$; $p < 0.0001$) and main effect of treatment ($F_{(3,12)} = 11.78$; $p < 0.001$). We next performed post-hoc analyses, which revealed a decrease in the dendritic length significantly evident when *Cebpd*^{-/-}-sham were compared to *Cebpd*^{-/-}-IR. Analysis revealed a significant decrease in dendritic length at 90–190 μ m (Holm-Sidak's multiple comparisons: 90 μ m,

$p < 0.05$; 100 μm , $p < 0.001$; 110–190 μm , $p < 0.0001$; Figure 3). We found no significant interactions between genotype and dendritic Sholl length ($F_{(29,174)} = 0.81$; $p = 0.74$; Figure 3) when *Cebpd*^{+/+}-sham were compared to *Cebpd*^{-/-}-sham. Nor was there a significant interaction between treatment and dendritic Sholl ($F_{(29,174)} = 0.92$; $p = 0.57$; Figure 3) when *Cebpd*^{+/+}-sham were compared to *Cebpd*^{+/+}-IR.

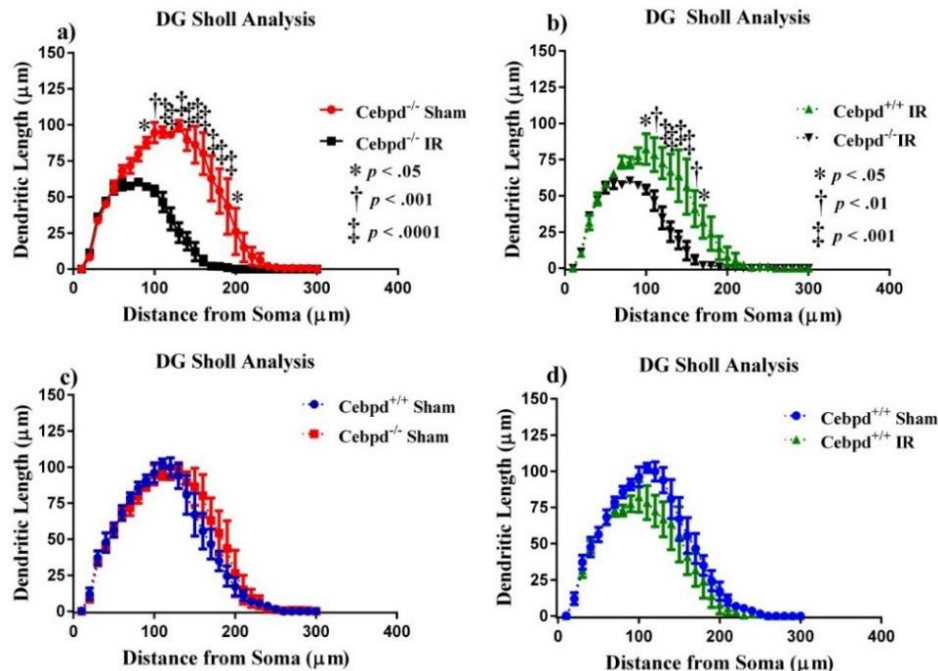


Figure 3. Sholl analyses of neurons in the dentate gyrus. (A) Dendritic length, measured by Sholl analysis, radiation greatly decreased length at 90–100 μm from the soma when *Cebpd*^{-/-}-sham were compared to *Cebpd*^{-/-}-IR. (B) Treatment decreased length at 100–170 μm from the soma when *Cebpd*^{+/+}-IR were compared to *Cebpd*^{-/-}-IR. There were no significant differences observed when (C) *Cebpd*^{+/+}-sham were compared to *Cebpd*^{-/-}-sham or (D) *Cebpd*^{+/+}-sham were compared to *Cebpd*^{+/+}-IR. Average \pm SEM ($n = 5$); * $p < 0.05$, † $p < 0.01$. ‡ $p < 0.001$.

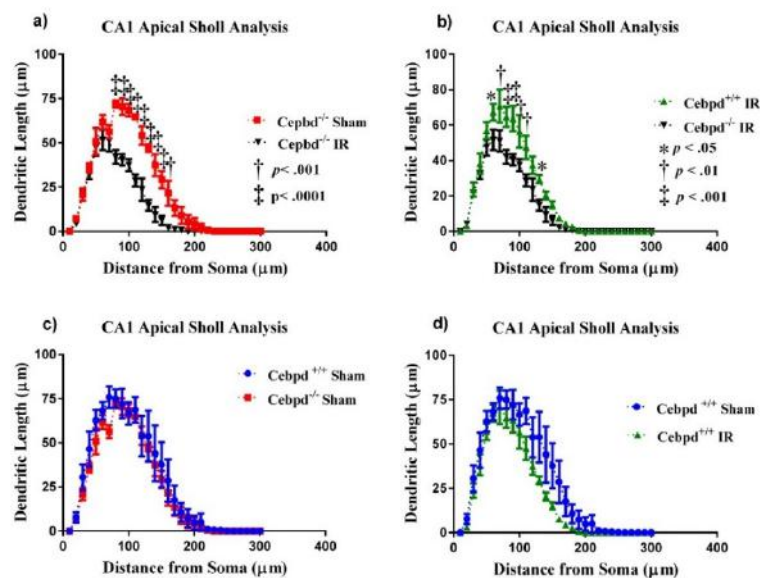
2.2.2. Dendritic Morphology of CA1 Apical Neurons is Significantly Altered in Irradiated *Cebpd*^{-/-} Mice

We next examined dendritic complexity in the CA1 neurons between treatment groups. An ANOVA found differences in dendritic complexity ($F_{(3, 12)} = 6.50$; $p < 0.01$). Multiple comparisons show a marked decrease in complexity between *Cebpd*^{+/+}-sham compared to *Cebpd*^{+/+}-IR ($p < 0.05$). We also observed decreases in dendritic length ($F_{(3, 12)} = 9.06$; $p < 0.01$) and total branch points ($F_{(3, 12)} = 7.80$; $p < 0.01$; see Table 2) in both dosage groups.

We report significant interactions between treatment groups and dendritic Sholl length in the CA1 apical neurons. Similar to what was seen in the DG, we detected significant interactions between treatment and dendritic length ($F_{(87,348)} = 2.54$; $p < 0.0001$). We also found significant main effects of Sholl dendritic length ($F_{(29,348)} = 127.1$; $p < 0.0001$) and main effect of treatment ($F_{(3, 12)} = 11.78$; $p < 0.001$). We next performed post-hoc analyses, which revealed a decrease in the dendritic length significantly evident when *Cebpd*^{-/-}-sham were compared to *Cebpd*^{-/-}-IR. Analysis revealed a significant decrease in dendritic length at 80–160 μm (Holm-Sidak's multiple comparisons: 80–150 μm , $p < 0.0001$; 160 μm , $p < 0.001$; Figure 4). We found no significant interactions between genotype and dendritic Sholl length ($F_{(29,174)} = 0.41$; $p = 0.99$; Figure 4) when *Cebpd*^{+/+}-sham were compared to *Cebpd*^{-/-}-sham. Nor was there a significant interaction between treatment and dendritic Sholl ($F_{(29,174)} = 1.10$; $p = 0.34$; Figure 4) when *Cebpd*^{+/+}-sham were compared to *Cebpd*^{+/+}-IR.

Table 2. Analysis of CA1 apical and basal neurons in aged *Cebpd*^{+/+} and *Cebpd*^{-/-} mice. **** Bold figures represent significant compared to *Cebpd*^{-/-}-IR.

| Cell Type and Measurements | <i>Cebpd</i> ^{+/+} -Sham (mean ± SEM) | <i>Cebpd</i> ^{-/-} -Sham (mean ± SEM) | <i>Cebpd</i> ^{+/+} -IR (mean ± SEM) | <i>Cebpd</i> ^{-/-} -IR (mean ± SEM) |
|-------------------------------|---|---|---|---|
| CA1 Apical | | | | |
| Total Dendritic Length | 839.8 ± 82.52 | 677.6 ± 74.02 | 519.1 ± 43.86 | 414.6 ± 32.46 |
| Total Number of Branch Points | 8.00 ± 0.96 | 7.13 ± 0.58 | 5.3 ± 0.39 | 4.05 ± 0.45 |
| Complexity | 43356 ± 9937 | 29426 ± 6042 | 17154 ± 1491 | 8699 ± 1649 |
| CA1 Basal Measurements | | | | |
| Total Dendritic Length | 1301 ± 173.34 | 823.01 ± 52.91 | 788.8 ± 22.93 | 472.6 ± 28.61 |
| Total Number of Branch Points | 9.90 ± 1.35 | 7.00 ± 0.64 | 6.95 ± 0.49 | 3.85 ± 0.52 |
| Complexity | 20722 ± 5219 | 8366 ± 1556 | 9275 ± 1671 | 3749 ± 540.5 |

**Figure 4.** Sholl analyses of neurons in the CA1 apical. (A) Dendritic length, measured by Sholl analysis radiation decreased length at 80–160 μm from the soma when *Cebpd*^{-/-}-sham were compared to *Cebpd*^{-/-}-IR. (B) Treatment greatly decreased length at 80–160 μm from the soma when *Cebpd*^{+/+}-IR were compared to *Cebpd*^{-/-}-IR. There were no significant differences observed when (C) *Cebpd*^{+/+}-sham were compared to *Cebpd*^{-/-}-sham or (D) *Cebpd*^{+/+}-sham were compared to *Cebpd*^{+/+}-IR. Average \pm SEM ($n = 5$) * $p < 0.05$, † $p < 0.01$, ‡ $p < 0.001$.

2.2.3. Dendritic Morphology of CA1 Basal Neurons is Significantly Altered in Irradiated *Cebpd*^{-/-} Mice

In the CA1 basal pyramidal dendrites, the ANOVA also found differences in dendritic complexity ($F_{(3,12)} = 6.35$; $p < 0.01$). Multiple comparisons show a significant decrease in complexity when *Cebpd*^{+/+}-IR were compared to *Cebpd*^{-/-}-IR ($p < 0.05$). We also observed decreases in dendritic length ($F_{(3,12)} = 13.64$; $p < 0.001$) and total branch points ($F_{(3,12)} = 8.80$; $p < 0.01$; see Table 2). We detected significant interactions between treatment and dendritic length ($F_{(87,348)} = 8.06$; $p < 0.0001$). We also found significant main effects of Sholl dendritic length ($F_{(29,348)} = 178.5$; $p < 0.0001$) and main effect of treatment ($F_{(3,12)} = 12.31$; $p < 0.001$). Post-hoc analyses revealed a significant decrease in the dendritic length when *Cebpd*^{+/+}-sham were compared to *Cebpd*^{+/+}-IR at 90–140 μm from the soma (Holm-Sidak's multiple comparison: 90 μm , $p < 0.01$; 100–130 μm , $p < 0.001$; 140 μm , $p < 0.01$ Figure 5).

When *Cebpd*^{+/+}-sham were compared to *Cebpd*^{-/-}-sham, analysis revealed a significant decrease in dendritic length at 90–130 μm (Holm-Sidak's multiple comparisons: 90 μm , $p < 0.01$; 100–120 μm , $p < 0.0001$; 130–140 μm , $p < 0.05$; Figure 5). When *Cebpd*^{-/-}-sham were compared to *Cebpd*^{-/-}-IR, analysis revealed a significant decrease in dendritic length at 50–110 μm (Holm-Sidak's multiple comparisons: 50–100 μm , $p < 0.0001$; 110 μm , $p < 0.001$; Figure 5).

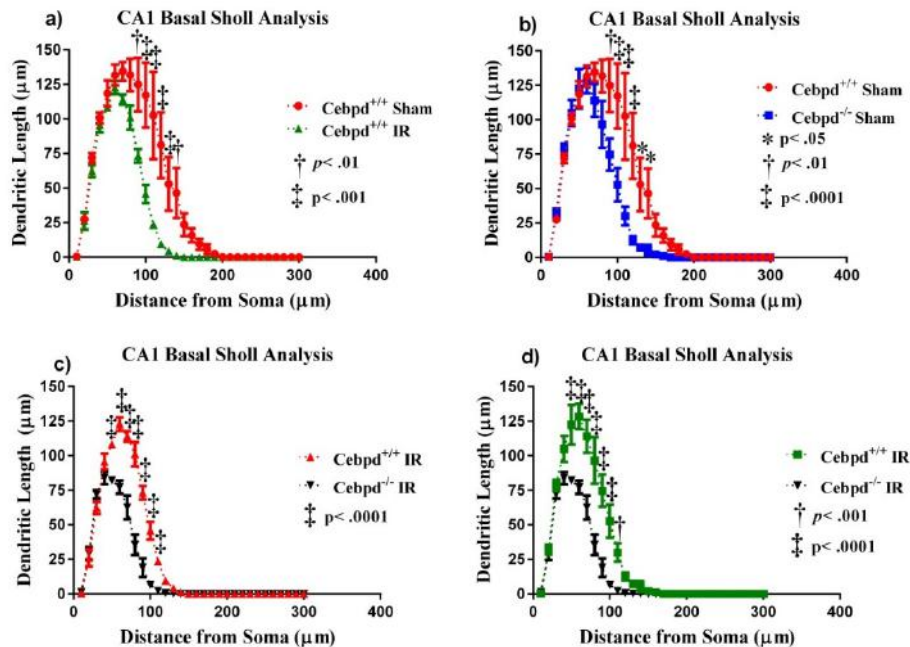


Figure 5. Sholl analyses of neurons in the CA1 basal. (A) Dendritic length, measured by Sholl analysis radiation decreased length at 90–140 μm from the soma when *Cebpd*^{+/+}-sham were compared to *Cebpd*^{+/+}-IR. (B) There was a decrease in length at 90–140 μm from the soma when *Cebpd*^{+/+}-sham were compared to *Cebpd*^{-/-}-sham. (C) Radiation decreased length at 50–110 μm from the soma when *Cebpd*^{+/+}-IR were compared to *Cebpd*^{-/-}-IR. (D) Treatment greatly decreased length at 50–110 μm from the soma when *Cebpd*^{-/-}-sham were compared to *Cebpd*^{-/-}-IR. Average \pm SEM ($n = 5$).

2.3. Irradiated *Cebpd*^{-/-} Mice Show Impaired Expression of Antioxidant Response Proteins, but no Change in the Expression of Inflammatory Markers in the Hippocampus

Exposure to IR is known to induce the expression of toll-like receptor 4 (TLR4) and pro-inflammatory cytokines which promote the increased recruitment of immune cells to clear the damaged tissue and/or dying cells. The activation of TLR4 is primarily in the microglia, so we also examined the expression of CD68, a marker of activated glia in the hippocampal extracts. We did not observe a significant difference in the expression of TLR4 nor CD68, which suggests that *Cebpd*-deficiency in aged mice did not further exacerbate IR-induced inflammation compared to unirradiated *Cebpd*^{+/+} mice (Figure 6).

Exposure to IR induces increased oxidative stress and damage to cellular constituents and leads to cell death and damage to the tissues. The hippocampus, which is the center for neurogenesis, is sensitive to IR-induced oxidative stress which can be counteracted by the antioxidant response proteins such as nuclear factor (erythroid-derived 2)-like 2 (NRF2), superoxide dismutase 2 (SOD2), catalase (CAT), and gamma-glutamyl cysteine ligase subunit m (γ -GCSm). There was no significant difference between the genotypes in sham or irradiated groups in the expression of antioxidant response proteins such as NRF2 or γ -GCSm which is involved in the synthesis of the cellular antioxidant glutathione. The expression of SOD2 was significantly upregulated in *Cebpd*^{-/-}-sham mice compared to *Cebpd*^{+/+}-sham mice. Exposure to IR led to downregulation of the overall expression of SOD2 in *Cebpd*^{+/+} mice, however *Cebpd*^{-/-} mice still showed significantly higher expression (Figure 7). We also found that the post-IR hippocampal expression of CAT was significantly decreased in *Cebpd*^{-/-} mice

compared to *Cebpd*^{+/+} mice (Figure 7). These results point to impairment in the oxidative stress response proteins and is suggestive of increased oxidative damage in the hippocampus which may play a role in neurocognitive deficits observed in *Cebpd*^{-/-} mice.

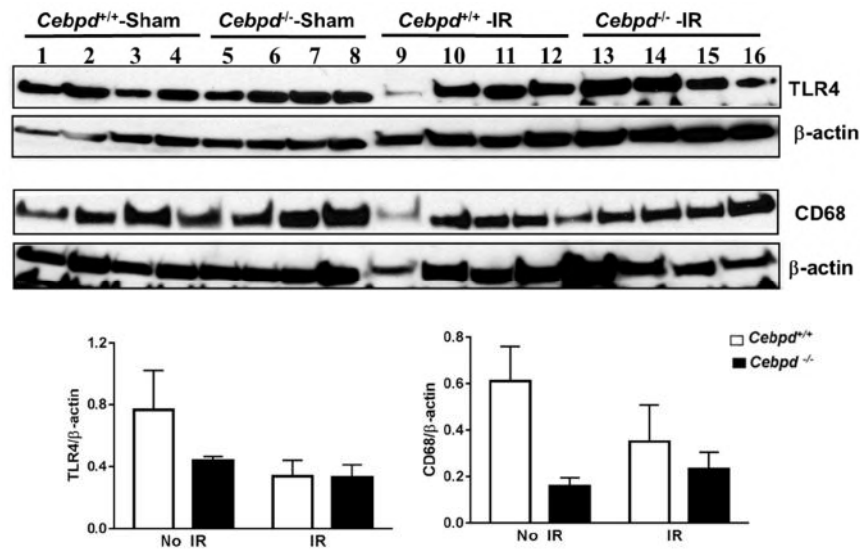


Figure 6. Expression of markers of inflammation and activated microglia in sham and irradiated *Cebpd*^{+/+} and *Cebpd*^{-/-} hippocampal extracts of aged mice. Immunoblotting of TLR4 and CD68 normalized to β -actin used as a loading control, $n = 4$ mice per genotype per treatment.

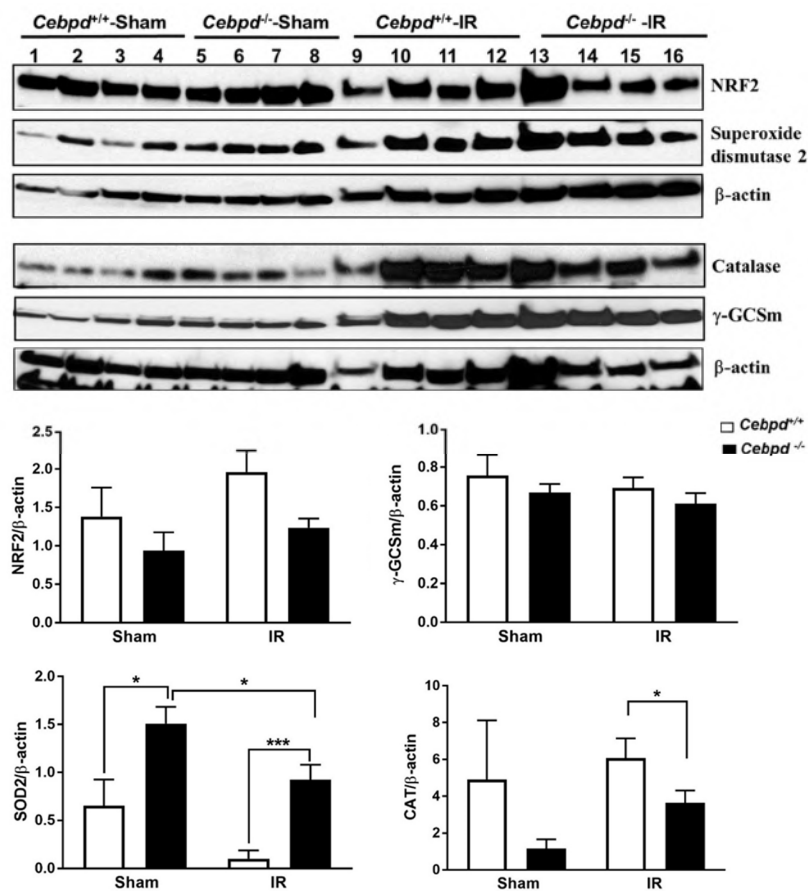


Figure 7. Expression of antioxidant response proteins in hippocampal extracts of sham and irradiated *Cebpd*^{+/+} and *Cebpd*^{-/-} mice. Immunoblotting of hippocampal extracts probed for NRF2, SOD2, CAT, γ -GCSm and β -actin, $n = 4$ mice per genotype per treatment. * $p < 0.05$; *** $p < 0.001$.

3. Discussion and Conclusions

Most of the clinical observations on radiation-induced neurocognitive impairments are based on the uncontrolled accidental exposure to radiation or the controlled cranial radiotherapy in cancer patients. Radiation exposure of the brain disrupts neurotransmission and elicits varying degrees of cognitive dysfunction [9–11]. While severe macroscopic tissue destruction and functional central nervous system (CNS) injury generally occur only after high radiation doses, lower doses do elicit moderate, acute changes [10]. Exposure to radiation gives rise to oxidative stress and neuroinflammation neurochemical mechanism detrimental to proper functionality of the CNS [40]. In young adult mice, significant reductions in proliferating and immature neurons are seen shortly after irradiation (i.e., 48 h) after irradiation [41]. In juvenile mice (age p21) 48 h after irradiation, the number of immature neurons is reduced 12% after 2 Gy to 75% after 10 Gy [42].

C/EBP δ expression is low to undetectable in most cell types and tissues. Activation of C/EBP δ has been observed in age-associated inflammatory diseases such as Alzheimer's disease and Parkinson's disease [32,33]. Sterneck et al. previously demonstrated that *Cebpd* is expressed in distinct neuronal populations, including the granule neurons of the dentate gyrus and the pyramidal neurons of the hippocampus, and that young *Cebpd*^{-/-} mice display an enhancement in contextual fear conditioning but not spatial learning in the Morris task [43]. Microarray analysis of genes expressed in the brains of young versus old mice revealed that the expression of *Cebpd* is not influenced by age [44].

The Y-maze is a simple 2-trial recognition test for measuring spatial recognition memory in animal experiments. The Y-maze test is based on the instinctive curiosity of rodents to explore novel areas without negative or positive reinforcements to the animals [45]. In the present study, one of the interesting findings was that aged *Cebpd*^{+/+} mice that received whole body radiation were not affected cognitively. However, *Cebpd*^{-/-}-IR animals' lack of curiosity about the novel arm, implying the inability to remember the start or the familiar arms, suggests deficits in the hippocampus-dependent process of short-term recall [46].

Recognition, a subtype of declarative memory, is composed of familiarity and recollection, which are processes dependent upon the hippocampus [38]. Recent findings are categorizing organized electrical activity in response to NOR within the hippocampus [23,38,47]. The dorsal hippocampus in particular is implicated in novel-object signaling. Within the dorsal hippocampus, the CA1 is paramount for object-novelty processing, as it is the main hippocampal output of the tri-synaptic pathway and broadcasts environmental novelty [48,49]. Our data showed that NOR was impaired significantly in *Cebpd*^{-/-}-IR mice compared to *Cebpd*^{-/-}-sham and *Cebpd*^{+/+}-sham and *Cebpd*^{+/+}-IR cohorts. However, since *Cebpd*^{-/-}-IR mice explore objects equally during familiarization and exhibit no signs of neophobia, deficits in NOR are likely due to impaired learning and/or memory rather than reduced curiosity.

Dendritic branching alterations and spine morphology can disrupt synapse formation and/or stability, which ultimately can lead to neurological and cognitive disorders, such as autism spectrum disorders, Alzheimer's disease, schizophrenia, anxiety, and depression [50]. Loss of dendritic arborization complexity would prohibit information processing and learning and memory formation that can manifest as cognitive dysfunction [51,52]. Neurons were once thought to be radioresistant cells because they do not divide, but we now know that they respond negatively to radiation. Our data showed significantly decreased dendritic length in the DG and CA1 regions of the hippocampus of irradiated *Cebpd*^{-/-} mice. In the DG, Sholl analysis of *Cebpd*^{+/+}-sham mice compared with *Cebpd*^{+/+}-IR mice revealed significant reductions in dendritic length at 80–190 μ m from the soma, with similar reductions at 90–190 μ m in *Cebpd*^{-/-}-sham mice when compared with *Cebpd*^{-/-}-IR mice. Dendritic morphology has been implicated in the health of neurons [53]; these data suggest that C/EBP δ -deficiency enhanced neuronal damage after exposure to radiation. Our findings of changes in dendritic morphology are aligned with findings in the literature showing abnormal morphology and decreased complexity are associated with impaired learning and memory on behavioral testing [54].

It is known that cumulative oxidative stress and inflammation play a contributory role in the process of aging and are also associated with radiation injury [2,55–57]. In the present study, we did not find any significant changes in the expression of markers of inflammation such as TLR4 or in the expression levels of the marker for activated microglia, CD68. It is known that aging is also associated with chronic inflammation partly mediated by increased levels of damage-associated molecular patterns, which activate pattern recognition receptors of the innate immune system such as TLR4 [58]. It is perhaps possible that due to the baseline inflammation present in the aged mice, radiation does not further upregulate the expression of TLR4. Alternatively, it may be possible that the inflammatory peak is an early effect post-IR exposure and perhaps TLR4 may be upregulated at early time points in *Cebpd*^{-/-} mice, as observed in other tissues such as the intestine [59].

However, we found significant alterations in the post-irradiation expression of the antioxidant proteins, SOD2, and CAT between aged *Cebpd*^{-/-} and *Cebpd*^{+/+} mice. It is known that the generation of ROS is considered the main cause of radiation-induced tissue injuries, and elevated levels of oxidative stress persist long after the initial irradiation [60]. We found significant upregulation of SOD2 in sham as well as irradiated *Cebpd*^{-/-} mice. Interestingly, a study with proton irradiation reported that SOD2-deficient mice were protected from radiation-induced neurocognitive deficits compared to SOD2-wild type mice [61]. The hydrogen peroxide produced by SOD2 is further detoxified by the enzyme CAT which was found to be significantly downregulated in irradiated *Cebpd*^{-/-} mice. These findings are further supported by our previous studies with a transgenic mouse model overexpressing mitochondrial CAT which showed extended longevity [62] and significant protection of radiation-induced neurocognitive deficits [63]. Further studies are needed to investigate the impaired expression of SOD2 and CAT in the specific neuronal cells of the hippocampus by immunostaining and whether SOD2 knockdown or CAT overexpression can alleviate the post-irradiation loss of cognitive functions in *Cebpd*^{-/-} mice.

Taken together, our results show that *Cebpd*-deficiency promotes radiation-induced deficits in short-term memory and spatial learning in aged mice that may be due to an impaired ability to detoxify IR-induced oxidative stress.

4. Materials and Methods

4.1. Ethics Statement

This study was carried out in strict accordance with the recommendations in the Guide for the Care and Use of Laboratory Animals of the National Institutes of Health and approved by the Institutional Animal Care and Use Committee of the University of Arkansas for Medical Sciences, animal use protocol number #3511, approved on 5/20/2014).

4.2. Animals

Cebpd-heterozygous breeder mice were backcrossed for more than 20 generations to the C57BL/6 strain background. Genotyping was done as described previously [34]. In all the studies, 15-month-old male *Cebpd*^{+/+} and *Cebpd*^{-/-} littermate mice were used. The animals were housed in the Division of Laboratory Medicine (DLAM, University of Arkansas for Medical Sciences, Little Rock, AR, USA) under standardized conditions with controlled temperature and humidity and a 12-h day, 12-h night light cycle. Brain tissues were harvested from sham mice and from irradiated mice at day 11 post-IR following isoflurane inhalation to minimize suffering and the animals were euthanized by cervical dislocation.

4.3. Irradiation of Mice

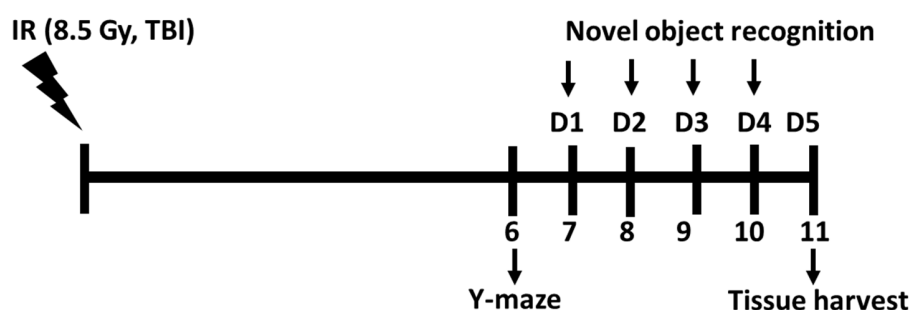
Cebpd^{+/+} and *Cebpd*^{-/-} mice were exposed to TBI administered in a Mark I irradiator (J. L. Shepherd & Associates, San Fernando, CA, USA). Dose uniformity was assessed by an independent company (Ashland Specialty Ingredients, Wilmington, DE, USA) with radiographic film and alanine

tablets. Alanine tablets were analyzed by the National Institute of Standards and Technology (Gaithersburg, MD, USA) and demonstrated a dose rate of 1.14 Gy/min at 21 cm from the source. For each experiment, the dose rate was corrected for decay.

The total dose of TBI used in the present study was 8.5 Gy. We have previously reported that 3-month-old *Cebpd*^{+/+} mice exposed to 8.5 Gy led to 100% mortality by days 9–13 post-TBI compared to *Cebpd*^{+/+} mice, which showed 40% mortality by days 11–13 post-TBI [34]. Aged (15 months old) *Cebpd*^{-/-} mice display about 55% mortality by days 8–12 compared to 12.5% mortality at day 15 post-TBI dose of 8.5 Gy (Pawar et al., unpublished results, data not shown). Hence, we chose the timepoint of 7–10 days post-irradiation for the behavior studies followed by tissue harvest on day 11 post-irradiation to examine the morphological changes and molecular changes in the hippocampus.

4.4. Behavioral Methods

In the sham group, $n = 5$ mice for each genotype, where in the IR group, *Cebpd*^{+/+} mice ($n = 7$) and *Cebpd*^{-/-} mice ($n = 5$) were used for the behavior studies. The figure below depicts the timepoints for the behavior studies that were conducted prior to tissue harvest.



4.4.1. Y-Maze

At day 6 post-irradiation, *Cebpd*^{+/+} and *Cebpd*^{-/-} mice were first tested in the Y-maze, which did not rely on either negative or positive reinforcement. The maze was constructed out of acrylic and consisted of three similar arms (45L x 7W x 14H cm): a “start” arm where animals were placed initially, a “familiar” arm, and a “novel” arm. The familiar and novel arms each contained an object of different size and shape mounted at the end of the arm. Animals were placed in the start arm facing away from the center of the maze. The familiarization session consisted of free exploration of the start and familiar arms for 10 min. Four hours later, the testing session was held; animals were again placed in the maze, this time with access to all arms. Allocation of arms (start, familiar, or novel) was counterbalanced between each experimental group. Trials lasted for 10 min, and center- and nose-points were recorded throughout each session. An arm entry was counted when all four limbs of the mouse entered an arm. All experimental arenas were wiped clean with 20% ethanol after each trial. All behavioral experiments were conducted during the light cycle under dimly-lit (white light) conditions, after a minimum of one hour of acclimation. Behavioral experiments were recorded on a charge-coupled device video camera, located above the maze for automatic behavioral analysis with EthoVision XT software version 11 (Noldus Information Technology, Leesburg, VA, USA) as described previously [23].

4.4.2. Novel Object Recognition

On day 7 post-irradiation, *Cebpd*^{+/+} and *Cebpd*^{-/-} mice were tested for novel object recognition (NOR) with a 4-day procedure in which animals freely explored an arena for 10 min each day. The arena was a cube consisting of an aluminum floor, acrylic walls (41L x 41W x 35H cm), and an open ceiling. The first two days (days 7 and 8 post-TBI) served as habituation learning days, in which mice were able to explore the empty arena (effectively serving as open field tests); locomotor activity was measured at this stage. The familiarization phase occurred on day 3 (day 9 post-TBI), when animals explored an

arena containing two identical objects (cell-culture flasks filled with sand). Novel object recognition testing occurred on day 4 (day 10 post-TBI); here, a now-familiar object was replaced with a novel object (large LEGO® blocks assembled to the size of the cell-culture flasks) [64]. Animals were placed in the center of the arena parallel to the objects to avoid bias. NOR testing relies on the animals' natural inclination to explore novel objects in their environment (untreated animals should spend significantly more time exploring the novel object). The tracking software was programmed to track animal center-points for the habituation trials and nose-points during familiarization and testing trials.

4.4.3. Golgi Staining

Shortly after behavioral testing, animals were euthanized, and their brains were collected at day 11 post-8.5 Gy and dissected along the midsagittal plane and half of the hippocampus was harvested for Golgi staining. The Golgi method of staining has long proven to be a reliable method for assessing dendrite and dendritic spine dynamics due to various treatments, because of its resistance to fading or photobleaching over time [65,66]. We adapted a staining protocol and used the reagents contained in the superGolgi kit (Bioenno Tech, Santa Ana, CA, USA) [67]. Right hemispheres were immediately impregnated in a potassium dichromate solution for two weeks ($n = 5$). Next, sections were immersed for at least 48 h in a post-impregnation buffer. Samples were sectioned at 200 μm in $1 \times$ PBS along the coronal plane. Samples were then transferred into wells and washed with 0.01 M PBS buffer (pH 7.4) with Triton X-100 (0.3%) (PBS-T). Immediately after washing, samples were stained with ammonium hydroxide and then immersed in a post-staining buffer. Sections were again washed in PBS-T, mounted on 1% gelatin-coated slides, and allowed to dry. Sections were finally dehydrated with ethanol solutions, followed by cleaning in xylene, and coverslipped with Permount™ (Thermo Fisher Scientific, Waltham, MA, USA).

4.4.4. Dendritic Morphology Quantification

All dendritic morphology data were collected blinded with regard to experimental conditions on $n = 5$ mice per genotype per treatment group. We performed quantification of morphological characteristics of the granular and pyramidal neurons contained in the hippocampal formation using techniques that included Sholl analyses (Figure S2, Supplementary Materials), total dendritic length, number of branch points, and dendritic complexity index (DCI). Multiple Z-stack images of neurons were collected with the aid of a computer-assisted neuron tracing using the Neuroexplorer component of the NeuroLucida program (Ver. 11, MicroBrightfield, Inc., Williston, VT, USA). Sholl analysis was used to assess the amount and distribution of the arbor at increasing radial distances from the cell body [68]. Radii were set to extend in 10 μm intervals from the soma. The length of each dendritic branch, within each progressively larger circle, was counted from the soma, with respect to three dimensions. This provided information about the amount and distribution of individual dendrites.

We then performed branch-point analyses. Branch points occur at bifurcations of the dendrite when a branch divides into two sub-branches. Branch-point analysis depends on the number of bifurcations and the order of the points [69]. Lower branch-point orders represent proximal regions of the tree, whereas larger branch-point orders characterize distal regions. We used the branch-point analysis to determine the complexity of dendritic arborization, because the complexity of the dendritic tree is an important phenotypic component of branching analysis. DCI was determined by the following equation: $\text{DCI} = \sum (\text{branch tip orders} + \# \text{ of branch tips}) \times (\text{total dendritic length} / \text{total number of primary dendrites})$. In the CA1 apical and basal regions, dendrites were analyzed separately.

4.4.5. Immunoblotting of Hippocampal Extracts

Hippocampal tissues were harvested from sham and irradiated *Cebpd*^{+/+} and *Cebpd*^{-/-} mice at day 11 post-irradiation and protein extracts were prepared using an IBI Scientific DNA/RNA/Protein Extraction kit (MIDSCI, St. Louis, MO, USA), and the protein was quantified using a Nanodrop 2000c A280 (Thermo Scientific, Waltham, MA, USA). The protein samples were mixed with $2 \times$ sodium

dodecyl sulfate polyacrylamide gel electrophoresis sample buffer and boiled for 5 min. A 35 µg portion of total protein per sample was separated by a 4–20% gradient sodium dodecyl sulfate polyacrylamide gel electrophoresis, electrotransferred to polyvinylidene fluoride (PVDF) filters at 40 V and 4 °C for 120 min, blocked with 5% non-fat milk at room temperature for 1 h, and incubated with primary antibodies specific to NRF2 (sc-722), SOD2 (sc-30080), CAT (sc-50508), γ -GCSm (sc-55586), TLR4 (sc-293072), and CD68 (sc-59103) (Santa Cruz Biotechnology, Dallas, TX, USA), and β -actin (4790, Cell Signaling Technology, Danvers, MA, USA) monoclonal antibodies overnight at 4 °C. The membranes were washed three times with Tris-buffered saline/Tween-20 (TBST), incubated with secondary antibody for 60 min, washed three times with TBST, and visualized by enhanced chemiluminescence. β -actin expression was used as the internal reference. The band intensities were measured by densitometry using NIH ImageJ analysis.

4.4.6. Statistical Analyses

We expressed data as a mean \pm the standard error of the mean (SEM). We analyzed the behavioral data throughout the 10-minute length of each test. Behavioral assays comparing visits or time spent in apparatus areas by individual treatment groups were analyzed via ANOVA. NOR discrimination ratio (DR) was calculated by the following formula: (NOR) DR = (novel object visits - familiar object visits)/(novel object visits + familiar object visits). For measures of dendritic length, two-way repeated-measures ANOVA was conducted for the effects of radiation (between-subjects variable) and distance from the cell soma (Sholl radius, repeated-measures variable); Holm's correction to control for multiple comparisons post-hoc tests followed, when appropriate. Densitometry data were analyzed by unpaired Student's *t*-test. All statistical analyses were conducted with GraphPad Prism 7.0 software (La Jolla, CA, USA) in a 95% confidence interval, and $p < 0.05$ was considered significant.

Supplementary Materials: The following are available online at <http://www.mdpi.com/1422-0067/20/4/885/s1>, Figure S1: Discrimination ratio of sham and irradiated aged *Cebpd*^{+/+} and *Cebpd*^{-/-} mice. Figure S2: Combined Sholl analyses of neurons in DG and CA1 apical and CA1 basal regions depicted in Figures 3–5. Figure S3: Representative tracings of DG granule neurons superimposed over concentric rings (10 µm) used for Sholl analysis.

Author Contributions: A.R.A. and S.A.P. conceived, designed and directed the experiments; S.B., T.A., D.M., T.G., F.K., J.W., and A.G. performed the experiments; J.W. and A.R.A. analyzed the data; A.R.A. and S.A.P. contributed reagents, materials, and analysis tools; S.B., S.A.P., and A.R.A. wrote the paper.

Funding: This research was funded by National Institute of General Medical Sciences supported COBRE-Center for Host Responses to Cancer Therapy Grant P20GM109005 (ARA, SAP); Department of Defense Congressionally Directed Medical Research Program Award W81XWH-15-1-0489 (SAP), and the Arkansas Bioscience Institute (SAP). The authors also wish to acknowledge the support provided by the core facilities of the National Institute of General Medical Sciences supported Center for Translational Neuroscience (P30 GM110702).

Acknowledgments: The authors would like to thank Esta Sterneck (National Cancer Institute, Frederick, MD, USA) for kindly providing us the *Cebpd* heterozygous mice to generate the experimental animals. The authors acknowledge Randolph Mildred, Gail Wagoner, Bianca Schutte, Rebecca Mitchell, Jeannie Holland and Bridgette Angie from the Division of Laboratory Animals and Medicine for excellent animal care.

Conflicts of Interest: The authors declare no conflict of interest. The funding sponsors had no role in the design of the study; in the collection, analyses, or interpretation of data; in the writing of the manuscript; and in the decision to publish the results.

References

1. Hladik, D.; Tapio, S. Effects of ionizing radiation on the mammalian brain. *Mutat. Res. Rev. Mutat. Res.* **2016**, *770*, 219–230. [[CrossRef](#)] [[PubMed](#)]
2. Hernandez, L.; Terradas, M.; Camps, J.; Martin, M.; Tusell, L.; Genesca, A. Aging and radiation: Bad companions. *Aging Cell* **2015**, *14*, 153–161. [[CrossRef](#)] [[PubMed](#)]
3. Monje, M.L.; Toda, H.; Palmer, T.D. Inflammatory blockade restores adult hippocampal neurogenesis. *Science* **2003**, *302*, 1760–1765. [[CrossRef](#)] [[PubMed](#)]
4. Voloboueva, L.A.; Giffard, R.G. Inflammation, mitochondria, and the inhibition of adult neurogenesis. *J. Neurosci. Res.* **2011**, *89*, 1989–1996. [[CrossRef](#)] [[PubMed](#)]

5. Huang, T.-T.; Leu, D.; Zou, Y. Oxidative stress and redox regulation on hippocampal-dependent cognitive functions. *Arch. Biochem. Biophys.* **2015**, *576*, 2–7. [[CrossRef](#)] [[PubMed](#)]
6. Betlazar, C.; Middleton, R.J.; Banati, R.B.; Liu, G.-J. The impact of high and low dose ionising radiation on the central nervous system. *Redox Biol.* **2016**, *9*, 144–156. [[CrossRef](#)]
7. Lumniczky, K.; Szatmári, T.; Sáfrány, G. Ionizing Radiation-Induced Immune and Inflammatory Reactions in the Brain. *Front. Immunol.* **2017**, *8*, 517. [[CrossRef](#)]
8. Roman, D.D.; Sperduto, P.W. Neuropsychological effects of cranial radiation: Current knowledge and future directions. *Int. J. Radiat. Oncol. Biol. Phys.* **1995**, *31*, 983–998. [[CrossRef](#)]
9. Fike, J.R.; Gobbel, G.T. Central nervous system radiation injury in large animal models. In *Radiation Injury to the Nervous System*; Gutin, P.H., Leibel, S.A., Sheline, G.E., Eds.; Raven Press, Ltd.: New York, NY, USA, 1991; pp. 113–135.
10. Tofilon, P.J.; Fike, J.R. The radioresponse of the central nervous system: A dynamic process. *Radiat. Res.* **2000**, *153*, 357–370, Epub 2000/05/08. [[CrossRef](#)]
11. Abayomi, O.K. Pathogenesis of irradiation-induced cognitive dysfunction. *Acta Oncol.* **1996**, *35*, 659–663. [[CrossRef](#)]
12. Son, Y.; Yang, M.; Wang, H.; Moon, C. Hippocampal dysfunctions caused by cranial irradiation: A review of the experimental evidence. *Brain Behav. Immun.* **2015**, *45*, 287–296. [[CrossRef](#)] [[PubMed](#)]
13. Greene-Schloesser, D.; Moore, E.; Robbins, M.E. Molecular Pathways: Radiation-Induced Cognitive Impairment. *Clin. Cancer Res.* **2013**, *19*, 2294–2300. [[CrossRef](#)] [[PubMed](#)]
14. Broadbent, N.J.; Squire, L.R.; Clark, R.E. Spatial memory, recognition memory, and the hippocampus. *Proc. Natl. Acad. Sci. USA* **2004**, *101*, 14515–14520. [[CrossRef](#)] [[PubMed](#)]
15. Casciati, A.; Dobos, K.; Antonelli, F.; Benedek, A.; Kempf, S.J.; Bellés, M.; Balogh, A.; Tanori, M.; Heredia, L.; Atkinson, M.J.; et al. Age-related effects of X-ray irradiation on mouse hippocampus. *Oncotarget* **2016**, *7*, 28040–28058. [[CrossRef](#)] [[PubMed](#)]
16. Beckervordersandforth, R.; Ebert, B.; Schäffner, I.; Moss, J.; Fiebig, C.; Shin, J.; Moore, D.L.; Ghosh, L.; Trinchero, M.F.; Stockburger, C.; et al. Role of Mitochondrial Metabolism in the Control of Early Lineage Progression and Aging Phenotypes in Adult Hippocampal Neurogenesis. *Neuron* **2017**, *93*, 560.e6–573.e6. [[CrossRef](#)]
17. Knobloch, M.; Jessberger, S. Metabolism and neurogenesis. *Curr. Opin. Neurobiol.* **2017**, *42*, 45–52. [[CrossRef](#)]
18. Wu, P.H.; Coultrap, S.; Pinnix, C.; Davies, K.D.; Taylor, R.; Ang, K.K.; Browning, M.D.; Grosshans, D.R. Radiation induces acute alterations in neuronal function. *PLoS ONE* **2012**, *7*, e37677. [[CrossRef](#)]
19. Kumar, M.; Haridas, S.; Trivedi, R.; Khushu, S.; Manda, K. Early cognitive changes due to whole body gamma-irradiation: A behavioral and diffusion tensor imaging study in mice. *Exp. Neurol.* **2013**, *248*, 360–368. [[CrossRef](#)]
20. Chakraborti, A.; Allen, A.; Allen, B.; Rosi, S.; Fike, J.R. Cranial Irradiation Alters Dendritic Spine Density and Morphology in the Hippocampus. *PLoS ONE* **2012**, *7*, e40844. [[CrossRef](#)]
21. Parihar, V.K.; Limoli, C.L. Cranial irradiation compromises neuronal architecture in the hippocampus. *Proc. Natl. Acad. Sci. USA* **2013**, *110*, 12822–12827. [[CrossRef](#)]
22. Parihar, V.K.; Pasha, J.; Tran, K.K.; Craver, B.M.; Acharya, M.M.; Limoli, C.L. Persistent changes in neuronal structure and synaptic plasticity caused by proton irradiation. *Brain Struct. Funct.* **2015**, *220*, 1161–1171. [[CrossRef](#)]
23. Kiffer, F.; Howe, A.K.; Carr, H.; Wang, J.; Alexander, T.; Anderson, J.E.; Groves, T.; Seawright, J.W.; Sridharan, V.; Carter, G.; et al. Late effects of (1)H irradiation on hippocampal physiology. *Life Sci. Space Res.* **2018**, *17*, 51–62. [[CrossRef](#)] [[PubMed](#)]
24. Shuryak, I.; Sachs, R.K.; Brenner, D.J. Cancer risks after radiation exposure in middle age. *J. Natl. Cancer Inst.* **2010**, *102*, 1628–1636. [[CrossRef](#)] [[PubMed](#)]
25. Ramji, D.P.; Foka, P. CCAAT/enhancer-binding proteins: Structure, function and regulation. *Biochem. J.* **2002**, *365*, 561–575. [[CrossRef](#)] [[PubMed](#)]
26. Sarkar, T.R.; Sharan, S.; Wang, J.; Pawar, S.A.; Cantwell, C.A.; Johnson, P.F.; Morrison, D.K.; Wang, J.M.; Sterneck, E. Identification of a Src tyrosine kinase/SIAH2 E3 ubiquitin ligase pathway that regulates C/EBPdelta expression and contributes to transformation of breast tumor cells. *Mol. Cell Biol.* **2012**, *32*, 320–332. [[CrossRef](#)]

27. Pawar, S.A.; Sarkar, T.R.; Balamurugan, K.; Sharan, S.; Wang, J.; Zhang, Y.; Dowdy, S.F.; Huang, A.M.; Sterneck, E. C/EBP delta targets cyclin D1 for proteasome-mediated degradation via induction of CDC27/APC3 expression. *Proc. Natl. Acad. Sci. USA* **2010**, *107*, 9210–9215. [[CrossRef](#)] [[PubMed](#)]
28. Thangaraju, M.; Rudelius, M.; Bierie, B.; Raffeld, M.; Sharan, S.; Hennighausen, L.; Huang, A.M.; Sterneck, E. C/EBPdelta is a crucial regulator of pro-apoptotic gene expression during mammary gland involution. *Development* **2005**, *132*, 4675–4685. [[CrossRef](#)]
29. Huang, A.M.; Montagna, C.; Sharan, S.; Ni, Y.; Ried, T.; Sterneck, E. Loss of CCAAT/enhancer binding protein delta promotes chromosomal instability. *Oncogene* **2004**, *23*, 1549–1557. [[CrossRef](#)]
30. Hour, T.C.; Lai, Y.L.; Kuan, C.I.; Chou, C.K.; Wang, J.M.; Tu, H.Y.; Hu, H.T.; Lin, C.S.; Wu, W.J.; Pu, Y.S.; et al. Transcriptional up-regulation of SOD1 by CEBPD: A potential target for cisplatin resistant human urothelial carcinoma cells. *Biochem. Pharmacol.* **2010**, *80*, 325–334. [[CrossRef](#)]
31. Wang, J.; Sarkar, T.R.; Zhou, M.; Sharan, S.; Ritt, D.A.; Veenstra, T.D.; Morrison, D.K.; Huang, A.M.; Sterneck, E. CCAAT/enhancer binding protein delta (C/EBPdelta, CEBPD)-mediated nuclear import of FANCD2 by IPO4 augments cellular response to DNA damage. *Proc. Natl. Acad. Sci. USA* **2010**, *107*, 16131–16136. [[CrossRef](#)]
32. Cardinaux, J.R.; Allaman, I.; Magistretti, P.J. Pro-inflammatory cytokines induce the transcription factors C/EBPbeta and C/EBPdelta in astrocytes. *Glia* **2000**, *29*, 91–97. [[CrossRef](#)]
33. Li, R.; Strohmeyer, R.; Liang, Z.; Lue, L.F.; Rogers, J. CCAAT/enhancer binding protein delta (C/EBPdelta) expression and elevation in Alzheimer's disease. *Neurobiol. Aging* **2004**, *25*, 991–999. [[CrossRef](#)] [[PubMed](#)]
34. Pawar, S.A.; Shao, L.; Chang, J.; Wang, W.; Pathak, R.; Zhu, X.; Wang, J.; Hendrickson, H.; Boerma, M.; Sterneck, E.; et al. C/EBP delta Deficiency Sensitizes Mice to Ionizing Radiation-Induced Hematopoietic and Intestinal Injury. *PLoS ONE* **2014**, *9*, e94967. [[CrossRef](#)]
35. Banerjee, S.; Aykin-Burns, N.; Krager, K.J.; Shah, S.K.; Melnyk, S.B.; Hauer-Jensen, M.; Pawar, S.A. Loss of C/EBP δ enhances IR-induced cell death by promoting oxidative stress and mitochondrial dysfunction. *Free Radic. Biol. Med.* **2016**, *99*, 296–307. [[CrossRef](#)]
36. Dellu, F.; Fauchey, V.; Le Moal, M.; Simon, H. Extension of a new two-trial memory task in the rat: Influence of environmental context on recognition processes. *Neurobiol. Learn. Mem.* **1997**, *67*, 112–120. [[CrossRef](#)]
37. Ran, Y.; Yan, B.; Li, Z.; Ding, Y.; Shi, Y.; Le, G. Dityrosine administration induces novel object recognition deficits in young adulthood mice. *Physiol. Behav.* **2016**, *164*, 292–299. [[CrossRef](#)]
38. Cohen, S.J.; Stackman, R.W., Jr. Assessing rodent hippocampal involvement in the novel object recognition task. A review. *Behav. Brain Res.* **2015**, *285*, 105–117. [[CrossRef](#)] [[PubMed](#)]
39. Burke, S.N.; Wallace, J.L.; Nematollahi, S.; Uprety, A.R.; Barnes, C.A. Pattern separation deficits may contribute to age-associated recognition impairments. *Behav. Neurosci.* **2010**, *124*, 559–573. [[CrossRef](#)] [[PubMed](#)]
40. Hofer, T.; Duale, N.; Muusse, M.; Eide, D.M.; Dahl, H.; Boix, F.; Andersen, J.M.; Olsen, A.K.; Myhre, O. Restoration of Cognitive Performance in Mice Carrying a Deficient Allele of 8-Oxoguanine DNA Glycosylase by X-ray Irradiation. *Neurotox. Res.* **2018**, *33*, 824–836. [[CrossRef](#)] [[PubMed](#)]
41. Mizumatsu, S.; Monje, M.L.; Morhardt, D.R.; Rola, R.; Palmer, T.D.; Fike, J.R. Extreme sensitivity of adult neurogenesis to low doses of X-irradiation. *Cancer Res.* **2003**, *63*, 4021–4027. [[PubMed](#)]
42. Romanko, M.J.; Rola, R.; Fike, J.R.; Szele, F.G.; Dizon, M.L.; Felling, R.J.; Brazel, C.Y.; Levison, S.W. Roles of the mammalian subventricular zone in cell replacement after brain injury. *Prog. Neurobiol.* **2004**, *74*, 77–99. [[CrossRef](#)] [[PubMed](#)]
43. Sterneck, E.; Paylor, R.; Jackson-Lewis, V.; Libbey, M.; Przedborski, S.; Tessarollo, L.; Crawley, J.N.; Johnson, P.F. Selectively enhanced contextual fear conditioning in mice lacking the transcriptional regulator CCAAT/enhancer binding protein delta. *Proc. Natl. Acad. Sci. USA* **1998**, *95*, 10908–10913. [[CrossRef](#)] [[PubMed](#)]
44. Sharman, E.H.; Bondy, S.C.; Sharman, K.G.; Lahiri, D.; Cotman, C.W.; Perreau, V.M. Effects of melatonin and age on gene expression in mouse CNS using microarray analysis. *Neurochem. Int.* **2007**, *50*, 336–344. [[CrossRef](#)] [[PubMed](#)]
45. Sarnyai, Z.; Sibille, E.L.; Pavlides, C.; Fenster, R.J.; McEwen, B.S.; Toth, M. Impaired hippocampal-dependent learning and functional abnormalities in the hippocampus in mice lacking serotonin(1A) receptors. *Proc. Natl. Acad. Sci. USA* **2000**, *97*, 14731–14736. [[CrossRef](#)] [[PubMed](#)]

46. Gruber, M.J.; Gelman, B.D.; Ranganath, C. States of curiosity modulate hippocampus-dependent learning via the dopaminergic circuit. *Neuron* **2014**, *84*, 486–496. [[CrossRef](#)]
47. Kiffer, F.; Alexander, T.; Anderson, J.E.; Groves, T.; Wang, J.; Sridharan, V.; Boerma, M.; Allen, A.R. Late Effects of (16)O-Particle Radiation on Female Social and Cognitive Behavior and Hippocampal Physiology. *Radiat. Res.* **2019**. [[CrossRef](#)] [[PubMed](#)]
48. Larkin, M.C.; Lykken, C.; Tye, L.D.; Wickelgren, J.G.; Frank, L.M. Hippocampal output area CA1 broadcasts a generalized novelty signal during an object-place recognition task. *Hippocampus* **2014**, *24*, 773–783. [[CrossRef](#)] [[PubMed](#)]
49. Stepan, J.; Dine, J.; Eder, M. Functional optical probing of the hippocampal trisynaptic circuit in vitro: Network dynamics, filter properties, and polysynaptic induction of CA1 LTP. *Front. Neurosci.* **2015**, *9*, 160. [[CrossRef](#)] [[PubMed](#)]
50. Kulkarni, V.A.; Firestein, B.L. The dendritic tree and brain disorders. *Mol. Cell. Neurosci.* **2012**, *50*, 10–20. [[CrossRef](#)] [[PubMed](#)]
51. Nimchinsky, E.A.; Sabatini, B.L.; Svoboda, K. Structure and function of dendritic spines. *Annu. Rev. Physiol.* **2002**, *64*, 313–353. [[CrossRef](#)] [[PubMed](#)]
52. Segal, M. Dendritic spines and long-term plasticity. *Nat. Rev. Neurosci.* **2005**, *6*, 277–284. [[CrossRef](#)] [[PubMed](#)]
53. Yuste, R.; Bonhoeffer, T. Morphological changes in dendritic spines associated with long-term synaptic plasticity. *Annu. Rev. Neurosci.* **2001**, *24*, 1071–1089. [[CrossRef](#)] [[PubMed](#)]
54. Raber, J.; Allen, A.R.; Sharma, S.; Allen, B.; Rosi, S.; Olsen, R.H.; Davis, M.J.; Eiwaz, M.; Fike, J.R.; Nelson, G.A. Effects of Proton and Combined Proton and (56)Fe Radiation on the Hippocampus. *Radiat. Res.* **2016**, *185*, 20–30. [[CrossRef](#)] [[PubMed](#)]
55. Sydow, A.; Hochgrafe, K.; Konen, S.; Cadinu, D.; Matenia, D.; Petrova, O.; Joseph, M.; Dennissen, F.J.; Mandelkow, E.M. Age-dependent neuroinflammation and cognitive decline in a novel Ala152Thr-Tau transgenic mouse model of PSP and AD. *Acta Neuropathol. Commun.* **2016**, *4*, 17. [[CrossRef](#)] [[PubMed](#)]
56. Richardson, R.B. Ionizing radiation and aging: Rejuvenating an old idea. *Aging* **2009**, *1*, 887–902. [[CrossRef](#)]
57. Glass, C.K.; Saijo, K.; Winner, B.; Marchetto, M.C.; Gage, F.H. Mechanisms underlying inflammation in neurodegeneration. *Cell* **2010**, *140*, 918–934. [[CrossRef](#)]
58. Wilhelm, I.; Nyul-Toth, A.; Kozma, M.; Farkas, A.E.; Krizbai, I.A. Role of pattern recognition receptors of the neurovascular unit in inflamm-aging. *Am. J. Physiol. Heart Circ. Physiol.* **2017**, *313*, H1000–H1012. [[CrossRef](#)]
59. Banerjee, S.F.Q.; Shah, S.K.; Ponnappan, U.; Melnyk, S.B.; Hauer-Jensen, N.; Pawar, S.A. Role of TLR4 in the pathogenesis of radiation-induced intestinal injury in C/EBP δ -knockout mice. In *SHOCK*; Lippincott Williams & Wilkins: Fort Lauderdale, FL, USA, 2017.
60. Robello, E.; Bonetto, J.G.; Puntarulo, S. Cellular Oxidative/Antioxidant Balance in gamma-Irradiated Brain: An Update. *Mini-Rev. Med. Chem.* **2016**, *16*, 937–946. [[CrossRef](#)]
61. Fishman, K.; Baure, J.; Zou, Y.; Huang, T.-T.; Andres-Mach, M.; Rola, R.; Suarez, T.; Acharya, M.; Limoli, C.L.; Lamborn, K.R.; et al. Radiation-induced reductions in neurogenesis are ameliorated in mice deficient in CuZnSOD or MnSOD. *Free Radic. Biol. Med.* **2009**, *47*, 1459–1467. [[CrossRef](#)]
62. Dai, D.F.; Chiao, Y.A.; Martin, G.M.; Marcinek, D.J.; Basisty, N.; Quarles, E.K.; Rabinovitch, P.S. Mitochondrial-Targeted Catalase: Extended Longevity and the Roles in Various Disease Models. *Prog. Mol. Biol. Transl. Sci.* **2017**, *146*, 203–241.
63. Parihar, V.K.; Allen, B.D.; Tran, K.K.; Chmielewski, N.N.; Craver, B.M.; Martirosian, V.; Morganti, J.M.; Rosi, S.; Vlkolinsky, R.; Acharya, M.M.; et al. Targeted overexpression of mitochondrial catalase prevents radiation-induced cognitive dysfunction. *Antioxid. Redox Signal.* **2015**, *22*, 78–91. [[CrossRef](#)]
64. Leger, M.; Quiedeville, A.; Bouet, V.; Haelewyn, B.; Boulouard, M.; Schumann-Bard, P.; Freret, T. Object recognition test in mice. *Nat. Protoc.* **2013**, *8*, 2531–2537. [[CrossRef](#)] [[PubMed](#)]
65. Zhao, Z.H.; Zheng, G.; Wang, T.; Du, K.J.; Han, X.; Luo, W.J.; Shen, X.F.; Chen, J.Y. Low-level Gestational Lead Exposure Alters Dendritic Spine Plasticity in the Hippocampus and Reduces Learning and Memory in Rats. *Sci. Rep.* **2018**, *8*, 3533. [[CrossRef](#)] [[PubMed](#)]
66. Mikolaenko, I.; Rao, L.M.; Roberts, R.C.; Kolb, B.; Jinnah, H.A. A Golgi study of neuronal architecture in a genetic mouse model for Lesch-Nyhan disease. *Neurobiol. Dis.* **2005**, *20*, 479–490. [[CrossRef](#)] [[PubMed](#)]
67. Groves, T.R.; Wang, J.; Boerma, M.; Allen, A.R. Assessment of Hippocampal Dendritic Complexity in Aged Mice Using the Golgi-Cox Method. *J. Vis. Exp. JoVE* **2017**. [[CrossRef](#)] [[PubMed](#)]

68. Sholl, D.A. Dendritic organization in the neurons of the visual and motor cortices of the cat. *J. Anat.* **1953**, *87*, 387–406. [[PubMed](#)]
69. Morley, B.J.; Mervis, R.F. Dendritic spine alterations in the hippocampus and parietal cortex of alpha7 nicotinic acetylcholine receptor knockout mice. *Neuroscience* **2013**, *233*, 54–63. [[CrossRef](#)] [[PubMed](#)]



© 2019 by the authors. Licensee MDPI, Basel, Switzerland. This article is an open access article distributed under the terms and conditions of the Creative Commons Attribution (CC BY) license (<http://creativecommons.org/licenses/by/4.0/>).



Loss of C/EBP δ enhances IR-induced cell death by promoting oxidative stress and mitochondrial dysfunction



Sudip Banerjee^a, Nukhet Aykin-Burns^a, Kimberly J. Krager^a, Sumit K. Shah^a,
Stepan B. Melnyk^b, Martin Hauer-Jensen^{a,c}, Snehalata A. Pawar^{a,*}

^a Division of Radiation Health, Department of Pharmaceutical Sciences, College of Pharmacy, University of Arkansas for Medical Sciences, Little Rock, AR 72205, United States

^b Arkansas Children's Hospital Research Institute, Little Rock, AR 72205, United States

^c Surgical Services, Central Arkansas Veterans Healthcare System, Little Rock, AR 72205, United States

ARTICLE INFO

Article history:

Received 1 April 2016

Received in revised form

26 July 2016

Accepted 17 August 2016

Available online 20 August 2016

Keywords:

Ionizing radiation

Reactive oxygen species

Oxidative stress

Mitochondrial dysfunction

CCAAT enhancer binding protein delta

Glutathione

ABSTRACT

Exposure of cells to ionizing radiation (IR) generates reactive oxygen species (ROS). This results in increased oxidative stress and DNA double strand breaks (DSBs) which are the two underlying mechanisms by which IR causes cell/tissue injury. Cells that are deficient or impaired in the cellular antioxidant response are susceptible to IR-induced apoptosis. The transcription factor CCAAT enhancer binding protein delta (*Cebpd*, C/EBP δ) has been implicated in the regulation of oxidative stress, DNA damage response, genomic stability and inflammation. We previously reported that *Cebpd*-deficient mice are sensitive to IR and display intestinal and hematopoietic injury, however the underlying mechanism is not known. In this study, we investigated whether an impaired ability to detoxify IR-induced ROS was the underlying cause of the increased radiosensitivity of *Cebpd*-deficient cells.

We found that *Cebpd*-knockout (KO) mouse embryonic fibroblasts (MEFs) expressed elevated levels of ROS, both at basal levels and after exposure to gamma radiation which correlated with increased apoptosis, and decreased clonogenic survival. Pre-treatment of wild type (WT) and KO MEFs with polyethylene glycol-conjugated Cu-Zn superoxide dismutase (PEG-SOD) and catalase (PEG-CAT) combination prior to irradiation showed a partial rescue of clonogenic survival, thus demonstrating a role for increased intracellular oxidants in promoting IR-induced cell death. Analysis of mitochondrial bioenergetics revealed that irradiated KO MEFs showed significant reductions in basal, adenosine triphosphate (ATP)-linked, maximal respiration and reserved respiratory capacity and decrease in intracellular ATP levels compared to WT MEFs indicating they display mitochondrial dysfunction. KO MEFs expressed significantly lower levels of the cellular antioxidant glutathione (GSH) and its precursor- cysteine as well as methionine. In addition to its antioxidant function, GSH plays an important role in detoxification of lipid peroxidation products such as 4-hydroxynonenal (4-HNE). The reduced GSH levels observed in KO MEFs correlated with elevated levels of 4-HNE protein adducts in irradiated KO MEFs compared to respective WT MEFs.

We further showed that pre-treatment with the GSH precursor, N-acetyl L-cysteine (NAC) prior to irradiation showed a significant reduction of IR-induced cell death and increases in GSH levels, which contributed to the overall increase in clonogenic survival of KO MEFs. In contrast, pre-treatment with the GSH synthesis inhibitor- buthionine sulfoximine (BSO) further reduced the clonogenic survival of irradiated KO MEFs.

This study demonstrates a novel role for C/EBP δ in protection from basal as well as IR-induced oxidative stress and mitochondrial dysfunction thus promoting post-radiation survival.

© 2016 Published by Elsevier Inc.

Abbreviations: ATP, Adenosine triphosphate; BSO, Buthionine sulfoximine; CAT, Catalase; C/EBP δ /*Cebpd*, CCAAT enhancer binding protein delta; CHO, Chinese hamster ovary; DSBs, DNA double strand breaks; GSH, Glutathione, L- γ -glutamyl-L-cysteinyl-glycine; GSSG, Glutathione disulfide; H₂O₂, Hydrogen peroxide; 4-HNE, 4-Hydroxynonenal; IR, Ionizing Radiation; KO, Knockout; MEFs, Mouse embryonic fibroblasts; NAC, N-acetyl L-cysteine; NAD⁺, Nicotinamide adenine dinucleotide; NADH, Dihydroxynicotinamide-adenine dinucleotide; NADP⁺, Nicotinamide adenine dinucleotide; NADPH, Dihydroxynicotinamide-adenine dinucleotide; OCR, Oxygen Consumption Rate; PEG, Polyethylene glycol; PEG-CAT, Polyethylene glycol conjugated catalase; PEG-SOD, Polyethylene glycol conjugated Cu-Zn superoxide dismutase 1; PBS, phosphate buffered saline; ROS, Reactive oxygen species; O₂^{•-}, Superoxide; S.E.M., Standard error mean; SOD1, Cu-Zn Superoxide dismutase 1; TBST, 10mM Tris HCl, pH7.5, 150mM NaCl, 0.05% Tween-20; WT, Wild type

* Corresponding author.

E-mail address: SAPawar@uams.edu (S.A. Pawar).

<http://dx.doi.org/10.1016/j.freeradbiomed.2016.08.022>

0891-5849/© 2016 Published by Elsevier Inc.

1. Introduction

Exposure to IR during cancer radiotherapy inevitably results in normal tissue toxicity to the rapidly renewing cell systems such as the hematopoietic tissues and the gastrointestinal tract mucosa [1–3]. The acute side-effects arise due to radiation-induced apoptotic and clonogenic cell death, and functional changes in various cellular compartments and microenvironments [1]. Although, several studies using cell lines and murine knockout models have demonstrated the role of genetics and genomics in toxic side-effects of radiotherapy, the molecular mechanism(s) of IR-induced injury in normal tissues remains unclear [2,3]. Knowledge of the underlying mechanisms is therefore critical for developing novel interventions to mitigate radiation-induced injury to the normal tissues [3].

IR exposure induces free radical generation and increased oxidative stress, which result in DSBs that are the primary causes of injury to cells and tissues [4–7]. It is known that exposure to IR induces a plethora of responses by cells to counteract oxidative stress, DNA damage response and inflammation by inducing the expression of antioxidants, DNA damage repair proteins and inflammatory and anti-inflammatory cytokines [7–11]. Cells have developed an antioxidant defense system to control the ROS [8,12,13]. If cells are deficient in the production of antioxidants to scavenge IR-induced oxidative stress and/or are impaired in the repair of IR-induced DSBs, they could be more sensitive to IR-induced apoptosis or become genetically unstable if they survive the initial IR insult [10,14]. Additionally, IR also affects the mitochondrial metabolism, which can lead to elevated levels of $O_2^{\bullet-}$ and thus perpetuate the damaging effects of IR in cells and tissues [14–17]. Most cellular ROS is generated in mitochondria, thus they play a key role in ROS-mediated apoptosis [15]. In the cells, ROS are mainly formed due to electron leakage naturally occurring in complex I and III of the mitochondrial electron transport chain [16]. Excessive and acute ROS accumulation triggers apoptotic pathway leading to cell death [17,18]. ROS, including superoxide ($O_2^{\bullet-}$) and hydrogen peroxide (H_2O_2) can cause oxidative damage via oxidation of DNA, proteins and lipids that may result in mitochondrial dysfunction [6,19]. The increase in ROS production leads to decreased ATP production, increased levels of protein carbonyls, and increased nitration of cellular proteins [20–22]. A balance between the production of ROS and the defensive capacity to produce antioxidants determines the ability of the cell to overcome oxidative damage [10,23].

The most abundant endogenous intracellular antioxidant present in the cells is the tripeptide L- γ -glutamyl-L-cysteinyl-glycine, GSH [24–27]. One of the major roles of GSH is to maintain the redox state that is critical for cellular activities [28,29]. Deficiency of GSH results in an increased pro-oxidizing shift and elevated oxidative stress [30,31]. The cellular biochemical machinery responsible for the metabolic production of free radicals and other reactive oxygen and nitrogen species derived from superoxide and nitric oxide could remain perturbed for minutes, hours, days and even years after exposure to IR [7].

The transcription factor C/EBP δ is a member of the basic leucine-zipper family of transcription factors that is implicated in the regulation of diverse biological processes in a cell-specific context such as acute phase response, proliferation, differentiation, growth arrest, apoptosis, hyperoxia, genomic stability, tumor suppression and self-renewal of stem cells [32–38]. The antioxidant enzyme SOD1 is a transcriptional target that is upregulated by C/EBP δ in cisplatin-treated human urothelioma cells and represents yet another important function for this protein [39].

Exposure to IR leads to increased oxidative stress, DNA-damage and inflammation, and although C/EBP δ is implicated in the

regulation of these processes, how it regulates these processes in the context of IR is not clear [32,36,39–42]. We have recently reported that C/EBP δ -deficiency promotes increased radiation lethality primarily due to injury to the gastrointestinal and hematopoietic tissues, however the underlying mechanism has not been elucidated [43].

Here we investigated the role of C/EBP δ in modulating IR-induced oxidative stress and mitochondrial dysfunction to prevent cells from undergoing IR-induced cell death.

We report that C/EBP δ -deficiency is associated with increased oxidative stress and oxidative damage and results in an increased sensitivity of MEFs to IR-induced cell death. The increased oxidative stress and mitochondrial dysfunction and increased sensitivity of C/EBP δ -deficient cells is due to the reduced levels of the cellular antioxidant GSH and its precursor amino acid- cysteine as well as methionine.

2. Materials and methods

2.1. Ethics statement

This study was carried out in strict accordance with the recommendations in the Guide for the Care and Use of Laboratory Animals of the National Institutes of Health and approved by the Institutional Animal Care and Use Committee of the University of Arkansas for Medical Sciences (animal use protocol number: 3511).

2.1.1. Generation of primary mouse embryo fibroblasts (MEFs)

Primary MEFs were isolated from 13.5 day old *Cebpd*-KO and WT embryos as described previously [36] and grown in T-75 flasks in DMEM supplemented with 10% FBS, 2 mM glutamine, 0.5% penicillin-streptomycin, 50 μ M β -mercaptoethanol, 1 mM sodium pyruvate. The cells were cultured at 37 °C in a humidified incubator with 5% CO_2 and 95% air. All studies were carried out on 2–3 pairs of early passage primary WT and KO MEFs (passage 3–7) in the presence of serum containing medium.

2.2. Reagents

NAC (Cat# A7250, St. Louis, MO) was prepared as 1 mM stock solutions with sodium bicarbonate and pH of 7.0. To prevent oxidation, NAC stocks were prepared fresh just before addition to the culture. BSO (cat# sc-200824, Santacruz Biotechnology, Dallas, TX), was dissolved in phosphate buffered saline (PBS) and prepared as a 10 mM stock solution.

2.3. Irradiation of MEFs

Irradiation (gamma-rays) of MEFs was performed in a Shepherd Mark I model 25 ^{137}Cs irradiator (J. L. Shepherd & Associates, San Fernando, CA). Dose uniformity was assessed by an independent company (Ashland Specialty Ingredients, Wilmington, DE) with radiographic film and alanine tablets. Alanine tablets were analyzed by the National Institute of Standards and Technology (Gaithersburg, MD) and demonstrated a dose rate of 1.14 Gy/min at 21 cm from the source. For each experiment the dose rate was corrected for decay.

2.3.1. Flow cytometry

2.3.1.1. Measurement of apoptosis

IR-induced cell death was measured with Annexin V FITC apoptosis detection kit (Cat # 556420, BD Biosciences, San Jose, CA, USA) and cleaved-caspase-3 expression. WT and KO MEFs (2×10^5 cells) were seeded per 60 mm dish in triplicates and 18 h

later exposed to 10 Gy, and harvested at 0, 6 h and 24 h post-irradiation. The cells were detached with Accutase (Cat# AT104, Innovative Cell Technologies, Inc, San Diego, CA). Another set of dishes were treated with NAC (5 mM) for 2 h prior to IR exposure at 10 Gy. At 3 h post-irradiation, NAC containing media was replaced with a NAC-free medium and cells were harvested at 0 and 24 h post-irradiation and processed similarly for Annexin V staining as described above.

Staining of cleaved caspase-3 was used to further confirm late-apoptosis. 2×10^5 cells were seeded in 60 mm dishes and exposed to 10 Gy and harvested at 0 and 24 h post-irradiation. The cells were detached, washed with chilled PBS, stained with antibody specific for cleaved caspase-3 (Cat# 9644, Cell Signaling Technology, Danvers, MA, USA) and processed as per the manufacturer's instructions.

Cells stained for Annexin V as well as cleaved caspase-3 were analyzed immediately on a BD FACS Calibur 488 nm excitation wavelength with 530/30 nm (FL1) emission filter. For each analysis, 20,000 cells were assayed for fluorescence and the data were analyzed using FlowJo (FlowJo, LLC, Ashland, OR, USA) and results are expressed as mean fluorescence intensity of 20,000 cells \pm standard error mean (S.E.M.).

2.3.1.2. Measurement of ROS

WT and KO MEFs were seeded at a density of 2×10^5 cells per 60 mm dish in triplicates and 18–20 h later exposed to 2 Gy. The cells were harvested 24 h later for measurement of ROS levels. At 24 h post-irradiation, cells were detached with 0.05% trypsin (Cat# 25300054, Thermo Fisher Scientific, Grand Island, NY), followed by a wash with PBS and were stained with 2 μ M MitoSOX Red (Cat# M36008, Life technologies, Grand Island, NY, USA) at 37 °C for 15 min. Unirradiated WT and KO MEFs were processed similarly as irradiated groups. The stained cells were washed and suspended in 200 μ l PBS and analyzed immediately on a BD FACS Calibur using 405 nm excitation wavelength with 585/642 nm (FL2) emission filter to detect ROS signal [44,45]. Results are expressed as mean fluorescence intensity of 20,000 cells \pm S.E.M.

2.3.1.3. Clonogenic survival assay-dose curve

Clonogenic survival of MEFs was performed to compare the ability of cells to recover from radiation exposure and measure the differences in survival between WT and KO MEFs. Chinese hamster ovary (CHO) cells exposed to 35 Gy, were seeded at a density of 3×10^4 cells per well in six-well plates to serve as a feeder layer for the primary MEFs as has been described previously [46]. The irradiated CHO cells secrete growth factors into the medium which aid the growth of the primary MEFs.

WT and KO MEFs (2×10^5) cells were seeded in 60 mm petridishes, and 18 h later were exposed to irradiation doses of 0, 2, 4 and 8 Gy. The cells were re-seeded on the CHO feeder layers at low densities (50–300 cells/well) 3 h post-irradiation. Unirradiated WT and KO MEFs were treated similarly and seeded at various cell densities to measure the plating efficiency and used to calculate the percent survival as described previously [47]. By day 10–14 post-seeding, the CHO cells undergo cell death by mitotic catastrophe, while the MEFs form colonies. A negative control dish with no MEFs is included as a control and shows no colonies. At 2 weeks post-seeding, the colonies were fixed with chilled methanol (100%) for 30 min, followed by staining with Giemsa stain and were counted with a stereomicroscope. Colonies were defined as containing at least 50 cells. The plating efficiency and surviving fractions were calculated as described previously [47].

2.3.1.4. Clonogenic assay with antioxidant enzymes

PEG-SOD and PEG-CAT

(Sigma, St. Louis) were dissolved in sterile PBS at 5000 U per ml

or 50,000 U per ml for stock solutions respectively. WT and KO MEFs were treated at a concentration of 50 U per ml for 2 h prior to irradiation at 2 Gy with PEG-SOD/PEG-CAT or in combination. PEG alone was used as a control. The cells were seeded on the irradiated CHO feeder layer and processed similarly as described above.

2.3.1.5. Clonogenic assay with NAC and BSO

For determining the effects of GSH levels on clonogenic survival, MEFs were treated with 5 mM NAC for 2 h prior to irradiation (2 Gy) and removed 3 h post-irradiation, when cells were re-seeded for the clonogenic assay in NAC-free medium. An aliquot of the treated cells was frozen for GSH measurements.

We also examined whether inhibition of GSH biosynthesis would further increase sensitivity of KO MEFs to IR. WT and KO MEFs (2×10^5) were seeded in 60mm dishes and 18h later treated with 10 μ M BSO for 24 h prior to irradiation at 2 Gy. Cells were re-seeded 3 h post-irradiation in BSO-free medium on the irradiated CHO feeder layer and processed similarly as described above.

2.3.1.6. Immunoblotting

WT and KO MEFs (2×10^5) were seeded in 60 mm dishes and 18 h later exposed to 2 Gy. The cells were harvested and whole cell extracts were prepared at 0, 2 h, 4 h and 24 h post-irradiation. 50 μ g protein was run on SDS-PAGE gels and immunoblotted. The blot was blocked with 5% milk in 10 mM Tris·HCl at pH7.5, 150mMNaCl and 0.05%Tween20 (1X TBST) probed with rabbit polyclonal serum against 4-HNE (1:10,000) in 1 X TBST. The blots were developed using peroxidase-conjugated anti-rabbit secondary IgGs and visualized by ECL. Ponceau S staining of the blot served as a loading control for each sample per lane.

2.3.1.7. Mitochondrial cellular bioenergetics

We used the Seahorse Extracellular Flux 96 Analyzer (Agilent Biotechnologies, Santa Clara, CA, USA) to measure the oxygen consumption rate (OCR), an indicator of mitochondrial respiration in real-time in WT and KO MEFs. Briefly, 2×10^5 MEFs were seeded in 60 mm dishes and 18 h later exposed to 2 Gy. At 6 h post-irradiation, cells were trypsinized and 10^4 cells/well were seeded in Seahorse XF96 cell culture microplates and allowed to grow overnight at 37 °C. The cells were washed and subsequently changed to unbuffered seahorse assay medium at 24 h post-irradiation and the oxygen consumption rate (OCR) was measured using a 2 min mix, 4 min read cycling protocol as described previously [48]. The basal respiration, ATP-linked respiration, maximal respiration, reserved respiratory capacity, non-mitochondrial respiration and proton leak was calculated [49].

2.3.1.8. Measurement of ATP levels

WT and KO MEFs (8×10^5) were seeded in 100 mm dishes and 18 h later exposed to 2 Gy and cells were collected 24 h post-irradiation and flash frozen. Adenosine 5'-triphosphate (ATP) levels were measured using the ATP Bioluminescent Assay kit (Cat# FLAA, Sigma-Aldrich, St. Louis, MO) as per the manufacturer's instructions [50]. Standard curve for ATP was generated and total ATP levels were extrapolated and expressed as nmoles per cell.

2.3.1.9. Measurement of NADH, NAD, NADP, NADPH, GSH, GSSG, Methionine and Cysteine

WT and KO MEFs were seeded at a density of 8×10^5 cells per 100 mm dishes in triplicates and 18 h later were exposed to 2 Gy. The cell were harvested 24 h post-irradiation, snap-frozen in liquid nitrogen and stored at -80 °C until HPLC analysis. Nicotinamide adenine dinucleotide (NAD^+) and dihydronicotinamide adenine dinucleotide (NADH); nicotinamide adenine dinucleotide (NADP^+) and dihydronicotinamide adenine dinucleotide (NADPH)

were measured as described [51] utilizing a Dionex UltiMate 3000 HPLC-UV system (Dionex Inc., Sunnyvale, CA). C18 Gemini column (5 μ m, 3 \times 150 mm; Phenomenex, Torrance, CA) at 254 nm wavelength. Concentrations were calculated from peak areas of standard calibration curves using HPLC software. Results are expressed per mg protein using BCA Protein Assay Kit (Pierce Inc., Rockford, IL, USA).

For quantification of intracellular free GSH, glutathione disulfide (GSSG), methionine and cysteine, thawed cells were lysed by sonication in 112.5 μ l ice-cold PBS followed by the addition of 37.5 μ l ice-cold 10% meta-phosphoric acid. This mixture was incubated for 30 min on ice followed by centrifuging for 15 min at 18,000 \times g at 4 $^{\circ}$ C. The metabolites were eluted using a Shimadzu Solvent Delivery System (ESA model 580; ESA Inc., Chelmsford, MA) and a reverse-phase C18 column (3 μ m, 4.6 \times 150 mm; Shiseido Co., Tokyo, Japan). A 20 μ l aliquot of cell extract was directly injected onto the column using an ESA Inc. Autosampler (model 507E), and the metabolites were quantified using a model 5200A Coulochem II and CoulArray electrochemical detection system (ESA) equipped with a dual analytical cell (model 5010), a 4-channel analytical cell (model 6210), and a guard cell (model 5020) as described previously [52].

2.3.1.10. Statistical analyses

Statistical analysis was performed using GraphPad Prism 7.0 (GraphPad Software, San Diego, California). Data were expressed as average \pm standard error mean (S.E.M.) unless otherwise specified. One-way ANOVA with Tukey's post-analysis was used to study the differences among 3 or more means. $P < 0.05$ was considered statistically significant.

3. Results

3.1. *Cebpd*-deficiency increased IR-induced cell death in MEFs

We have shown that *Cebpd* plays an important role in the post-irradiation survival of mice [43], so we first examined whether KO MEFs were also sensitive to IR exposure. Under basal conditions and at 6 h post-irradiation at 10 Gy, there were slightly more Annexin V positive KO MEFs than WT MEFs, but these differences were not significant. However, at 24 h post-irradiation, the number of Annexin V-positive KO MEFs was 1.8-fold higher than the respective WT MEFs (Fig. 1A).

We then examined the production of cleaved caspase-3, a marker of late apoptosis under basal conditions and 24 h

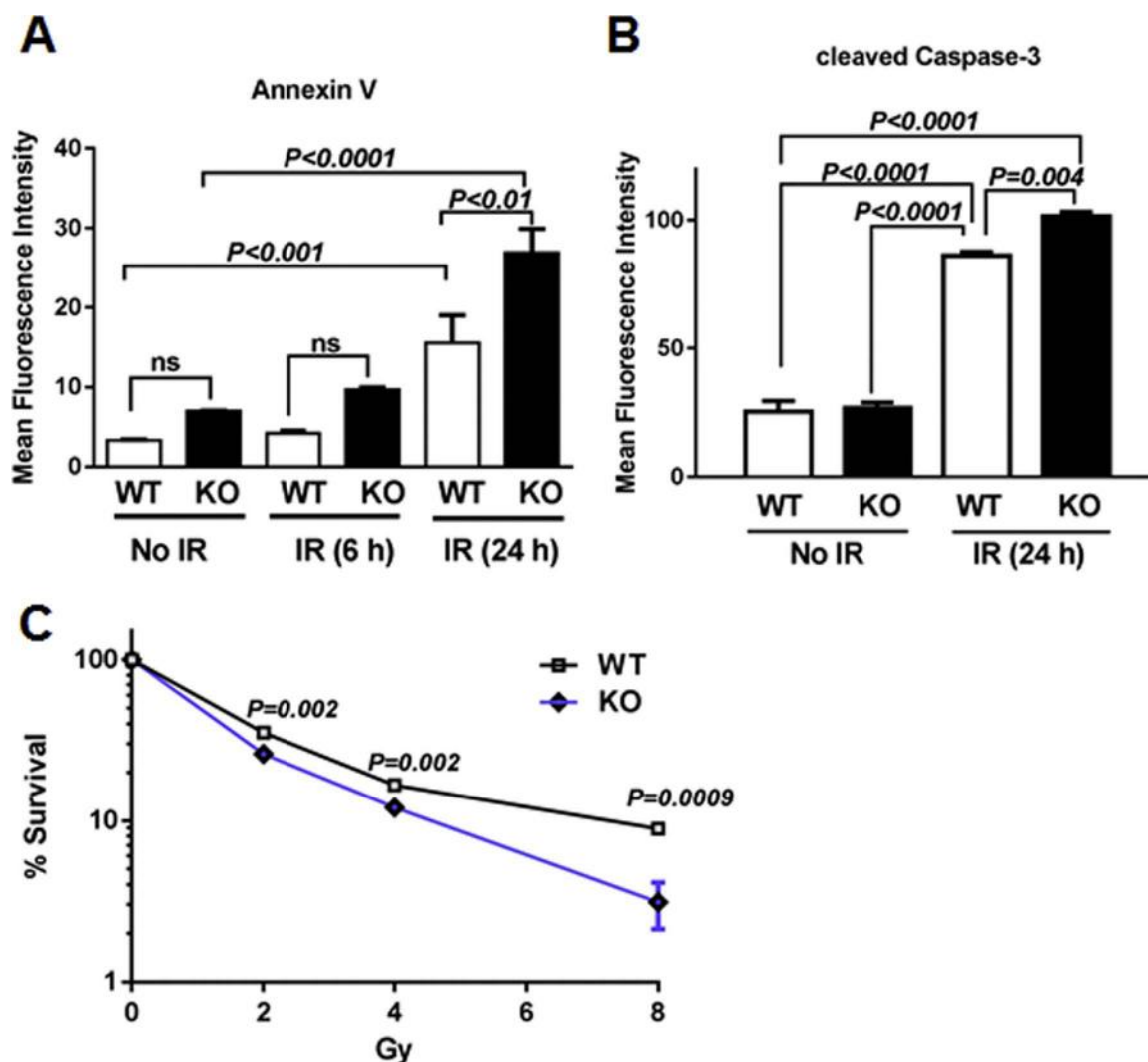


Fig. 1. *Cebpd*-KO MEFs show increased apoptosis and decreased clonogenic survival after exposure to IR. WT and KO MEFs were seeded in triplicates and harvested at 0, 6 h and 24 h post-irradiation (10 Gy), for (A) Annexin V staining and (B) cleaved caspase-3 staining and analyzed by flow cytometry. Data are represented as mean fluorescence intensity \pm SEM. (C) KO and WT MEFs were exposed to 0–8 Gy and re-seeded 3 h later in triplicates. Colonies were scored 2 weeks later after staining with Giemsa. The data are presented as an average of 3 dishes seeded per treatment group, ns-not significant.

post-10 Gy exposure. Under basal conditions, there were no significant changes in cleaved caspase-3 expression between WT and KO MEFs. However 24 h post-irradiation, there was a robust increase in the amount of cleaved caspase-3 positive cells in both WT (3.4-fold) and KO MEFs (3.8-fold) compared to unirradiated WT controls. Irradiated KO MEFs expressed about 1.2-fold higher cleaved caspase-3 positive cells compared with irradiated WT MEFs (Fig. 1B), thus confirming that these cells undergo IR-induced apoptosis.

Next, we utilized the clonogenic survival assay to determine the effect of increasing doses of radiation on recovery and survival of MEFs and whether C/EBP δ -deficiency resulted in a differential response. While there were no significant differences in the number of clones in the unirradiated group between the genotypes (*data not shown*), KO MEFs showed a remarkable dose-dependent decline in survival of clones with increasing doses of IR compared to respective WT MEFs (Fig. 1C). These results suggest that C/EBP δ is essential to promote post-radiation survival which may be dependent upon its role in the modulation of radiation-induced oxidative stress.

3.2. Cebpd-deficiency promotes increased levels of intracellular oxidants

In order to investigate whether the increased sensitivity of KO MEFs to IR was due to the increased levels of oxidants, we first compared the cellular ROS levels at steady state levels and 24 h post-2 Gy exposure in WT and KO MEFs. WT and KO MEFs were stained with MitoSOX at 0 and 24 h post-2 Gy exposure and MitoSOX oxidation was analyzed by flow cytometry. Irradiated WT MEFs did not show a significant increase in MitoSOX oxidation compared to unirradiated WT MEFs (Fig. 2A-B). In contrast, we found that the basal levels of MitoSOX oxidation in KO MEFs were 1.8-fold higher compared to that of WT MEFs. At 24 h post-irradiation, KO MEFs showed 2.2-fold higher levels of MitoSOX oxidation compared to the WT MEFs (Fig. 2A-B). Although the basal levels of ROS are elevated in the KO MEFs, they are able to proliferate normally. However in response to an external stressor such as IR, KO MEFs show increased production of IR-induced ROS levels suggestive of an impaired oxidant/anti-oxidant balance as well as impaired mitochondrial function, since mitochondria are a

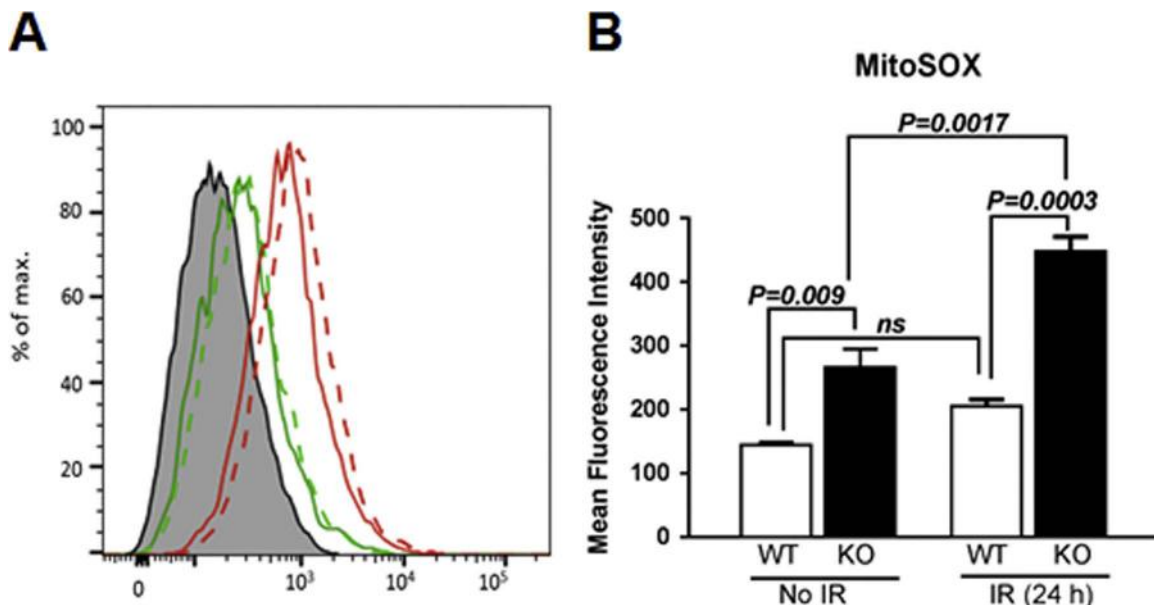


Fig. 2. Cebpd-KO MEFs express increased ROS levels. WT and KO MEFs were exposed to 0 and 2 Gy, and 24 h later stained with MitoSOX and analyzed by flow cytometry. The data is presented as an average of 3 dishes seeded per treatment group and represented as mean fluorescence intensity \pm S.E.M.

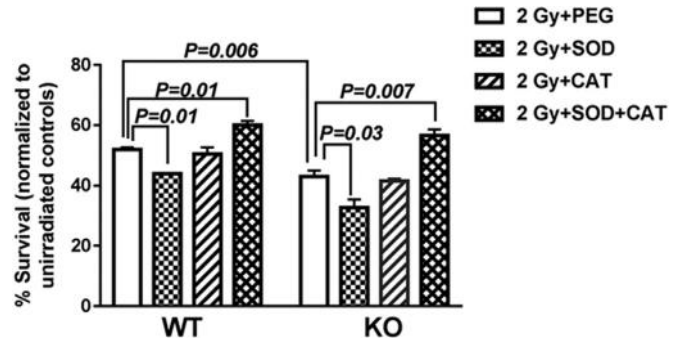


Fig. 3. PEG-SOD + CAT treatment prior to irradiation show a slight increase in post-radiation clonogenic survival of WT and KO MEFs. WT and KO MEFs were treated with PEG alone, PEG-SOD, PEG-CAT and or PEG-SOD + CAT for 2 h prior to irradiation at 2 Gy. The cells were re-seeded 3 h post-irradiation in triplicates and colonies were counted two weeks later and normalized to respective unirradiated dishes. The data are presented as an average of 2 biological replicates \pm S.E.M. of 3 dishes seeded per treatment group.

significant source of superoxide.

3.3. Pre-treatment with exogenous antioxidant enzymes increased post-radiation clonogenic survival of Cebpd-KO MEFs

Based on our MitoSOX data, we hypothesized that KO MEFs are more radiosensitive than WT MEFs because they are unable to modulate the IR-induced oxidative stress. To determine whether impaired oxidative stress modulation is the underlying cause of the increased radiosensitivity of KO MEFs, we examined the clonogenic survival of WT and KO MEFs in the presence of exogenously added antioxidant enzymes. Since IR is known to induce $O_2^{\bullet-}$ and H_2O_2 , we utilized superoxide dismutase which dismutates $O_2^{\bullet-}$ to form H_2O_2 and catalase that catalyzes the breakdown of H_2O_2 to water and molecular oxygen. WT and KO MEFs were pre-treated with PEG-SOD or PEG-CAT alone or in combination prior to irradiation.

Interestingly, pre-treatment of MEFs with PEG-SOD prior to IR exposure led to a 0.82-fold reduction in survival of WT MEFs and a 0.63-fold reduction in clonogenic survival of KO MEFs compared with PEG alone. These results suggest that the IR-induced $O_2^{\bullet-}$

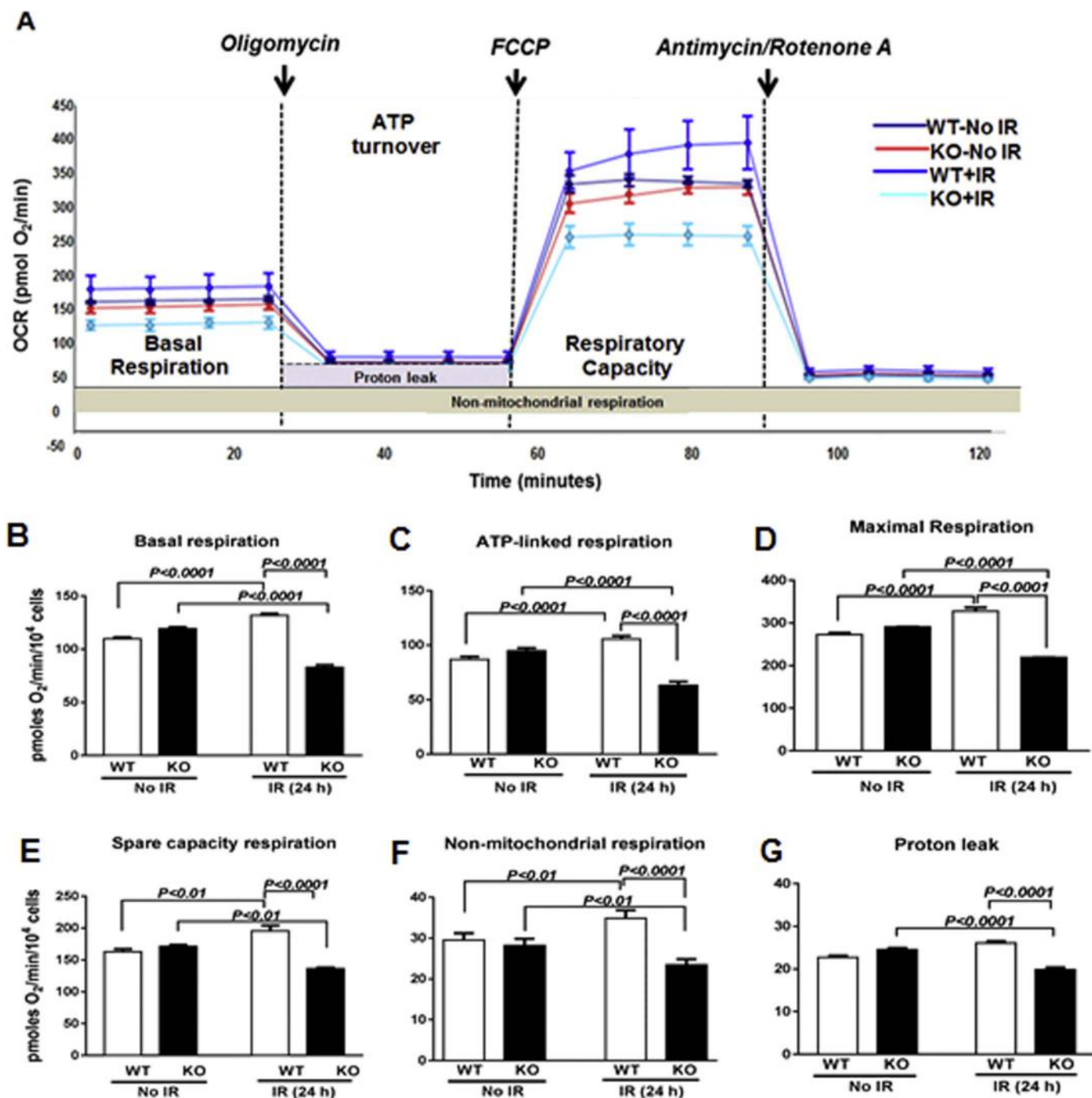


Fig. 4. *Cebpd*-KO MEFs showed decrease in mitochondrial bioenergetics after IR exposure. (A) Mitochondrial bioenergetics profiles were measured by seahorse XF-analyzer in sham and irradiated WT and KO MEFs. The arrows indicate the time of addition of mitochondrial inhibitors: oligomycin (1 μ m), FCCP (5 μ m) or rotenone and antimycin A (10 μ m). (B) basal respiration; (C) ATP-dependent respiration; (D) Maximal respiration rate; (E) Reserved respiratory capacity; (F) non-mitochondrial respiration and (G) proton leakage between WT and KO MEFs. The data are presented as average \pm S.E.M. of $n=4-8$ wells per treatment group.

species are converted to H₂O₂. The endogenous catalase in the irradiated WT and KO MEFs is not effective in catalyzing the increased H₂O₂ levels and thus leads to reduced clonogenic survival when compared to respective PEG-alone controls.

In contrast pre-treatment with PEG-CAT alone prior to IR exposure did not show any significant change in clonogenic survival in both irradiated WT and KO MEFs compared to their respective PEG alone groups. These results suggest that the IR-induced cell death that occurs in both WT and KO MEFs is perhaps due to the

increased IR-induced O₂^{•-} and that the endogenous Cu-Zn SOD and Mn-SOD are not efficient in dismutation of O₂^{•-} or may be inactivated by IR-induced oxidative stress.

However PEG-SOD+CAT combination treatment prior to IR exposure showed a modest but significant increase in clonogenic survival of both WT and KO MEFs compared to respective PEG alone groups (Fig. 3). Thus these data indicate that the underlying sensitivity of KO MEFs to IR may be in part via an impaired ability to control IR-induced oxidative stress.

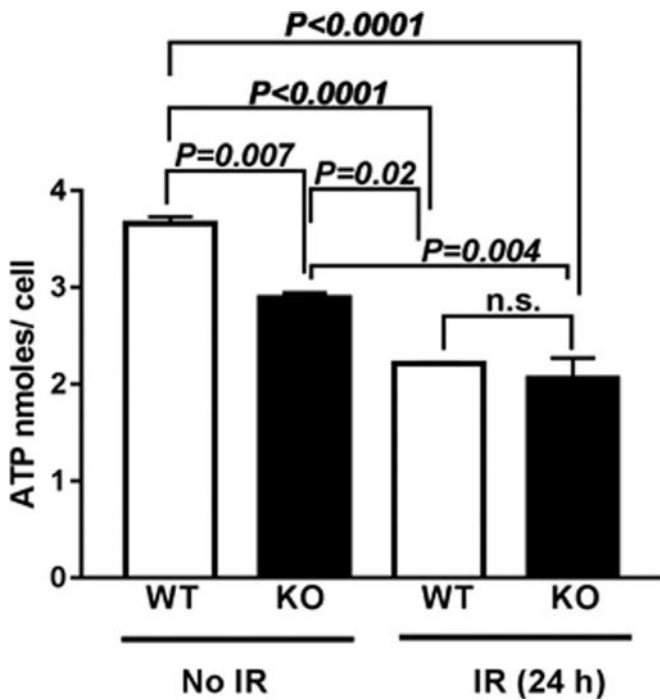


Fig. 5. *Cebpd*-KO MEFs showed significant reduction in ATP levels at 24 h post-irradiation. WT and KO MEFs were harvested at 0 and 24h post-irradiation (2 Gy) and whole cell extracts were prepared and analyzed for ATP levels. The data is plotted as an average of three biological replicates \pm S.E.M.

3.4. *Cebpd*-KO MEFs show mitochondrial dysfunction after exposure to IR

Several studies have demonstrated that the exposure of cells to IR adversely affects the mitochondrial electron transport chain and respiration [21,53]. The cellular bioenergetics and cellular respiration in unirradiated versus irradiated WT and KO MEFs were measured using the Sea-horse XF flux analyzer (Fig. 4A). There were no significant differences between the WT and KO MEFs in their basal, ATP-linked, maximal, reserved respiratory capacity, non-mitochondrial respiration and proton leakage. However, at 24 h post-irradiation, KO MEFs showed significant reductions in basal respiration (0.63-fold), ATP-linked respiration (0.6-fold), maximal respiration (0.66-fold), reserved respiratory capacity (0.69-fold), proton leakage (0.76-fold) and non-mitochondrial respiration (0.67-fold) compared to respective WT MEFs (Fig. 4B-G). These results suggest that the mitochondria in the KO MEFs display severe dysfunction and are unable to cope up with the IR-induced oxidative stress.

3.5. *Cebpd*-KO MEFs express significantly reduced ATP levels after IR exposure

It is well known that mitochondrial dysfunction and IR-induced oxidative stress leads to reduction in ATP synthesis due to disruption of the proton gradient across the mitochondrial membrane [20]. We next investigated whether the mitochondrial dysfunction led to alterations in ATP production. KO MEFs showed a 0.8-fold decrease in ATP levels under basal conditions which showed a further 0.56-fold decrease at 24 h post-2 Gy exposure compared to unirradiated WT MEFs (Fig. 5). The reduced ATP levels could arise due to oxidation of the coenzymes NADH/NADPH of the mitochondrial electron transport chain.

We therefore examined whether there was increased oxidation of the coenzymes NADH/ NADPH. Contrary to our expectation, we found no significant differences in the levels of oxidized to

reduced forms of the coenzymes NADH and NADPH between both the genotypes (Supplementary Fig. 1).

3.6. *Cebpd*-deficient MEFs expressed low levels of GSH, Cysteine and Methionine

Although we saw that ATP levels were significantly reduced in KO MEFs post-2 Gy exposure, we did not find any significant changes in the oxidation of the coenzymes NADH/NADPH of the mitochondrial electron transport chain. We next investigated whether the expression of the cellular antioxidant GSH, which is known to protect against radiation-induced oxidative damage [28] is impaired in the KO MEFs.

Interestingly, we found that KO MEFs expressed significantly lower levels of reduced GSH and GSSG compared to WT MEFs in irradiated as well as unirradiated conditions (Fig. 6A-B), which correlated with the increased ROS levels as shown by MitoSOX oxidation (Fig. 2). While the total GSH levels and GSH/GSSG were lower in KO MEFs, than WT MEFs (supplementary Fig. 2A, B). The decreased levels of GSH further correlated with reduced levels of its precursor amino acid-cysteine as well as methionine (Fig. 6C-D). Particularly the essential amino acid methionine is a precursor for cysteine, a rate limiting amino acid for GSH synthesis.

3.7. *Cebpd*-deficient MEFs accumulate high levels of 4-HNE protein adducts

It is known that increased oxidative stress results in increased chemical modifications of cellular proteins namely protein carbonylations and formation of 4-HNE adducts [54]. GSH plays a critical role in detoxification of 4-HNE and thus protects the cellular components from oxidative damage. Therefore, the expression of HNE-protein adduct formation as a marker of oxidative damage to the cellular proteins was examined in KO and WT MEFs at various timepoints post-irradiation. WT and KO MEFs express similar HNE-protein adduct formation under basal conditions, which was significantly elevated in KO MEFs after irradiation as compared to respective WT MEFs (Fig. 7). These results demonstrate an impaired ability to modulate endogenous ROS levels in irradiated cells leading to increased oxidative damage of the cellular proteins in KO MEFs.

3.8. Post-radiation survival of *Cebpd*-KO MEFs was rescued by pre-treatment with NAC and inhibited by BSO

To determine whether decreased GSH was the underlying cause of decreased post-radiation survival and increased radiosensitivity of KO MEFs, we assessed the effect of the GSH precursor- NAC on IR-induced cell death. We found that treatment with NAC (5 mM) for 2 h prior to irradiation and 3 h post-irradiation did not have any significant effects on cell death measured by Annexin V staining in WT MEFs under basal condition or after exposure to 10 Gy (Fig. 8A). In contrast, unirradiated KO MEFs showed a 0.63-fold decrease when compared with respective WT MEFs. Compared to irradiated WT MEFs, irradiated KO MEFs showed a 0.43-fold decrease in cell death when treated with NAC which was significant (Fig. 8A).

Further we wanted to determine whether treatment of NAC led to improved clonogenic survival of WT and KO MEFs after exposure to IR. We found that treatment with NAC (5 mM) for 2 h prior to irradiation and 3 h post-irradiation showed a robust rescue of clonogenic survival of both irradiated WT and KO MEFs (Fig. 8B).

We also verified whether NAC treatment led to significant increase in GSH levels and was the underlying basis of increased clonogenic survival and decreased cell death in KO MEFs. NAC

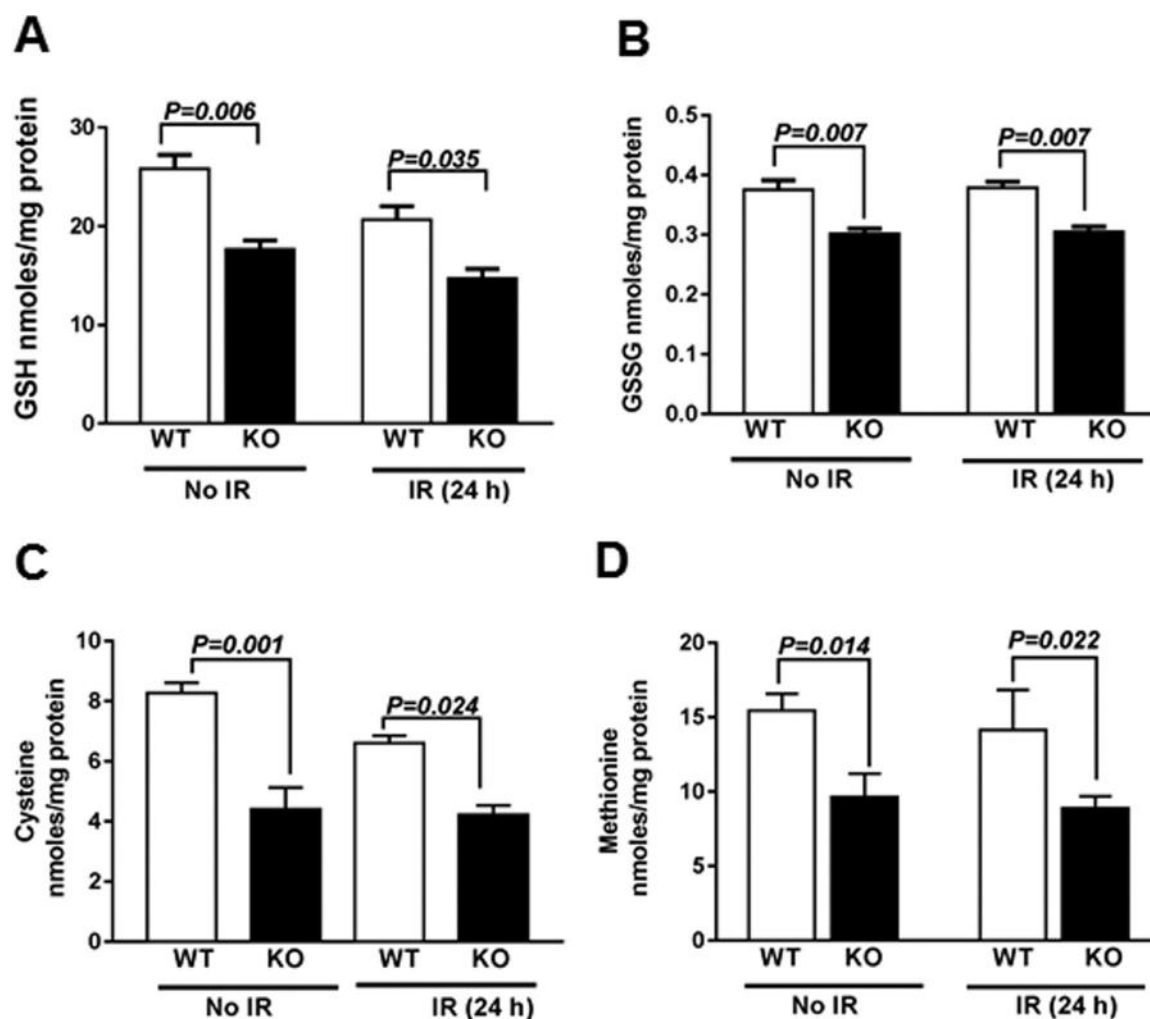


Fig. 6. *Cebpd*-KO MEFs show reduced expression of GSH and its precursor amino acid –cysteine as well as methionine. WT and KO MEFs were harvested at 0 and 24 h post-irradiation (2 Gy) and analyzed for the (A) GSH; (B) GSSG; (C) Cysteine and (D) Methionine and normalized to protein content. The data is plotted as an average of three biological replicates \pm S.E.M.

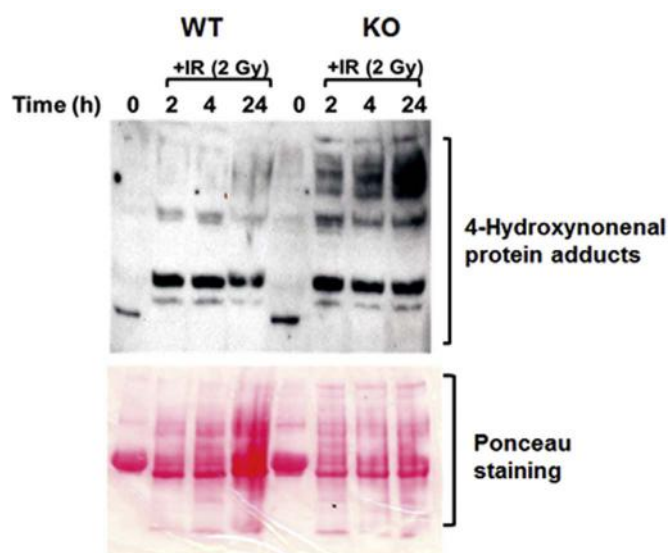


Fig. 7. *Cebpd*-KO MEFs display increased oxidative damage after IR exposure. WT and KO MEFs were harvested at 0, 2, 4 and 24 h post-IR (2 Gy) and probed with an antibody specific for 4-HNE. This is a representative blot showing the increased 4-HNE–protein adduct formation in KO MEFs at various timepoints post-irradiation. Ponceau S staining of the blot serves as a loading control.

treatment led to 1.35-fold increase in WT MEFs and 1.46-fold increase in GSH levels in the KO MEFs compared to respective irradiated WT and KO MEFs (Fig. 8C).

To further confirm the role of reduced GSH levels in the increased sensitivity of KO MEFs to IR exposure, we examined the effect of inhibition of the gamma-glutamyl cysteine ligase, the rate limiting step of GSH biosynthesis by BSO on clonogenic survival of irradiated and unirradiated WT and KO MEFs. Here, pre-treatment with BSO stimulated the survival of unirradiated WT MEFs by 1.3-fold compared to KO MEFs (Fig. 8D). In the irradiated groups, BSO pre-treatment further decreased the survival of KO MEFs by 1.6-fold compared to that of WT MEFs and by 1.9-fold compared to that of KO MEFs. These data demonstrate that the underlying sensitivity of KO MEFs to IR is in part via the reduced GSH levels.

4. Discussion

In this study we describe a novel role for C/EBP δ in regulating IR-induced oxidative stress and induced mitochondrial dysfunction and thereby promoting post-radiation survival. The major findings of this study are that a loss of C/EBP δ results in increased basal as well as IR-induced ROS levels and mitochondrial dysfunction which led to increased apoptosis. Further we showed that

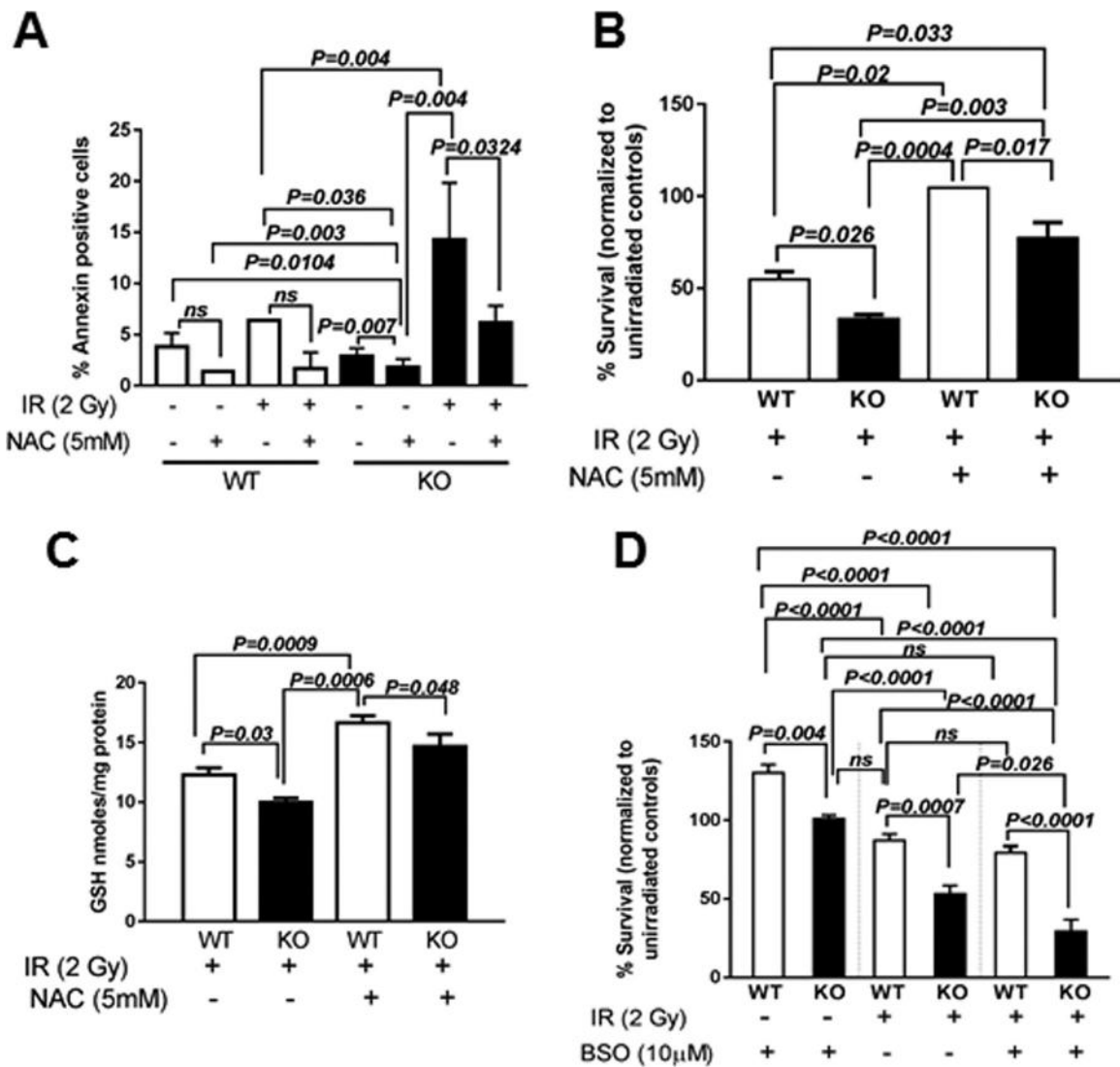


Fig. 8. The GSH-precursor NAC rescues post-radiation survival but the GSH inhibitor-BSO reduces survival of *Cebpd*-KO MEFs. WT and KO MEFs were treated with NAC (5 mM) for 2 h prior to IR exposure (10 Gy) and analyzed at indicated timepoints for (A) apoptosis using FITC Annexin V; (B) WT and KO MEFs were treated with NAC (5 mM) for 2 h prior to irradiation at 2 Gy and re-seeded for clonogenic assay 3 h post-irradiation and (C) cells were also harvested for GSH measurements; (D) KO and WT MEFs were treated with BSO (10 µM) for 24 h prior to irradiation at 2 Gy and re-seeded for clonogenic assay 3 h post-irradiation. The data for A and C are plotted as an average of 2–3 dishes ± S.E.M. The data for B and D are plotted as an average of 6 dishes each for the 2 biological replicates ± S.E.M.

C/EBP δ -deficiency led to decreased levels of GSH and its precursor amino acid-cysteine and its precursor-methionine. Thus our studies point to a novel role of C/EBP δ in redox regulation via modulation of GSH levels.

C/EBP δ is a transcription factor that has been implicated in the regulation of gene targets involved in inflammation, DNA damage response and oxidative stress, processes that also play a critical role in response of cells or tissues to IR exposure [32,36,39–42]. Survival of cells in response to IR exposure is dependent upon their ability to recover from IR-induced oxidative stress, DNA damage and inflammation [32,36,39–42]. A previous study has shown a role for C/EBP δ in detoxification of cisplatin-induced ROS levels by transcriptional upregulation of SOD1 [39]. Cells that overexpress SOD1 are known to be protected from IR-induced apoptosis [55–57]. It is possible that *Cebpd*-WT MEFs may upregulate antioxidant response genes which are perhaps impaired in the KO MEFs, thereby making them more susceptible to IR-induced cell death. Similar to the anti-apoptotic role of CEBP δ described in mammary epithelial cells and pancreatic beta cells [58,59], we found that *Cebpd*-WT MEFs protected from IR-induced apoptosis and promoted clonogenic survival compared to KO MEFs

(Fig. 1), which correlated with decreased ROS levels (Fig. 2).

The clonogenic survival of WT and KO MEFs upon pre-treatment with PEG-CAT prior to irradiation did not show significant change compared to the respective PEG-alone group, suggesting that the increased IR-induced cell death may be due to the increased O $_2^{\bullet-}$ levels. In contrast, PEG-SOD pre-treatment led to a further decrease in post-radiation clonogenic survival of both WT and KO MEFs compared to PEG-alone group. These results suggest that the cells accumulate increased H $_2$ O $_2$ due to dismutation of IR-induced increased O $_2^{\bullet-}$ levels and points to a contributory role of IR-induced mitochondrial superoxide in promoting cell death. KO MEFs as well as WT MEFs showed a partial rescue of clonogenic survival, when treated with a combination of PEG-SOD+CAT, rather than individual treatment of PEG-SOD or PEG-CAT alone (Fig. 3). Overall these results suggest that both O $_2^{\bullet-}$ and H $_2$ O $_2$ may contribute to the decrease in post-radiation survival in *Cebpd*-KO MEFs.

We also further investigated whether the increased ROS levels led to alterations of mitochondrial function in KO MEFs in response to IR. Although unirradiated KO MEFs show elevated ROS levels as shown by MitoSOX oxidation, there were no significant

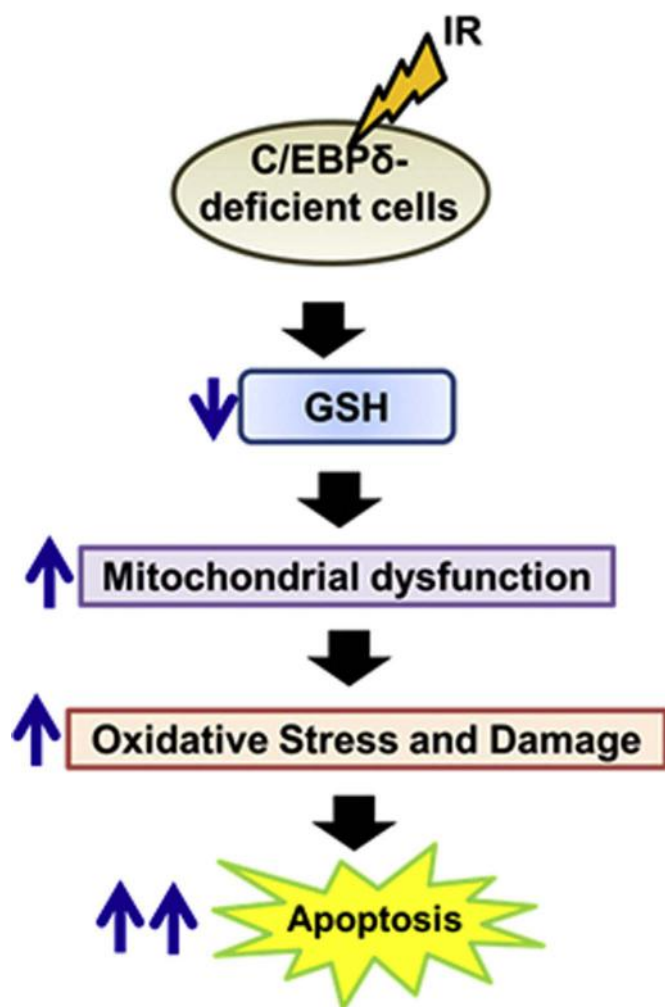


Fig. 9. Schematic model depicting the increased oxidative stress, mitochondrial dysfunction and reduced GSH levels that lead to IR-induced apoptosis of C/EBP δ -deficient cells.

differences in the mitochondrial function compared to that of WT MEFs as measured by OCR (Fig. 4A–B). This could be due to the robust induction of antioxidant genes under basal conditions in the KO MEFs but not after exposure to IR (*data not shown*). However post-irradiation, KO MEFs showed significant decreases in basal, ATP-dependent, maximal and reserved respiratory capacity as well as a decrease in proton leakage, indicative of mitochondrial dysfunction compared to WT MEFs (Fig. 4) which correlated with reduced ATP levels (Fig. 5). The decrease in reserved respiratory capacity of KO MEFs points to a deficiency in energy demanding bioenergetics response against IR-induced stress as described for *Sirt3*-knockdown cells [60].

In contrast WT MEFs showed an increase in the basal, ATP-dependent, maximal, reserved respiratory capacity and non-mitochondrial respiration, which is indicative of an adaptive response to IR-induced oxidative stress. The increased ROS levels in KO MEFs however did not show any impairment in the NAD⁺/NADH and NADP⁺/NADPH ratios, both under irradiated and unirradiated conditions, which led us to investigate the role of the cellular antioxidant GSH (Supplementary Fig. 1).

GSH plays a key role in maintaining the redox state that is critical for cellular activities [28,29]. It is known that the cellular antioxidant GSH protects against radiation-induced oxidative damage and the oxidation of GSH is an indicator of oxidative stress. Increased levels of GSH are known to suppress apoptosis [25,28]. We found that the KO MEFs express reduced levels of GSH

compared to WT MEFs (Fig. 6A–B). In addition to reduced GSH levels, we also found that KO MEFs expressed reduced cysteine and methionine content (Fig. 6C–D).

Apart from its role in maintaining redox state of the cells, GSH is also involved in detoxification of ROS/RNS by direct interactions with enzymes like GSH-peroxidase and GSH-S-transferase [25,27]. 4-HNE is a lipid peroxidation-derived product, highly associated with the generation of ROS, hence used as a marker of oxidative stress [54]. 4-HNE is rapidly removed from the cells by phase II pathway using glutathione-S-transferases which use GSH as one of the substrates leading to its short half-life. We investigated whether the reduced GSH levels led to increased oxidative damage in the irradiated KO MEFs. The increased accumulation of 4-HNE protein adducts in the irradiated KO MEFs could be due to decreased clearing of 4-HNE protein adducts and correlates with the reduced GSH levels (Fig. 7). These studies suggest that reduced GSH levels contribute to the increased oxidative stress and increased sensitivity of KO MEFs post-IR exposure.

To further confirm the role of reduced GSH in promoting IR-induced cell death, we investigated the effects of the GSH precursor-NAC on IR-induced cell death of WT and KO MEFs. Although unirradiated and irradiated WT MEFs did not show significant reductions in apoptosis with NAC treatment, they showed a significant increase in GSH levels and rescue of clonogenic survival (Fig. 8A–C). These results suggest that GSH-independent pathways may also play a role in the post-radiation survival of WT MEFs.

In contrast, KO MEFs showed significant reductions in cell death in both unirradiated and irradiated groups, and significant increases in GSH levels compared to respective radiation alone treatment groups which explain the robust rescue of clonogenic survival (Fig. 8A–C). These results confirm the reduced GSH levels as one of the major players in the increased radiosensitivity of *Cebpd*-KO MEFs.

As expected we found that upon inhibiting GSH biosynthesis by BSO treatment for 24 h prior to irradiation, KO MEFs were further sensitized to IR and showed a decline in clonogenic survival compared to irradiated WT MEFs (Fig. 8D). While unirradiated WT and KO MEFs did not show any effect of BSO treatment, post-irradiation there was a significant decrease in post-radiation survival of BSO treated KO MEFs compared to radiation alone, but not in respective WT MEFs groups.

We speculate that *Cebpd*-KO MEFs may have defects in either GSH biosynthesis pathways or the GSH regeneration pathways similar to the *Nrf2*^{-/-} MEFs [61]. This phenotype needs further investigation. Studies are currently underway utilizing a proteomics approach to identify the C/EBP δ -targets that may be downregulated in KO MEFs, leading to increased radiosensitivity. Overall, this study demonstrates a novel role of C/EBP δ in modulating oxidative stress via regulating the mitochondrial functions and maintaining the cellular levels of GSH (Fig. 9). Further studies are needed to investigate whether C/EBP δ may regulate genes involved in mitochondrial biogenesis and GSH metabolism.

Author contributions

SB, SAP, SKS, NAB, KJK and SBM: designed, performed experiments; SB, SAP, NAB and MHJ: analyzed results and wrote the paper.

Conflict of interest

None.

Acknowledgments

The authors acknowledge Dr. Randolph Mildred, Gail Wagoner, Erika Nicholson, Rebecca Mitchell, Jeannie Holland and Bridgette Angie for excellent animal care. We would like to thank Dr. Esta Sterneck (National Cancer Institute) for kindly providing us the *Cebpd* heterozygous mice from which we obtained the MEFs. We thank Dr. Sharda Singh (UAMS) for the kind gift of the HNE-polyclonal rabbit antibody and Dr. Michael J. Borrelli (UAMS) for the kind gift of the CHO cell line. The authors wish to acknowledge the technical assistance provided by Ms. Andrea Harris at the Flow cytometry Core Facility supported in part by the Center for Microbial Pathogenesis and Host Inflammatory Responses grant P20GM103625 through the NIH National Institute of General Medical Sciences (NIGMS) Centers of Biomedical Research Excellence (COBRE).

This work was supported by an Institutional Development Award (IDeA) from the NIGMS of the National Institutes of Health under grant number P20 GM109005 (SAP, NAB, MHJ); and awards from the Department of Defense W81XWH-15-1-0489 (SAP, MHJ); NIH 1R15ES022781 (NAB, KJK); Arkansas Science and Technology Authority 15-B-19 (NAB, KJK) and the Arkansas Bioscience Institute (SAP, SBM, NAB) is gratefully acknowledged. This manuscript was edited by the UAMS Office of Grants and Scientific Publications. We recommend you disclose that the manuscript was edited.

Appendix A. Supplementary material

Supplementary data associated with this article can be found in the online version at <http://dx.doi.org/10.1016/j.freeradbiomed.2016.08.022>.

References

- Hall E. J. a. G., A.J., *Radiobiology for the Radiologist*, 6th edn, 2006.
- C.N. Andreassen, J. Isner, Genetic variants and normal tissue toxicity after radiotherapy: a systematic review, *Radiat. Oncol.* 92 (2009) 299–309.
- P. Prasanna, H. Stone, R. Wong, J. Capala, V., B. C. Coleman, Normal tissue protection for improving radiotherapy: where are the Gaps? *Transl. Cancer Res.* 1 (2012) 35–48.
- M.E. Robbins, W. Zhao, Chronic oxidative stress and radiation-induced late normal tissue injury: a review, *Int. J. Radiat. Biol.* 80 (2004) 251–259.
- W. Zhao, D.I. Diz, M.E. Robbins, Oxidative damage pathways in relation to normal tissue injury, *Br. J. Radiol.* 80 (2007) S23–S31.
- S.W. Ryter, H.P. Kim, A. Hoetzel, J.W. Park, K. Nakahira, X. Wang, A.M. Choi, Mechanisms of cell death in oxidative stress, *Antioxid. Redox Signal.* 9 (2007) 49–89.
- D.R. Spitz, M. Hauer-Jensen, Ionizing radiation-induced responses: where free radical chemistry meets redox biology and medicine, *Antioxid. Redox Signal.* 20 (2014) 1407–1409.
- P. Okunieff, S. Swarts, P. Keng, W. Sun, W. Wang, J. Kim, S. Yang, H. Zhang, C. Liu, J.P. Williams, A.K. Huser, L. Zhang, Antioxidants reduce consequences of radiation exposure, *Adv. Exp. Med. Biol.* 614 (2008) 165–178.
- W.L. Santivasi, F. Xia, Ionizing radiation-induced DNA damage, response, and repair, *Antioxid. Redox Signal.* 21 (2014) 251–259.
- E.I. Azzam, J.P. Jay-Gerin, D. Pain, Ionizing radiation-induced metabolic oxidative stress and prolonged cell injury, *Cancer Lett.* 327 (2012) 48–60.
- R.L. Auten, J., M. Davis, Oxygen toxicity and reactive oxygen species: the devil is in the details, *Pediatr. Res.* 66 (2009) 121–127.
- J. Sun, Y. Chen, M. Li, Z. Ge, Role of antioxidant enzymes on ionizing radiation resistance, *Free Radic. Biol. Med.* 24 (1998) 586–593.
- G. Leonarduzzi, B. Sottero, G. Poli, Targeting tissue oxidative damage by means of cell signaling modulators: the antioxidant concept revisited, *Pharmacol. Ther.* 128 (2010) 336–374.
- D. Spitz, E. Azzam, J. Jian Li, D. Gius, Metabolic oxidation/reduction reactions and cellular responses to ionizing radiation: a unifying concept in stress response biology, *Cancer and Metastasis Reviews*, Kluwer Academic Publishers, Dordrecht, The Netherlands, 2004.
- D.R. Green, J.C. Reed, Mitochondria and apoptosis, *Science* 281 (1998) 1309–1312.
- J.F. Turrens, Mitochondrial formation of reactive oxygen species, *J. Physiol.* 552 (2003) 335–344.
- H.U. Simon, A. Haj-Yehia, F. Levi-Schaffer, Role of reactive oxygen species (ROS) in apoptosis induction, *Apoptosis* 5 (2000) 415–418.
- S. Kobashigawa, G. Kashino, K. Suzuki, S. Yamashita, H. Mori, Ionizing radiation-induced cell death is partly caused by increase of mitochondrial reactive oxygen species in normal human fibroblast cells, *Radiat. Res.* 183 (2015) 455–464.
- C.H. Wang, S.B. Wu, Y.T. Wu, Y.H. Wei, Oxidative stress response elicited by mitochondrial dysfunction: implication in the pathophysiology of aging, *Exp. Biol. Med.* 238 (2013) 450–460.
- J.J. Hwang, G.L. Lin, S.C. Sheu, F.J. Lin, Effect of ionizing radiation on liver mitochondrial respiratory functions in mice, *Chin. Med. J.* 112 (1999) 340–344.
- D. Dayal, S.M. Martin, K.M. Owens, N. Aykin-Burns, Y. Zhu, A. Boominathan, D. Pain, C.L. Limoli, P.C. Goswami, F.E. Domann, D.R. Spitz, Mitochondrial complex II dysfunction can contribute significantly to genomic instability after exposure to ionizing radiation, *Radiat. Res.* 172 (2009) 737–745.
- R. Kulkarni, B. Marples, M. Balasubramaniam, R.A. Thomas, J.D. Tucker, Mitochondrial gene expression changes in normal and mitochondrial mutant cells after exposure to ionizing radiation, *Radiat. Res.* 173 (2010) 635–644.
- Y.T. Yeung, K.L. McDonald, T. Grewal, L. Munoz, Interleukins in glioblastoma pathophysiology: implications for therapy, *Br. J. Pharmacol.* 168 (2013) 591–606 [Review].
- D.A. Dickinson, H.J. Forman, Glutathione in defense and signaling: lessons from a small thiol, *Ann. N. Y. Acad. Sci.* 973 (2002) 488–504.
- D.A. Dickinson, H.J. Forman, Cellular glutathione and thiols metabolism, *Biochem. Pharm.* 64 (2002) 1019–1026.
- R. Franco, J.A. Cidlowski, Apoptosis and glutathione: beyond an antioxidant, *Cell Death Differ.* 16 (2009) 1303–1314.
- V.I. Lushchak, Glutathione homeostasis and functions: potential targets for medical interventions, *J. Amino Acids* 2012 (2012) 26.
- A. Chatterjee, Reduced glutathione: a radioprotector or a modulator of DNA-repair activity? *Nutrients* 5 (2013) 525–542.
- Y.C. Awasthi, P. Chaudhary, R. Vatsyayan, A. Sharma, S. Awasthi, R. Sharma, Physiological and pharmacological significance of glutathione-conjugate transport, *J. Toxicol. Environ. Health Part B Crit. Rev.* 12 (2009) 540–551.
- R.V. Sekhar, S.G. Patel, A.P. Guthikonda, M. Reid, A. Balasubramanyam, G. E. Taffet, F. Jahoor, Deficient synthesis of glutathione underlies oxidative stress in aging and can be corrected by dietary cysteine and glycine supplementation, *Am. J. Clin. Nutr.* 94 (2011) 847–853.
- P. Diaz-Vivancos, A. de Simone, G. Kiddle, C.H. Foyer, Glutathione linking cell proliferation to oxidative stress, *Free Radic. Biol. Med.* 89 (2015) 1154–1164.
- D.P. Ramji, P. Foka, CCAAT/enhancer-binding proteins: structure, function and regulation, *Biochem. J.* 365 (2002) 561–575.
- X. Yu, J. Si, Y. Zhang, J. DeWille, CCAAT/Enhancer Binding Protein-delta (C/EBP-delta) regulates cell growth, migration and differentiation, *Cancer Cell Int.* 10 (2010) 48.
- J.P. O'Rourke, G.C. Newbound, J.A. Hutt, J. Dewille, CCAAT/enhancer-binding protein delta regulates mammary epithelial cell G0 growth arrest and apoptosis, *J. Biol. Chem.* 274 (1999) 16582–16589.
- A.M. Choi, S. Sylvester, L. Otterbein, N.J. Holbrook, Molecular responses to hyperoxia in vivo: relationship to increased tolerance in aged rats, *Am. J. Respir. Cell Mol. Biol.* (1995).
- A.M. Huang, C. Montagna, S. Sharan, Y. Ni, T. Ried, E. Sterneck, Loss of CCAAT/enhancer binding protein delta promotes chromosomal instability, *Oncogene* 23 (2004) 1549–1557.
- T.R. Sarkar, S. Sharan, J. Wang, S.A. Pawar, C.A. Cantwell, P.F. Johnson, D. K. Morrison, J.M. Wang, E. Sterneck, Identification of a Src tyrosine kinase/SIAH2 E3 ubiquitin ligase pathway that regulates C/EBPdelta expression and contributes to transformation of breast tumor cells, *Mol. Cell Biol.* 32 (2012) 320–332.
- V. Barbaro, A. Testa, I.E. Di, F. Mavilio, G. Pellegrini, L.M. De, C/EBPdelta regulates cell cycle and self-renewal of human limbal stem cells, *J. Cell Biol.* 177 (2007) 1037–1049.
- T.C. Hour, Y.L. Lai, C.I. Kuan, C.K. Chou, J.M. Wang, H.Y. Tu, H.T. Hu, C.S. Lin, W. J. Wu, Y.S. Pu, E. Sterneck, A.M. Huang, Transcriptional up-regulation of SOD1 by CEBPD: a potential target for cisplatin resistant human urothelial carcinoma cells, *Biochem. Pharmacol.* 80 (2010) 325–334.
- S.A. Pawar, T.R. Sarkar, K. Balamurugan, S. Sharan, J. Wang, Y. Zhang, S. F. Dowdy, A.M. Huang, E. Sterneck, C/EBP delta targets cyclin D1 for proteasome-mediated degradation via induction of CDC27/APC3 expression, *Proc. Natl. Acad. Sci. USA* 107 (2010) 9210–9215.
- J. Wang, T.R. Sarkar, M. Zhou, S. Sharan, D.A. Ritt, T.D. Veenstra, D.K. Morrison, A.M. Huang, E. Sterneck, CCAAT/enhancer binding protein delta (C/EBPdelta, CEBPD)-mediated nuclear import of FANCD2 by IPO4 augments cellular response to DNA Damage, *Proc. Natl. Acad. Sci. USA* 107 (2010) 16131–16136.
- K. Balamurugan, E. Sterneck, The many faces of C/EBPdelta and their relevance for inflammation and cancer, *Int. J. Biol. Sci.* 9 (2013) 917–933.
- S.A. Pawar, L. Shao, J. Chang, W. Wang, R. Pathak, X. Zhu, J. Wang, H. Hendrickson, M. Boerma, E. Sterneck, D. Zhou, M. Hauer-Jensen, C/EBP delta deficiency sensitizes mice to ionizing radiation-induced hematopoietic and intestinal injury, *PLoS One* 9 (2014) e94967.
- K.M. Robinson, M.S. Janes, J.S. Beckman, The selective detection of mitochondrial superoxide by live cell imaging, *Nat. Protoc.* 3 (2008) 941–947.
- J. Zielonka, B. Kalyanaram, Hydroethidine- and MitoSOX-derived red fluorescence is not a reliable indicator of intracellular superoxide formation: another inconvenient truth, *Free Radic. Biol. Med.* 48 (2010) 983–1001.
- M.J. Borrelli, L.L. Thompson, W.C. Dewey, Evidence that the feeder effect in

- mammalian cells is mediated by a diffusible substance, *Int. J. Hyperth.* 5 (1989) 99–103.
- [47] A. Munshi, Marvette Hobbs, E. Meyn Raymond, Clonogenic cell survival assay, *Methods Mol. Med.* 110 (2005) 7.
- [48] R. Pathak, S.A. Pawar, Q. Fu, P.K. Gupta, M. Berbee, S. Garg, V. Sridharan, W. Wang, P.G. Biju, K.J. Krager, M. Boerma, S.P. Ghosh, A.K. Cheema, H. P. Hendrickson, N. Aykin-Burns, M. Hauer-Jensen, Characterization of transgenic Gfp knock-in mice: implications for tetrahydrobiopterin in modulation of normal tissue radiation responses, *Antioxid. Redox Signal.* 20 (2014) 1436–1446.
- [49] M. Wu, A. Neilson, A.L. Swift, R. Moran, J. Tamagnine, D. Parslow, S. Armistead, K. Lemire, J. Orrell, J. Teich, S. Chomicz, D.A. Ferrick, Multiparameter metabolic analysis reveals a close link between attenuated mitochondrial bioenergetic function and enhanced glycolysis dependency in human tumor cells, *Am. J. Physiol. Cell Physiol.* 292 (2007) C125–C136.
- [50] S. Banerjee, S.B. Melnyk, K.J. Krager, N. Aykin-Burns, L.G. Letzig, L.P. James, J. A. Hinson, The neuronal nitric oxide synthase inhibitor NANT blocks acetaminophen toxicity and protein nitration in freshly isolated hepatocytes, *Free Radic. Biol. Med.* 89 (2015) 750–757.
- [51] V. Stocchi, L. Cucchiaroni, M. Magnani, L. Chiarantini, P. Palma, G. Crescentini, Simultaneous extraction and reverse-phase high-performance liquid chromatographic determination of adenine and pyridine nucleotides in human red blood cells, *Anal. Biochem.* 146 (1985) 118–124.
- [52] S. Melnyk, M. Pogribna, I. Pogribny, R.J. Hine, S.J. James, A new HPLC method for the simultaneous determination of oxidized and reduced plasma amino thiols using coulometric electrochemical detection, *J. Nutr. Biochem.* 10 (1999) 490–497.
- [53] N. Aykin-Burns, B.G. Slane, A.T. Liu, K.M. Owens, M.S. O'Malley, B.J. Smith, F. E. Domann, D.R. Spitz, Sensitivity to low-dose/low-LET ionizing radiation in mammalian cells harboring mutations in succinate dehydrogenase subunit C is governed by mitochondria-derived reactive oxygen species, *Radiat. Res.* 175 (2011) 150–158.
- [54] H. Zhong, H. Yin, Role of lipid peroxidation derived 4-hydroxynonenal (4-HNE) in cancer: focusing on mitochondria, *Redox Biol.* 4 (2015) 193–199.
- [55] Y. Peter, G. Rotman, J. Lotem, A. Elson, Y. Shiloh, Y. Groner, Elevated Cu/Zn-SOD exacerbates radiation sensitivity and hematopoietic abnormalities of Atm-deficient mice, *EMBO J.* 20 (2001) 1538–1546.
- [56] G. Guo, Y. Yan-Sanders, B.D. Lyn-Cook, T. Wang, D. Tamae, J. Ogi, A. Khaletskiy, Z. Li, C. Weydert, J.A. Longmate, T.T. Huang, D.R. Spitz, L.W. Oberley, J.J. Li, Manganese superoxide dismutase-mediated gene expression in radiation-induced adaptive responses, *Mol. Cell. Biol.* 23 (2003) 2362–2378.
- [57] A. Hosoki, S.I. Yonekura, Q.L. Zhao, L. Wei, I. Takasaki, Y. Tabuchi, L.L. Wang, S. Hasuike, T. Nomurat, A. Tachibana, K. Hashiguchi, S. Yonei, T. Kondo, Q. M. Zhang-Akiyama, Mitochondria-targeted Superoxide Dismutase (SOD2) regulates radiation resistance and radiation stress response in HeLa cells, *J. Radiat. Res.* 53 (2012) 58–71.
- [58] J.A. Hutt, J.W. DeWille, Oncostatin M induces growth arrest of mammary epithelium via a CCAAT/enhancer-binding protein delta-dependent pathway, *Mol. Cancer Ther.* 1 (2002) 601–610.
- [59] F. Moore, I. Santin, T.C. Nogueira, E.N. Gurzov, L. Marselli, P. Marchetti, D. L. Eizirik, The transcription factor C/EBP delta has anti-apoptotic and anti-inflammatory roles in pancreatic beta cells, *PLoS One* 7 (2012) e31062.
- [60] J. Pflieger, M. He, M. Abdellatif, Mitochondrial complex II is a source of the reserve respiratory capacity that is regulated by metabolic sensors and promotes cell survival, *Cell Death Dis.* 6 (2015) e1835.
- [61] C. Gorrini, I.S. Harris, T.W. Mak, Modulation of oxidative stress as an anticancer strategy, *Nat. Rev. Drug Discov.* 12 (2013) 931–947.

UAMS
College of Pharmacy


C/EBP delta Protects Mice from Radiation-induced Gastrointestinal injury

Sudip Banerjee, PhD
Post-Doctoral Fellow

Division of Radiation Health
Department of Pharmaceutical Sciences,
College of Pharmacy
University of Arkansas for Medical Sciences
Little Rock, AR

Scenarios of Exposure to Ionizing Radiation


Exposure of Military personnel/Civilians



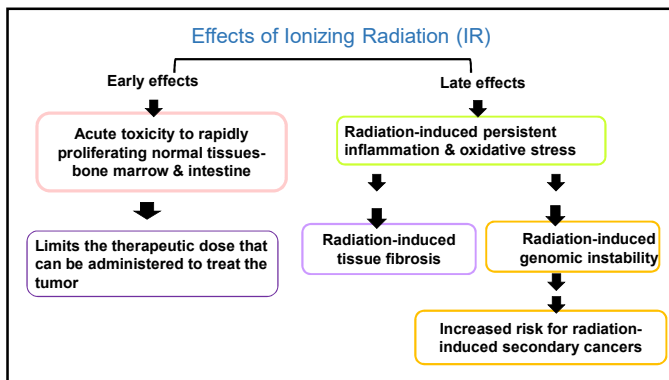
<https://www.iaea.org/newscenter/focus/fukushima>

- Nuclear terrorism
- Nuclear disasters- eg. Chernobyl, Fukushima

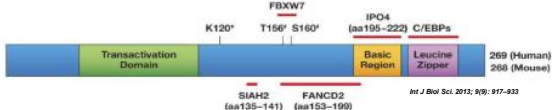
Exposure of Patients



- Radiation Therapy used as a treatment modality for 50% of all cancer types

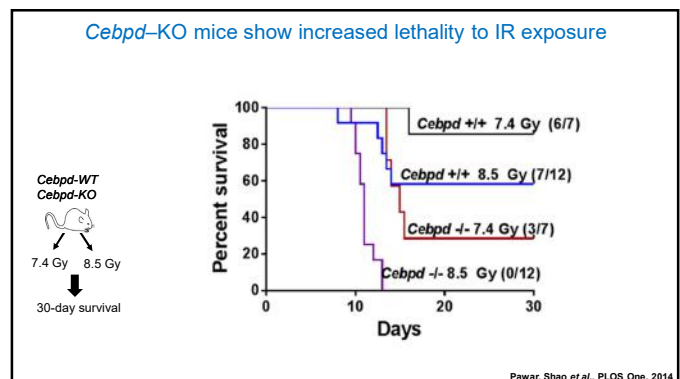
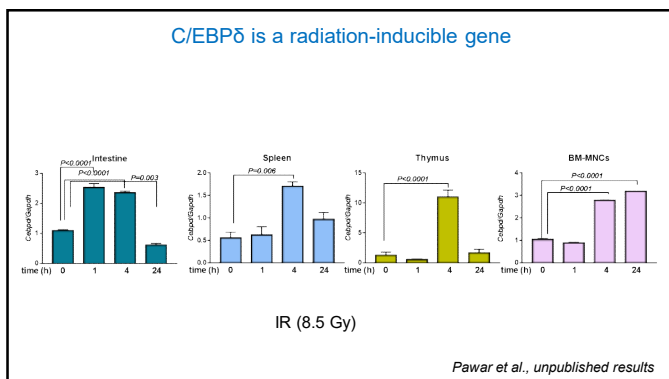


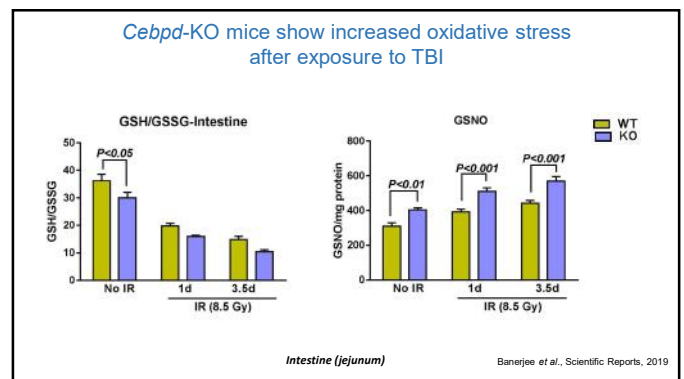
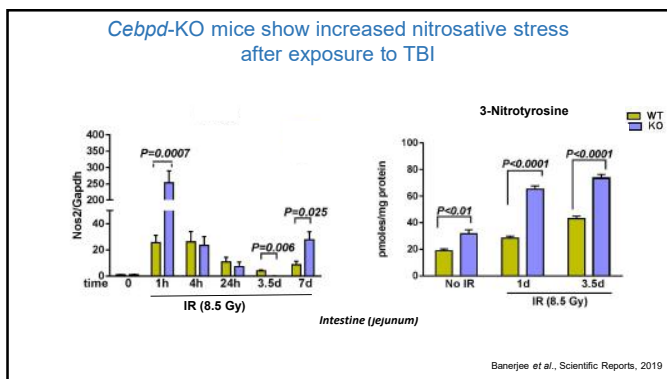
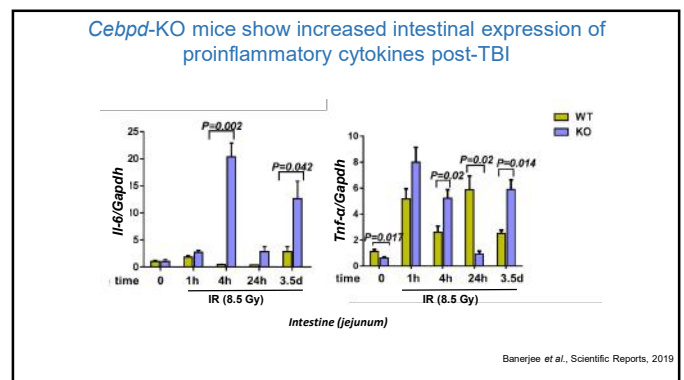
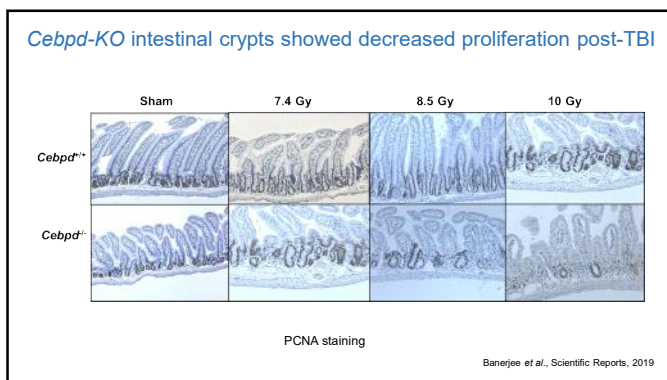
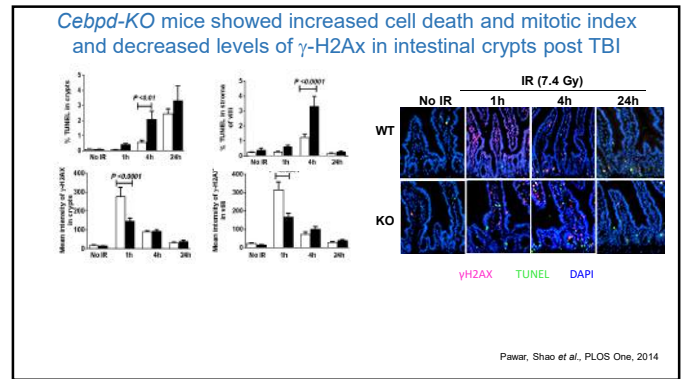
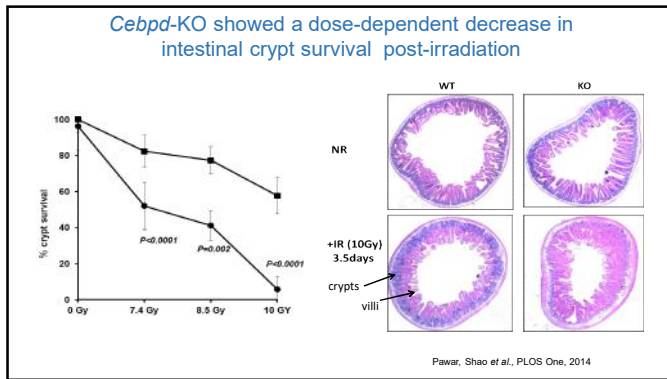
CCAAT enhancer binding protein delta (C/EBP δ)

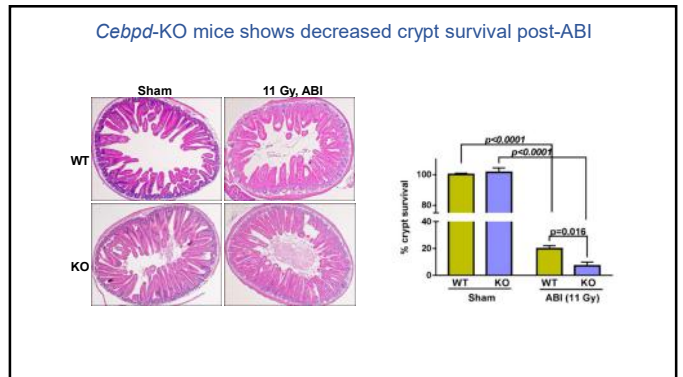
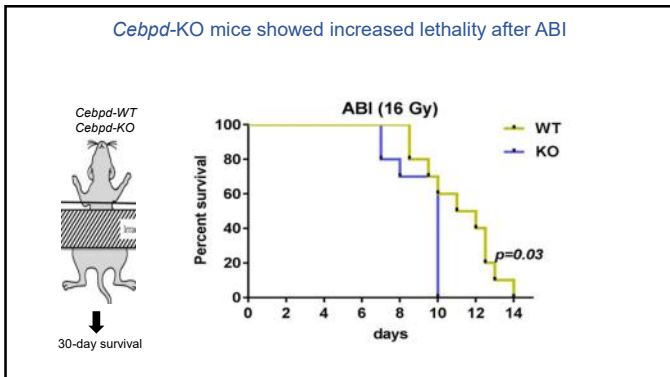
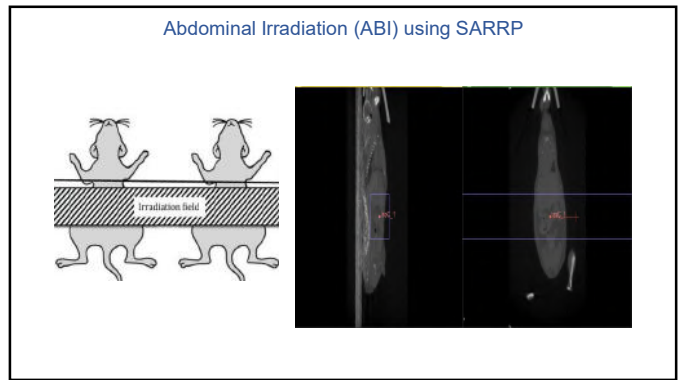
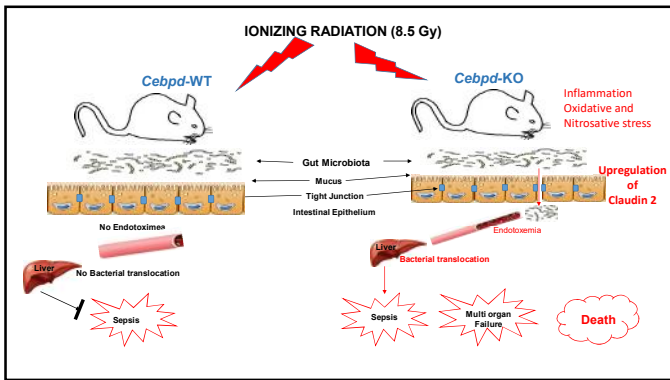
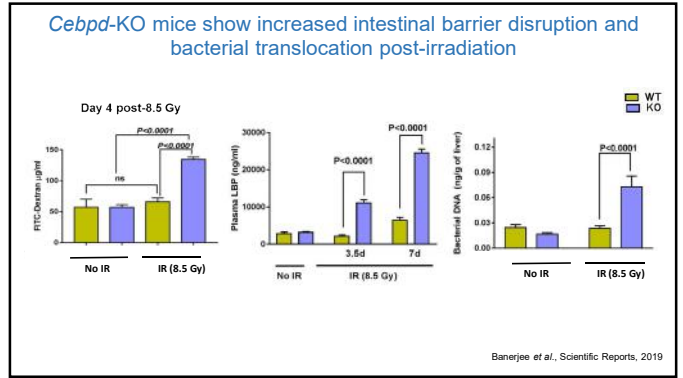
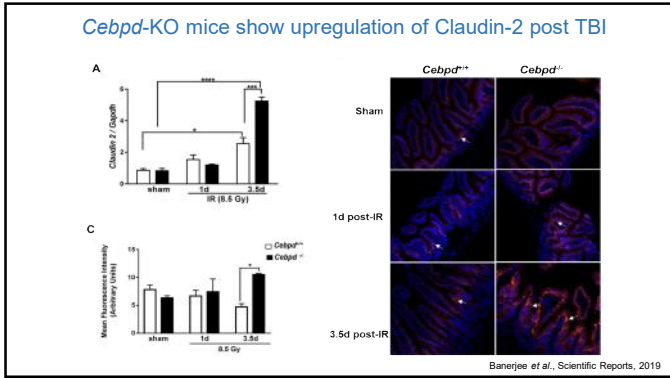


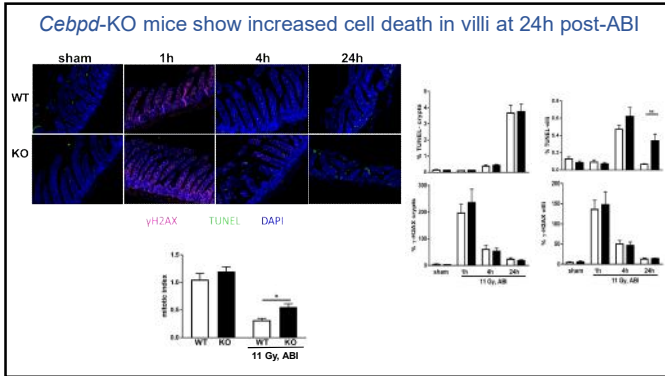
Various synonyms : CELF; CRP3; C/EBP-delta; NF-IL6-beta; CEBPD
chromosome: 8; Location: 8p11.2-p11.1

- Basic leucine zipper containing transcription factor
- Basal expression is very low
- Transiently inducible by cell-type specific stimuli – TNF- α , Interleukins-1 & 6, Interferon- γ and stress response such as UV
- Downstream target of TLR4/Myd88, STAT3





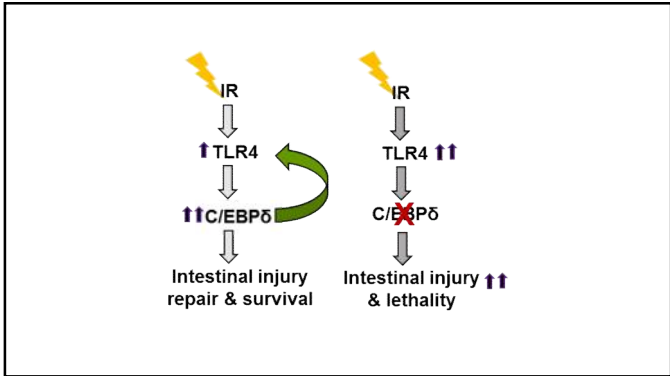
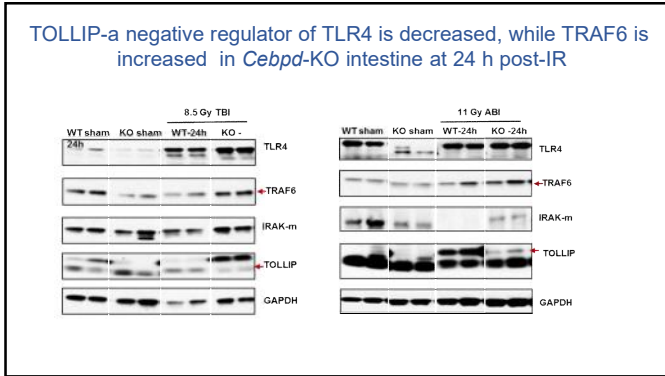
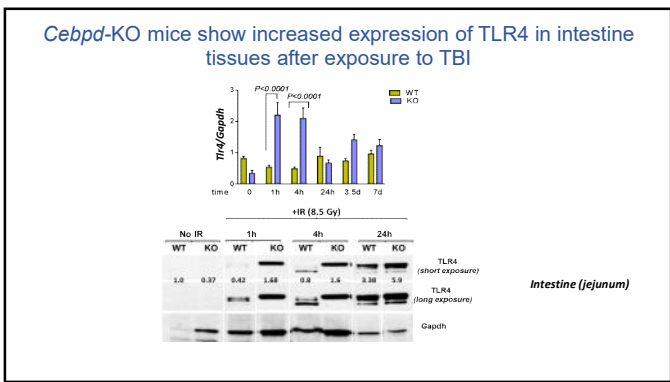


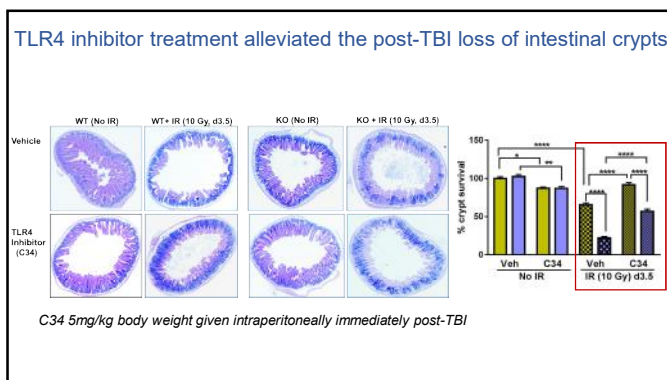
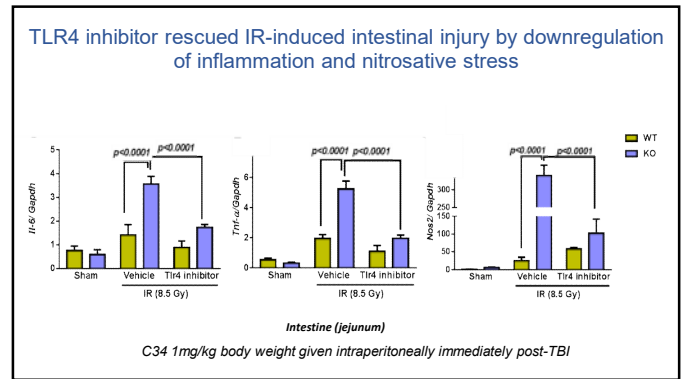
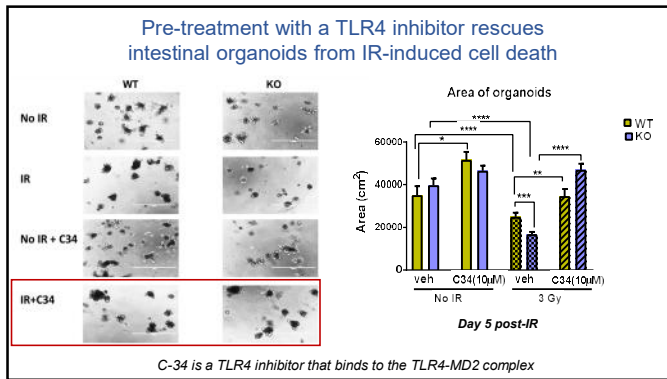


Role of Toll-like receptor signaling in IR-induced intestinal injury?

Toll-like receptors (TLRs) and Intestine

- TLRs play a critical role in host defense against infection by detecting conserved components of invading microbial pathogens.
- TLRs play a role in intestinal homeostasis.
- Intestinal epithelial barrier breakdown leads to exposure of the TLR ligands produced by commensal bacteria to TLR expressing cells (tissue resident macrophages and or intestinal epithelial cells) –resulting in inflammatory response, intestinal inflammation and injury.
- TLR2, TLR3, and TLR4 activation specifically upregulates the oxidative stress in intestinal epithelial cells (*Latorre et al., 2014*).





Summary

- *Cebpd*-KO mice show IR-induced upregulation of TLR4 expression which promotes increased intestinal injury.
- TOLLIP protein levels in are decreased resulting in upregulation of TLR4 signaling in irradiated *Cebpd*-KO mice.
- TLR4 inhibitors may have potential as an agent to alleviate IR-induced intestinal injury.

Acknowledgements

Division of Radiation Health, UAMS
 Snehalata Pawar, PhD
 Sumit Shah, MBBS, MPH
 Debajyoti Majumdar, M. Pharm

Funding

- NIH/NIGMS COBRE-P20GM109005
- Department of Defense W81XWH-15-1-0489

Martin Hauer-Jensen, MD, PhD
 Qiang Fu, MD, PhD

COBRE Irradiation Core, UAMS
 Marjan Boerma, PhD
 Kimberly Krager, PhD

Arkansas Children's Research Institute, Little Rock, AR
 Stepan Melnyk, PhD

C/EBPδ: A Novel Player in Normal Tissue Responses to Ionizing Radiation

Snehalata Pawar, PhD
 Assistant Professor of Pharmaceutical Sciences
 Division of Radiation Health
 UAMS College of Pharmacy
 Little Rock, AR



1. Introduction on IR & cellular response to IR
2. Significance for studying normal tissue responses to IR
3. Background on C/EBPδ
4. Research
 - Role of C/EBPδ in IR-induced hematopoietic injury
 - Role of C/EBPδ in IR-induced intestinal injury
 - Role of C/EBPδ in modulating IR-induced oxidative stress
5. Other ongoing projects/Future Directions

Scenarios of Exposure to Ionizing Radiation

Exposure of Patients



- Radiation Therapy used as a treatment modality for 50% of all cancer types

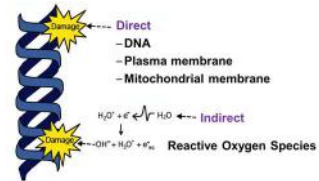
Exposure of Military personnel/Civilians



<https://www.iaea.org/newscenter/focus/fukushima>

- Nuclear terrorism
- Nuclear disasters- eg. Chernobyl, Fukushima

Cellular Damage from Ionizing Radiation



Cellular Responses to IR

- Activation of cell cycle checkpoints
- DNA damage response- γ -H2AX, DNA repair proteins
- Oxidative stress response- antioxidant enzymes
- Inflammatory responses- cytokines and chemokines

Effects of Ionizing Radiation (IR)

Early effects

Acute toxicity to rapidly proliferating normal tissues- bone marrow & intestine

Late effects

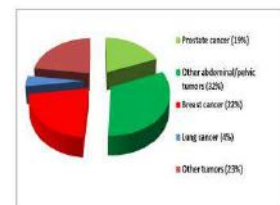
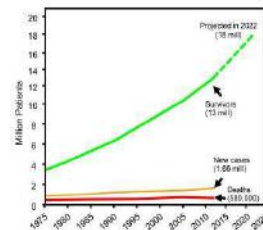
Radiation-induced persistent inflammation & oxidative stress

Radiation-induced tissue fibrosis

Radiation-induced genomic instability

Increased risk for radiation-induced secondary cancers

Overall 5-year cancer survival rates in the United States



Hauer-Jensen et al., 2014, Nat. Rev Gastroenterol. Hepatol, 11: 47-479

Significance

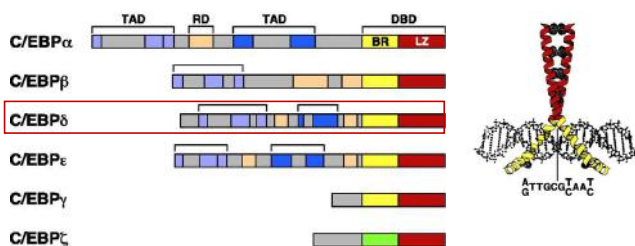
- Lack of selective radioprotectants for normal tissues
 - limits the therapeutic doses that can be delivered to treat cancers
- Lack of agents to protect from acute toxicity in the setting of total whole body radiation exposure

Significance

Understanding the normal tissue mechanisms in response to IR exposure is critical for the development of novel interventions:

- 1) To reduce the adverse effects of IR on normal tissues
- 2) To prevent the late complications of IR exposure
 - IR-induced carcinogenesis
 - Fibrosis

The CCAAT/Enhancer Binding Proteins



Johnson, P. F. *J Cell Sci* 2005;118:2545-2555

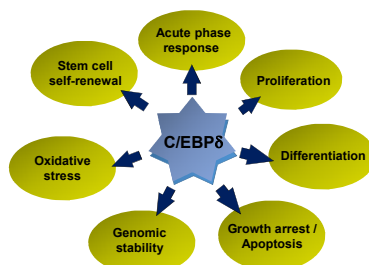
CCAAT enhancer binding protein delta (C/EBP δ)



Various synonyms : CELF; CRP3; C/EBP-delta; NF-IL6-beta; CEBPD
chromosome: 8; Location: 8p11.2-p11.1

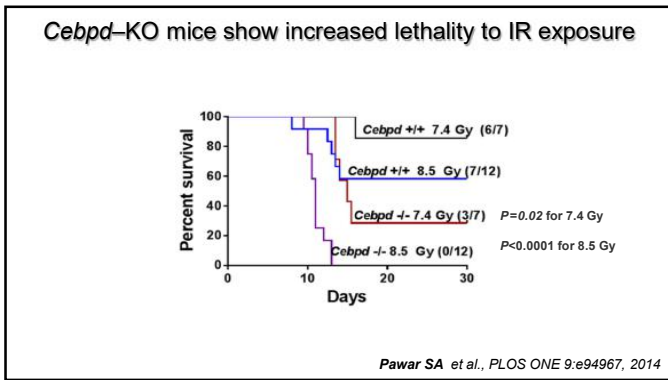
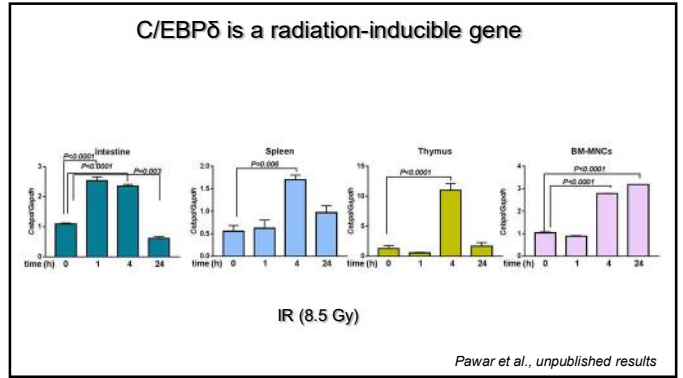
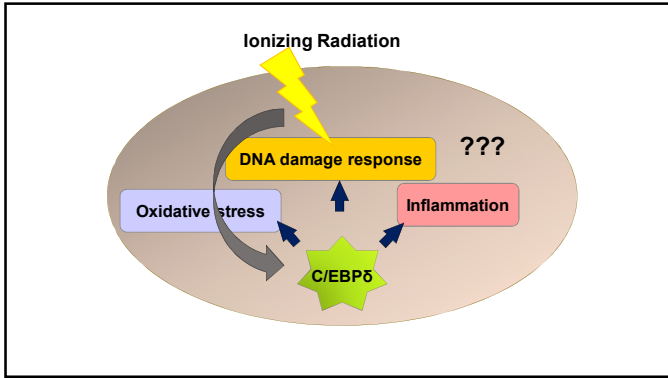
- Basic leucine zipper containing transcription factor
- Basal expression is very low
- Transiently inducible by cell-type specific stimuli –
TNF- α , Interleukins-1 & 6, Interferon- γ and stress response such as UV
- Downstream target of TLR4/Myd88, STAT3

Diverse Biological Functions of C/EBP δ

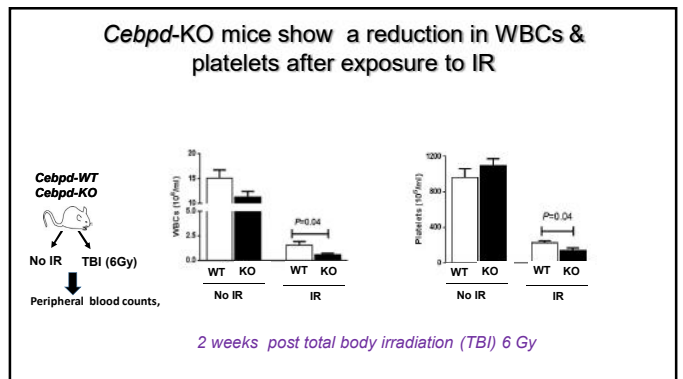
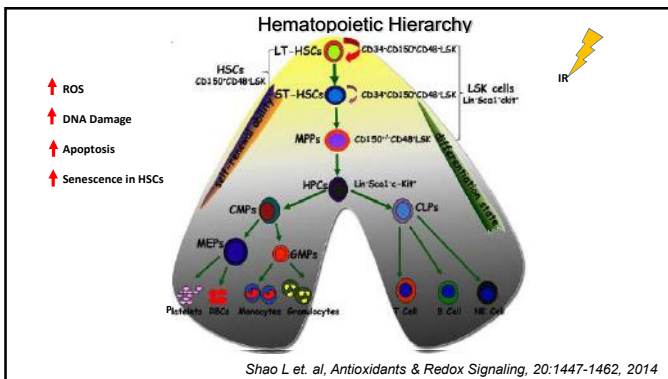


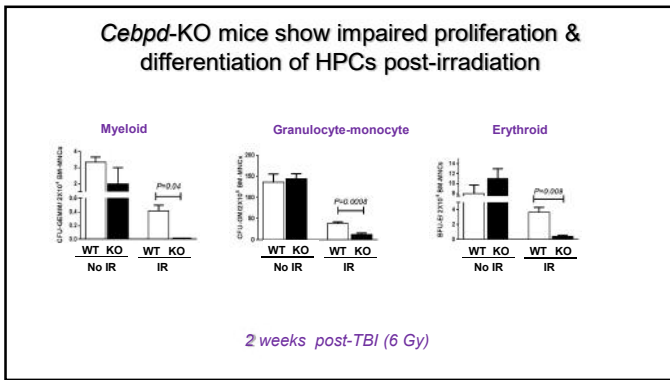
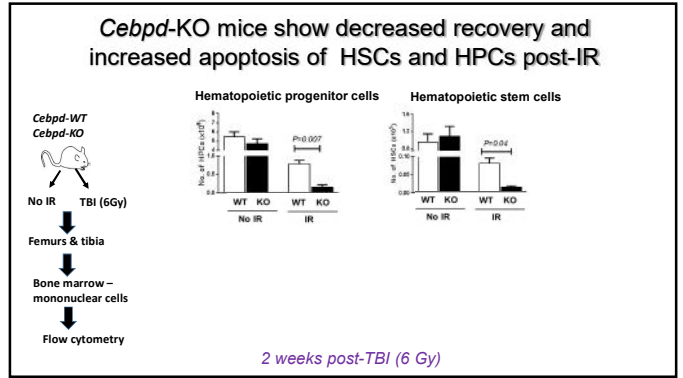
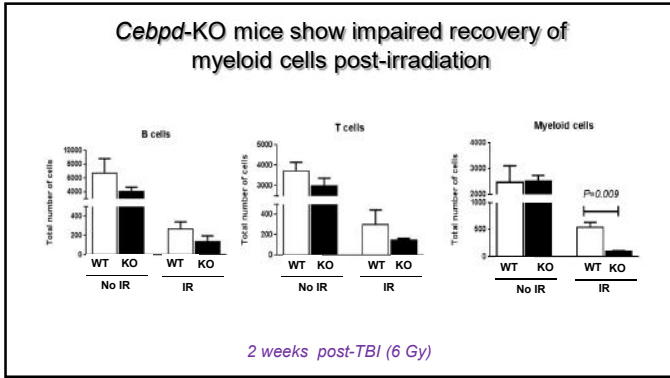
C/EBP δ –Role in DNA damage, Genomic Instability & Oxidative Stress

- C/EBP δ downregulates cyclin D1 and protects genomic stability in mouse embryonic fibroblasts (*Huang et al., Oncogene, 2004; Pawar et al., PNAS, 2010*).
- C/EBP δ interacts with FANCD2 to augment cellular response to DNA damage by Mitomycin C (*Wang et al., PNAS, 2010*).
- C/EBP δ regulates oxidative stress via the transcriptional upregulation of superoxide dismutase 1 (SOD1) (*Hour et al., Biochem. Pharmacol., 2010*)



Does C/EBPδ-deficiency promote IR-induced lethality due to hematopoietic injury ?

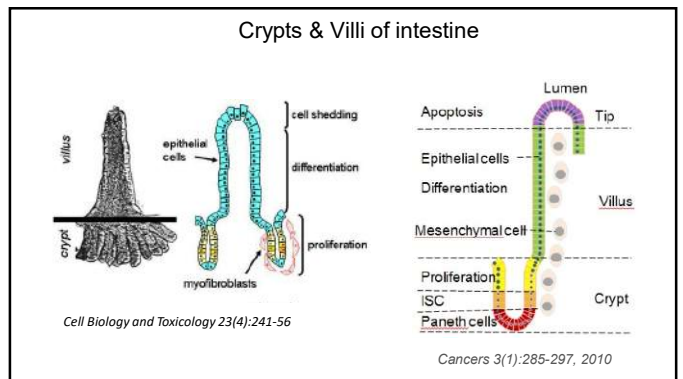


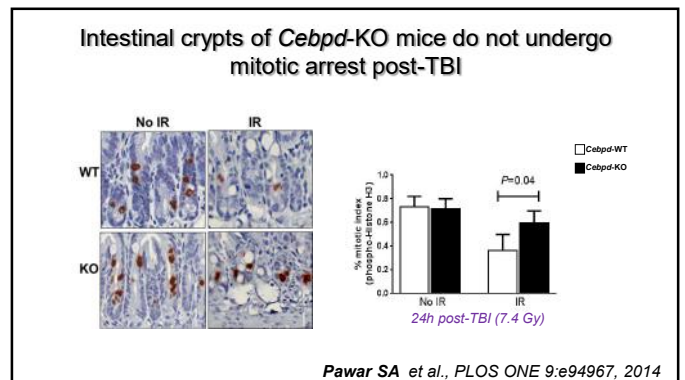
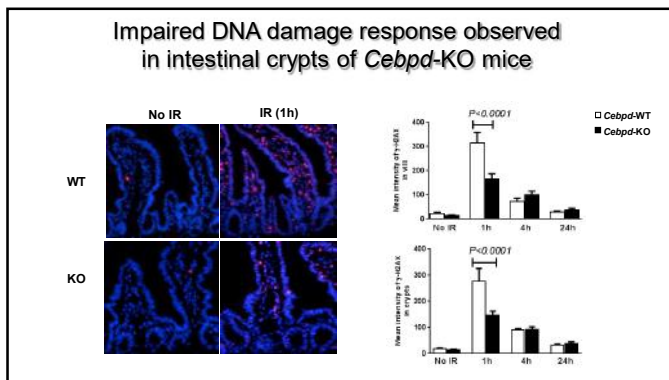
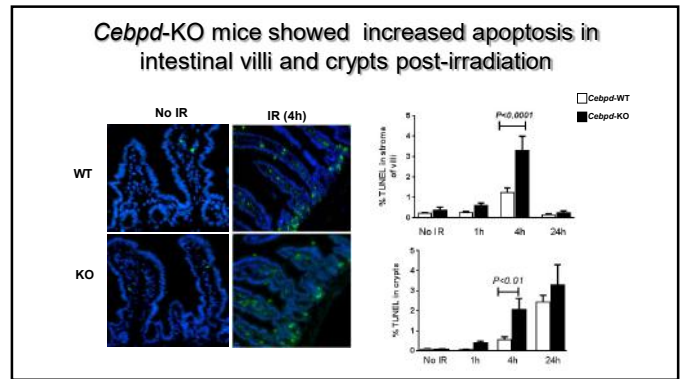
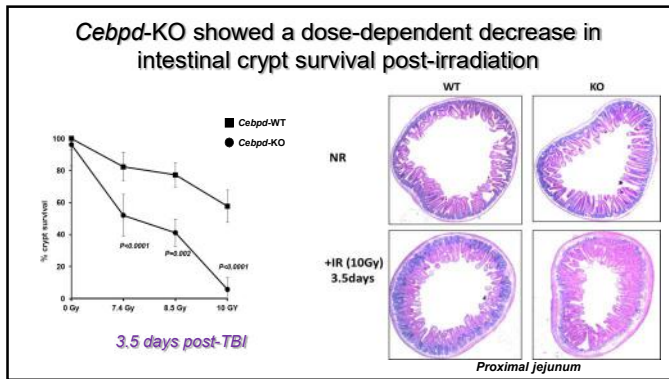


Summary

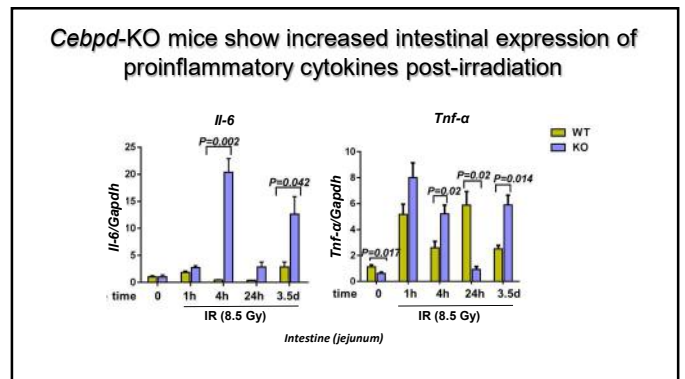
- Cebpd-KO mice display injury to the bone marrow after TBI
- decreased WBCs, platelets and myeloid cells
- increased IR-induced apoptosis of hematopoietic stem and progenitor cells
- reduced proliferation and differentiation of hematopoietic progenitors

Does C/EBPδ-deficiency promote IR-induced lethality due to intestinal injury ?

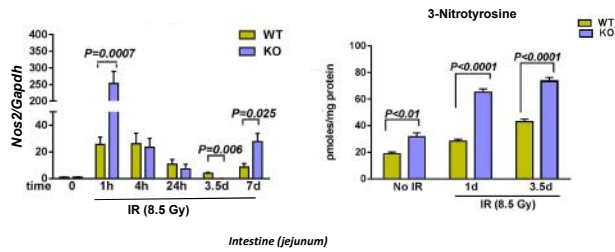




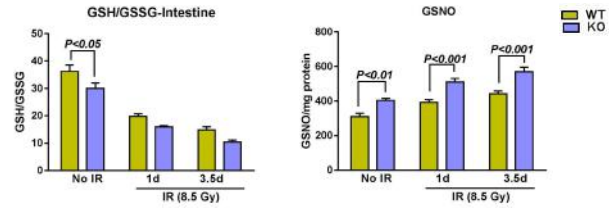
Role of impaired inflammatory signals in promoting radiation-induced intestinal injury of *Cebpd*-KO mice?



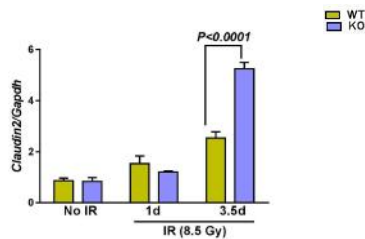
Cebpd-KO mice show increased nitrosative stress after exposure to IR



Cebpd-KO mice show increased oxidative stress after exposure to IR



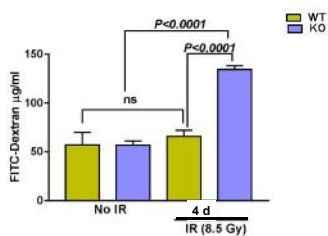
Cebpd-KO mice show increased expression of Claudin-2 post-irradiation



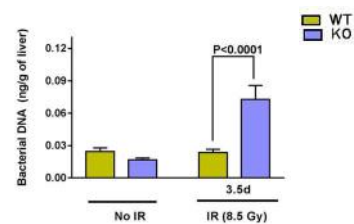
Claudin-2 is a mediator of a leaky gut barrier

- Claudin-2 is a protein involved in paracellular transport of water and cations such as Na⁺ ions (*J Cell Sci.* 123:1913-21, 2010; *Elife.* 4:e09906, 2015; *World J Gastroenterol.* 2016 Mar 21;22(11):3117-26)
- Claudin-2 is upregulated in intestinal epithelial cells by inflammatory cytokines such as IL-6 & TNF- α (*Cell Tissue Res.* 336, 67-77, 2009; *J. Biol. Chem.* 286, 31263-71, 2011; *PLoS One.* Mar 24;9(3):e85345, 2014)
- Claudin-2 is upregulated by oxidative stress (*Antioxid. Redox Signal.* 15, 1255-1270, 2011; *Molecular Medicine Reports,* 11: 4639-4644, 2015)
- Claudin-2 as a mediator of leaky gut barrier during intestinal inflammation. (*Lab Invest.* 88(10): 1110-1120, 2008; *Tissue Barriers.* 1(3): e24978, 2013; *Tissue Barriers.* 3: e977176, 2015).

Cebpd-KO mice show increased intestinal permeability post-TBI



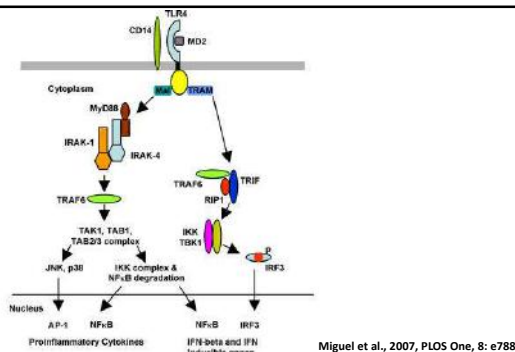
Cebpd-KO mice show increased bacterial translocation to the liver post-irradiation



Does dysregulated Toll-like receptor signaling promote increased IR-induced intestinal injury in *Cebpd*-KO mice?

Toll-like receptors (TLRs) and Intestine

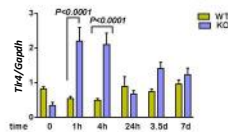
- TLRs play a critical role in host defense against infection by detecting conserved components of invading microbial pathogens.
- TLRs play a role in intestinal homeostasis.
- Intestinal epithelial barrier breakdown leads to exposure of the TLR ligands produced by commensal bacteria to TLR expressing cells (tissue resident macrophages and or intestinal epithelial cells) –resulting in inflammatory response, intestinal inflammation and injury.
- TLR2, TLR3, and TLR4 activation specifically upregulates the oxidative stress in intestinal epithelial cells (*Latorre et al., 2014*).



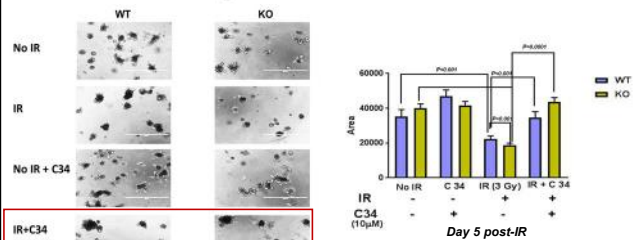
TLRs and Radiation Response

- TLR agonists lipopolysaccharide (LPS), flagellin, and the flagellin-derived CBL502 confer protection against IR-induced intestinal injury and the acute radiation syndrome in mouse models.
- *TLR4*-KO mice show increased radiosensitivity (*Cai et al., 2013*).
- The expression of TLR4 is upregulated by IR (*Schaue 2013*).

Cebpd-KO mice show increased expression of TLR4 in intestinal tissues after exposure to IR



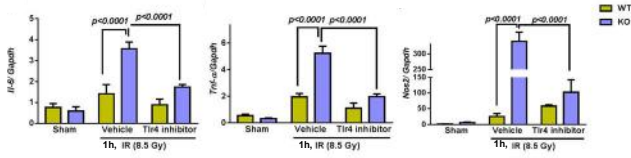
Pre-treatment with a TLR4 inhibitor rescues intestinal organoids from IR-induced cell death



C-34 is a TLR4 inhibitor that binds to the TLR4-MD2 complex

TLR4 inhibitor treatment downregulated IR-induced inflammation & nitrosative stress

C-34 is a TLR4 inhibitor that binds to the TLR4-MD2 complex



C34 1mg/kg body weight given intraperitoneally immediately post-TBI

Summary

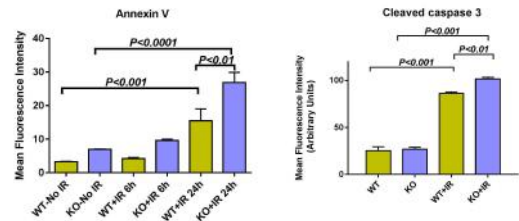
Cebpd-KO mice show increased IR-induced intestinal injury

- increased cell death in intestinal crypts and villi, decreased crypt colony survival
- impaired DNA damage response mechanism
- increased inflammatory response as well as nitrosative /oxidative stress
- Increased Claudin 2, intestinal barrier disruption and bacterial translocation
- Impaired TLR4 signaling promotes increased injury

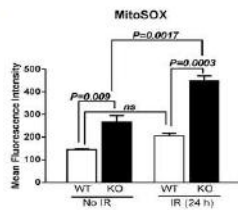
Cebpd-KO mice show increased IR-induced mortality due to injury to the bone marrow as well as intestine tissues.

Does C/EBPδ-deficiency lead to an impaired ability to detoxify IR-induced oxidative stress?

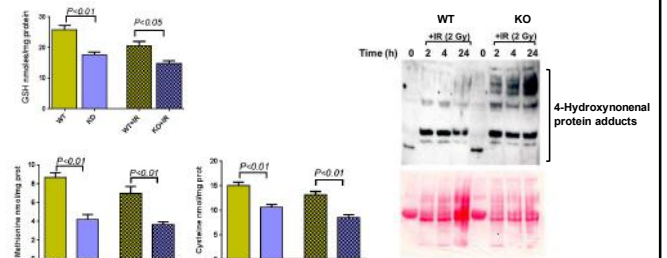
Cebpd-KO MEFs show increased apoptosis in response to IR



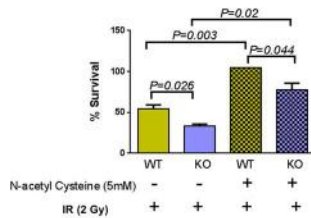
Cebpd-KO MEFs show increased superoxide levels



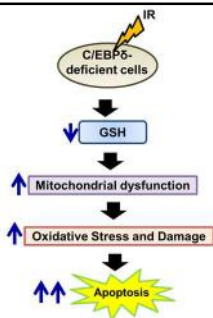
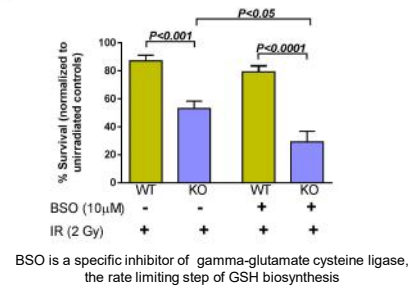
Cebpd-KO MEFs show reduced GSH levels indicative of increased oxidative damage after exposure to IR



Pre-treatment with N-acetyl Cysteine showed a rescue of post-radiation survival of *Cebpd*-KO MEFs



Pre-treatment with Buthionine sulfoximine (BSO) reduced the post-radiation survival of *Cebpd*-KO MEFs



Banerjee et al., *Free Radical Biology and Medicine*, 99:296-307, 2016

Summary

- C/EBP δ protects from IR-induced cell death.
- *Cebpd*-KO MEFs display increased oxidative stress under basal conditions.
- *Cebpd*-KO MEFs display IR-induced oxidative stress and mitochondrial dysfunction.
- Increased sensitivity of *Cebpd*-KO MEFs to IR is due to reduced levels of GSH and its precursor amino acid- cysteine as well as methionine.

Ongoing Projects

1. Investigate the role of C/EBP δ in IR-induced hematopoiesis.
2. Investigate the role of C/EBP δ in polarization of macrophages to a M2-phenotype in the context of radiation-induced ionizing radiation.
3. Investigate whether C/EBP δ -deficiency promotes gut injury in localized radiation models of abdominal radiation.
4. Investigate whether TLR4 inhibitors can be used to sensitize the tumors to IR, and prevent normal tissue side effects.
5. Identify the underlying basis for radiation-induced mitochondrial dysfunction in C/EBP δ -deficient MEFs.

Future Directions

1. Identify the underlying mechanism of TLR4 upregulation in C/EBP δ -deficient intestinal epithelial cells.
2. Identify the upstream regulators of C/EBP δ in response to IR as well as other genotoxic stressors such as chemotherapeutics.
3. Determine whether C/EBP δ -deficiency promotes radiation-induced carcinogenesis.

Acknowledgments

Pawar Lab

Sudip Banerjee, PhD
Sumit Shah, MBBS, MPH
Debajyoti Majumdar, M. Pharm

Martin Hauer-Jensen, MD, PhD
Qiang Fu, MD, PhD

Daohong Zhou, MD
Lijian Shao, MD, PhD
Jianhui Chang, PhD

Stepan Melnyk, PhD
Arkansas Children's Hospital Research Institute

Esta Sterneck, PhD
National Cancer Institute, Frederick, MD


Eric Pietras, PhD
University of Colorado Denver
Aurora, CO USA

Funding
NIH/NIGMS COBRE-P20GM109005
Department of Defense W81XWH-15-1-0489

TLR4 Inhibition Attenuates Radiation-induced Inflammation And Oxidative Stress To Protect Mice From Gastrointestinal Injury


Sudip Banerjee, PhD
Post-Doctoral Fellow

Division of Radiation Health
Department of Pharmaceutical Sciences




Scenarios of Exposure to Ionizing Radiation

Exposure of Patients

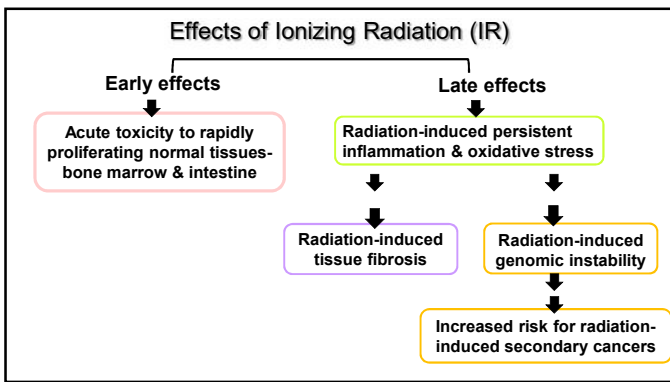


Exposure of Military personnel/Civilians



<https://www.iaea.org/newscenter/focus/fukushima>

- Radiation Therapy used as a treatment modality for 50% of all cancer types
- Nuclear terrorism
• Nuclear disasters- eg. Chernobyl, Fukushima



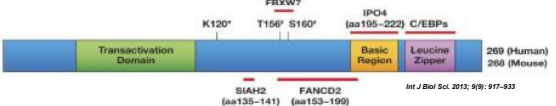
Significance

- Lack of selective radioprotectants for normal tissues - limits the therapeutic doses that can be delivered to treat cancers
- Lack of agents to protect from acute toxicity in the setting of total whole body radiation exposure

Understanding the normal tissue mechanisms in response to IR exposure is critical for the development of novel interventions:

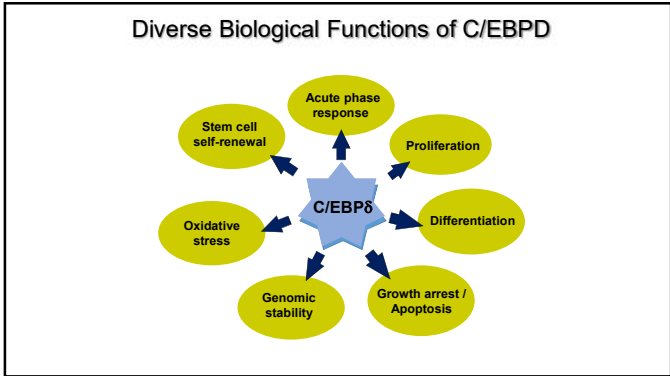
- To reduce the adverse effects of IR on normal tissues
- To prevent the late complications of IR exposure
 - IR-induced carcinogenesis
 - Fibrosis

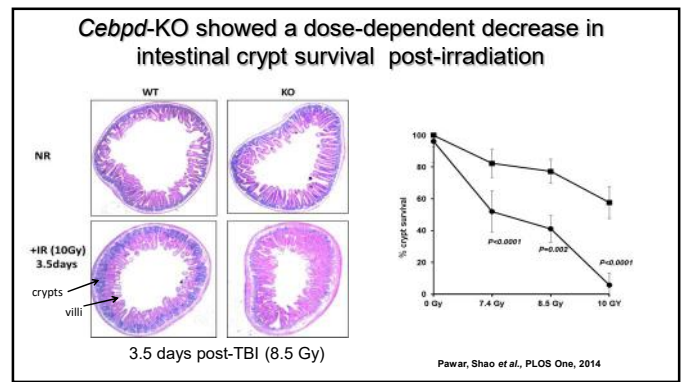
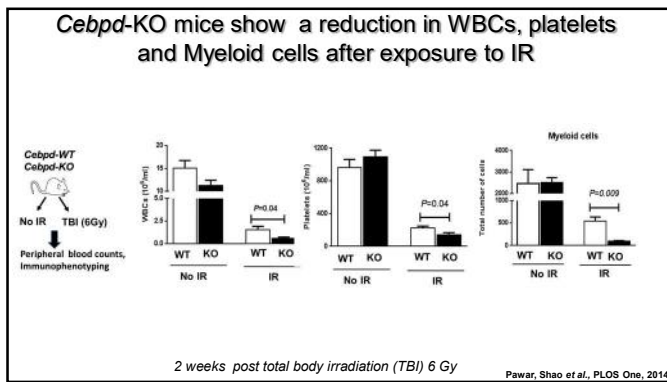
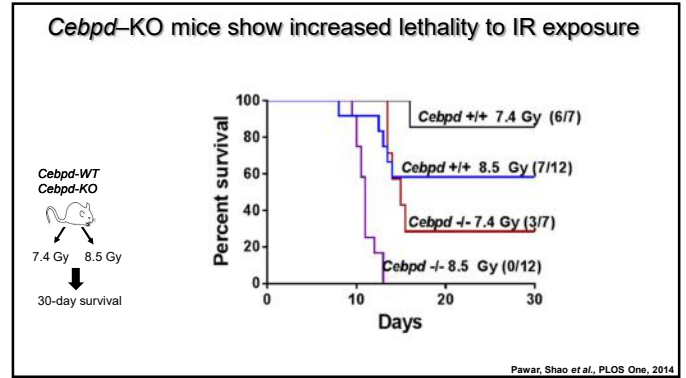
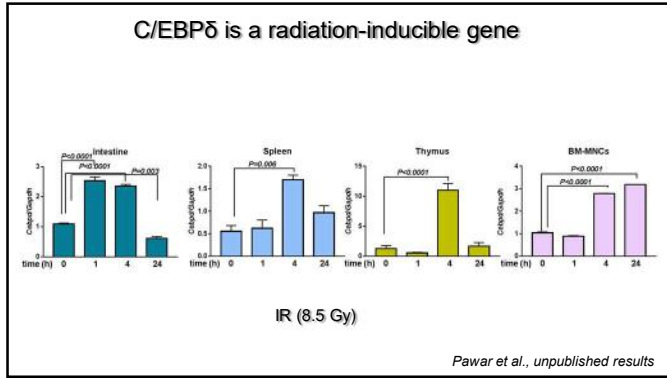
CCAAT enhancer binding protein delta (C/EBPδ)



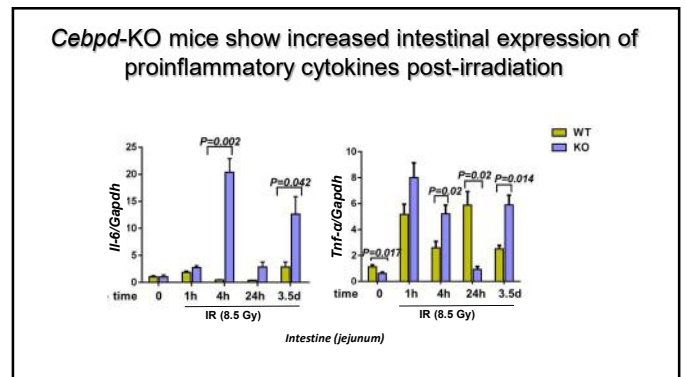
Various synonyms : CELF; CRP3; C/EBP-delta; NF-IL6-beta; CEBPD
chromosome: 8; Location: 8p11.2-p11.1

- Basic leucine zipper containing transcription factor
- Basal expression is very low
- Transiently inducible by cell-type specific stimuli – TNF-α, Interleukins-1 & 6, Interferon-γ and stress response such as UV
- Downstream target of TLR4/Myd88, STAT3

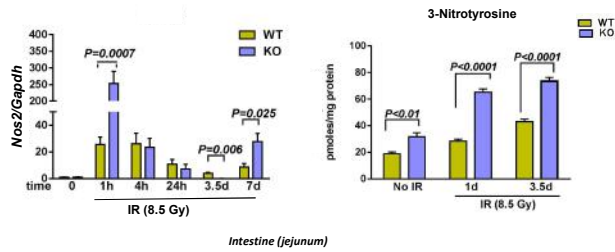




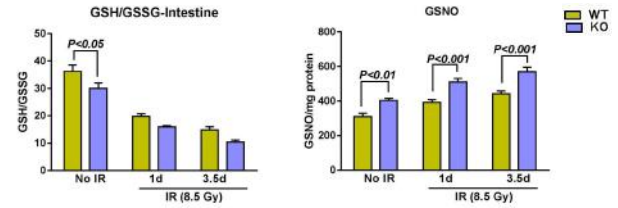
Role of impaired inflammatory signals in promoting radiation-induced intestinal injury of *Cebpd*-KO mice?



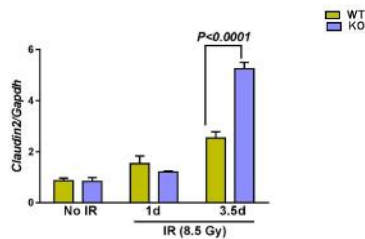
Cebpd-KO mice show increased nitrosative stress after exposure to IR



Cebpd-KO mice show increased oxidative stress after exposure to IR



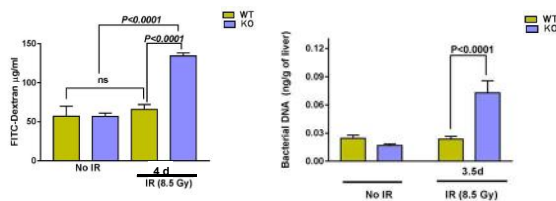
Cebpd-KO mice show increased expression of Claudin-2 post-irradiation



Claudin-2 is a mediator of a leaky gut barrier

- Claudin-2 is a protein involved in paracellular transport of water and cations such as Na⁺ ions (*J Cell Sci.* 123:1913-21, 2010; *Elife.* 4:e09906, 2015; *World J Gastroenterol.* 2016 Mar 21;22(11):3117-26)
- Claudin-2 is upregulated in intestinal epithelial cells by inflammatory cytokines such as IL-6 & TNF- α (*Cell Tissue Res.* 336, 67-77, 2009; *J. Biol. Chem.* 286, 31263-71, 2011; *PLoS One.* Mar 24;9(3):e85345, 2014)
- Claudin-2 is upregulated by oxidative stress (*Antioxid. Redox Signal.* 15, 1255-1270, 2011; *Molecular Medicine Reports*, 11: 4639-4644, 2015)
- Claudin-2 as a mediator of leaky gut barrier during intestinal inflammation. (*Lab Invest.* 88(10): 1110-1120, 2008; *Tissue Barriers.* 1(3): e24978, 2013; *Tissue Barriers.* 3: e977176, 2015).

Cebpd-KO mice show increased intestinal permeability post-TBI



Role of Toll-like receptor signaling in IR-induced intestinal injury?

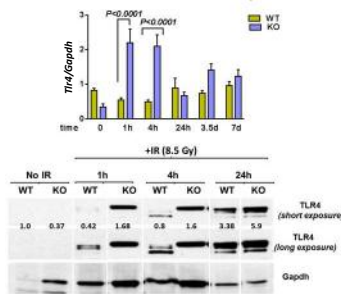
Toll-like receptors (TLRs) and Intestine

- TLRs play a critical role in host defense against infection by detecting conserved components of invading microbial pathogens.
- TLRs play a role in intestinal homeostasis.
- Intestinal epithelial barrier breakdown leads to exposure of the TLR ligands produced by commensal bacteria to TLR expressing cells (tissue resident macrophages and or intestinal epithelial cells) –resulting in inflammatory response, intestinal inflammation and injury.
- TLR2, TLR3, and TLR4 activation specifically upregulates the oxidative stress in intestinal epithelial cells (*Latorre et al., 2014*).

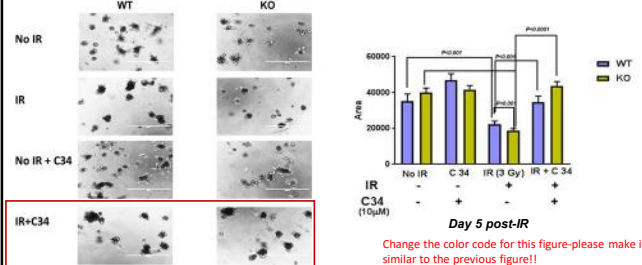
TLRs and Radiation Response

- TLR agonists lipopolysaccharide (LPS), flagellin, and the flagellin-derived CBL502 confer protection against IR-induced intestinal injury and the acute radiation syndrome in mouse models.
- *TLR4-KO mice show increased radiosensitivity* (Cai *et al.*, 2013).
- The expression of TLR4 is upregulated by IR (Schaue 2013).

Cebpd-KO mice show increased expression of TLR4 in intestine tissues after exposure to IR

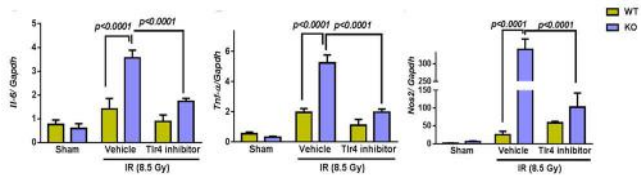


Pre-treatment with a TLR4 inhibitor rescues intestinal organoids from IR-induced cell death



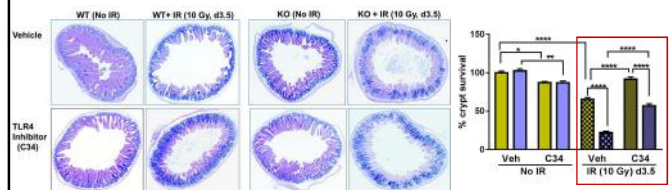
C-34 is a TLR4 inhibitor that binds to the TLR4-MD2 complex

Pre-treatment with a TLR4 inhibitor rescued IR-induced intestinal injury by downregulation of inflammation and nitrosative stress



C34 1mg/kg body weight given intraperitoneally immediately post-TBI

TLR4 inhibitor treatment alleviated the post-radiation loss of intestinal crypts



C34 5mg/kg body weight given intraperitoneally immediately post-TBI

Summary

- *Cebpd*-KO mice display increased IR-induced inflammation, oxidative and nitrosative stress.
- Irradiated *Cebpd*-KO mice show leaky gut due to increased claudin-2 leading to bacterial translocation, endotoxemia finally causing sepsis and death.
- *Cebpd*-KO mice show IR-induced upregulation of TLR4 expression which promotes increased intestinal injury.
- TLR4 inhibitors may have potential as an agent to alleviate IR-induced intestinal injury.

Future Directions

- Determine the effect of TLR4 inhibitor administered either before or after IR exposure (6h, 24h post-IR exposure) on intestinal crypt colony survival.
- Examine the effect of TLR4 inhibitor on 30-day survival.
- Determine whether TLR4 inhibitor stimulates post-IR proliferation of intestinal stem cells.

Acknowledgements

Division of Radiation Health

UAMS, Little Rock, AR

Snehalata Pawar, PhD

Martin Hauer-Jensen, MD, PhD

Qiang Fu, MD, PhD

Sumit Shah, MBBS, MPH

Debajyoti Majumdar, M. Pharm

National Cancer Institute,

Frederick, MD

Esta Sterneck, PhD

Arkansas Children's Research Institute,

Little Rock, AR

Stepan Melnyk, PhD

Arkansas Children's Hospital Research Institute, Little

Rock, AR

Funding

NIH/NIGMS COBRE-P20GM109005

Department of Defense W81XWH-15-1-0489

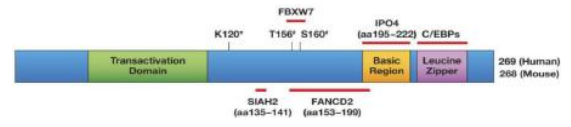

Center for Studies of Host Response to Cancer Therapy

Identification of C/EBPδ-targets Involved in Regulation of Radiation-induced Oxidative Stress Utilizing a Proteomics Approach

Snehalata Pawar, PhD
 Assistant Professor
 Division of Radiation Health
 University of Arkansas for Medical Sciences, Little Rock, AR

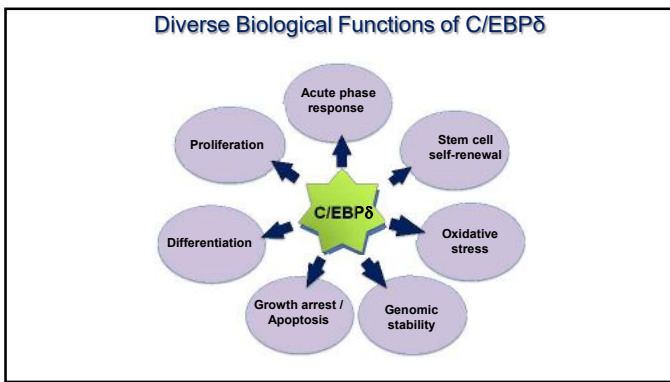
6th Biennial NISBRE Conference

CCAAT enhancer binding protein delta (C/EBPδ)

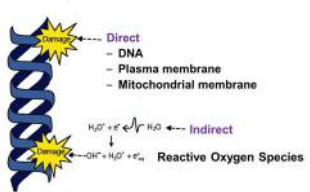


Kuppuswamy & Sternick, *Int J Biol Sci.* 2013; 9(9): 917-932

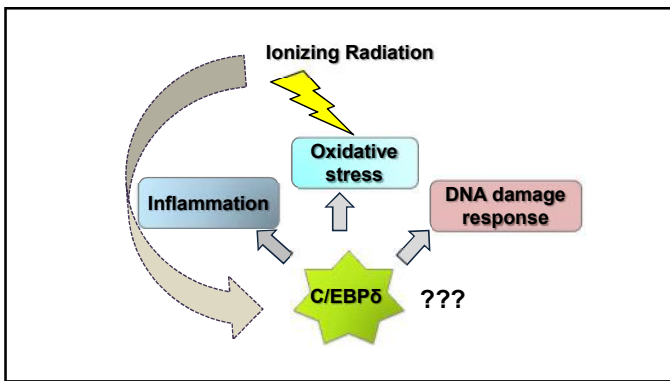
- Basic leucine zipper containing transcription factor
- Basal expression is very low & is transiently inducible by cell-type specific stimuli such as TNF-α, Interleukins 1 & 6, Interferon-γ and stress response such as UV, IR
- Downstream target of TLR4/Myd88, STAT3



Cellular Response to Ionizing Radiation (IR)

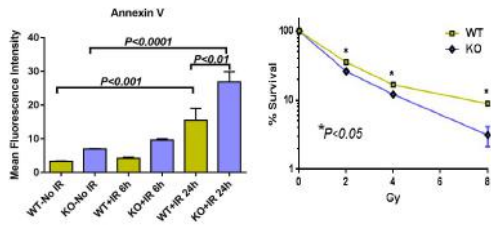


- Activation of cell cycle checkpoints
- DNA damage response- γ-H2AX, DNA repair proteins
- Oxidative stress response- antioxidant enzymes
- Inflammatory responses- cytokines and chemokines

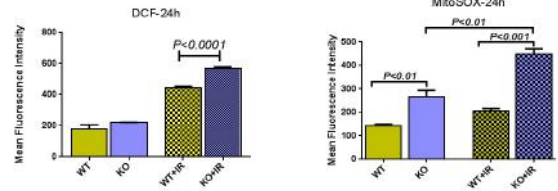


Does C/EBPδ-deficiency in cells lead to an impaired ability to detoxify IR-induced oxidative stress?

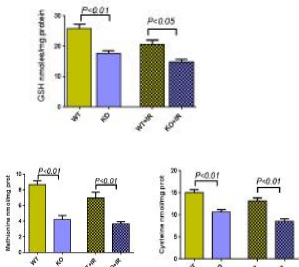
Cebpd-KO MEFs show increased apoptosis in response to IR



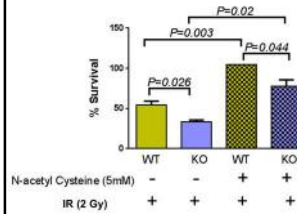
Cebpd-KO MEFs show increased levels of cellular hydroperoxides and superoxide



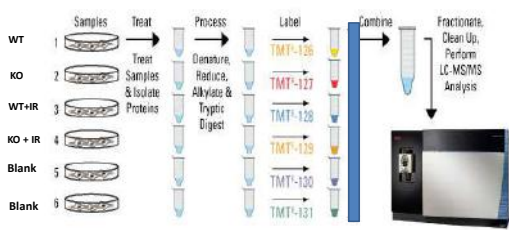
Cebpd-KO MEFs show reduced GSH levels indicative of increased oxidative damage after exposure to IR



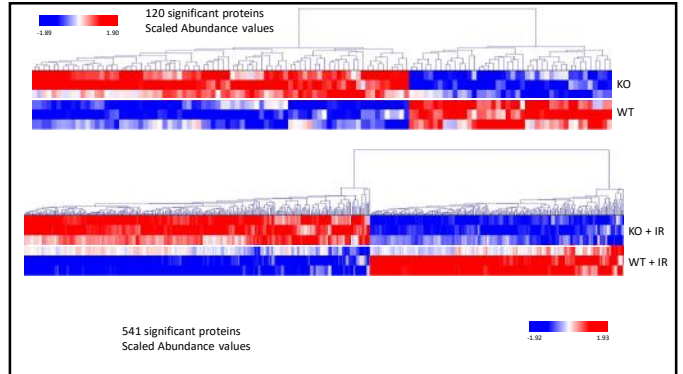
Pre-treatment with N-acetyl Cysteine showed a rescue of post-radiation survival of Cebpd-KO MEFs

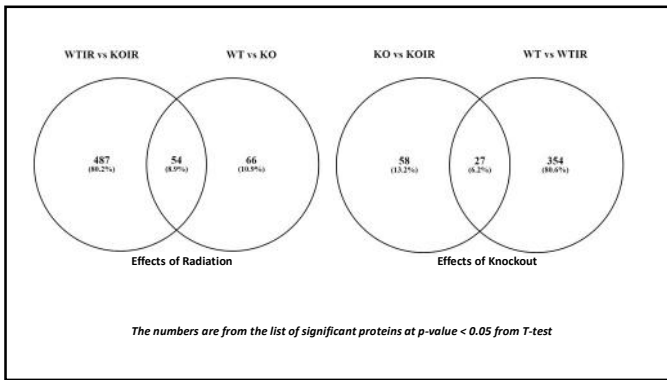
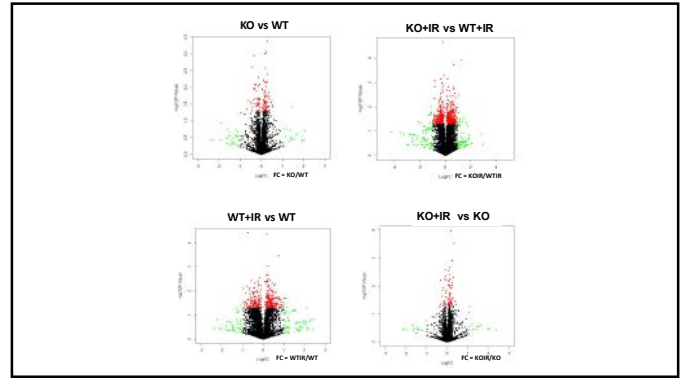
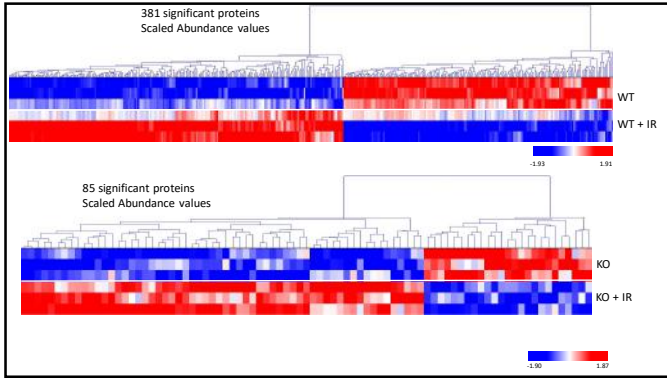


TMT labeled-Proteomics analysis of WT and KO MEFs



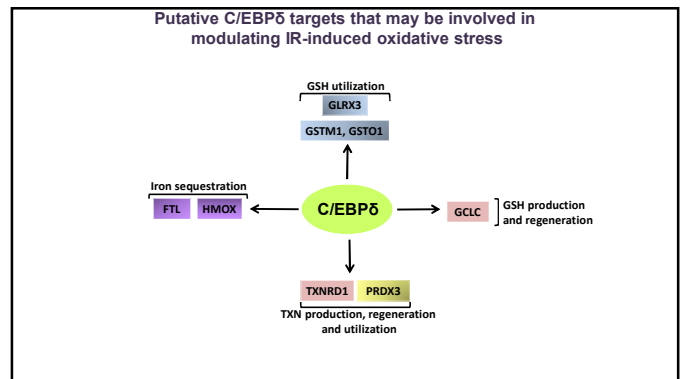
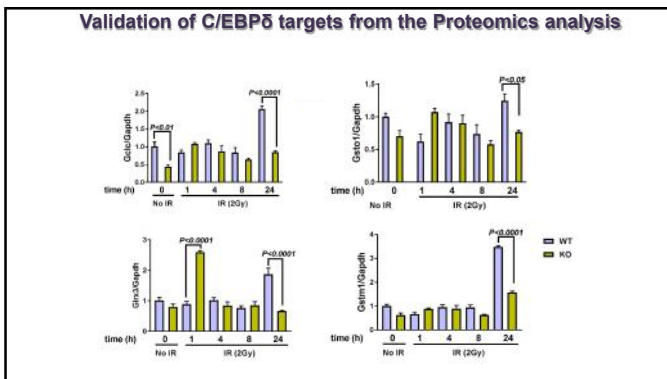
TMT quantification was performed using Thermo Fisher Proteome Discoverer software to determine significantly differential levels of protein (> 2-fold change) between the KO and WT MEFs and subjected to Ingenuity Pathway Analysis





Differentially regulated genes between *Cebpd*-WT and KO MEFs in the unirradiated and irradiated groups

| PROTEINS | No IR | IR (24h) |
|---|-------------|-------------|
| | KO/WT | KO/WT |
| Glutathione S-transferase O 1, <i>Gsto1</i> | 1.020617775 | 0.743485024 |
| Glutathione S-transferase Mu 1, <i>Gstm1</i> | 0.572 | 0.565 |
| Glutathione S-transferase Mu 2, <i>Gstm2</i> | 0.826 | 0.343 |
| Glutamate-cysteine ligase catalytic subunit, <i>Gclc</i> | 0.815867434 | 0.858574945 |
| Glutaredoxin-3, <i>Grx3</i> | 0.886 | 0.400 |
| Cystathionine gamma lyase | 0.601 | 0.060 |
| Thioredoxin, <i>Txn</i> | 0.944 | 0.438 |
| Thioredoxin reductase 1, cytoplasmic, <i>Txnrd1</i> | 1.697 | 0.616 |
| Thioredoxin-dependent peroxide reductase, mitochondrial, <i>Prdx3</i> | 1.202 | 0.761 |
| Heme oxygenase 1, <i>Hmox1</i> | 0.839859354 | 0.571681413 |
| Peroxioredoxin 5, <i>Prdx5</i> | 0.915807562 | 0.692582349 |



Acknowledgements

Division of Radiation Health, UAMS

Pawar Lab

Sudip Banerjee, PhD

Vaibhav Aher, PhD

Sumit Shah, MD

Debajyoti Majumdar, M. Pharm

Martin Hauer-Jensen, MD, PhD, FACS

Qiang Fu, MD, PhD

Junru Wang, MD, PhD

Sarita Garg, PhD

Rupak Pathak, PhD

Daohong Zhou, MD

Lijian Shao, MD, PhD

Jianhui Chang, PhD

Nukhet Arkin-Burns, PhD

Kimberly Krager, PhD

Dept. of Microbiology & Immunology, UAMS

Usha Ponnappan, PhD

Dept. of Biochemistry & Molecular Biology, UAMS

Alan Tackett, PhD

Stephanie Byrum, PhD

Lisa Orr, BS

Arkansas Children's Research Institute

Stepan Melnyk, PhD

National Cancer Institute, Frederick-MD

Está Sterneck, PhD

Funding

NIH/NIGMS COBRE-P20GM109005

Department of Defense W81XWH-15-1-0489

INTRODUCTION

Exposure to total body irradiation (TBI) results in injury to the rapidly proliferating tissues such as the hematopoietic and gastrointestinal (GI) tract in response. Acute injury to the GI tract is characterized by a massive loss of functional intestinal epithelia resulting in fatal pathological loss of fluid, electrolyte imbalances, intestinal bleeding and sepsis.

Loss in the progenitor cell compartment, microvascular endothelial cell death and mucosal inflammation are characteristic of radiation-induced GI damage. The production of reactive oxygen/nitrogen species, the induction of apoptosis and clonogenic cell death, mucosal breakdown, and the activation of the transcription of several pro-inflammatory cytokines, chemokines, and growth factors initiate the inflammatory response induced by radiation. Damage to the intestinal epithelial barrier leads to vascular leakage and translocation of the intestinal microflora in the blood leading to an inflammatory cascade resulting in sepsis-induced mortality.

The transcription factor CCAAT enhancer binding protein delta (*Cebpd*, C/EBP δ) is a basic leucine zipper protein that is implicated in the regulation of target genes that modulate oxidative stress, DNA damage response, genomic stability and inflammation. We have recently shown that C/EBP δ -deficiency in mice promotes intestinal and hematopoietic injury and is the underlying cause of TBI-induced lethality.

Toll-like receptors (TLRs) are pattern recognition receptors that recognize microbial components and activate intracellular signaling pathways to induce transcription of genes for inflammatory responses and are induced by ionizing radiation (IR).

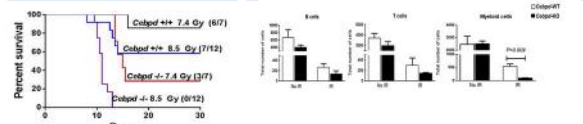
In the present study we investigated whether impaired TLR4 expression led to the increased inflammation and oxidative/nitrosative stress and was the underlying cause of IR-induced intestinal injury in *Cebpd*-knockout (KO) mice.

BACKGROUND

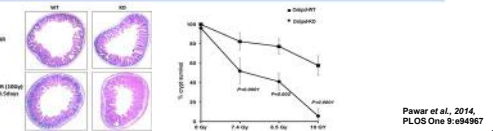
CCAAT Enhancer Binding Protein delta (*Cebpd*, C/EBP δ)

- Basic leucine zipper containing transcription factor.
- Basal expression is very low and is transiently inducible by cell-type specific stimuli such as cytokines –TNF- α , Interleukins 1 & 6, Interferon- γ and stress response such as UV.
- Implicated in diverse biological processes in a cell-type specific manner- acute phase response, proliferation, differentiation, growth arrest, apoptosis, stem cell self-renewal.

Cebpd-KO mice show increased lethality to TBI *Cebpd*-KO mice show impaired recovery of myeloid cells post-irradiation

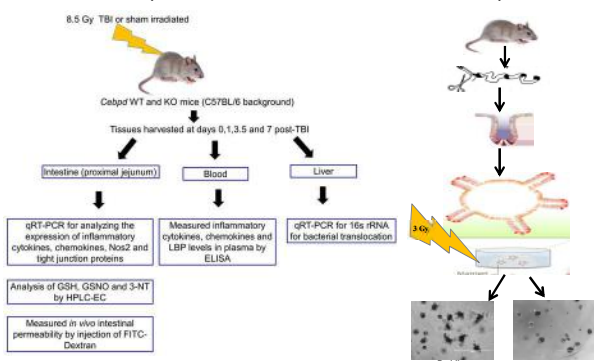


Cebpd-KO showed a dose-dependent decrease in intestinal crypt survival post-TBI



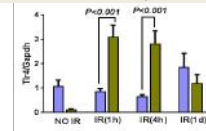
METHODS

In Vivo Experiment

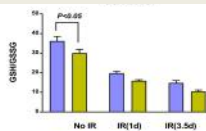


RESULTS

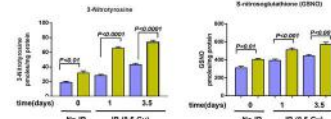
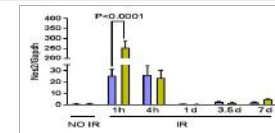
Cebpd-KO MEFs show increased expression of *Tlr4* in intestine post-TBI



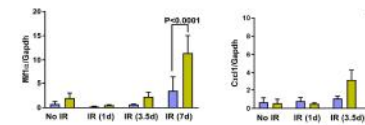
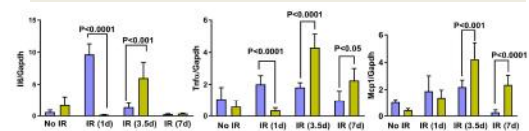
Cebpd-KO mice show reduced GSH/GSSG ratio indicative of oxidative stress



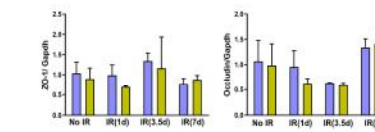
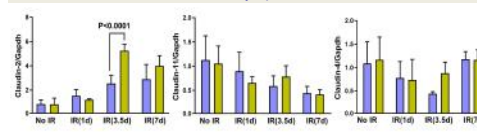
Cebpd-KO MEFs show increased nitrosative stress post-TBI



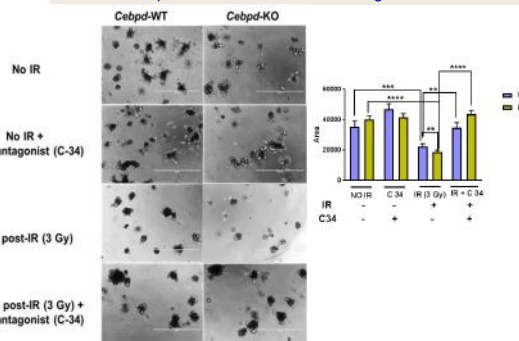
Cebpd-KO MEFs show increased expression of pro-inflammatory cytokines & chemokines in intestine post-TBI



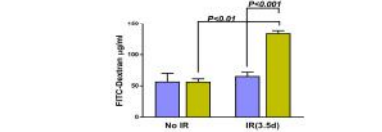
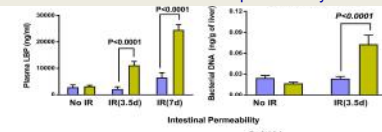
Cebpd-KO mice show increased expression of Claudin-2 at 3.5 days post-TBI



Pre-treatment with TLR4 inhibitor rescued intestinal organoids from *Cebpd*-KO mice from IR-induced growth inhibition



Cebpd-KO mice show increased levels of LBP & bacterial translocation to liver at day 3.5 post-TBI, which correlated with *in vivo* intestinal permeability



CONCLUSIONS & FUTURE DIRECTIONS

- KO mice displayed significantly elevated expression of *Tlr4* as well as *Nos2*, pro-inflammatory cytokines and chemokines in the intestine after exposure to TBI compared to *Cebpd*-wild type (WT) mice.
 - KO mice showed reduced oxidative stress and increased nitrosative stress compared to WT mice.
 - Irradiated KO mice show increased mRNA levels of *Claudin-2*, a marker associated with intestinal barrier disruption at day 3.5 post TBI & increased intestinal permeability which correlated with increased levels of plasma LBP and bacterial translocation to the liver.
 - Intestinal organoids from *Cebpd*-KO mice showed decrease in the total area post IR compared to the WT type organoids.
 - Inhibition of TLR4 was able to rescue the intestinal organoids from IR-induced cell death and promote survival.
- Our studies confirm that the increased IR-induced intestinal injury in *Cebpd*-KO occurs due to the upregulation of *Tlr4*, promotes the increased expression of the pro-inflammatory cytokines & chemokines, increased oxidative/nitrosative which leads to disruption of the intestinal barrier & bacterial translocation and was reversed by pre-treatment with a TLR4 inhibitor prior to irradiation.
- These results may have implications for utilizing TLR4 as a therapeutic target to protect the intestine from IR-induced normal tissue injury and in radiation-induced sepsis. Future studies will investigate the role of C/EBP δ in the regulation of target proteins that may inhibit the TLR4 pathway in response to IR.

INTRODUCTION

Myelosuppression as a result of chemotherapy or radiation therapy is a common side-effect of toxicity to the hematopoietic tissue that results in limiting the therapeutic dose that can be administered to treat the tumors. Additionally myelosuppression is a key hallmark of sepsis.

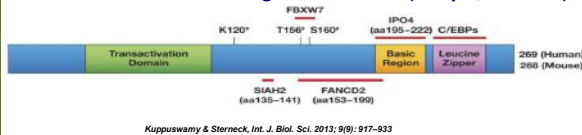
Although the key regulatory proteins of steady-state myelopoiesis have been elucidated, not much is known about the key regulatory factors involved in stress-induced myelopoiesis. Therefore, studies in this direction are essential to enable the development of therapeutic interventions to treat myelosuppression.

The transcription factor CCAAT/enhancer-binding protein delta (*Cebpd*, C/EBPδ) plays an important role in regulation of the inflammatory and stress responses as well as in innate and adaptive immune responses. Previous work by us revealed that *Cebpd*-knockout (KO) mice show increased ionizing radiation (IR)-induced injury to the hematopoietic and intestinal tissues. The hematopoietic injury in KO mice was characterized by increased myelotoxicity.

In the present study, we investigated whether C/EBPδ plays an essential role in the post-irradiation (IR) expansion of the various hematopoietic stem cells (HSCs) and hematopoietic progenitor cells (HPCs) as well as in the functional activity of differentiated myeloid cell types such as bone marrow-derived macrophages (BMDMs).

BACKGROUND

CCAAT Enhancer Binding Protein delta (*Cebpd*, C/EBPδ)

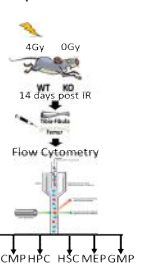


Kuppuswamy & Sternick, Int. J. Biol. Sci. 2013; 9(9): 917-933

- Basic leucine zipper containing transcription factor.
- Basal expression is very low and is transiently inducible by cell-type specific stimuli such as cytokines –TNF-α, Interleukins 1 & 6, Interferon-γ and stress response such as UV.
- Implicated in diverse biological processes in a cell-type specific manner- acute phase response, proliferation, differentiation, growth arrest, apoptosis, stem cell self-renewal.

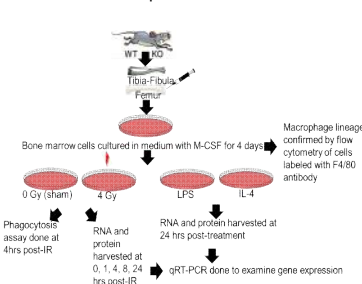
METHODS

In vivo experiments



CLP: Common Lymphoid Progenitors
CMP: Common Myeloid Progenitors
HPC: Hematopoietic Progenitor Cells
HSC: Hematopoietic Stem Cells
MEP: Megakaryocyte Erythrocyte Progenitors
GMP: Granulocyte Monocyte Progenitors

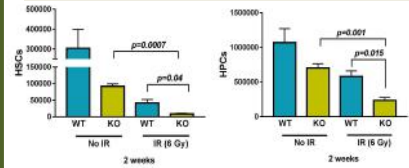
In vitro experiments



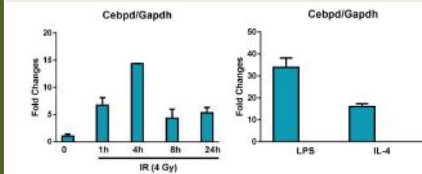
Phagocytosis assay done at 4hrs post-IR
RNA and protein harvested at 0, 1, 4, 8, 24 hrs post-IR
qRT-PCR done to examine gene expression

RESULTS

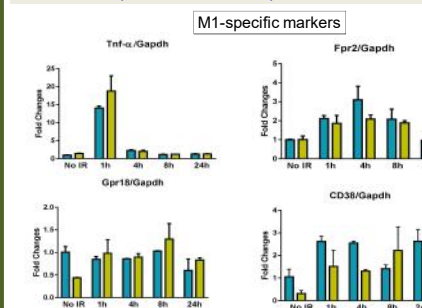
Cebpd-KO mice show reduced post-TBI recovery of hematopoietic stem and progenitor cells



Cebpd is induced by IR, LPS and IL-4 treatment in BMDMs



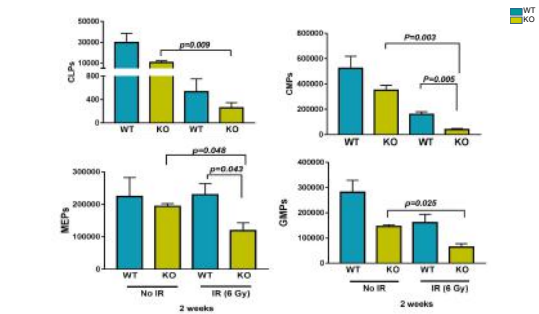
KO-BMDMs showed slightly decreased expression of CD38 at 4h post-irradiation compared to WT-BMDMs



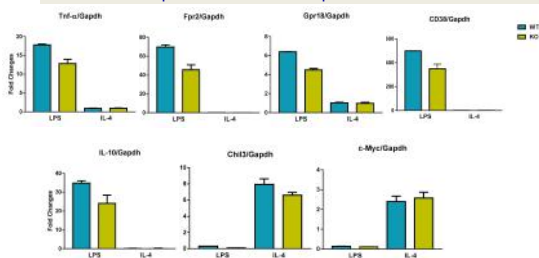
M1-specific markers

M2-specific markers

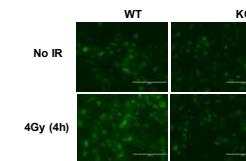
Cebpd-KO mice show reduced post-TBI recovery of CMPs & MEPs



Cebpd-KO mice show impaired expression of M1 macrophage specific markers in response to LPS



KO-BMDMs show reduced phagocytosis activity post-irradiation



CONCLUSIONS & FUTURE DIRECTIONS

- *Cebpd*-KO mice showed significantly reduced numbers of HSCs and HPCs as well as CMPs & MEPs compared to *Cebpd*-wild type (WT) mice at 2 weeks post-irradiation.
 - We found that the *Cebpd* gene is induced rapidly at early timepoints after IR, or after LPS or IL-4 exposure in WT-BMDMs.
 - *CD38*, a M1-macrophage specific marker was significantly upregulated in WT-BMDMs compared to KO-BMDMs in response to LPS and IR exposure.
 - *CD38* is a key player in phagocytosis, and its reduced expression correlated with the decreased phagocytic function in KO-BMDMs following irradiation.
- These results suggest that C/EBPδ is essential for stress-induced hematopoiesis and also plays a critical role in macrophage phagocytic function in response to stress such as IR.

- Future studies will investigate whether the IR-induced decrease in *Cebpd*-KO HSCs & HPCs occur due to intrinsic or extrinsic mechanism. We will also determine whether impaired DNA damage response or oxidative stress response promote the IR-induced apoptosis in HSCs & HPCs of KO mice.
- Chromatin immunoprecipitation assay will be carried out to ascertain whether *CD38* is a direct transcriptional target of C/EBPδ. Additionally we will determine whether overexpression of *CD38* can rescue the phagocytic function of KO BMDMs.
- Lastly we will use small molecule inhibitors to manipulate macrophages to the M1 polarization state which is essential for their ability to clear cells that have suffered IR-induced damage.

SYNOPSIS

Myeloid cells are the key components of the innate immune system, forming a bridge between innate and adaptive immunity by producing several cytokines, and phagocytosing and presenting antigens to the adaptive immune system. The common myeloid progenitor (CMP) cells give rise to the entire myeloid lineage (monocytes, macrophages, neutrophils, basophils, eosinophils).

Macrophages are derived from circulating monocytes at various sites of the body. There are two functionally distinct phenotypes of macrophages-M1 and M2. The M1 phenotype is associated with pro-inflammatory responses needed to counter pathogen invasion whereas the M2 phenotype is associated with immuno-suppressive activities that aid in tissue remodeling. The M2 macrophages are better at phagocytosing apoptotic cells, whereas M1 macrophages specialize in phagocytosing pathogens.

The transcription factor CCAAT enhancer binding protein delta [Cebpd (gene); C/EBPδ (protein)] regulates inflammatory and stress response as well as innate and adaptive immune response. C/EBPδ expression is induced in a MyD88/Irk-4-dependent manner in response to LPS in macrophages.

We have recently shown that C/EBPδ-deficiency sensitized mice to ionizing radiation (IR)-induced lethality primarily due to injury to the intestine and bone marrow tissues. The increased lethality of Cebpd-knockout (KO) mice occurred primarily due to injury to the hematopoietic stem cells (HSCs), hematopoietic progenitor cells (HPCs) and intestinal stem and epithelial cells. KO mice showed significant reduction in white blood cells, neutrophils, platelets and impaired recovery of myeloid cells (Pawar *et al.*, Plos One, 9: e94967, 2014).

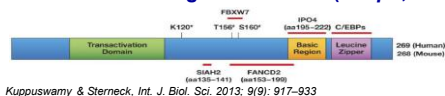
In the IR-induced gut injury model, studies have shown that the M1 macrophages play an important role in transmitting regenerative signals to the intestinal stem cells whereas the M2b macrophages promote bacterial translocation and subsequent sepsis (Kobayashi *et al.*, Journal of Immunology, 189: 296-303, 2012). Interestingly, a recent study showed that reduced expression of C/EBPδ promotes polarization of macrophages towards the M2 phenotype (Banerjee *et al.*, J. Immunol., 190: 6542-6549).

In view of the above findings, we hypothesized that C/EBPδ-deficiency may play a critical role in stress-induced myelopoiesis and may skew the macrophage function to a M2-like phenotype in the context of IR exposure. Utilizing *in vivo* as well as *in vitro* studies to investigate the role of C/EBPδ in myeloid lineage determination as well as function in IR stress, the key findings of our studies revealed that:

- KO mice showed an impaired recovery of CMPs at 2 weeks after exposure post-irradiation.
- Cebpd-KO bone marrow-derived macrophages (BMDMs) display increased inflammatory responses such as Il-6 and Tnf-α, but reduced expression of Nos2 compared to wild type (WT) BMDMs after exposure to IR.
- Cebpd-KO BMDMs display increased expression of Il-10 and reduced expression of Arg-1 compared to WT BMDMs after exposure to IR.
- Cebpd-KO BMDMs display a decrease in phagocytic function compared to WT BMDMs after exposure to IR.

BACKGROUND

CCAAT Enhancer Binding Protein delta (Cebpd, C/EBPδ)

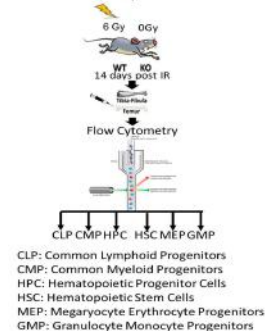


Kuppuswamy & Sterneck, *Int. J. Biol. Sci.* 2013; 9(9): 917-933

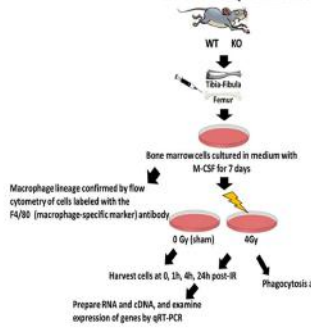
- Basic leucine zipper containing transcription factor.
- Basal expression is very low and is transiently inducible by cell-type specific stimuli such as cytokines –TNF-α, Interleukins 1 & 6, Interferon-γ and stress response such as UV.
- Implicated in diverse biological processes in a cell-type specific manner- acute phase response, proliferation, differentiation , growth arrest, apoptosis, stem cell self-renewal.

METHODS

In vivo experiments

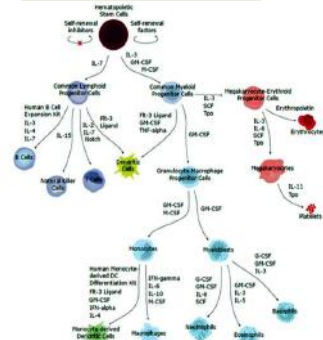


In vitro experiments



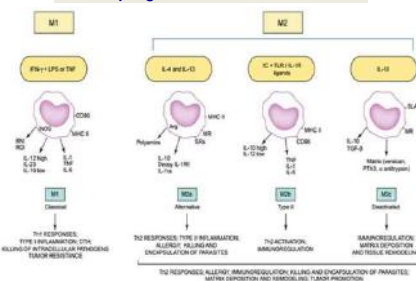
RESULTS

Development of myeloid lineage



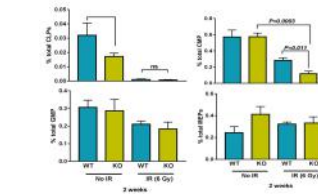
<https://www.mdssystems.com/pathways/hematopoietic-stem-cell-differentiation-pathways-lineage-specific-markers>

Macrophage Functional Classification



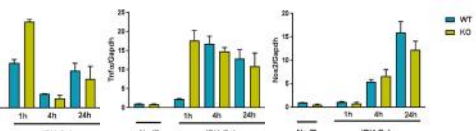
Mantovani *et al.* *Trends in Immunology*, 25(12): 677-686, 2004

Cebpd-deficiency results in impaired recovery of CMPs after exposure to IR

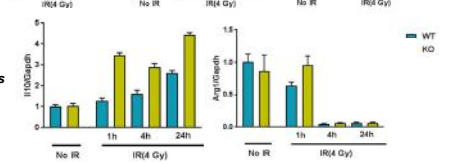


Cebpd-KO BMDMs display a M2b-like phenotype after exposure to IR

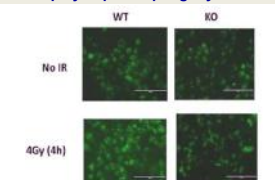
M1-specific genes



M2-specific genes



Cebpd-KO BMDMs display impaired phagocytic activity after exposure to IR



CONCLUSIONS

- Cebpd-KO mice showed an impaired recovery of CMPs after exposure to IR.
 - Cebpd-KO BMDMs display increased inflammatory cytokines such as Il-6 and Tnf-α, reduced Nos2 expression and increased expression of the anti-inflammatory Il-10 compared to WT BMDMs after exposure to IR, indicative of a M2b-like phenotype in the KO BMDMs.
 - Cebpd-KO BMDMs display impaired phagocytic activity compared to WT BMDMs after exposure to IR.
- Overall, these results point towards impaired myelopoiesis and myeloid function which undermines the immune system and makes the Cebpd-KO mice more susceptible to IR-induced injury to the bone marrow and intestine and the underlying lethality.

FUTURE DIRECTIONS

Future plans :

- Determine the expression of C/EBPδ in the various hematopoietic lineages in WT mice at various timepoints post radiation (0, 1, 2, 4, 8 & 24 h) by real-time PCR and by ImageStream flow cytometry.
- Determine whether C/EBPδ is essential for differentiation of granulocytes versus monocytes.
- Determine genes that are differentially regulated in the WT and KO CMPs by single-cell PCR based microarray and perform target validation by real-time PCR and or chromatin immunoprecipitation assays.
- Determine whether the impaired recovery of CMPs is due to impaired DNA damage response by staining cells for γ-H2AX and/or Comet assay.
- Examine expression of the DNA repair proteins-Non-homologous end joining pathway such as Ku70, DNA-PK, and homologous recombination pathway such Rad51 by Western Blotting, in CMPs from KO and WT mice.
- Determine whether CMPs display increased oxidative damage by measuring markers of oxidative stress such as oxidation of dichlorofluorescein-diacetate or measure 8-hydroxy-2'-deoxyguanosine (8-OHdG) levels by flow cytometry.
- Compare the effect of M-CSF versus GM-CSF on the polarization of KO and WT BMDMs.

Acknowledgments: This work was funded by Centers of Biomedical Research Excellence (COBRE)-Center for Host responses to Cancer Therapy at UAMS from NIGMS under grant number P20GM109005 and the Department of Defense W81XWH-15-1-0489.

INTRODUCTION

Bone marrow (BM) suppression is a common side-effect of toxicity to the hematopoietic tissue both in the clinical setting as well as in case of total body irradiation (TBI) exposure in the event of nuclear terrorism or nuclear disasters. Although a lot is known about the key regulatory proteins of steady-state hematopoiesis, not much is known about the key regulatory factors involved in stress-induced hematopoiesis. Studies in this direction are needed to aid in the development of therapeutic interventions to treat IR-induced BM injury.

The transcription factor CCAAT/enhancer-binding protein delta (*Cebpd*) plays an important role in the regulation of inflammatory and stress responses, oxidative stress and DNA damage response and in the innate and adaptive immune response.

Previously we have previously reported that *Cebpd*-knockout (KO) mice show increased ionizing radiation (IR)-induced BM injury characterized by myelosuppression and increased apoptosis of hematopoietic stem and progenitor cells (HSCs and HPCs) (Pawar *et al.*, 2014).

In the present study, we investigated the underlying mechanism of BM injury in *Cebpd*-knockout (KO) mice. The key findings of our study were:

- 1) Hind leg shielding of both *Cebpd*-WT and KO mice rescued the IR-induced mortality, which suggests that the lethality occurs primarily due to bone marrow injury.
- 2) We found that *Cebpd*-KO mice show reduced numbers of HSCs, HPCs, common myeloid progenitors (CMPs) and myeloid-erythroid progenitors (MEPs) compared to *Cebpd*-WT mice at 2 weeks post-6 Gy.
- 3) Preliminary results indicate increased presence of reactive oxygen species (ROS) in *Cebpd*-KO bone marrow mononuclear cells (BM-MNCs) at 4h post-irradiation.
- 4) There was no overall difference between the genotypes in the expression of the DNA damage marker, γ -H2AX at 1 hour post-3 Gy in BM-MNCs.

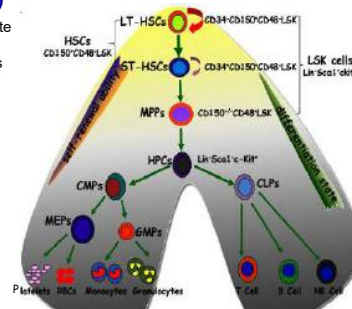
BACKGROUND

CCAAT Enhancer Binding Protein delta (*Cebpd*, C/EBP δ)

Previous studies from our laboratory indicate that C/EBP δ protects mouse embryonic fibroblasts from IR-induced oxidative stress and mitochondrial dysfunction (Banerjee *et al.*, 2016).

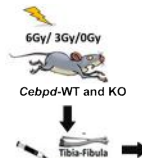


Hematopoietic Hierarchy



Shao *et al.* Antioxidants & Redox Signaling, 2019; 1447-1462, 2014.

METHODS

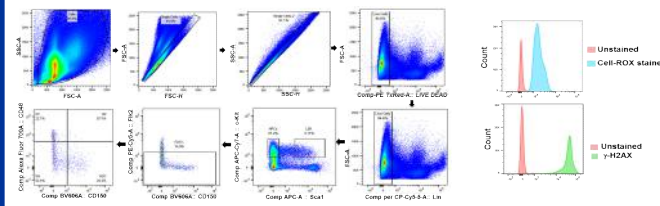


Flow Cytometry Analysis

- LSK: Lin⁻Sca1⁺cKit⁺ Cells
- CLP: Lin⁻Sca1⁺cKit⁺CD137⁺CD135⁻
- CMP: Lin⁻Sca1⁺cKit⁺CD34⁺CD116/32⁻
- MEP: Lin⁻Sca1⁺cKit⁺CD34⁺CD16/32⁻
- HPC: Lin⁻Sca1⁺cKit⁺
- GMP: Lin⁻Sca1⁺cKit⁺CD34⁺CD116/32⁻
- ST-HSCs: Lin⁻Sca1⁺cKit⁺CD135⁺CD48⁺CD150⁺
- LT-HSCs: Lin⁻Sca1⁺cKit⁺CD135⁺CD48⁺CD150⁻

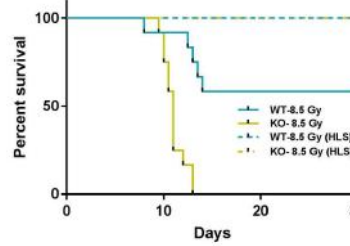
Analysis of LSK, HPCs, CMPs, CLPs, MEPs & GMPs and γ -H2AX, n=5 per treatment group/genotype
Analysis of ROS in various BM lineages, n=3 per treatment group/genotype

Scheme for detection of ST- and LT-HSCs, ROS and DNA damage

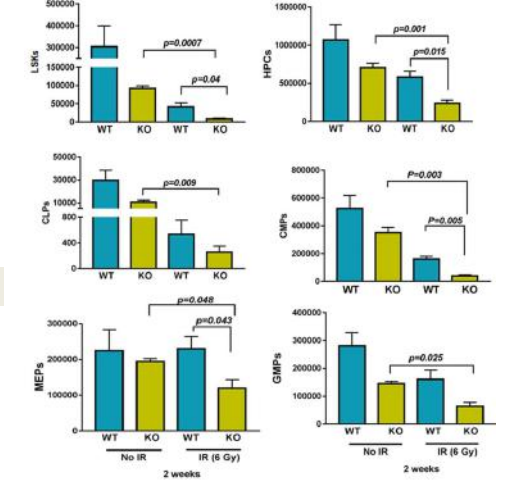


RESULTS

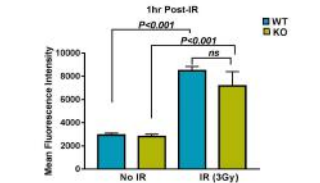
Bone marrow shielding rescues *Cebpd*-KO mice from IR-induced lethality



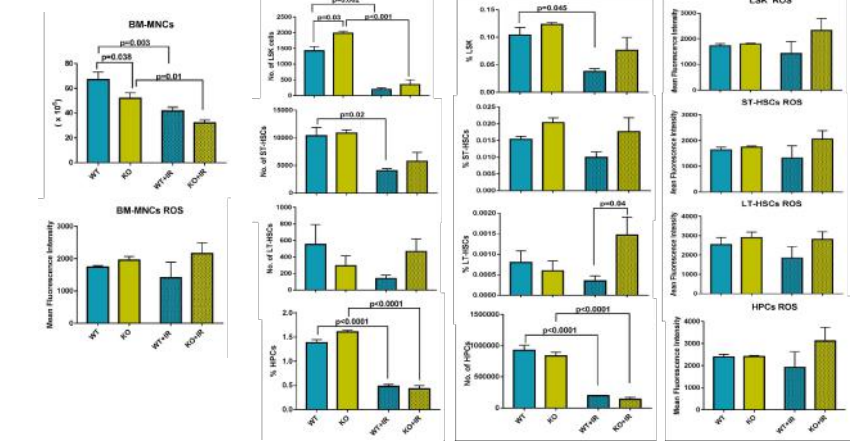
Cebpd-KO mice display significant reduction in total HSCs, HPCs, lymphoid and myeloid progenitors at 2 weeks post-irradiation



No significant difference in γ -H2AX levels in BM-MNCs at 1h post-irradiation



Cebpd-KO mice display slightly increased ROS levels at 4h post-irradiation




CONCLUSIONS & FUTURE DIRECTIONS

- Leg shielding experiments revealed that *Cebpd*-KO mice display lethality to IR primarily due to BM injury.
- *Cebpd*-KO mice showed significant reduction in LSKs, HPCs, CMPs and MEPs at 2 weeks post-IR exposure.
- Preliminary results in BM-MNCs did not show a significant difference in the expression of the DNA damage marker, γ -H2AX at 1 h post-irradiation.
- Preliminary studies showed that *Cebpd*-KO mice display increased accumulation of ROS in LSK and HPCs at 4h post-irradiation.
- Future studies will be directed to-
 - a) Confirm the roles of ROS and DNA damage in the LT-HSCs and ST-HSCs in *Cebpd*-WT and KO mice at 24h, 7 days and 14 days post-irradiation.
 - b) Investigate whether stem self-renewal of HSCs is impaired in *Cebpd*-KO mice after exposure to sublethal IR.

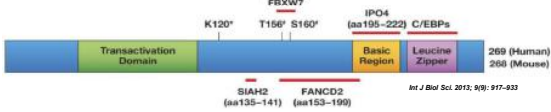
TLR4 Inhibition Attenuates Radiation-induced Inflammation And Oxidative Stress To Protect Mice From Gastrointestinal Injury

Sudip Banerjee, PhD
Post-Doctoral Fellow

Division of Radiation Health
Department of Pharmaceutical Sciences

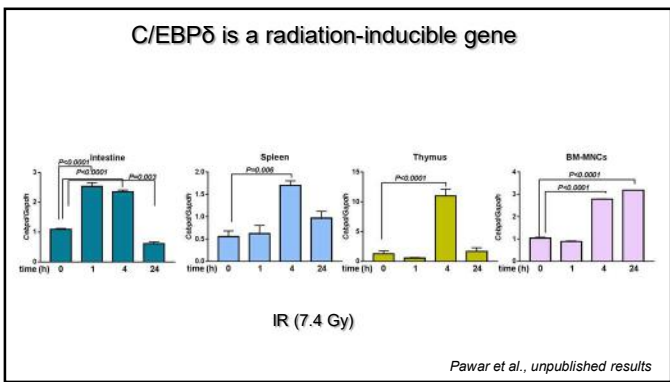
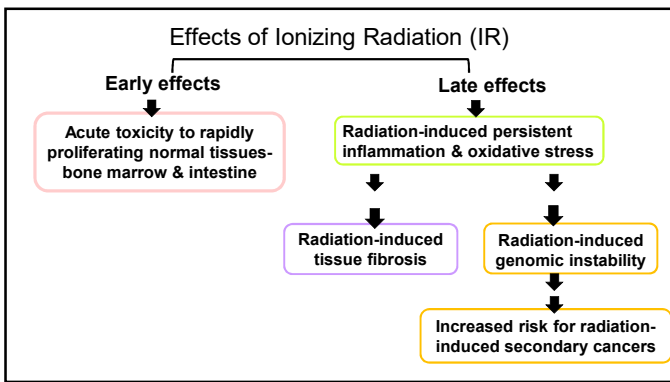


CCAAT enhancer binding protein delta (C/EBPδ)



Various synonyms : CELF; CRP3; C/EBP-delta; NF-IL6-beta; CEBPD
chromosome: 8; Location: 8p11.2-p11.1

- Basic leucine zipper containing transcription factor
- Basal expression is very low
- Transiently inducible by cell-type specific stimuli – TNF-α, Interleukins-1 & 6, Interferon-γ and stress response such as UV
- Downstream target of TLR4/Myd88, STAT3

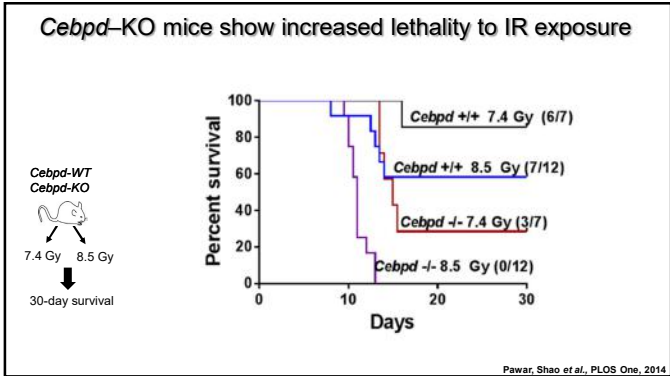


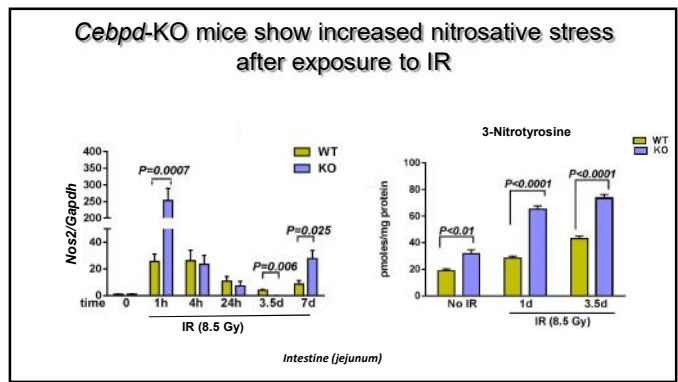
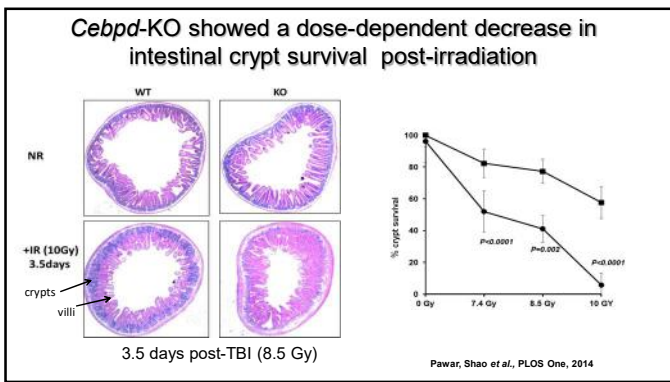
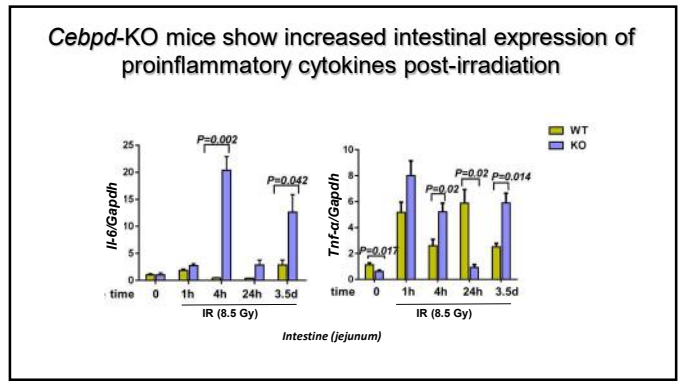
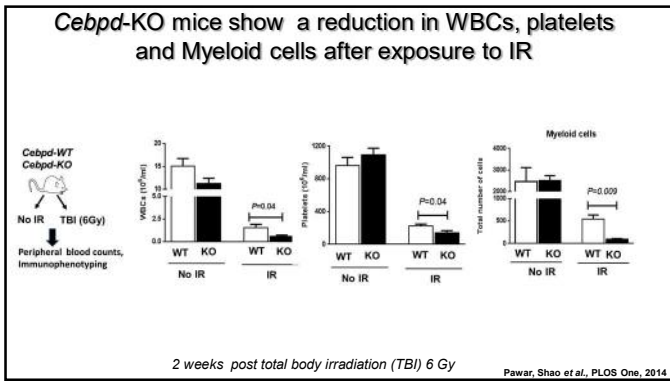
Significance

- Lack of selective radioprotectants for normal tissues
 - limits the therapeutic doses that can be delivered to treat cancers
- Lack of agents to protect from acute toxicity in the setting of total whole body radiation exposure

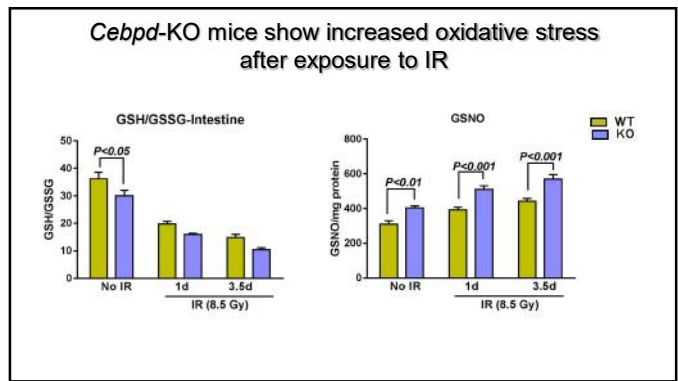
Understanding the normal tissue mechanisms in response to IR exposure is critical for the development of novel interventions:

- To reduce the adverse effects of IR on normal tissues
- To prevent the late complications of IR exposure
 - IR-induced carcinogenesis
 - Fibrosis

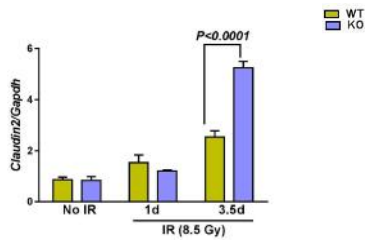




Role of impaired inflammatory signals in promoting radiation-induced intestinal injury of *Cebpd*-KO mice?



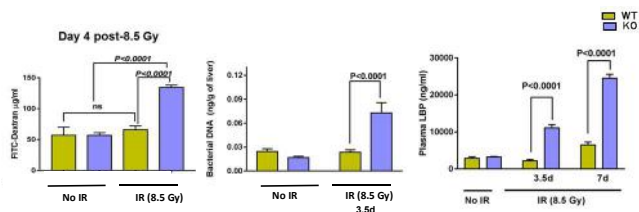
Cebpd-KO mice show increased expression of Claudin-2 post-irradiation



Toll-like receptors (TLRs) and Intestine

- TLRs play a critical role in host defense against infection by detecting conserved components of invading microbial pathogens.
- TLRs play a role in intestinal homeostasis.
- Intestinal epithelial barrier breakdown leads to exposure of the TLR ligands produced by commensal bacteria to TLR expressing cells (tissue resident macrophages and or intestinal epithelial cells) –resulting in inflammatory response, intestinal inflammation and injury.
- TLR2, TLR3, and TLR4 activation specifically upregulates the oxidative stress in intestinal epithelial cells (*Latorre et al., 2014*).

Cebpd-KO mice show increased intestinal barrier disruption and bacterial translocation post-irradiation

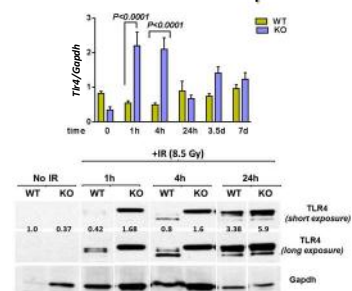


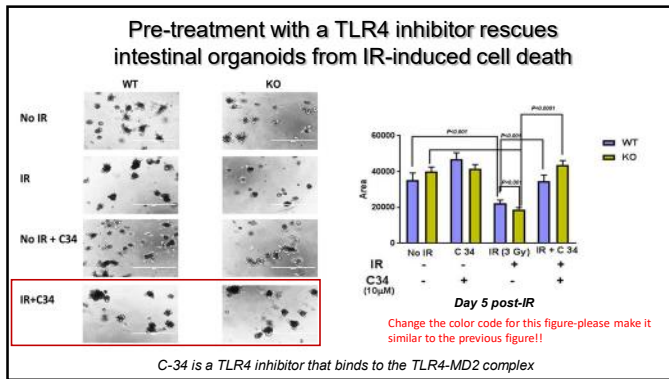
TLRs and Radiation Response

- TLR agonists lipopolysaccharide (LPS), flagellin, and the flagellin-derived CBL502 confer protection against IR-induced intestinal injury and the acute radiation syndrome in mouse models.
- *TLR4-KO* mice show increased radiosensitivity (*Cai et al., 2013*).
- The expression of TLR4 is upregulated by IR (*Schae 2013*).

Role of Toll-like receptor signaling in IR-induced intestinal injury?

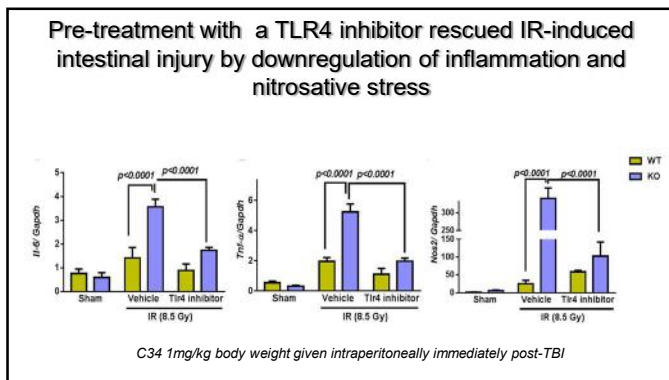
Cebpd-KO mice show increased expression of TLR4 in intestine tissues after exposure to IR





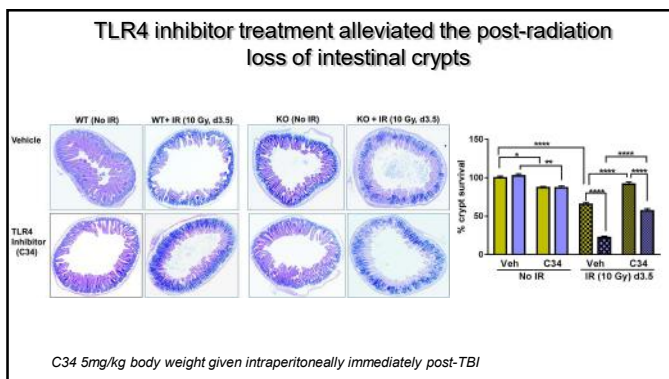
Summary

- *Cebpd*-KO mice display increased IR-induced inflammation, oxidative and nitrosative stress.
- Irradiated *Cebpd*-KO mice show leaky gut due to increased claudin-2 leading to bacterial translocation, endotoxemia finally causing sepsis and death.
- *Cebpd*-KO mice show IR-induced upregulation of TLR4 expression which promotes increased intestinal injury.
- TLR4 inhibitors may have potential as an agent to alleviate IR-induced intestinal injury.



Future Directions

- Determine the effect of TLR4 inhibitor administered either before or after IR exposure (6h, 24h post-IR exposure) on intestinal crypt colony survival.
- Examine the effect of TLR4 inhibitor on 30-day survival.
- Determine whether TLR4 inhibitor stimulates post-IR proliferation of intestinal stem cells.



Acknowledgements

Division of Radiation Health
UAMS, Little Rock, AR
Snehalata Pawar, PhD
 Sumit Shah, MBBS, MPH
 Debajyoti Majumdar, M. Pharm

National Cancer Institute,
Frederick, MD
Esta Sterneck, PhD

Martin Hauer-Jensen, MD, PhD
 Qiang Fu, MD, PhD

Arkansas Children's Research Institute,
Little Rock, AR
Stepan Melnyk, PhD
 Arkansas Children's Hospital Research Institute,
 Little Rock, AR

Funding
 NIH/NIGMS COBRE-P20GM109005
 Department of Defense W81XWH-15-1-0489

THANK YOU!

ABSTRACT

Lethality to ionizing radiation (IR) exposure in the event of nuclear terrorism or disaster occurs primarily due to bone marrow (BM) injury. IR exposure damages hematopoietic stem and progenitor cells (HSPCs), alongside the hematopoietic microenvironment. One of the major limitations of hematopoietic growth factors used to alleviate BM injury, is their inability to prevent long-term BM suppression due to exhaustion of HSCs. Thus, delineating the mechanism underlying the effects of IR stress-induced hematopoiesis is critical for developing novel interventions.

We have previously reported that mice lacking the transcription factor CCAAT enhancer binding protein delta (*Cebpd*, C/EBP δ) show increased lethality to total body irradiation (TBI), due to increased apoptosis of hematopoietic stem/progenitor cells (HSPCs) (Pawar et al., PLOS One 2014). In the present study, we investigated (a) whether *Cebpd*-deficiency impaired post-irradiation recovery of myeloid progenitors and (b) whether increased IR-induced reactive oxygen species (ROS) or DNA damage or impaired cell cycle regulation promote impaired recovery of HSPCs.

The key findings of our study revealed that:

- Unirradiated *Cebpd*-KO mice show increased numbers of short-term (ST)-HSCs, hematopoietic progenitors (HPCs), pre-megakaryocyte-erythroid progenitors (Pre-MEP), pre-megakaryocyte progenitors (Pre-Mkp) and pre-granulocyte-monocyte progenitors (Pre-GMs) compared to wild type (WT) mice.
- *Cebpd*-KO show significant decrease in lineage: c-kit⁺Sca1⁺(LSK), HSCs, LT-HSCs, multipotent progenitor 1 (MPP1) and in the myeloid lineage progenitors including common myeloid progenitors (CMPs), Pre-MEP, Pre-MegE, CFU-ProEry, Pre-GM and granulocyte-monocyte progenitors (GMPs) at 2 weeks post-6 Gy exposure.
- *Cebpd*-KO LSK and ST-HSCs from No IR group showed significant increase in G0 and decrease in G1 phase of the cell cycle.
- At 4h post-irradiation, there was a significant decrease in G0 in LSK, HSCs, ST-HSCs and HPCs, while HSCs and ST-HSCs of *Cebpd*-KO mice showed increased G1 phase of the cell cycle.
- *Cebpd*-KO mice show significantly increased expression of γ -H2AX at 4h post-IR exposure.
- *Cebpd*-KO LSK, HSCs, LT-HSCs and HPCs show significantly elevated ROS levels at 24h post-IR exposure.

BACKGROUND

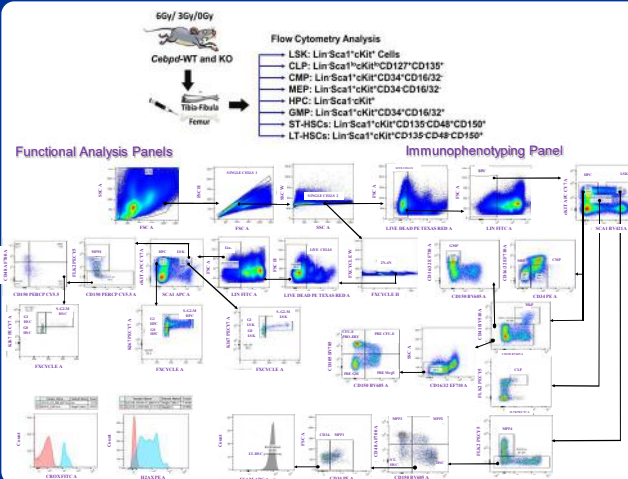
CCAAT Enhancer Binding Protein delta (*Cebpd*, C/EBP δ)

- Exposure to IR invokes signaling mechanisms that modulate oxidative stress, apoptosis, DNA damage repair, cell cycle arrest, and pro-inflammatory responses—C/EBP δ is implicated in the regulation of these very same processes.
- C/EBP δ plays an important role in the regulation of inflammatory and stress responses, as well as in innate and adaptive immunity.
- We were the first to report a novel role for C/EBP δ in promoting post-radiation survival. We showed that C/EBP δ -deficient mice exhibit increased lethality to total body irradiation (TBI), which occurs primarily due to injury to hematopoietic stem and progenitor cells and a decrease in myeloid cells after exposure to TBI (Pawar et al., 2014).
- We demonstrated a role for C/EBP δ in modulating basal and IR-induced oxidative stress and mitochondrial dysfunction in mouse embryonic fibroblasts (MEFs) (Banerjee et al., 2016).
- We further showed that *Cebpd*-deficiency promotes lethality due to increased inflammation and nitrosative stress which results in sepsis-induced lethality (Banerjee et al., 2019).

Based on our own studies and those by others, we hypothesize that C/EBP δ may protect cells from IR-induced damage by suppressing IR-induced oxidative stress and DNA damage response

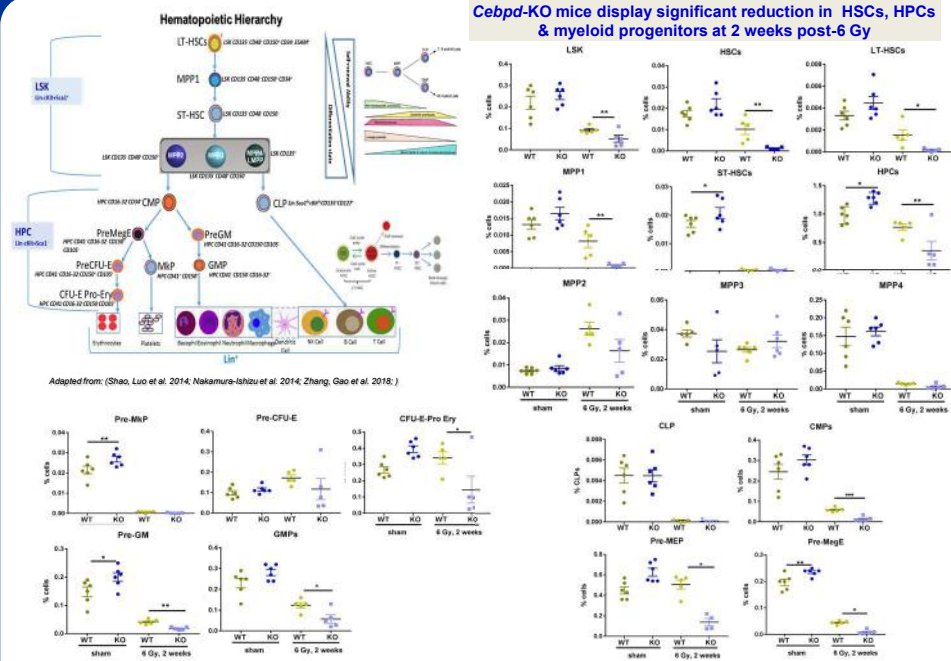


METHODS

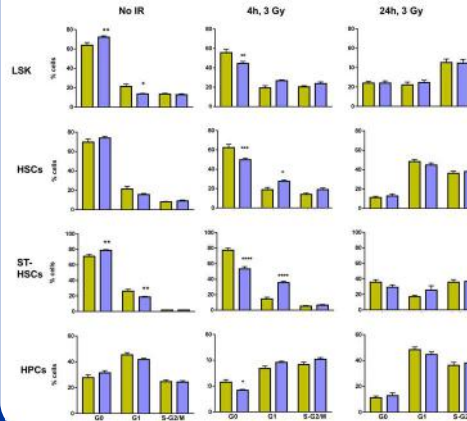


RESULTS

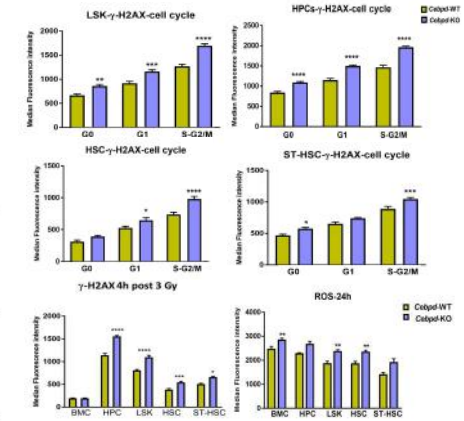
***Cebpd*-KO mice display significant reduction in HSCs, HPCs & myeloid progenitors at 2 weeks post-6 Gy**



***Cebpd*-deficiency promotes decrease in G0 in all cell types, but increased G1 in HSCs and ST-HSCs post-IR exposure**



***Cebpd*-KO mice display slightly increased γ -H2AX and ROS levels at 4h and 24h post-IR exposure**



CONCLUSIONS & FUTURE DIRECTIONS

- *Cebpd*^{-/-} mice showed significant reduction in numbers of HSCs, LT-HSCs, MPP1, HPCs, and the myeloid progenitors at 2 weeks post-irradiation.
- *Cebpd*^{-/-} HSPCs also show heightened cycling alongside increased levels of gamma-H2AX in all cell cycle phases, but specifically in S-G2/M at 4h post-IR exposure.
- *Cebpd*^{-/-} HSPCs show increased ROS levels at 24h post-3 Gy.

Conclusions: Overall these results indicate that *Cebpd* may regulate the cell-intrinsic properties such as IR-induced oxidative stress and DNA damage response to protect LT-HSCs and HPCs specifically the myeloid progenitors from injury.

- Future studies will identify the differentially-expressed targets of C/EBP δ that modulate oxidative stress and DNA damage response using a RNA-Seq approach.

INTRODUCTION

Etoposide is a chemotherapy drug that inhibits topoisomerase II which induces DNA double strand breaks and an increase in reactive oxygen species (ROS) to produce cell cytotoxicity and eventual apoptosis in tumor cells. However not much is known about the key target proteins that mediate the cytotoxic effects of etoposide.

CCAAT enhancer binding protein delta (*Cebpd*/C/EBPδ) is a basic leucine zipper transcription factor implicated in the regulation of oxidative stress, DNA damage response, genomic stability and inflammation. In this study we investigated whether C/EBPδ-deficiency may promote the cytotoxic effects of etoposide in mouse embryonic fibroblasts (MEFs).

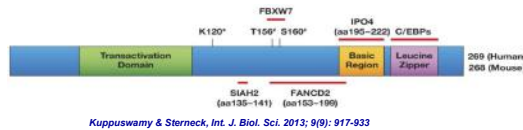
The goal of this project is to delineate the role of C/EBPδ in response to etoposide induced cytotoxicity. Based on the known roles of etoposide in modulating oxidative stress and DNA damage in the context of ionizing radiation, we **hypothesize** that C/EBPδ-deficient cells will experience increased cell death and sensitivity in response to etoposide treatment.

Key findings of this study were:

- *Cebpd*-knockout (KO) MEFs display decreased post-etoposide survival as measured by MTT cell proliferation assay and increased apoptosis.
- KO MEFs display increased levels of mitochondrial superoxide and increased levels of the DNA damage marker γ-H2AX compared to *Cebpd*-wild type (WT) MEFs in response to etoposide treatment.
- Compared to WT, KO MEFs showed increased mitochondrial mass post etoposide treatment.
- Electron Microscopy showed disrupted mitochondrial cristae in KO MEFs compared to WT MEFs at higher doses of etoposide.

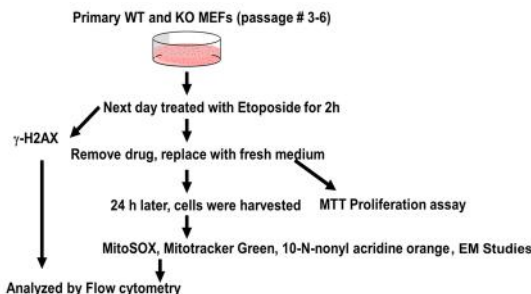
BACKGROUND

CCAAT Enhancer Binding Protein delta (C/EBPδ)



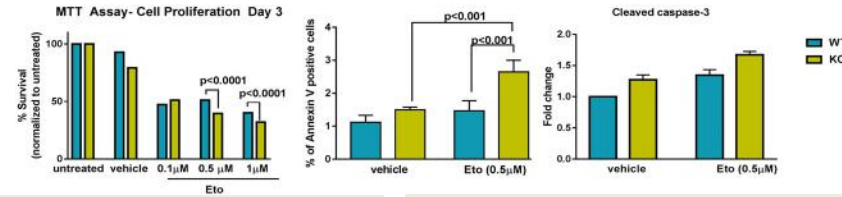
- Basic leucine zipper containing transcription factor.
- Implicated in diverse biological processes in a cell-type specific manner- acute phase response, proliferation, differentiation, growth arrest, apoptosis, stem cell self-renewal.
- Previous studies from our laboratory indicate that C/EBPδ plays an important role in responding to radiation and in protection from radiation-induced injury.

METHODS

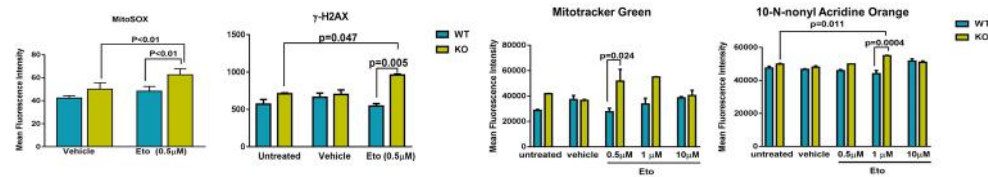


RESULTS

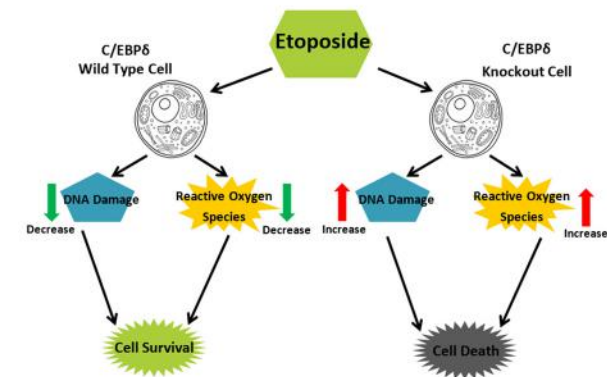
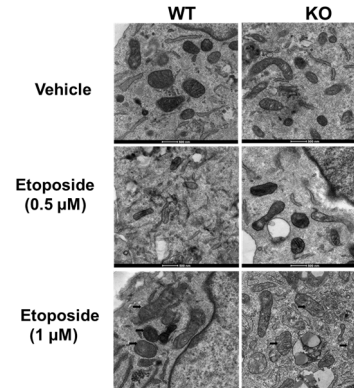
Cebpd-KO MEFs show decreased cellular proliferation and increased apoptosis post etoposide treatment



Cebpd-KO MEFs display increased DNA damage and levels of ROS post etoposide treatment



Cebpd-KO MEFs show increased mitochondrial damage in response to etoposide treatment



CONCLUSIONS & FUTURE DIRECTIONS

- *Cebpd*-KO MEFs displayed increased sensitivity and cell death to etoposide compared to WT MEFs.
- *Cebpd*-KO MEFs showed increased DNA damage and increased mitochondrial superoxide in response to etoposide treatment when compared to WT MEFs.
- *Cebpd*-KO MEFs showed increased etoposide-induced mitochondrial mass which may be indicative of mitochondrial biogenesis or a defect in mitophagy.
- Electron microscopy reveals increased disruption of mitochondrial cristae in etoposide-treated KO MEFs compared to WT MEFs.

Future research plans-

1. Measure the effect of etoposide on mitochondrial respiration in *Cebpd*-KO and WT MEFs using the seahorse XF96 flux analyzer.
2. Examine for markers of mitophagy and mitochondrial biogenesis.
3. Examine the expression of proteins involved in oxidative stress response and DNA damage response in WT and KO MEFs treated with etoposide and respective untreated, & vehicle controls.

ACKNOWLEDGMENTS

Funding by the Center of Biomedical Research Excellence (COBRE)-Center for Host responses to Cancer Therapy at UAMS from NIGMS grant - P20GM109005 & DoD through the Peer Reviewed Medical Research Program under Award No: W81XWH-15-1-0489 is gratefully acknowledged.

Snehalata Pawar *nee* Bhosale, PhD

Assistant Professor

Department of Pharmaceutical Sciences

Division of Radiation Health

University of Arkansas for Medical Sciences

4301 W. Markham Street, #522-10

Little Rock, AR 72205

Tel: 501-686-5784, Fax: 501-686-6057

E-mail: SAPawar@uams.edu

EDUCATION

- | | |
|-----------|--|
| 1987-1990 | B. Sc. (Microbiology), University of Bombay, Mumbai, India |
| 1990-1992 | M. Sc. (Biochemistry), Maharaja Sayajirao University, Baroda, India |
| 1993-1999 | Ph. D. (Biochemistry), National Chemical Laboratory <i>affiliated to</i> University of Pune, Pune, India |

PROFESSIONAL EXPERIENCE

- | | |
|------------------|---|
| 03/2000-01/2005 | Postdoctoral Fellow, Department of Molecular Genetics, The University of Texas M. D. Anderson Cancer Center, Houston, TX |
| 02/2005-10/2008 | Postdoctoral Fellow, Laboratory of Cell & Developmental Signaling, National Cancer Institute (NCI), Frederick, MD |
| 07/2009-06/2010 | Instructor, Division of Radiation Health, Department of Pharmaceutical Sciences, University of Arkansas for Medical Sciences (UAMS), Little Rock, AR |
| 07/02010-present | Assistant Professor, Division of Radiation Health, Department of Pharmaceutical Sciences, UAMS, Little Rock, AR |

AWARDS and HONORS

- | | |
|-----------|---|
| 1993-1998 | Junior & Senior Research Fellowship, Council of Scientific and Industrial Research Fellowship, New Delhi, India |
| 2008 | Travel Award, 8 th Annual Fellows & Young Investigators Colloquium, Ocean City, MD |
| 2017 | Nominated for Dr. and Mrs. Jon Wolfe Annual Endowed Award for Faculty Excellence, College of Pharmacy, UAMS, Little Rock, AR |
| 2017 | Early Career Investigator Travel Award, 63 rd Annual meeting of Radiation Research Society, Cancun, Mexico |
| 2017 | Arkansas-IDeA Networks of Biomedical Research Excellence (INBRE) Investigator Travel award, Morgantown, WV |
| 2018 | Early Career Investigator Travel Award, 64 th Annual meeting of Radiation Research Society, Chicago, IL |

RESEARCH SUPPORT

Active Support

| | | |
|---|-----------------------|-------------------|
| W81XWH1910737 | Pawar (PI) | 2.4 cal mths |
| Department of Defense | 09/15/2019-09/14/2022 | \$754,102 (total) |
| Peer Reviewed Medical Research Expansion Award, PR181863 | | |

Role of TLR4 in radiation-induced cardiomyopathy

This project investigates the role of TLR4 signaling in promoting radiation-induced cardiomyopathy and whether TLR4 inhibitors can alleviate the adverse effects of total body and localized radiation to the heart.

| | | |
|-------------------------|-----------------------|-------------------|
| HHS-NIH-NIAID-BAA2019-1 | Dirk Pleimes (PI) | 2.4 cal mths |
| Broad Agency | 05/01/2020-04/30/2021 | \$250,000 (total) |

Development of Myelo001 as medical countermeasure for the treatment of Acute Radiation

This project will investigate the role of imidazolyl ethanamide pentandioic Acid (IEPA, Myelo001), as a novel radiation countermeasure agent to protect from acute radiation syndrome and delineate the underlying mechanism via which it imparts protection against hematopoietic injury.

Role: Pawar (subcontractor)

Grants in planning (Feb 2020)

| | | |
|-------------------------------------|-----------------------|---------------------|
| W81XWH18SBAA | Pawar (PI) | 2.4 cal mths |
| Broad Agency, Department of Defense | 01/01/2020-05/31/2022 | \$1,250,000 (total) |

Role of TLR4 inhibitors as a novel agent to mitigate radiation-induced gastrointestinal injury

This project will investigate the role of TLR4 inhibitor as a novel radiation countermeasure agent to protect from acute radiation syndrome and delineate the underlying mechanism of radioprotection.

| | | |
|--------------|------------------------|---------------------|
| R01, NCI/NIH | Pawar (PI) | 2.4 cal mths |
| | 07/01/2020- 06/30/2025 | \$1,250,000 (total) |

Role of C/EBP δ /TLR4 nexus in radiation-induced intestinal injury

This project will delineate the role of TLR4 in myeloid versus epithelial cells in promoting radiation-induced localized intestinal injury using tissue specific models of C/EBP δ depletion. In this project, we will elucidate the molecular mechanism of C/EBP δ -mediated TLR4 downregulation in the context of radiation injury.

| | | |
|--------------|-----------------------|---------------------|
| R01, NCI/NIH | Pawar (PI) | 2.4 cal mths |
| | 07/01/2020-06/30/2025 | \$1,250,000 (total) |

Role of C/EBP δ in genotoxic stress-induced bone marrow dysfunction

This project will elucidate the functional role of C/EBP δ in hematopoietic stem cells in response to chemotherapy/ionizing radiation exposure and further utilize a myeloid-specific depletion of C/EBP δ depletion.

Completed Research Support

| | | |
|---------------------------------|-----------------------|--------------|
| W81XWH-15-1-0489 | Pawar (PI) | 4.8 cal mths |
| PR140967, Department of Defense | 09/01/2015-08/31/2019 | \$1,438,032 |

Role of C/EBP δ in IR-induced sepsis

This project investigates 1) whether IR-induced intestinal injury in *Cebpd*-knockout (KO) mice is due to increased toll-like receptor 4 (TLR4)-mediated inflammatory response, and 2) whether *Cebpd*-KO mice show perturbed macrophage response post-IR.

| | | |
|-------------|-------------------|--------------|
| P20GM109005 | Hauer-Jensen (PI) | 6.0 cal mths |
|-------------|-------------------|--------------|

| | | |
|---|--------------------------|-------------------|
| NIH/NIGMS | 06/24/2015-03/31/2018 | \$804,597 (total) |
| COBRE Center for Studies of Host Response to Cancer Therapy | Pawar (Project 2 Leader) | |

Project 2: Molecular mechanisms of C/EBP delta in ionizing radiation response

The goal of this project is to investigate the role of C/EBP δ in a) ionizing radiation (IR)-induced normal tissue injury to gastrointestinal and hematopoietic system, b) radiation-induced genomic instability, in bone marrow cells, and c) elucidate the underlying mechanism via which C/EBP δ protects from injury to normal tissue and genomic instability in response to IR.

| | | |
|---|-----------------------|---------------|
| P20GM103625 | Pawar (PI) | 12.0 cal mths |
| Center for Microbial Pathogenesis and Host Inflammatory Responses Pilot Award | 07/01/2013-06/30/2014 | \$50,000 |

Role of C/EBP delta in radiation-induced sepsis

This project examined the role of C/EBP δ -deficiency in ionizing radiation induced intestinal injury and role of altered macrophage responses in promoting gut-associated sepsis.

| | | |
|---|-----------------------|---------------|
| 2012 UAMS Medical Research Endowment Fund | Pawar (PI) | 12.0 cal mths |
| | 01/01/2012-12/31/2012 | \$15,000 |

Role of C/EBP delta in normal tissue radiation injury

This project examines the role of C/EBP δ in normal tissue injury in the gastrointestinal and hematopoietic systems in a genetic knockout mouse model of C/EBP δ .

| | | |
|---|----------------------|--------------|
| Arkansas Biosciences Institute Pilot Project Proposal | Pawar (PI) | 3.0 cal mths |
| | 03/01/2010-6/30/2010 | \$64,853 |

The role of CCAAT enhancer binding protein delta in response to ionizing radiation

This project was seed-money for initiating the studies on the role of C/EBP δ in ionizing radiation response.

PEER-REVIEWED PUBLICATIONS

1. Gupta S, **Bhosale S**, Pandya K. Effect of low level exposure of lead and cadmium on δ -ALAD and acetylcholinesterase in rats. **Indian Journal of Experimental Biology**, **32**, 819-821, 1994. [citations:6]
2. **Bhosale SH**, Rao MB, Srinivasan MC and Deshpande VV. Thermostability of high activity alkaline protease from *Conidiobolus coronatus* (NCL 86.8.20). **Enzyme Microbial Technology**, **17**, 136-139, 1995. [citations:98]
3. **Bhosale SH**, Rao MB and Deshpande VV. Molecular and industrial aspects of glucose isomerase. **Microbiological Reviews**, **60**, 281-290, 1996. [citations:564]
4. **Bhosale SH**, Ghatge MS and Deshpande VV. Molecular cloning and expression of glucose/xylose isomerase from *Streptomyces* sp. NCIM 2730 in *E.coli*. **FEMS Microbiology Letters**, **145**, 95-100, 1996. [citations:6]
5. Paul A, **Bhosale SH**, Maity TK, and Deshpande VV. Effect of coordinated addition of specific amino acids on the synthesis of recombinant glucose isomerase. **Enzyme Microbial Technology**. **23**, 506-510, 1998. [citations:6]
6. **Pawar SA** and Deshpande VV. Characterization of acid-induced unfolded intermediates of glucose/xylose isomerase from *Streptomyces* sp. NCIM 2730. **European Journal of Biochemistry** **267**, 6331-6338, 2000. [citations:59]
7. Szentirmay MN, Yang X-H, **Pawar SA**, Vinson C and Sawadogo M. The IGF2 receptor (*IGF2R*) is a USF2-specific target in mammary epithelial cells, but not in breast cancer cells. **Journal of Biological Chemistry**, **278**, 37231-37240, 2003. [Impact factor: 5.886, citations:37]
8. **Pawar SA**, Szentirmay M, Hermeking H and Sawadogo M. Evidence for a gene-specific switch at the CDK4 promoter with loss of control by both USF and c-Myc. **Oncogene**, **23**, 6125-6135, 2004. [Impact factor: 5.886, citations:32]

9. Chen N, Szentirmay MN, **Pawar SA**, Sirito M, Wang J, Wang Z, Zhai Q, Yang H-X, Peehl DM, Ware JL and Sawadogo M. Tumor-suppression functions of transcription factor USF2 in prostate carcinogenesis. **Oncogene**, **25**, 579-87, 2006. [Impact factor: 5.886, citations:19]
10. **Pawar SA**, Roy-Sarkar T, Kuppaswamy B, Wang J, Zhang Y, Dowdy S, Huang A, Sharan S and Sterneck E. C/EBP δ targets cyclin D1 for proteasome-mediated degradation via induction of CDC27/APC3 expression. **Proceedings of the National Academy of Sciences, USA**, **107**: 9210-5, 2010. [Impact factor: 9.771, citations:57]
11. Roysarkar T, Sharan S, Wang J, **Pawar SA**, Cantwell CA, Johnson PF, Morrison DK, Wang JM, Sterneck E. Identification of a Src tyrosine kinase/SIAH2 E3 ubiquitin ligase pathway that regulates C/EBP δ expression and contributes to transformation of breast tumor cells. **Molecular and Cellular Biology**, **32**:320-332, 2012. [Impact factor: 6.05, citations:54]
12. Geiger H, **Pawar SA**, Kerschen EJ, Nattamai KJ, Hernandez I, Liang H-P, Fernández JA, Cancelas JA, Ryan MA, Kustikova O, Schambach A, Fu Q, Wang J, Fink LM, Petersen K-U, Zhou, D, Griffin JF, Baum C, Weiler H, Hauer-Jensen M. Pharmacological targeting of the thrombomodulin–protein C pathway mitigates radiation toxicity. **Nature Medicine**, **18**:1123-1129, 2012. [Impact factor: 28.439, citations:91]
13. Pathak R, **Pawar SA**, Gupta P, Fu Q, Berbée M, Garg S, Sridharan V, Wang W, Biju PG, Kragerly K, Boerma M, Ghosh SP, Cheema AK, Hendrickson HP, Aykin-Burns N and Hauer-Jensen M. Characterization of transgenic Gfrp knock-in mice: Implications for BH4 in modulation of radiation response. **Antioxidants Redox Signaling**, **20**:1436-46, 2014. [Impact factor: 7.407, citations:15]
14. **Pawar SA***, Shao L, Chang J, Wang W, Pathak R, Wang J, Zhu X, Boerma M, Sterneck E, Zhou, D and Hauer-Jensen M. C/EBP δ deficiency sensitizes mice to ionizing radiation-induced hematopoietic and intestinal injury. **PLOS One**, **9**:e94967, 2014. [Impact factor: 4.7, citations:13]
15. Banerjee S, Aykin-Burns N, Krager KJ, Shah SK, Melnyk SB, Hauer-Jensen M, **Pawar SA***. Loss of C/EBP δ enhances IR-induced cell death by promoting oxidative stress and mitochondrial dysfunction. **Free Radical Biology and Medicine**, **99**:296-307, 2016. [Impact factor: 5.886, citations:15]
16. Banerjee S, Shah, SK, Melnyk SB, Pathak R, Hauer-Jensen and **Pawar SA***. C/EBP δ is essential for gamma tocotrienol-mediated protection against radiation-induced hematopoietic and intestinal injury. **Antioxidants**, **7**: 55, 2018. [Impact factor: 4.183, citations:3]
17. Banerjee S, Tyler A, Majumdar D, Groves T, Wang J, Gorantla A, Allen AR* and **Pawar SA***. Loss of C/EBP δ exacerbates radiation-induced neurocognitive decline by suppression of oxidative stress in aged mice. **Int. J. Mol. Sci.** **20**: 885, 2019. [Impact factor: 3.687]
18. Garg S, Sadhukhan R, Banerjee S, Savenka AL, Basnakian AG, McHargue V, Wang J, **Pawar SA**, Ghosh SP, Ware J, Hauer-Jensen M, Pathak R*. Gamma-tocotrienol protects the intestine from radiation potentially by accelerating mesenchymal immune cell recovery. **Antioxidants**. **8**, 57, 2019. [Impact factor: 4.52]
19. Banerjee S, Fu Q, Melnyk SB, Shah SK, Sterneck E, Hauer-Jensen M, **Pawar SA***. C/EBP δ protects from radiation-induced intestinal injury and sepsis by suppression of inflammatory and nitrosative stress. **Sci. Rep.**, **9**:13953, 2019. <https://doi.org/10.1038/s41598-019-49437-x>

Manuscripts to be submitted

20. Shah SK[#], Banerjee S[#], Ponnappan U, Stumhofer J, Hauer-Jensen M and **Pawar SA***. IL17A does not play a role in radiation-induced intestinal injury. **Int. J. Mol. Sci.**
21. Byrum SD, Banerjee S, Orr L, Ponnappan U, Tackett AJ and **Pawar SA***. Identification of C/EBP δ -targets involved in regulation of radiation response utilizing a proteomics approach. **Journal of Proteomics & Bioinformatics**
22. Banerjee S, Shah SK, Hauer-Jensen M and **Pawar SA***. Impaired TLR4 signaling promotes radiation-induced intestinal injury in *Cebpd*-deficient mice. **Innate Immunity**.
23. Majumdar D and **Pawar SA***. Analysis of murine hematopoietic stem cell proliferation, DNA damage and ROS after exposure to radiation-induced damage. **Cytometry**.

24. Majumdar D and **Pawar SA***. C/EBP δ -deficiency does not alter the radiation response of M1 and M2 genes in bone marrow derived macrophages. **Cell & Biosciences**.
25. Orton J[#], Raley R[#], Vue S[#], Coates C, Banerjee S, Kuppasamy B, Sterneck E and **Pawar SA***. C/EBP δ -deficiency sensitizes cells to etoposide-induced cytotoxicity due to impaired DNA damage response. **Cell Death & Disease**

Manuscripts in preparation

26. **Pawar SA***, Banerjee S, Gill K and Cheema AK. C/EBP δ -deficiency promotes gut dysbiosis after radiation exposure and correlates with metabolomics changes. **Journal of Proteome Research**.
27. Majumdar D and **Pawar SA***. C/EBP δ does not play a pertinent role in stress-induced hematopoiesis in aged mice. **American Journal of Hematology**.
28. Majumdar D, Chavez JC, Pietras EM, and **Pawar SA***. C/EBP δ protects from radiation-induced bone marrow failure by suppression of ROS-induced DNA damage and cell cycle proliferation. **Hematologica**.
29. Chavez JC[#], Majumdar D, **Pawar SA*** and Pietras EM*. C/EBP δ -deficiency promotes impaired myeloid differentiation in response to chronic inflammation. **Blood**.
30. Majumdar D, **Pawar SA**, Chowdhury P, Griffin R, Narayanasamy G, Dobretsov M, Hauer-Jensen M and Pathak R*. Simultaneous exposure to chronic low-grade irradiation and simulated microgravity promotes increased oxidative stress in hematopoietic stem cells. **Scientific Reports**.
31. **Pawar SA***, Nguyen-Ngoc K-Y, Sharan S and Sterneck E. Identification of mouse mammary gland involution associated C/EBP δ -dependent targets. **Genes, 2020**.

Manuscripts in planning

32. **Pawar SA***, Banerjee S, Majumdar D and Hauer-Jensen M. C/EBP δ -deficiency in aged mice promotes increased radiation-induced intestinal injury. *PLOS One*.
33. Davis E, Zhang M, Banerjee S, **Pawar SA**, Steppenbach T, Liu J*. Delineating the critical role of myeloid-specific caspase 11 in inflammatory bowel disease. *Gastroenterology*
34. Majumdar D and **Pawar SA***. C/EBP δ - a novel player in ionizing radiation-induced normal tissue response. *Cell Death & Inflammation (Review article)*.
35. Majumdar D and **Pawar SA***. Advantages of drug delivery via polysaccharide-based nanoparticles to the GI. *(Review article)*

(*Corresponding author since independent Faculty position; # equal contributions)

SCIENTIFIC PRESENTATIONS

Invited Talks

NIH

1. Role of transcription factor USF in CDK4 regulation, Laboratory of Protein Dynamics and Signaling, National Cancer Institute, Frederick, MD, Aug 1, 2004.
2. Investigating the molecular mechanisms of growth inhibition by C/EBP δ , Laboratory of Molecular Pathology, NCI, Bethesda, MD, Oct 25, 2007.
3. Mechanistic insights into the growth inhibitory function of C/EBP δ , Laboratory of Genomic Physiology, NIDDK, Bethesda, MD, Nov 14, 2007.
4. Mechanistic insights into the growth inhibitory function of C/EBP δ , Mammary Biology & Tumorigenesis Laboratory, NCI, Bethesda, MD, Feb 1, 2008.
5. Does C/EBP δ inhibit tumor cell growth by repression of cyclin D1 expression? 8th Annual Fellows & Young Investigators Colloquium, Ocean City, MD, Mar 3-5, 2008.
6. Molecular mechanism of growth inhibition by C/EBP δ : Dual regulation of cyclin D1 in breast tumor cells, NCI-Frederick Postdoc seminar series, Frederick, MD, April 8, 2008.

7. Molecular mechanism of growth inhibition by C/EBP δ : Dual regulation of cyclin D1 in breast tumor cells, NCI Fellows Presentation Skills seminar series, NIH, Bethesda, MD, April 22, 2008.
8. C/EBP δ inhibits mammary epithelial cell growth by repression of cyclin D1 expression, LCDS-LPDS-LCMB Combined Retreat, NCI, Frederick, MD, June 3, 2008.

UAMS

9. Molecular mechanisms of growth inhibition by C/EBP δ , College of Pharmacy, UAMS, Little Rock, AR, Sep 4, 2009.
10. CCAAT enhancer binding protein delta: Role in radiation response, Division of Radiation Health Research Conference, UAMS, Little Rock, AR, July 10, 2012.
11. Role of C/EBP δ in IR response-the story so far..., Division of Radiation Health Research Conference, UAMS, Little Rock, AR, May 14, 2013.
12. Does C/EBP δ protect from radiation-induced injury and sepsis-induced lethality? Center for Biomedical Research Excellence (COBRE) External Advisory Committee Meeting, UAMS, Little Rock, AR, Jan 13, 2014.
13. Role of C/EBP δ in radiation sepsis-induced lethality, Department of Microbiology & Immunology, COBRE work-in-progress meeting, UAMS, Little Rock, AR, March 28, 2014.
14. Investigating the C/EBP δ /TLR pathway in radiation injury, Division of Radiation Health New Investigator Research Forum, UAMS, Little Rock, AR, April 8, 2014.
15. Molecular mechanism of C/EBP δ in ionizing radiation response, Center for Biomedical Research Excellence External Advisory Committee Meeting, UAMS, Little Rock, AR, Nov 6, 2015.
16. C/EBP δ protects from radiation-induced intestinal injury by downregulation of inflammation, COBRE New Investigator Research Forum, UAMS, UAMS, Little Rock, AR, Jan 12, 2016.
17. C/EBP δ - a novel player in radiation-induced normal tissue injury, Winthrop P. Rockefeller Cancer Research Forum Seminar, UAMS, Little Rock, AR, April 25, 2016.
18. Molecular mechanism of C/EBP δ in ionizing radiation response, Center for Biomedical Research Excellence External Advisory Committee Meeting, UAMS, Little Rock, AR, Nov 3, 2016.
19. What makes a great paper, Host Response & Radiological Sciences Program Meeting, UAMS, Little Rock, AR, April 25, 2017.
20. Targeting the C/EBP δ /TLR4 nexus protects from radiation-induced gut injury, Department of Physiology & Biophysics, UAMS, Little Rock, AR, Oct 26, 2017.
21. Molecular mechanism of C/EBP δ in ionizing radiation response, Center for Biomedical Research Excellence External Advisory Committee Meeting, UAMS, Little Rock, AR, Nov 6, 2017.

Other Institutions

22. C/EBP δ - a novel player in radiation response, National Cancer Institute, Frederick, MD, June 29, 2016.
23. C/EBP δ - a novel player in radiation response, Armed Forces Research in Radiobiology Institute, Bethesda, MD, June 30, 2016.
24. C/EBP δ - A novel player in normal tissue responses to ionizing radiation, Free Radical and Radiation Biology Division, Department of Radiation Oncology, University of Iowa, Iowa City, IA, April 3, 2017.
25. C/EBP δ : A novel player in normal tissue responses to ionizing radiation, Division of Radiation Research, Department of Radiology, Rutgers New Jersey Medical School, Newark, NJ, April 10, 2018.
26. C/EBP δ : A Novel Target to Alleviate Radiation-induced normal tissue toxicity, Masonic Medical Research Institute, Utica, NY, May 21, 2019.
27. C/EBP δ : A novel player in normal tissue responses to ionizing radiation, Department of Radiation Oncology, Upstate Medical University, Syracuse, NY, May 23, 2019.

Oral Presentations

1. **Pawar SA.** Role of C/EBP δ in radiation-induced injury of normal tissues, Joint UAMS-AFRRI Conference on Normal Tissue Radiation Effects and Countermeasures (CONTREC), at Winthrop Rockefeller Institute Conference Center, Morrilton, AR, April 26, 2010.
2. **Pawar SA,** Berbee M, Fu Q, Garg S, Wang J, Sreekumar K and Hauer-Jensen M. Gamma-tocotrienol confers radio-protection by modulation of the tetrahydrobiopterin biosynthetic pathway. 2010 Chemical and Biological Defense Science and Technology Conference, Orlando, FL, Nov 15-19, 2010.
3. **Pawar SA,** Banerjee S, Byrum SD, Orr L, Tackett AJ, Ponnappan U and Hauer-Jensen M. A proteomics approach to delineate the role of C/EBP δ in ionizing radiation-induced oxidative stress. Southeast Regional IDeA Conference, Cell signaling session, Biloxi, MS, Nov 11-13, 2015.
4. Banerjee S, Byrum SD, Orr L, Tackett A, Ponnappan U, Hauer-Jensen M and **Pawar SA.** Identification of C/EBP δ targets involved in regulation or IR-induced oxidative stress. National IDeA Symposium for Biomedical Research Excellence, Washington, DC, June 26-28, 2016.
5. Banerjee S, Fu Q, Shah SK, Melnyk SB, Hauer-Jensen M and **Pawar SA.** Aberrant TLR4 signaling promotes radiation-induced intestinal injury in *Cebpd*-deficient mice. Conference on Normal Tissue Radiation Effects and Countermeasures (CONTREC), Morrilton, AR, May 14-17, 2018.
6. Banerjee S, Fu Q, Shah SK, Melnyk SB, Hauer-Jensen M and **Pawar SA.** TLR4 inhibition attenuates radiation-induced inflammation and oxidative stress to protect mice from gastrointestinal injury. 64th Annual meeting of the Radiation Research Society, Chicago, IL, Sep 14-17, 2018.
7. Banerjee S, Krager K, Majumdar D, Boerma M, Hauer-Jensen M and **Pawar SA.** C/EBP δ protects from radiation-induced gastrointestinal injury. 65th Annual meeting of the Radiation Research Society, San Diego, CA, Nov 3-6, 2019.

Poster Presentations

1. **Pawar SA** and Sawadogo M. Poster entitled "E-box dependent transactivation of CDK4 promoter by Upstream Stimulatory Factor." Genes & Development Retreat 2001, Corpus Christi, TX, Mar 27- 31, 2001.
2. **Pawar SA** and Sawadogo M. E-box dependent transactivation of CDK4 promoter by Upstream Stimulatory Factor. Trainee Recognition Day, M. D. Anderson Cancer Center, Houston, TX, April 24-26, 2001.
3. **Pawar SA** and Sawadogo M. Regulation of the CDK4 promoter activity in human breast epithelial cells by Upstream Stimulatory Factor. Trainee Recognition Day, M. D. Anderson Cancer Center, Houston, TX, May 8-10, 2002.
4. **Pawar SA,** Szentirmay MN, Hermeking H and Sawadogo M. USF2 and c-Myc jointly control CDK4 expression in non-tumorigenic mammary epithelial cells, but not in breast cancer cells. AACR 95th Annual meeting, Orlando, FL, Mar 27-31, 2004.
5. **Pawar SA** and Sterneck E. Promoter regulation of the pro-apoptotic transcription factor C/EBP δ in breast cancer cells. Combined Breast Faculty Retreat, Rocky Gap, Cumberland, MD, July 20-22, 2005.
6. Chen N, **Pawar SA,** Szentirmay MN and Sawadogo M. Transcription factor USF2 suppresses the malignant phenotype of prostate cancer cells. AACR 96th Annual meeting, Anaheim, CA, April 16-20, 2005.
7. **Pawar SA** and Sterneck E. Identification of target genes of the pro-apoptotic transcription factor C/EBP δ in breast tumor cells by ChIP. 6th Annual Fellows & Young Investigators Retreat, Ocean City, MD, Feb 28-Mar 2, 2006.
8. **Pawar SA,** Sharan S and Sterneck E. C/EBP δ regulates Cyclin D1 expression in breast tumor cells. Spring Research Festival, NCI, Frederick, MD, May 17-18, 2006.
9. **Pawar SA,** Sharan S and Sterneck E. Identification of target genes mediating growth inhibition by transcription factor C/EBP δ . 25th International Congress on Breast Cancer Research, Montreal, Canada, Sep 15-18, 2006.

10. **Pawar SA**, Sharan S and Sterneck E. C/EBP δ inhibits breast epithelial cell growth in part by repression of the cyclin D1 promoter. 7th Annual CCR Fellows and Young Investigators Retreat, Ocean City, MD, Feb 27-Mar 1, 2007.
11. **Pawar SA**, Sharan S and Sterneck E. C/EBP δ inhibits breast epithelial cell growth in part by repression of the cyclin D1 promoter. Spring Research Festival, NCI, Fredrick, MD, May 16-17, 2007.
12. **Pawar SA**, Sharan S and Sterneck E. The growth inhibitory role of C/EBP δ is mediated via cyclin D1 repression in breast epithelial cells. Mechanisms and Models of Cancer, Salk Institute, San Diego, CA, Aug 8-12, 2007.
13. **Pawar SA**, Sharan S and Sterneck E. Molecular mechanism of growth inhibition by C/EBP δ : Dual mechanism of cyclin D1 repression in breast epithelial cells. Spring Research Festival, NCI, Frederick, MD, May 14-15, 2008.
14. Nguyen-Ngoc KV, **Pawar SA** and Sterneck E. Verification and characterization of apoptosis-related target genes of CCAAT/enhancer binding protein delta (C/EBP δ). Spring Research Festival, NCI, Frederick, MD, May 14-15, 2008.
15. Nguyen-Ngoc KV, **Pawar SA** and Sterneck E. Verification and characterization of apoptosis-related target genes of CCAAT/enhancer binding protein delta (C/EBP δ). LCDS–LPDS–LCMB Combined Department Retreat, NCI, Frederick, MD, June 3, 2008.
16. Nguyen-Ngoc KV, **Pawar SA** and Sterneck E. The C/EBP δ -regulated Interleukin 1 family member 9 (IL-1F9, IL-1H1) is a potential survival factor for mammary epithelial and breast tumor cells. NCI-CCR NIAID Symposium: “Manipulation of the Host Immune Response: Exploring the Crossroads of Infectious Disease and Cancer”, Bethesda, MD, June 12, 2008.
17. Sarkar TR, **Pawar SA** and Sterneck, E. The Src tyrosine kinase represses tumor suppressor CEBPD protein expression in breast cancer cells via regulation of SIAH Ubiquitin E3 Ligases. Ninth Annual Fellows and Young Investigators Colloquium. Hershey, PA, Mar 18-20, 2009.
18. Sarkar TR, **Pawar SA** and Sterneck E. The Src tyrosine kinase represses tumor suppressor CEBPD protein expression in breast cancer cells via regulation of SIAH ubiquitin E3 ligases. Spring Research Festival, NCI, Frederick, MD, April 29-30, 2009.
19. Balamurugan K, Sharan S, **Pawar SA** and Sterneck E. All mammary glands are not created equal: MMTV-neu x C/EBP delta null mouse analysis provokes consideration of body axis location for mechanisms of tumor development. AACR, San Diego, CA, Oct 13-16, 2009.
20. **Pawar SA**, Fu Q, Wang J, Petersen K-U, Weiler H, Fink LM and Hauer-Jensen M. Targeting the endothelial Thrombomodulin- Protein C pathway to mitigate radiation lethality. 56th Annual Meeting of the Radiation Research Society, Maui, HI, Sep 25-29, 2010.
21. Roy Sarkar T, Wang J, Sharan S, **Pawar SA** and Sterneck E. The Src tyrosine kinase downregulates C/EBP Delta (CEBPD) protein expression via the SIAH2 E3 ubiquitin ligase to maintain motility of breast tumor cells. NIH Research Festival, Bethesda, MD, Oct 6-9, 2010.
22. Roy Sarkar T, Wang J, **Pawar S**, Sharan S and Sterneck E. The Src tyrosine kinase down-regulates CEBPD protein expression via the SIAH2 E3 Ubiquitin ligase to maintain motility of breast cancer cells. EMT and Cancer Progression and Treatment AACR, Arlington, VA, Feb 28-Mar 2, 2011.
23. Roy Sarkar T, Wang J, Sharan S, **Pawar SA**, Wang J-M, Sterneck E. Src tyrosine kinase downregulates C/EBP δ protein expression in breast tumor cells via the SIAH2 E3 ubiquitin ligase, which contributes to cell transformation. The Biology of Cancer: Microenvironment, Metastasis & Therapeutics, CSHL meeting, NY, April 26 – 30, 2011.
24. Roy Sarkar T, Raza A, Wang J, Sharan S, Cantwell CA, **Pawar SA**, Johnson P F, Wang JM, Caldas C and Sterneck E. Src kinase downregulates C/EBP δ through SIAH2 to promote human breast cancer cell transformation. 4th Annual Safeway Breast Cancer Research Retreat. Baltimore, MD, May 26, 2011.

25. Pathak R, **Pawar SA**, Gupta P, Fu Q, Berbée M, Biju PG, Garg S, Hendrickson, H and Hauer-Jensen M. Characterization of transgenic GFRP knock-in mice: Implications for BH4 in modulation of radiation response. 14th International Congress of Radiation Research, Warsaw, Poland, Aug 28-Sep 1, 2011.
26. **Pawar SA**, Pathak R, Wang J, Sterneck E and Hauer-Jensen M. Role of the transcription factor C/EBP delta in ionizing radiation response. 14th International Congress of Radiation Research, Warsaw, Poland, Aug 28-Sep 1, 2011.
27. **Pawar SA**, Pathak R, Wang J, Sterneck E and Hauer-Jensen M. Role of the transcription factor C/EBP delta in ionizing radiation response. Arkansas Biotechnology Institute Fall Research Symposium, Little Rock, AR, Sep 21, 2011.
28. Pathak R, Krager KJ, **Pawar SA**, Gupta P, Fu Q, Berbée M, Biju P, Garg S, Wang W, Hendrickson H, Hauer-Jensen M, Aykin-Burns N. De novo biosynthesis of BH4 is critical in protecting against ionizing radiation-induced injury. 58th Annual Meeting Radiation Research Society 2012 Annual Meeting, San Juan, PR, Sep 30-Oct 3, 2012.
29. **Pawar SA**, Zhu X, Wang W, Sterneck E. and Hauer-Jensen M. C/ebp delta displays tissue-specific responses and protects from radiation-induced lethality. 58th Annual Meeting Radiation Research Society 2012, San Juan, PR, Sep 30-Oct 3, 2012.
30. Krager KJ, Pathak R, **Pawar SA**, Gupta P, Fu Q, Berbée M, Biju P, Garg S, Wang W, Wang W, Hendrickson H, Hauer-Jensen M, and Aykin-Burns N. De novo biosynthesis of tetrahydrobiopterin is critical in protecting against ionizing radiation. Society for Free Radical Biology and Medicine, San Diego, CA, Nov 14-18, 2012.
31. **Pawar SA**, Shao L, Chang J, Zhou D and Hauer-Jensen M. C/EBP delta knockout mice display increased hematopoietic injury after exposure to sublethal TBI. 59th Annual Meeting Radiation Research Society 2013 Annual Meeting, New Orleans, LA, Sep 15-19, 2013.
32. **Pawar SA**, Zhu X, Wang W and Hauer-Jensen M. C/EBP δ -deficiency promotes radiation injury by an impaired DNA damage response. 60th Annual Meeting Radiation Research Society 2014 Annual Meeting, Las Vegas, NV, Sep 21-24, 2014.
33. **Pawar SA**, Zhu X, Wang W and Hauer-Jensen M. C/EBP δ -deficiency promotes radiation injury by an impaired DNA damage response. Women in Science poster session, Jack Stephens Spine Center, UAMS, Little Rock, AR, Oct 31, 2014.
34. Banerjee S, Aykin-Burns N, Krager KJ, Hauer-Jensen M and **Pawar SA**. C/EBP δ modulates reactive oxygen species to protect against IR-induced cell death. Society for Free Radical Biology and Medicine, Seattle, WA, Nov 19-23, 2014.
35. Banerjee S, Aykin-Burns N, Krager KJ, Melnyk SB, Hauer-Jensen M and **Pawar SA**. C/EBP δ modulates oxidative stress and mitochondrial dysfunction to promote post-radiation survival. Student Research Day, UAMS, Little Rock, AR, April 15, 2015.
36. Banerjee S, Aykin-Burns N, Krager KJ, Melnyk SB, Hauer-Jensen M and **Pawar SA**. C/EBP δ modulates oxidative stress and mitochondrial dysfunction to promote post-radiation survival. Conference on Normal Tissue Radiation Effects and Countermeasures (CONTREC), at Winthrop Rockefeller Institute Conference Center, Morrilton, AR, May 6-9, 2015.
37. Banerjee S, Aykin-Burns N, Krager KJ, Melnyk SB, Hauer-Jensen M and **Pawar SA**. C/EBP δ modulates oxidative stress and mitochondrial dysfunction to promote post-radiation survival. 61st Annual Meeting Radiation Research Society, Weston, FL, Sep 19-22, 2015.
38. Banerjee S, Aykin-Burns N, Krager KJ, Hauer-Jensen M and **Pawar SA**. C/EBP δ modulates oxidative stress and mitochondrial dysfunction to promote post-radiation survival. Southeast Regional IDeA Conference, Biloxi, MS, Nov 11-13, 2015.
39. **Pawar SA**, Banerjee S, Aykin-Burns N, Krager KJ, Melnyk SB, and Hauer-Jensen M. C/EBP δ modulates oxidative stress and mitochondrial dysfunction to promote post-radiation survival. Society for Redox Biology and Medicine, Boston, MA, Nov 18-22, 2015.

40. LoBianco FV, **Pawar SA**, Krager KJ, Breen PJ, Compadre CM, Hauer-Jensen M and Aykin-Burns N. Tocotrienol-rich DG3 as a therapeutic agent protects against ionizing radiation-induced intestinal injury. Student Research Day, UAMS, Little Rock, AR, April 13, 2016.
41. Banerjee S, Fu Q, Ponnappan U, Melnyk SB, Hauer-Jensen M and **Pawar SA**. Radiation-induced intestinal injury in *Cebpd*-knockout mice occurs due to aberrant inflammatory and oxidative stress response. 6th Biennial NIH/NIGMS National IDeA Symposium for Biomedical Research Excellence, Washington, DC, June 26-28, 2016.
42. Majumdar D*, Banerjee S, Hauer-Jensen M, and **Pawar SA**. C/EBP δ -deficient macrophages display altered inflammatory response to ionizing radiation. 6th Biennial NIH/NIGMS National IDeA Symposium for Biomedical Research Excellence, Washington, DC, June 26-28, 2016.
43. Shah SK, Banerjee S, Majumdar D, Ponnappan U, Stumhofer J, Hauer-Jensen M, and **Pawar SA**. IL-17 signaling may be dispensable for promoting radiation-induced intestinal injury. 6th Biennial NIH/NIGMS National IDeA Symposium for Biomedical Research Excellence, Washington, DC, June 26-28, 2016.
44. Banerjee S, Fu Q, Ponnappan U, Melnyk SB, Hauer-Jensen M and **Pawar SA**. Radiation-induced intestinal injury in *Cebpd*-knockout mice occurs due to aberrant inflammatory and oxidative stress response. Gordon Research Conference, "Extracellular vesicles": Biologic Effects and Therapeutic Potential of Extracellular Vesicles, Newry, ME, Aug 21-26, 2016.
45. Banerjee S, Fu Q, Ponnappan U, Melnyk SB, Hauer-Jensen M and **Pawar SA**. Radiation-induced intestinal injury in *Cebpd*-knockout mice occurs due to aberrant inflammatory and oxidative stress response. Arkansas Biosciences Institute Symposium, Stephens Spine Institute, UAMS, Little Rock, AR, Sep 13, 2016.
46. Shah SK, Banerjee S, Majumdar D, Ponnappan U, Stumhofer J, Hauer-Jensen M, and **Pawar SA**. IL-17 signaling may be dispensable for promoting radiation-induced intestinal injury. Arkansas Biosciences Institute Symposium, Stephens Spine Institute, UAMS, Little Rock, AR, Sep 13, 2016.
47. Banerjee S, Byrum S, Orr L, Tackett AJ, Ponnappan U, Hauer-Jensen M and **Pawar SA**. Identification of C/EBP δ -targets involved in regulation of radiation-induced oxidative stress utilizing a proteomics approach. 62nd Annual Meeting Radiation Research Society, Maui, HI, Oct 16-19, 2016.
48. LoBianco FV, **Pawar SA**, Krager KJ, Breen PJ, Compadre CM, Hauer-Jensen M, Aykin-Burns N. Tocotrienol-rich DG3 as a therapeutic agent protects against ionizing radiation-induced intestinal injury. 62nd Annual Meeting Radiation Research Society, Maui, HI, Oct 16-19, 2016.
49. Banerjee S, Fu Q, Ponnappan U, Melnyk SB, Hauer-Jensen M and **Pawar SA**. Radiation-induced intestinal injury in *Cebpd*-knockout mice occurs due to aberrant inflammatory and oxidative stress response. Annual Meeting of the South Central Chapter of Society of Toxicology, UAMS, Little Rock, AR, Oct 27-28, 2016.
50. Shah SK, Banerjee S, Majumdar D, Ponnappan U, Stumhofer J, Hauer-Jensen M, and **Pawar SA**. IL-17 signaling may be dispensable for promoting radiation-induced intestinal injury. Annual Meeting of the South Central Chapter of Society of Toxicology, UAMS, Little Rock, AR, Oct 27-28, 2016.
51. Majumdar D, Banerjee S, Hauer-Jensen M, and **Pawar SA**. C/EBP δ -deficient macrophages display altered inflammatory response to ionizing radiation. Annual Meeting of the South Central Chapter of Society of Toxicology, UAMS, Little Rock, AR, Oct 27-28, 2016.
52. Banerjee S, Fu Q, Ponnappan U, Melnyk SB, Hauer-Jensen M and **Pawar SA**. Radiation-induced intestinal injury in *Cebpd*-knockout mice occurs due to aberrant inflammatory and oxidative stress response. Basic Subcellular Mechanisms, Showcase of Medical Discoveries, UAMS, Little Rock, AR, Nov 9, 2016.
53. Banerjee S, Fu Q, Ponnappan U, Melnyk SB, Hauer-Jensen M and **Pawar SA**. Role of TLR4 in promoting radiation-induced intestinal injury. 40th Annual Conference of Shock Society, Fort Lauderdale, FL, June 3-6, 2017.
54. Majumdar D*, Chang J, Zhou D, Banerjee S, Hauer-Jensen M and **Pawar SA**. C/EBP δ -deficiency alters radiation-induced myeloid responses. Drug Discovery and Development Colloquium, UAMS, Little Rock, AR, June 15-17, 2017.

55. Banerjee S, Shah SK, Pathak R, Melnyk SB, Hauer-Jensen M and **Pawar SA**. Gamma-tocotrienol-mediated Protection Against Radiation-induced Injury is Dependent on C/EBP δ . Drug Discovery and Development Colloquium, UAMS, Little Rock, AR, June 15-17, 2017.
56. Murdock S, Majumdar D, Banerjee S, Hauer-Jensen M and **Pawar SA**. Investigating the role of C/EBP δ in macrophage response to ionizing radiation. Center for Diversity Affairs Summer Research Internship presentation, UAMS, Little Rock, AR, July 25, 2017.
57. Orton J, Raley R, Banerjee S, Eldred C, Hauer-Jensen M and **Pawar SA**. Investigating the role of C/EBP δ in etoposide-mediated cytotoxicity. Central Arkansas Undergraduate Summer Research Conference, UAMS, Little Rock, AR, July 26, 2017.
58. Eldred C, Orton J, Raley R, Banerjee S, Hauer-Jensen M and **Pawar SA**. C/EBP δ -deficiency promotes doxorubicin-induced cytotoxicity due to increased mitochondrial damage and dysfunction. 51st Fall Annual Seminar, Arkansas Association for Health Systems Pharmacists, Little Rock, AR, Oct 5-6, 2017.
59. Orton J*, Raley R, Banerjee S, Eldred C, Krager KJ, Aykin-Burns N and **Pawar SA**. C/EBP δ -deficient cells show increased toxicity to etoposide due to impaired DNA damage response, increased oxidative stress response and mitochondrial damage. 2017 Southeast IDeA Regional Meeting, Morgantown, WV, Oct 11-13, 2017.
60. Banerjee S, Fu Q, Ponnappan U, Melnyk SB, Hauer-Jensen M and **Pawar SA**[#]. Impaired TLR4 signaling promotes radiation-induced intestinal injury in *Cebpd*-deficient mice. 2017 Southeast IDeA Regional Meeting, Morgantown, WV, Oct 11-13, 2017.
61. Majumdar D, Banerjee S, Hauer-Jensen M and **Pawar SA**. C/EBP δ -deficiency results in impaired phagocytic response to ionizing radiation. 2017 Southeast IDeA meeting, Morgantown, WV, Oct 11-13, 2017.
62. Banerjee S, Fu Q, Ponnappan U, Melnyk SB, Hauer-Jensen M and **Pawar SA**[#]. Impaired TLR4 signaling promotes radiation-induced intestinal injury in *Cebpd*-deficient mice. 63rd Annual International meeting of the Radiation Research Society, Cancun, Mexico, Oct 15-18, 2017.
63. Majumdar D, Banerjee S, Hauer-Jensen M and **Pawar SA**. C/EBP δ -deficiency results in impaired phagocytic response to ionizing radiation. 4th Annual Graduate Student Association Fall Symposium, UAMS, Little Rock, AR, Oct 27, 2017.
64. Orton J, Raley R, Banerjee S, Eldred C, Hauer-Jensen M and **Pawar SA**. C/EBP δ -deficient cells show increased toxicity to etoposide due to impaired DNA damage response, increased oxidative stress response and mitochondrial damage. Annual INBRE conference, University of Arkansas-Fayetteville, AR, Oct 27-28, 2017.
65. Coates C, Banerjee S, Orton J, Hauer-Jensen M and **Pawar SA**. C/EBP δ protects cells from Doxorubicin cytotoxicity by suppression of DNA damage and mitochondrial dysfunction. Student Research Day, UAMS, Little Rock, AR, Mar 6, 2018.
66. Majumdar D, Wang X, Zhou D, Hauer-Jensen M, and **Pawar SA**. Role of C/EBP δ in radiation-induced hematopoietic injury. Student Research Day, UAMS, Little Rock, AR, Mar 6, 2018.
67. Pathak R, Sadhukhan R, Garg S, **Pawar SA**, Boerma M, Ware J and Hauer-Jensen M. Kruppel-like factor 2 (KLF2): A novel radiation target is suppressed in the mouse intestine. Conference on Normal Tissue Radiation Effects and Countermeasures (CONTREC), Morrilton, AR, May 14-17, 2018.
68. Gorantla A, Banerjee S, Tyler A, Chokhani P, Groves T, Allen AR and **Pawar SA**. Investigating the role of C/EBP δ in inflammaging and oxidative stress in the aging brain. Center for Diversity Affairs Summer Research Internship presentation, UAMS, Little Rock, AR, July 23, 2018.
69. Banerjee S, Shah SK, Melnyk SB, Hauer-Jensen M and **Pawar SA**. *Cebpd* is essential for gamma-tocotrienol mediated protection against radiation-induced hematopoietic and intestinal injury. Military Health System Research Symposium, Kissimmee, FL, Aug 20-23, 2018.
70. Banerjee S, Fu Q, Shah SK, Melnyk SB, Hauer-Jensen M and **Pawar SA**. TLR4 inhibition alleviates IR-induced intestinal injury and underlying sepsis in C/EBP δ -deficient mice. Military Health System Research Symposium, Kissimmee, FL, Aug 20-23, 2018.

71. Majumdar D, Stumhofer J, Pietras E, and **Pawar SA**. C/EBP δ protects hematopoietic stem cells and myeloid progenitor cells from radiation-induced injury. 64th Annual meeting of the Radiation Research Society, Chicago, IL, Sep 14-17, 2018.
72. Banerjee S, Shah SK, Melnyk SB, Hauer-Jensen M and **Pawar SA**[#]. *Cebpd* is essential for gamma-tocotrienol mediated protection against radiation-induced hematopoietic and intestinal injury. 64th Annual meeting of the Radiation Research Society, Chicago, IL, Sep 14-17, 2018.
73. Pathak R, Sadhukhan R, Garg S, **Pawar SA**, Boerma M, Ware J and Hauer-Jensen M. Kruppel-like factor 2 (KLF2): A novel radiation target, shear-responsive KLF2, is suppressed in the mouse intestine. 64th Annual meeting of the Radiation Research Society, Chicago, IL, Sep 14-17, 2018.
74. Majumdar D, Stumhofer J, Pietras E, and **Pawar SA**. Investigating the role of C/EBP δ -deficiency in radiation-induced bone marrow failure. 60th American Society of Hematology Annual Meeting & Exposition, San Diego, CA, Dec 1-4, 2018.
75. Majumdar D, Banerjee S, Pietras EM and **Pawar SA**. C/EBP δ promotes post-radiation recovery of hematopoietic stem cells by downregulating oxidative stress and DNA damage. 65th Annual meeting of the Radiation Research Society, San Diego, CA, Nov 3-6, 2019.
76. Sadhukhan R, Majumdar D, Garg S, **Pawar SA**, Chowdhury P, Griffin R, Narayanasamy G, Dobretsov M, Hauer-Jensen M and Pathak R. Simultaneous exposure to chronic low-grade irradiation and simulated microgravity alter immune cells phenotype in mice thymus and spleen. 65th Annual meeting of the Radiation Research Society, San Diego, CA, Nov 3-6, 2019.

(*travel award or [#]New Investigator or Early Career Investigator travel award)

TEACHING

| | |
|-----------|---|
| 2011 | Radiation Biology overview (PhPR 5562), UAMS Pharmacy core curriculum, P3 elective <i>Topics:</i> Introduction to Radiation Biology <i>Number of Students:</i> 30, <i>Contact hours:</i> 1.5 h |
| 2011 | Biological & Cellular Chemistry (PhSc 3214), UAMS Pharmacy core curriculum, P1 year <i>Topics:</i> Lipid metabolism, Amino Acid metabolism <i>Number of Students:</i> 116, <i>Contact hours:</i> 10 h |
| 2011-2016 | Biological & Cellular Chemistry (PhSc 3214 /7102), UAMS Pharmacy core curriculum, additional review sessions for students with D & F grade, P1 year <i>Topics:</i> Lipid metabolism, Amino acid metabolism, Digestion & Absorption of Macronutrients, Micronutrients <i>Number of Students:</i> 10-25, <i>Contact hours:</i> 7.5 h |
| 2012-2016 | Biological and Cellular Chemistry (PhSc 3214), UAMS Pharmacy core curriculum, P1 year <i>Topics:</i> Lipid metabolism, Amino acid metabolism, Digestion & Absorption of Macronutrients, Micronutrients <i>Number of Students:</i> 119-123, <i>Contact hours:</i> 12 h |

| | |
|-----------|--|
| 2015-16 | Biological and Cellular Chemistry (PhSc 3214/7102), Summer School remediation, UAMS Pharmacy core curriculum, P1 year <i>Topics:</i> Lipid metabolism, Amino acid metabolism, Digestion & Absorption of Macronutrients, Micronutrients <i>Number of Students:</i> 1-2, <i>Contact hours:</i> 12.5 h |
| 2017 | Molecular Biology & Biotechnology (PhSc 7204), UAMS Pharmacy core curriculum, P2 year <i>Topics:</i> Protein analysis & Proteomics <i>Number of Students:</i> 120, <i>Contact hours:</i> 3.0 h |
| 2017 | Radiation Biology (PhSc 6112), UAMS Pharmaceutical Sciences Graduate Course <i>Topics:</i> Radiation effects on gastrointestinal system <i>Number of Students:</i> 4, <i>Contact hours:</i> 3.0 h |
| 2017-2019 | Anatomy/Physiology/Pathology (PhSc 7101), UAMS Pharmacy core curriculum, P1 year <i>Topics:</i> Regulation of Gastrointestinal, Liver & Biliary Tract, Pathology of the Gastrointestinal Tract <i>Number of Students:</i> 75-124, <i>Contact hours:</i> 4.0 h |
| 2018 | Biological and Cellular Chemistry (PhSc 7102), UAMS Pharmacy core curriculum, P1 year <i>Topic:</i> Lipid metabolism <i>Number of Students:</i> 120, <i>Contact hours:</i> 4.0 h |
| 2018-2019 | Pharmacology-II (PhSc 7202), UAMS Pharmacy core curriculum, P2 year <i>Topic:</i> Coagulation, Dyslipidemia <i>Number of Students:</i> 120, <i>Contact hours:</i> 5.0 h |
| 2020 | Pharmacology-II (PhSc 7202), UAMS Pharmacy core curriculum, P2 year <i>Topic:</i> Dyslipidemia <i>Number of Students:</i> 120, <i>Contact hours:</i> 2.0 h |

MENTORING & TRAINING ACTIVITIES

Baccalaureate Students

| | |
|------|---|
| 2015 | Sajal Bharany, Hendrix College, Conway, AR |
| 2015 | Bernice Ofori, Philander Smith College, Little Rock, AR |
| 2016 | Sammie James, Rhodes College, Memphis, TN |
| 2016 | Robin Raley, University of Arkansas, Fayetteville, AR |
| 2017 | Jessica Orton, University of Arkansas, Fayetteville, AR |

2018 Purav Chokhani, University of Texas, Austin, TX
2019 Sarah Vue, Henderson State University, Arkadelphia, AR

UAMS Center for Diversity Affairs Fellows

2017 Steven Murdock, Virginia State University, Petersburg, VA
2018 Akshita Gorantla, Cupertino High School, Cupertino, CA

Pharm. D Students

2017 Charis Eldred-Coates (P2 student), UAMS, College of Pharmacy (COP), Little Rock, AR

Masters's students

1994-1995 Co-Mentor Aparna Paul, M. Tech.
National Chemical Laboratory, University of Pune, India
Thesis: Effect of coordinated addition of specific amino acids on the synthesis of recombinant glucose/xylose isomerase

2008 Co-Mentor Kim-Vy Nguyen Ngoc, MS,
National Cancer Institute, Frederick, MD
Thesis: Identification of targets of the transcription factor C/EBP δ during mouse mammary gland involution

2016-2017 Thesis Committee Member Francesca Lobianco, MS
UAMS, Interdisciplinary Biomedical Sciences Program
Thesis: Role of Sirtuin3 in radiation-induced liver injury

2018 Mentor Jyoti Gogoi, MS
Research Assistant, Department of Physiology & Biophysics,
College of Medicine, UAMS, mentored & trained in Molecular Biology techniques

Ph.D. Students

2015- Major Advisor Debajyoti Majumdar, M. Pharm
Pharmaceutical Sciences Graduate Program (PSGP),
(Radiation biology track)
Dissertation: Role of C/EBP δ in radiation-induced hematopoietic injury

2017-2018 Thesis Committee Member Tyler Alexander, BS
UAMS, Interdisciplinary Biomedical Sciences Program
Dissertation: Effects of acute lymphoblastic leukemia treatment on cognitive function and hippocampal physiology

Postdoctoral Fellows

| | | |
|-----------|------------------|--|
| 2008-2015 | Co-Mentor | Balamurugan Kuppusamy, PhD National Cancer Institute, Frederick, MD <u>Current position:</u> Staff Scientist National Cancer Institute, Frederick, MD |
| 2013 | Mentor | Rakhee Agarwal, PhD Pharmacology and Toxicology, UAMS <u>Current position:</u> Research Scientist, Alexion Pharmaceuticals Inc. Wilton, Connecticut |
| 2013-2017 | Mentor | Nirmala Parajuli, PhD Pharmacology and Toxicology, UAMS <u>Current position:</u> Assistant Professor Pharmacology and Toxicology, UAMS |
| 2014- | Advisor & Mentor | Sudip Banerjee, PhD Div. Radiation Health, Dept. of Pharm. Sci, COP, UAMS, Little Rock, AR |
| 2016 | Advisor & Mentor | Vaibhav Aher, M. Pharm, PhD Div. Radiation Health, Dept. of Pharm. Sci, COP, UAMS, Little Rock, AR <u>Current position:</u> Associate Professor, Matoshri College of Pharmacy, Nashik, India |
| 2018 | Mentor | Gauri Lamture, PhD Drug Discovery & Development, Department of Pharm. Sci, COP, UAMS, Little Rock, AR <u>Current position:</u> Postdoctoral fellow, FDA, Bethesda, MD |

Research Assistants

| | | |
|------------------|------------------|---|
| 2011- 2013 | Advisor & Mentor | Xiaoyan Zhu, MS Div. Radiation Health, Dept. of Pharm. Sci, COP, UAMS, Little Rock, AR <u>Current position:</u> Research Assistant, Dept. of Family Medicine, College of Medicine, UAMS |
| 2015- 2018 | Advisor & Mentor | Sumit Shah, MD Div. Radiation Health, Dept. of Pharm. Sci, COP, UAMS, Little Rock, AR <u>Current position:</u> Research Assistant, Dept. of Pathology, College of Medicine, UAMS |
| 2015- present | Advisor & Mentor | Gail Wagoner, BS Div. Radiation Health, Dept. of Pharm. Sci, COP, UAMS, Little Rock, AR |

AWARDS & HONORS OF MENTEES/TRAINEES

| | |
|-------------------------------|---|
| Sudip Banerjee, PhD | Received Scholar-in training travel award to present poster at Radiation Research Society Meeting, Weston, FL, Sep 19-22, 2015. |
| Debajyoti Majumdar, M. Pharm. | Received UAMS Graduate School travel award, 6 th Biennial NIH/NIGMS National IDeA Symposium for Biomedical Research Excellence meeting in Washington DC, June 26-28, 2016. |
| Sumit Shah, MBBS, MPH | Received 1 st prize in the student category (\$100 award), South Central Chapter of the Society of Toxicology, UAMS, Little Rock, AR, Oct 28, 2016. |
| Sudip Banerjee, PhD | Received 1 st prize non-student category (\$100 award), South Central Chapter of the Society of Toxicology Meeting, UAMS, Little Rock, AR, Oct 28, 2016. |
| Robin Raley | Selected for NIH- Summer Internship Program Fellowship, May-August 2017, based on her research project in my laboratory. |
| Sudip Banerjee, PhD | Selected for oral presentation, Drug Discovery and Development Colloquium, UAMS, Little Rock, AR, June 15-17, 2017. |
| Debajyoti Majumdar, M. Pharm | Received 3 rd prize for poster presentation in graduate student category (\$100 award), Drug Discovery and Development Colloquium, UAMS, Little Rock, AR, June 15-17, 2017. |
| Jessica Orton | Selected for the Graduate Student Boot Camp, Pratt School of engineering at Duke University, based on her summer research project done in my laboratory, Sep15, 2017. |
| Jessica Orton | Received Arkansas INBRE travel award, to present her summer research at the Southeast IDeA Meeting, Morgantown, WV, Oct 11-13, 2017. |
| Sudip Banerjee, PhD | Selected for oral presentation at the Conference on Normal Tissue Radiation Effects and Countermeasures, Morrilton, AR, May 14-17, 2018. |
| Sudip Banerjee, PhD | Received Scholar-in training travel award & selected for oral presentation at the 64 th Annual meeting of the Radiation Research Society, Chicago, IL, Sep 23-26, 2018. |
| Jessica Orton | Selected for Duke University's Pratt School of Engineering Summer REU Program, based on her previous summer research experience in my lab. |
| Sudip Banerjee, PhD | Received Scholar-in training travel award, selected for oral presentation at the 65 th Annual meeting of the Radiation Research Society, San Diego, CA, Nov 3-6, 2019. |
| Debajyoti Majumdar, M. Pharm. | Nominated as one of the top 10 submitted abstracts, received Scholar-in training travel award to present his poster at the 65 th Annual meeting of the Radiation Research Society, San Diego, CA, Nov 3-6, 2019. |

SERVICE

Master's Student Committee

2016-2017
Francesca Lobianco,
Advisory Member, Master's thesis committee,
Interdisciplinary Biomedical Sciences Program, UAMS

Graduate Student Committee

2015-present
Debajyoti Majumdar, M.Pharm.,
Major Advisor, Dissertation Committee,
Pharmaceutical Sciences Graduate Program (Radiation Biology track),
UAMS

2017-2018
Tyler Alexander, BS,
Advisory member, Dissertation Committee,
Interdisciplinary Biomedical Sciences Program, UAMS

College Committees

2011-present
2012
2013-present
2013-2015
2014-2017
2015-2017
2018-present
2018-present
College of Pharmacy (COP) Graduate Faculty
Search Committee, Director of Assessment for the College
COP Graduate Faculty Committee
COP Educational and Technology Committee
COP Student Research Committee
COP Educational and Technology Committee
Curriculum 2025 Working Group 6 Co-Leader
Curriculum 2025 working group 3 (Cardiovascular disease states),
member

University Committees

2011-present
2012-2018
2013-2016
2017-present
2018-present
2019-present
UAMS Graduate Faculty
Women's Faculty Development Caucus Research Committee member,
UAMS
Women's Faculty Development Caucus Mentoring Committee member,
UAMS
UALR-UAMS Joint Bioinformatics Program Graduate faculty
UAMS IACUC Committee Member
CAVHS Safety Committee, unaffiliated member

University Service

2007-2008
2010-2016
2010-2014
Co-organizer of an inter-departmental postdoc seminar series, "Signaling Mechanisms in Immunology, Cancer and Development," National Cancer Institute, Frederick, MD
Poster judge, Student Research Day Symposium, UAMS, Little Rock, AR
Organizer and Coordinator of Division of Radiation Health Research Conference Seminar Series, UAMS, Little Rock, AR

- 2013 Hosted Guest Speaker Dr. Esta Sterneck, National Cancer Institute, Frederick, MD for the Winthrop P. Rockefeller Cancer Research Forum seminar series, UAMS, Little Rock, AR
- 2013 Advertised the Pharmaceutical Sciences Graduate Program, UAMS, Little Rock, AR on Student Career Day
- 2013 Hosted Guest Speaker Dr. Edouard Azzam, RUTGERS, The State University of New Jersey, for the Winthrop P. Rockefeller Cancer Research Forum seminar series, UAMS, Little Rock, AR
- 2014-present Coordinator, Host Responses and Radiation Science Program, UAMS, Little Rock, AR
- 2014 Brief overview of academic life in biomedical research provided to students of South Arkansas University, Magnolia, AR
- 2014-present Mentor for Pharm. D. Summer Research Program, UAMS, Little Rock, AR
- 2014-2015 Coordinated and organized the COBRE New Investigator Research Forum Seminars, UAMS, Little Rock, AR
- 2015-present Mentor for INBRE Summer Research Program, UAMS, Little Rock, AR
- 2015 Brief overview about Pharmacy program provided to students of University of Monticello, Monticello, AR
- 2015 Participated in multiple mini-interviews for screening P1 students, UAMS, Little Rock, AR
- 2016 Poster judge, Graduate Student Association Research Symposium, UAMS, Little Rock, AR
- 2016- 2018 Co-facilitator for small group discussions with Pharm. D (P1, P2 & P3) students, UAMS, Little Rock, AR
- 2017 College of Pharmacy Summer Internship Program Mentor, UAMS, Little Rock, AR
- 2017 Gave an overview of research to high school students in Medical Application of Science for Health (MASH) Program at UAMS, Little Rock, AR
- 2017, 2018 Mentor for Center for Diversity Affairs Summer Research Internship Program, UAMS, Little Rock, AR
- 2018, 2019 Poster judge, Student Research Day Symposium, UAMS, Little Rock, AR
- 2018 Participated in Health Careers Opportunity Program to promote interactions with high school students from minority and disadvantaged backgrounds
- 2018 Reviewer of Abstracts for Oral Presentations, Graduate Student Association Research Symposium, UAMS, Little Rock, AR
- 2019 Hosted Guest Speaker Dr. Eric Pietras, University of Colorado, Aurora, CO, for the Winthrop P. Rockefeller Cancer Research Forum seminar series, UAMS, Little Rock, AR

Professional Service

- 2015 Poster judge for undergraduate and graduate student posters, Southeast IDeA Meeting, Biloxi, MS

| | |
|--------------|--|
| 2015 | Chair, Topical Review at the 61 st Annual Radiation Research Society Meeting, Weston, FL |
| 2016 | Mentor for undergraduate and graduate students, Sixth Biennial National IDeA Symposium of Biomedical Research Excellence, Washington, DC |
| 2017 | Reviewer of Abstracts in Biological Sciences, American Association of Colleges of Pharmacy 2017 Annual Meeting, Nashville, TN |
| 2017-present | Junior Awards Committee Member, Society for Redox Biology & Medicine |
| 2017-present | Reviewer of Abstracts, Annual meeting of Society for Redox Biology & Medicine |
| 2019 | Grant Reviewer, DAIT/NIAID/ NIH Radiation and Nuclear Countermeasure Program |
| 2019-2023 | Awards and Honors Committee, Shock Society |

Editorial Service

| | |
|-------|--|
| 2017- | Journal of Molecular Biology & Biotechnology, Editorial board member |
| 2017- | SM Journal of Carcinogenesis, Editorial board member |
| 2018- | Reactive Oxygen Species (ROS), Editorial board member |

Manuscript Reviewer

American Journal of Therapeutics, Amino Acids, Antioxidant Redox Signaling, Biochemistry, Biomedicine & Pharmacotherapy, Cancer Chemotherapy and Pharmacology, Cancer Letters, Carcinogenesis, Cellular Physiology and Biochemistry, Cells, Current Drug Targets, Current Molecular Pharmacology, Experimental Neurology, International Journal of Molecular Sciences, International Journal of Radiation Biology, International Journal of Radiation Oncology, Biology, Physics, Journal of Life Sciences, Mediators of Inflammation, PLOS One, Radiation Research, Radiotherapy & Oncology, Reactive Oxygen Species, Royal Society of Chemistry Advances, Scientific Reports

PROFESSIONAL MEMBERSHIPS

| | |
|--------------|--|
| 1998 | Society of Biological Chemists, India |
| 2009-present | Radiation Research Society |
| 2009-2018 | American Association of Colleges of Pharmacy |
| 2012-present | Society for Redox Biology and Medicine |
| 2013-present | International Cytokine and Interferon Research Society |
| 2014 | American Association of Cancer Research |
| 2014-present | American Association for Advancement of Science |
| 2016-present | Shock Society |
| 2017-present | American Association of University Professors |
| 2018-present | American Society of Hematology |
| 2019-present | International Society for Experimental Hematology |